The interaction between the HPV E1^E4 protein and the cell cytoskeleton

A thesis submitted to the University of London for the degree of doctor of philosophy

Peter Laskey

Division of Virology
National Institute for Medical Research
The Ridgeway
Mill Hill
London
UK

2006

ProQuest LLC
789 East Eisenhower Parkway
P.O. Box 1346
Ann Arbor, MI 48106-1346

Acknowledgments

I would like to thank several people for their assistance for the duration of this research project.

Firstly I would like to thank my supervisor John Doorbar for initially selecting me for the project and his continual input throughout the duration of the work.

I am enormously grateful to Clare Davy and Pauline McIntosh for their continual assistance in the form of technical advice, and in the proof-reading of this manuscript.

I would also like to thank the other lab members and colleagues at the NIMR, Qian Wang, Deb Jackson, Woei Ling Peh, Rina Sorathia, Papia Das, Kate Sullivan, Ken Raj, Katie Copeland and Vivian Bechtold for their continual support and assistance in all areas of the project over the past few years, and for making the whole experience so enjoyable.

I am also very grateful to Rudolph Leube (Department of Anatomy, Johannes Gutenberg University Mainz, Becherweg 13, D-55128 Mainz, Germany), Bishr Omary (Department of Medicine, Palo Alto VA Medical Centre, Palo Alto, California 94304, USA) and Karl Sotlar (Institute of Pathology, University of Tuebingen, Germany) for supplying materials and reagents used in this study.

In addition to this I would like to say a special thanks to Alex Bolton, Nick Dennis, Chris How, and Bex McKay (my extended family) for moral support and keeping me sane over all these years, without whom things would be a whole lot less fun.

I would finally like to thank my parents for turning me in to a scientist from a ridiculously young age; turns out all those books on dinosaurs and how stuff works paid off in the end.... If only I learnt how to spell proper to.

Abstract

Papillomaviruses are small DNA viruses, which cause benign and malignant lesions in the differentiated epithelium of mammals and birds. A small subset of human papillomaviruses (HPV's), have been identified as the etiological agent of cervical cancer, with HPV 16 being found in over half of all cases. The HPV 16 E1^E4 protein is expressed late in the virus lifecycle. The protein can induce cell cycle arrest through an interaction with CyclinB/Cdk, and this is thought to facilitate viral genome amplification. E1^E4 can also associate with the cytokeratin network leading to its collapse, although this function is poorly understood.

The work described in this thesis shows that E1^E4s ability to bind to keratins is conserved amongst different members of the α HPV group, and to a lesser extent amongst members of the more distantly related γ-group. When expressed in SiHa cervical epithelial cells, 16 E1^E4 induced the collapse of affected keratin 8/18 network, and lead to the formation of Mallory body-like structures. Western blotting and immuno-precipitation revealed that the E1^E4/keratin association results in keratin phosphorylation and ubiquitination. 16 E1^E4 increases in abundance towards the epithelial surface, and coincides with keratin disruption in the upper epithelial layers. Immuno-fluorescence and biochemical analysis of HPV 2 and 16 lesions support the idea that keratin phosphorylation and ubiquitination may also occur *in vivo*. An effect of 16 E1^E4 on keratin dynamics was apparent when YFP-16E1^E4 was followed in monolayer cells by time-lapse microscopy. Although filament polymerisation and migration are not necessarily disrupted by 16 E1^E4, it appears that the progressive accumulation of E1^E4 can lead to filament stabilization, and eventually to keratin network disruption.

Contents

Figure Index

Abbreviations

Amp	Ampicillin
APS	Ammonium persulphate
APES	Aminopropyltriethoxysilane
AVP	Adenovirus protease
β-Gal	β-galactosidase
BPV	Bovine papillomavirus
BSA	Bovine serum albumin
CCE	Cornified cell envelope
cdc	cell division cycle
CDK	Cyclin dependant kinase
CFP	Cyan fluorescent protein
CIN	Cervical intraepithelial neoplasia
COPV	Canine oral papillomavirus
CPE	Cytopathic effect
CRPV	Cottontail rabbit papillomavirus
DAPI	4',6-diamidino-2-phenylindole
DMBA	Dimethylbenz(α)anthracene
DMEM	Dulbecco's modified Eagle's medium
DMSO	Dimethyl sulfoxide
DMP	Dimethylpimelimidate
DNA	Deoxyribonucleic acid
dNTPs	Deoxyribonucleoside triphosphates
dsDNA	Double-stranded deoxyribonucleic acid
DTT	Dithiothreitol
ECFP	Enhanced cyan fluorescent protein
ECL	Enhanced chemiluminescence
E.coli	*Escherichia coli*
E4-DBP	E4-DEAD box binding protein
EDTA	Ethylenediaminetetraacetic acid
EGF	Epidermal growth factor
EGFP	Enhanced green fluorescent protein
Em	emissions
EM	Electron microscopy
EtBr	Ethidium bromide
ETOH	Ethanol
EV	Epidermodysplasia verruciformis
Ex	Excitation
EYFP	Enhanced yellow fluorescent protein
FRAP	Fluorescence recovery after photobleaching
FAB	Fragment antibody
FCS	Foetal calf serum
GFP	Green fluorescent protein
GST	Glutathione S-transferase
H and E	Haematoxylin and eosin
HCMV	Human cytomegalovirus
HIV	Human immunodeficiency virus
HPV	Human papillomavirus

h	Hours
HRP	Horseradish peroxidase
HSPGs	heparin sulphate proteoglycans
IF	Intermediate filament
ICTV	International Committee on Taxonomy of Viruses
Ig	Immunoglobulin
kb	Kilobase
kDa	Kilo Daltons
LCR	Long control region
MAPK	Mitogen-activated protein kinase
MBP	Maltose binding protein
MCM	Mini-chromosome maintenance
MeOH	Methanol
MHC	Major histocompatibility complex
mRNA	Messenger ribonucleic acid
MWCO	Molecular weight cut off
NaAc	Sodium acetate
NaCl	Sodium chloride
NIMR	National Institute for Medical Research
NLS	Nuclear localisation sequence
NZW	New Zealand white
ORC	Origin recognition complex
ori	Origin of replication
PBS	Phosphate buffered saline
PCNA	Proliferating cell nuclear antigen
PCR	Polymerase chain reaction
PEN	Penicillin
PDGF	Platelet-derived growth factor
PKA	Protein kinase A
PML	Promyelocytic leukaemia protein
PV	Papillomavirus
QLM	Quantitative laser module
RNA	Ribonucleic acid
rAd	Recombinant adenovirus
r.t.	Room temperature
SCC	Squamous cell carcinoma
SDS	Sodium dodecyl sulphate
STREP	Streptomycin
TAD	Transactivation domain
TEMED	N,N,N,N,-Tetramethylethylenediamine
TRAIL	Tumour necrosis factor-related apoptosis-inducing ligand
TRIS	Tris hydroxymethylaminomethane
URR	Upstream regulatory region
UV	Ultraviolet
VLP	Virus-like particle
YFP	Yellow fluorescent protein

1 Introduction

1.1 Viruses

1.1.1 Virus discovery

Viruses have been responsible for countless disease outbreaks thoughout human history. Epidemics of smallpox have killed countless millions; an outbreak of flu in1918 is estimated to have killed 40 million people worldwide. The concept of a pathogen was first thought up back in 1880 when Robert Koch and Louis Pasteur published their now famous germ theory. It wasn't until 1892 that Pasteur identified the agent responsible for rabies which he referred to as a virus (Latin for poison) (reviewed in (Mendelsohn, 2002). A few years later in 1892, Dmitri Iwanowski was able to demonstrate that extracts of diseased tobacco plants which passed through ceramic filterers smaller than any known bacteria, were able to transmit disease. The magnitude of Iwanowski's discovery was not made clear until 1898 when Martinus Beijerinick referred to tobacco mosaic virus as contanium vivum fluidium (soluble living germs), so identifying viruses as a distinct new form of pathogen (Fields, 2001).

1.1.2 What is a virus?

Viruses are obligate intracellular parasites and lack the ability to replicate independently, hence are not considered to be living organisms. A virus is a microscopic particle that contains nucleic acid wrapped in a protein coat. The nucleic acid can be single or double stranded RNA or DNA depending on the virus type. The protein coat is typically made from repeating units of proteins which assemble into capsids. Viruses infect host cells where they unpackage their genetic material and hijack the cells transcriptional and translational machinery in order to replicate and package more viral genomes which are released as new virions.

1.1.3 Papillomaviruses

In 1907 it was discovered that common warts could be transmitted by cell free filtrates thus identifying the infectious agent as a virus (Ciuffo, 1907). Since then much has been learnt about papillomaviruses. Papillomaviruses consist of a large family of non-enveloped double stranded DNA viruses, with genomes of approximately 8 kb in size. Papillomavirus infections have been found in a wide variety of higher vertebrates, causing benign and malignant lesions of the epithelium (reviewed in (Doorbar, 2006; Laimins, 1996; Zur Hausen, 1996). Despite many variations, papillomaviruses all share a few key similarities. Papillomaviruses are highly tissue and host specific, virus lifecycle completion requires differentiating epithelium, viruses also share a common genome organisation and protein expression sequence.

The first papillomavirus to be identified in animals was the cotton tail rabbit papillomavirus (CRPV) identified in 1933 (Shope, 1933). Since then papillomaviruses have been identified in a wide variety of animals including ungulates(Koller *et al.*, 1971; Koller *et al.*, 1972), cats, dogs (Chambers *et al.*, 1959) and cetaceans (Lambertsen *et al.*, 1987; Van Bressem *et al.*, 1999a; Van Bressem *et al.*, 1999b). More recently papilloma viruses have been identified in a few species of birds (O'Banion *et al.*, 1992; Tachezy *et al.*, 2002). To date over 100 human papillomaviruses (HPVs) have been identified (reviewed in (de Villiers *et al.*, 2004). Although papillomaviruses have been identified in a wide variety of animal PVs show a high degree of species specificity and lack the ability to complete a productive life cycle when cross species infections occasionally occur (Howley, 1996).

1.1.4 Classification of papillomaviruses

Papillomaviruses were first classified according to the location and the pathology of the lesions they induced. As more research was done and new viruses discovered, classification switched to techniques based on the nucleotide sequence homology of the highly conserved genes E1, E6 and L1 (Chan *et al.*, 1992; Chan *et al.*, 1995b). Since then there have been several reworkings of the classification system (Villiers de, 2001). The currents classification system recognised by the international committee on the taxonomy of viruses states, that for papillomaviruses to be described as from the same genera they must share >60% identity in their L1 ORF. Isolates that are to be described as from the same species must share between 60-70 % L1 sequence homology. Isolates described as PV types, must have 71-89 % conservation within the L1 sequence. Viruses with 2-10 % sequence variation can be called subtypes whereas isolates with L1 sequence variations of less that 2 % can be defined as variants (de Villiers *et al.*, 2004). For the current papillomaviridae phylogenetic tree see (Fig 1.1)

Phylogenetically grouped viruses tend to share evolutionary related hosts (α papillomaviruses infect primates, δ papillomaviruses infect ungulates). The current papilloma taxonomy does however have its limitations. Phylogenetically grouped viruses can have very divergent characteristics and do not necessarily share tissue tropism, lesion morphology or risk of neoplastic progression.

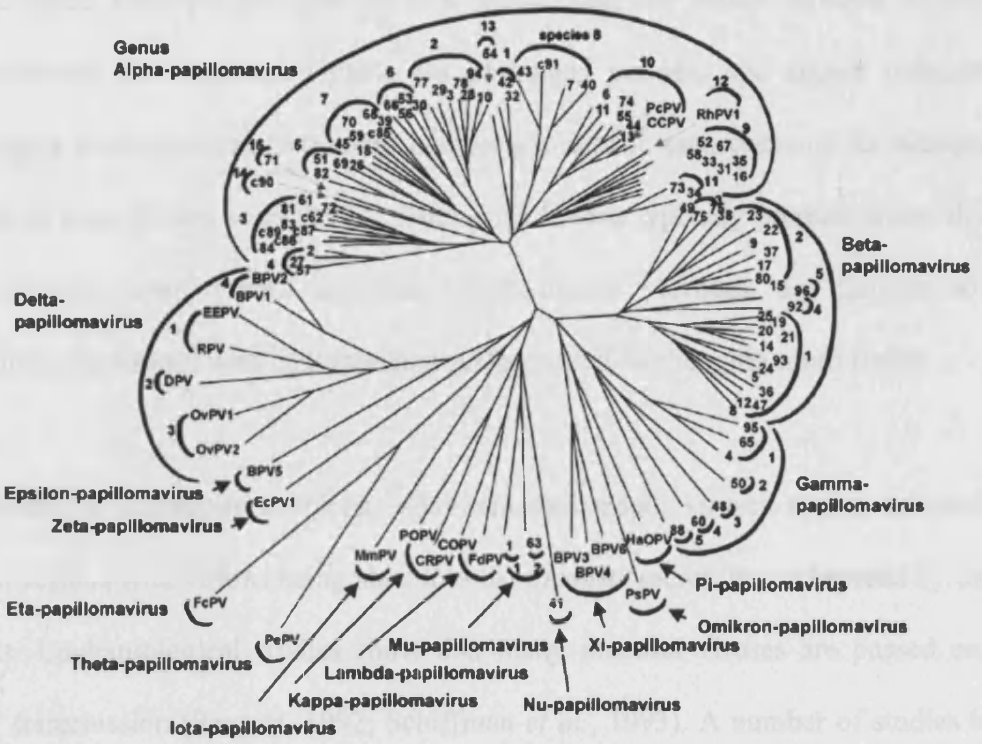

Figure1.1The papillomavirus phylogenetic tree
Figure shows the current papillomaviridae phylogenetic tree and contains sequences of 118 papillomavirus types. L1 ORF sequences were analyzed and used to construct the tree. The numbers at the ends of each branch identify an HPV type. C-numbers refer to candidate HPV types. All other abbreviations refer to animal papillomavirus types. The outer most semicircular symbols identify papillomavirus genera e.g. the genus alpha-papillomaviruses. The numbers in the inner circles refer to papillomavirus species. Image taken from (de Villiers et al., 2004).

1.1.5 Papillomavirus transmission

Productive papillomavirus lesions shed newly formed virions into the environment. Unlike blood born viruses such as HIV which degrade within minutes in hostile environments, PV virions are stable for prolonged periods, and appear resistant to desiccation allowing them to remain infectious in hostile environments for substantial periods of time (Roden *et al.*, 1997). Cutaneous lesions typically produce more virions than mucosal types. HPV2 infection which causes verrucas, are thought to be transmitted by contact with contaminated surfaces such as changing room floors.

In contrast to cutaneous subtypes, some mucosal tropic viruses appear to produce smaller lesions with virions being shed into the mucosal secretions and spread by direct contact. Epidemiological studies show that many mucosal viruses are passed on by sexual transmission (Sargent, 1992; Schiffman *et al.*, 1993). A number of studies have been able to find a direct correlation between the prevalence of infection and the number of sexual partners (Frega *et al.*, 2003). Some genital HPV types are rarely detected in people before they become sexually active (a fact which may cause controversy when targeting a future HPV vaccine).

Genital contact can lead to infection of oral mucosa by anogenital tropic HPV's (Panici *et al.*, 1992). Recent studies have revealed an increase in the prevalence of HPV-induced oral carcinomas that may be linked to changing sexual behaviour (Kreimer *et al.*, 2004). In addition to this, genital infections can be passed from mother to child during labour causing laryngeal infections. The appearance of genital lesions in non sexually active individuals suggests non-sexual transmission is also possible (Dunne *et al.*, 2005; Frega *et al.*, 2003; Handley *et al.*, 1993).

Some viruses cause large lesions which produce a large number of virions, and can regress in a matter of months, which suggests a burst-like strategy of transmission. In contrast many sexually transmitted mucosal viruses cause inapparent infections that persist for years.

1.1.6 Papillomavirus infection

Papillomaviruses are thought to infect mitotically active cells in the basal compartment of the epithelium with viruses gaining access to these cells through micro-wounds in the skin. The α6 integrin receptor has been proposed as a candidate for virion cell recognition (Evander *et al.*, 1997). Subsequent studies have revealed that neither HPV11 nor BPV viruses like particles (VLPs) require α6 integrin to bind cells (Joyce *et al.*, 1999; Sibbet *et al.*, 2000). More recent work has suggested that heparin sulphate proteoglycans (HSPGs) are required for PV infection (Bousarghin *et al.*, 2005; Giroglou *et al.*, 2001a).

HSPGs are found on the surface of most cells as well as in the extracellular matrix (Oksala *et al.*, 1995). The HSPG, syndecan-1, has been identified as a candidate receptor for HPV infections *in vivo* (Shafti-Keramat *et al.*, 2003). Furthermore, studies have shown that lactoferrin is able to inhibit HPV16 VLPs from entering cells. Lactoferrin is found in many bodily secretions and is known to inhibit herpesvirus and poliovirus from infecting cells by blocking heparin sulphate (Drobni *et al.*, 2004). Conflicting studies have confirmed that heparin sulphate is required for the infection of many cell lines, but are not required for the infection of natural host cells (keratinocytes) (Patterson *et al.*, 2005). A new as yet unidentified receptor component uniquely secreted into the basal extracellular matrix by keratinocytes which can facilitate infections that cannot be inhibited by heparin has recently been identified

(Culp *et al.*, 2006). The study also suggested that heparins sulphate binding may attach virions into wounds and that virus then use this second receptor to identify target cells.

After binding to cells it is thought that the papillomavirus can be endocytosed by a clathrin dependent pathway (Day *et al.*, 2003). This work was further supported by the finding that chlorpromazine, an inhibitor of the clathrin pathway was able to inhibit internalisation of both BPV and HPV16 VLPs. Interestingly the half-life of adsorption was found to be 4 h, verses 5-15 min for a typical ligand (Day *et al.*, 2003). These finding were confirmed in a second study which suggested that papillomaviruses infection is a slow process and remains susceptible to neutralisation hours after adsorption (Culp *et al.*, 2004). Mechanisms down stream of virus endocytosis may also be involved in tissue tropism. The virions lacking the L2 protein are 100 times less infectious (Holmgren *et al.*, 2005). L2 is required for egress of papillomavirus genomes from endosomes (Kamper *et al.*, 2006) and transport of the viral genome into the nucleus (Yang *et al.*, 2003b). These findings suggest that papillomavirus tissue specificity may be regulated at multiple levels including binding, entering and intracellular transport.

1.2 Site of infection

All papillomaviruses cause infections of mucosal and/or cutaneous epithelium. The skin is composed of three separate layers: the hypodermis, the dermis and the epidermis. The hypodermis is the lowest layer made of adipose and connective tissue and also contains the skins vascular infrastructure. The dermis is the principal mechanical barrier of the skin and contains smooth muscle, neurons and a network of elastic fibres that give the skin its elasticity. The epidermis (a type of epithelium) is the outer most layer of the skin and is composed of keratinised, stratified squamous epithelium. Skin epithelia can

be divided into two types, cutaneous and mucosal. Cutaneous epithelium covers most of the human body and forms a tough barrier against external insult and desiccation. Mucosal epithelium covers oral, anal and genital sites; and is moist with less mechanical strength (Alberts, 2002).

1.2.1 The epithelium

The epithelium is composed of several cell types, the principal of these being keratinocytes. In addition to these, dendritic cells are also present and are responsible for immuno-surveillance of the skin. Cutaneous epidermis also contains melanocytes which are involved in pigment production. The epidermis forms a protective barrier that is continually replacing itself as dead cells slough off from the surface. As cells move through the epithelium they undergo a process of differentiation, changing in morphology, protein expression and function (Fig 1.2). The basal layer is one cell thick and contains mitotically active cells continually producing daughter cells to replace those shed from the surface (Walker *et al.*, 2003). Basal cells are anchored to the basal lamina by hemi-desmosomal connections. Keratinocytes in the basal layer express a simple keratin 5 and 14 network (see Chapter 4 for further information).

The parabasal layer, also referred to in cutaneous epithelium as the spinous layer is defined as the first cell layer above the basal layer. Parabasal cells contain a mixed population of cells some maintaining expression of basal keratin with others expressing differentiation-specific keratins 1/10 (cutaneous) and 4/13 (mucosal) networks. Cells also begin to adhere to each other more tightly by up-regulating cadherins and integrins responsible for cell-cell adhesion junctions (Garrod, 2004; Nakano *et al.*, 2005). Cells in cutaneous epithelium undergo terminal differentiation to form the granular layer so called because of the presence of keratohyalin granules (Swanbeck *et al.*, 1965).

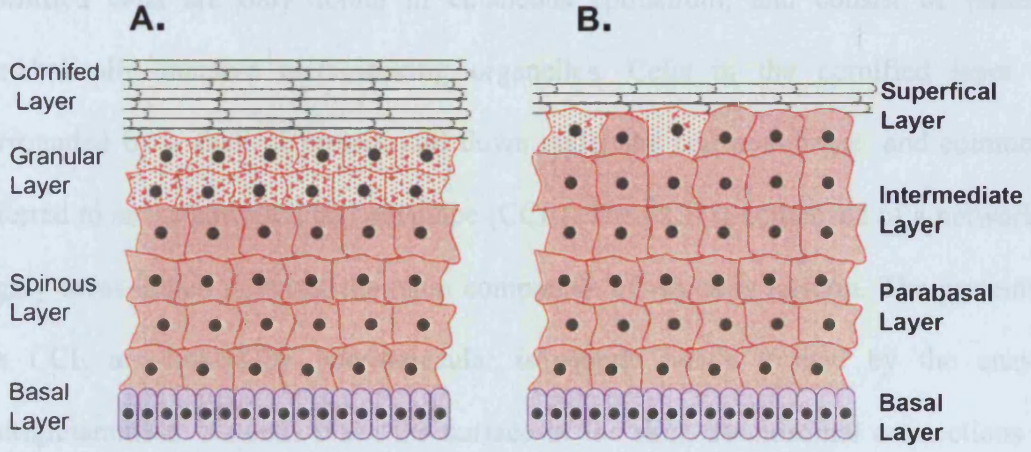

Figure 1.2 The organisation of squamous epithelial tissue
Two distinct types of epithelial tissue exist referred to mucosal and cutaneous epithelium. The basal layer of epithelium consists of largely undifferentiated mitotically active cells. In cutaneous epithelium (A) cells of the spinous layer become progressively less mitotically active and increasingly robust as they up-regulate desmosomal connections and keratin expression. The granular layer is only a few cells thick and acquired its name due to the presence of keratohyalin granules which contain loricrin and profilaggrin (the filaggrin precursor). The upper cornified layers are composed of dead cells surrounded by a cornified envelope and have lost intracellular organelles. In mucosal tissue (B) the layers are referred to as the parabasal, intermediate and superficial layers. Mucosal tissue organisation is similar but lacks granular cells, a cornified layer is generally much thinner. Mucosal epithelium is moist and is not required to protect the underlying tissue from desiccation.

Keratohyalin granules contain filaggrin precursors and loricrin. Filaggrin is a keratin associated protein that cross-links keratin filaments to form thick fibres increasing their resistance to mechanical stress (Lynley *et al.*, 1983).

Cornified cells are only found in cutaneous epithelium, and consist of flattened metabolically inactive cells lacking organelles. Cells in the cornified layer are surrounded by a shell of protein laid down under the cell membrane, and commonly referred to as the cornified cell envelope (CCE). The CCE is composed of a network of highly cross-linked proteins, the main component of which is loricrin. The proteins in the CCE are linked by intermolecular isopeptide bonds formed by the enzyme transglutaminase. As cells reach the surface of the skin, desmosomal connections are lost and dead cells slough off into the environment (Fuche *et al.*, 1994).

1.3 Papillomavirus related pathologies

Papillomaviruses are known to cause a wide variety of epithelial lesions in humans and animals. The lesions vary in severity from inapparent flat warts to the large horn like structures caused by cotton tail rabbit papillomavirus (CRPV). Papilloma related pathologies are further complicated by the ability of some PV infections to induce malignancies (Fig 1.3).

1.3.1 Animal papillomas

A recent attempt to find more by a group in Sweden involved a trip to the local zoo. Armed with skin swabs, the group managed to identify 53 new putative animal papillomaviruses in healthy animals (Antonsson *et al.*, 2002). It has recently been suggested that most mammals may harbour papillomaviruses although not all infections result in visible lesions (de Villiers *et al.*, 2004). These sections will discuss

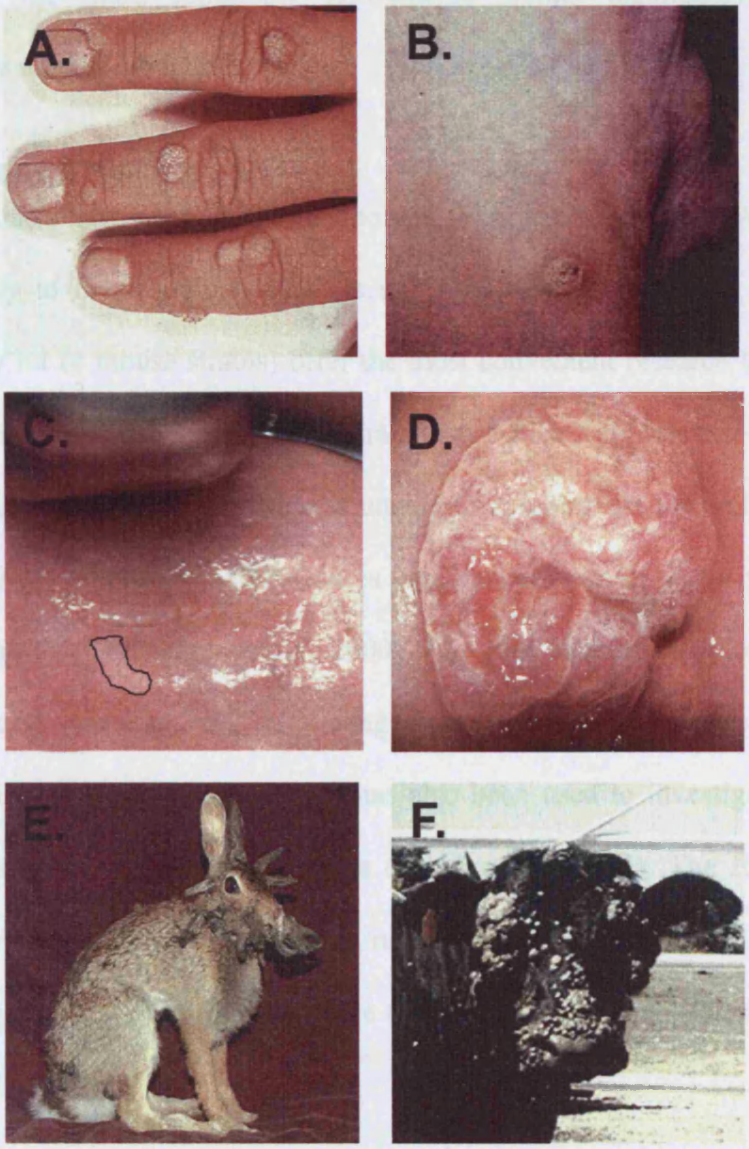

Figure 1.3 The papillomavirus causes a variety of lesions with varying pathologies in many different vertebrates
Image A shows HPV 2 induced flat wart of the hand, (B) shows an HPV 1 induced lesions of the foot (B.). (C) HPV 16 causes an inapparent flat wart of the cervix, such lesion can spontaneously regress but can also progress into cervical cancers (D) (images taken from (Gross and Barrasso, 1997). Papillomaviruses can infect a variety of different animal, some of which cause debilitating lesions such as cottontail rabbit papillomavirus (CRPV) (E)(image taken from (www.lafayette.edu/~hollidac/jacksforreal.html). (F) Bovine papillomaviruses (BPV's) can cause a variety of lesions in cattle (BPV2 pictured) some of which can result in epithelial malignancies (image taken from www.duke.usask.ca/-misra/virolgy/stud/2002/wart/spesies.html).

some of the more commonly encountered animal papillomaviruses which are commonly used as laboratory models.

1.3.2 Rabbit models

Rabbit models have been invaluable tools in the study of papillomaviruses. Rabbits are small, easy to breed animals that (as no papillomavirus have yet been identified in laboratory rat or mouse strains) offer the most convenient research tool. CRPV causes large horn-like structures in its natural host, which can regress, persist or induce malignancies (*see* Fig 1.3). CRPV is unable to complete its lifecycle in New Zealand white (NZW) rabbits and often causes carcinomas representing a valuable model of carcinogenesis (Christensen *et al.*, 2000). The link between papilloma infections and malignancies was made in CRPV long before the association was made in humans (reviewed in (Campo, 2002). CRPV has also been used to investigate the role of the immune system in clearing infections (Hopfl *et al.*, 1995). The first papillomavirus vaccine trials were also conducted on rabbits and demonstrated that both prophylactic and therapeutic vaccines may be viable (Breitburd *et al.*, 1995; Leachman *et al.*, 2000; Xiao *et al.*, 1996).

1.3.3 Bovine models

To date several BPVs have been identified belonging to two distinct branches of the papillomavirus phylogenetic tree. BPV 1 and 2 cause cutaneous and penile warts in cattle that can become so severe that infected animals have to be destroyed (*see* Fig 1.3). Interestingly BPV1 & 2 can cause abortive infections in horses, deer, mules and hamsters which can result in sarcoid carcinomas (Koller *et al.*, 1972; Lancaster *et al.*, 1977). The BPV-1 model has been used to identify some of the functions of papilloma virus proteins and their interactions with the host cell (Band *et al.*, 1993; Campo, 2002; Day *et al.*, 2003; Ham *et al.*, 1991; Ustav *et al.*, 1991).

BPV4 causes lesions of the oral mucosa with the potential to induce malignancies. A high incidence of cancer in cattle grazing on bracken ferns was first noticed in the late 1970's (Jarrett, 1980). It has since been demonstrated that brackens contain immunosuppressant and carcinogenic compounds which can cause malignancies in BPV 4 infected cattle (Campo *et al.*, 1992). The same phenomenon has been observed in humans, with mucosal HPV infection developing into carcinomas of the oesophagus after consuming bracken (Nagao *et al.*, 1989). BPV 4 were used extensively in the early development of papillomavirus vaccines (Campo *et al.*, 1993; Campo *et al.*, 1994)

1.4 Pathologies associated with human papillomavirus infections

1.4.1 Cutaneous pathologies in humans

To date over 100 complete HPVs genomes have been sequenced and several hundred more putative sequences identified (de Villiers *et al.*, 2004). The majority of papilloma infections are asymptomatic with dozens of papilloma DNA sequences showing up in the skin of healthy individuals (Antonsson *et al.*, 2000). This finding suggests that papillomaviruses are a part of the natural floral and fauna of human skin. Some papillomaviruses are known to be responsible for a number of clinically significant conditions. HPV1 are frequently associated with common warts of cutaneous epithelium found on the hands (Fig 1.3). HPV6 and 11 are the causative agent of genital warts (Walboomers *et al.*, 1999). HPV 2 cause deep plantar warts (verrucas) of the foot (Fig 1.3). Most HPV infections will spontaneously regress after a few months although HPV DNA can commonly be detected long after the lesion has disappeared (Hsu *et al.*, 2003; Sarian *et al.*, 2005; Schiffman *et al.*, 2002).

1.4.2 Epidermodysplasia verruciformis

Despite the connection between animal papilloma infections and cancer having been known about for several years it wasn't until the late 1970s that the link between HPV

and human cancers was discovered (Jablonska *et al.*, 1978; Orth *et al.*, 1977). The discovery was made in patients with the rare genetic condition epidermodysplasia verruciformis (EV) (Jablonska *et al.*, 1978; Lutzner *et al.*, 1980). EV patients have an increased susceptibility to papilloma infections and suffer from flat scaly warts and pigmented macula like lesions caused by HPV 5 and 8. Sun exposed EV lesions undergo neoplastic progression to non-melanoma skin cancer in approximately 50% of EV patients (Jablonska *et al.*, 1994). EV type HPV DNA has also been found in non-myeloma skin cancers of non EV patients, although the role of HPV infections in these cancers is currently uncertain. There is some limited evidence linking HPV 5 and 8 infections with psoriasis, although the role of the virus in this inflammatory skin condition is at present unclear (Favre *et al.*, 1998; Wolf *et al.*, 2004).

1.4.3 Mucosal Cancers

Cervical cancer is the second most prevalent cancer in women globally and is responsible for ~275,000 deaths annually (Ferlay *et al.*, 2001; Parkin *et al.*, 2005). A sub-set of papilloma viruses which infect mucosal epithelium and cause inapparent flat warts (Fig 1.3), and which are commonly referred to as the high risk papillomaviruses are the etiological agent of cervical cancer (Munoz *et al.*, 1994; Walboomers *et al.*, 1999). The most common is HPV 16, which is detected in over 50% of cases (Munoz *et al.*, 2003). Other high risk papillomaviruses commonly found in mucosal cancers (including oral and anal sites) include HPV 18, 31, 33, 35 and 42. As well as causing cervical cancers, high-risk papillomavirus DNA has been found in cancer of the oral mucosa (Kreimer *et al.*, 2004; Kundu *et al.*, 1995)

1.5 Papillomavirus models

The papillomaviruses require differentiated epithelium for productive infections. This makes the virus challenging to study in the laboratory. Over the years many different systems have been used to study various aspects of the virus lifecycle.

1.5.1 Monolayer cell culture

Unlike human immunodeficiency virus (HIV) and influenza, to date papillomavirus have not been made to replicate successfully inside monolayer cell culture systems. Despite this, such systems are an invaluable tool and are commonly used to study the function of individual viral proteins. The effect of viral proteins on host cell mechanisms such as the cell cycle has revealed a huge amount in recent years and allowed the identification of possible therapeutic targets for future drugs. Draw-backs of such experiments are that proteins expressed in such systems are not under endogenous promoter control and are commonly over-expressed, which may result in the reporting of interactions which do not occur *in vivo*.

1.5.2 Epithelial raft cultures

Epithelial raft cultures can be produced by seeding HPV-infected keratinocytes onto a fibroblast containing medium such as a collagen gel. The keratinocytes are grown at a liquid air interface where they undergo differentiation. Such systems require medium containing specific growth factors, serum and high calcium. The medium is absorbed though the tissue via capillary action producing a gradient which causes the keratinocytes to differentiate, (Chow *et al.*, 1997; Flores *et al.*, 1999). Raft cultures are technically demanding and hard to establish, but are currently the method of choice for the study of HPV lifecycle. It is possible to produce fully differentiated tissue, complete with cornified layer, in the laboratory. Such systems will support productive papilloma infections including virion production and release (Flores *et al.*, 1999). A major

advantage of such systems is the ability to study human rather than animal viruses. Cells containing mutant genomes can also be cultured in this system, allowing the role of individual or mutant proteins to be assessed with regards to the virus lifecycle (Dollard *et al.*, 1992; Steenbergen *et al.*, 1998; Wilson *et al.*, 2005). The major draw back of raft cultures is that the tissues lack an immune system so cannot be used in studies interested in the resolution of infection.

1.5.3 Xenographs

The species specificity of papilloma virus infections means that viruses will only produce productive infections in the correct tissue of their natural hosts. This fact makes the study of HPV infections very challenging as deliberately infecting humans with pathogens is ethically unacceptable. The discovery of two strains of immuno-compromised mice incapable of rejecting xenotransplants, provided a new model for use in papillomavirus research. Experiments in athymic (nude) mice showed that HPV11 infected human foreskin and cervical tissue grafted under the kidney capsule, were capable of supporting productive viral infections (Bryan *et al.*, 2001; Kreider *et al.*, 1986; Stoler *et al.*, 1990). Experiments that involved challenging skin from different areas of the human body to determine the tissue tropism of HPV 11, were conducted using the kidney capsule model (Kreider *et al.*, 1987), which was later used with foetal skin to study HPV 1 infections (Kreider *et al.*, 1990). Severe combined immunodeficiency mice SCID (Bosma *et al.*, 1983) suffer from a defective adaptive immune system, and are also capable of supporting human tissue grafts (Renz *et al.*, 1996). These provide another valuable model for the study of HPV infections. SCID mice have been shown to be capable of supporting productive high risk HPV infections such as with HPV16 that has been introduced into the animal by grafting infected foreskin keratinocytes onto the backs of the mice. Infections in SCID mice are

morphologically comparable to naturally occurring infections and produce correctly packaged infectious virions (Bonnez *et al.*, 1993; Brandsma *et al.*, 1995).

1.5.4 Clinical samples

Clinical samples are ultimately the most important source of data on HPV infections, as they are caused by the viruses of interest in their natural hosts (Humans). Despite this due to ethical and legal barriers, researchers in the United Kingdom struggle to gather samples of interest, and usually can only access material collected from patients having problematic lesions surgically removed. Many lesions are left to regress naturally or treated with topical agents such as salicylic acid or imiquimod (Micali *et al.*, 2004). As such most of what is known about high risk viruses like HPV 16, comes from CIN lesions where the virus life cycle has already begun to fail (Middleton *et al.*, 2003). It may well be that these viruses favour foreskin over cervical sites but as such lesions are not of medical significance and are difficult to obtain for study. Another limitation is that human infections cannot be artificially manipulated by researchers, so cannot be used in knock out or mutant studies.

1.5.5 Animal models

Animal models offer another source of valuable information as they can be used to study papilloma infections in their natural hosts. Animal models have been used to study latency and regression of papilloma lesions as well as the role played by the host immune system in resolving infections. None of the other laboratory systems offers these possibilities, and as a result of this animal models have played an invaluable role in the development of papillomavirus vaccines (Campo, 2002).

1.6 Overview of Papillomavirus lifecycle

The papillomavirus replication depends on finding the correct type of differentiating epithelium tissue in a permissible host for completion of its productive lifecycle. An

infection begins when a virus particle gains access to mitotically active cells in the basal layer of the epithelium (Egawa, 2003). Once inside a suitable host cell the genome is uncoated and the virus genome appears to undergo an initial round of replication in the nucleus with infected cells containing between 10-200 copies of the viral DNA (De Geest *et al.*, 1993). It is presumed that the expression of the early proteins E1 & E2 are required for this to occur although expression levels are such that no viral protein can be detected in basal cells (Ozbun *et al.*, 1998b; Wilson *et al.*, 2002). Expression of the E6 and E7 proteins then cause infected cells to undergo several rounds of replication to produce a pool of infected cells capable of viral production (reviewed in(Doorbar, 2006). The E6 & E7 proteins override barriers to, and apoptosis associated with unsanctioned cell cycle entry, by interacting with cellular checkpoint proteins including RB and p53 (Dyson *et al.*, 1989; Scheffner *et al.*, 1990; Werness *et al.*, 1990). The viral genome then undergoes a second round of replications to produce multiple copies of the viral genome for packaging. All the early proteins including E1^E4 and E5 are believed to be required for genome amplification (Fehrmann *et al.*, 2003; Peh *et al.*, 2004). L1 and L2 capsid proteins are expressed after genome amplification allowing assembly of virions (Ozbun *et al.*, 1998a). Newly formed virus particles then shed from the surface of the epithelium as terminally differentiated cells slough off (Fig 1.4).

1.6.1 Papillomavirus virions

Papillomavirus virions are non enveloped structures approximately 55nm in diameter (Kirnbauer *et al.*, 1992). The virion contains a single circular double stranded histone bound DNA molecule. The viral genome is contained within a protein capsid composed of the viral proteins L1 and L2 with a stoichiometry of 1:5

(Belnap *et al.*, 1996). The proteins associate into 72 rosette-like capsomeres, which

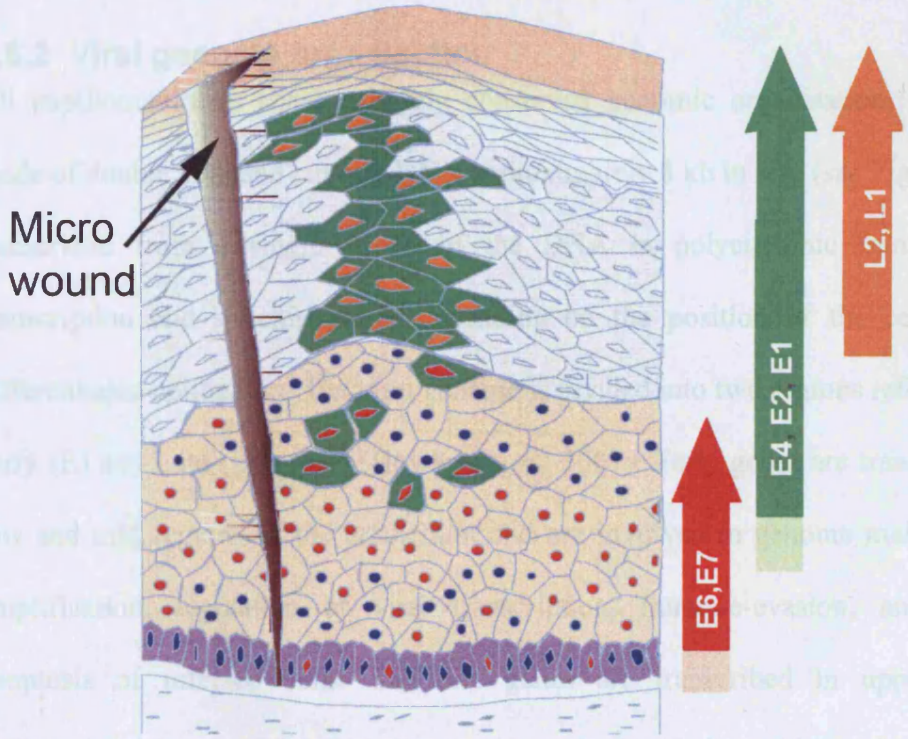

Figure 1.4 The papillomavirus lifecycle
The papillomavirus lifecycle begins when viruses infect cells of the basal layer, which they are though to do through a micro wound in the skin. The virus begins to express E1 and E2 which are involved in an initial burst of viral genome amplification. Expression of the E6 and E7 proteins induce proliferation of infected cells and increase the number of cell that can be used to produce progeny virions. Higher in the epithelium E1, E2 and E1^E4 levels increase allowing viral genome amplification to occur. The viral capsid proteins L1 and L2 are expressed towards the surface of the epithelium after genome amplification, allowing packaging of genomes. Newly formed infectious virions are though to be shed from the surface of the epithelium as terminally differentiated cells slough off into the environment.

self-assemble into an icosahedral shaped protein coat (Howley *et al.*, 2001; Zur Hausen, 1996)

1.6.2 Viral genome organisation

All papillomaviruses share a highly conserved genomic organisation. Genomes are made of double stranded circular DNA approximately 8 kb in size (*see* Fig 1.5). RNA is transcribed from a single strand of the DNA in polycistronic transcripts. RNA transcription and splicing varies depending on the position of the cell within the differentiated epithelium. The viral genome is divided into two regions referred to as the early (E) and Late (L) genes (Howley *et al.*, 2001). Early genes are transcribed in the low and mid regions of the epithelium and are involved in genome maintenance and amplification, regulation of viral transcription, immune-evasion, and preventing apoptosis of infected cells. The late genes are transcribed in upper terminally differentiated layers of the epithelium and encode the viral capsid proteins (reviewed in (Doorbar, 2005; O'Brien *et al.*, 2002). The viral genome also contains a non-coding region sandwiched between the L1 and E6 ORF's, referred to as the long control region (LCR), or the upstream regulatory region (URR). The LCR contains sequences involved in transcriptional regulation including binding sites of viral transcription factors such as the viral protein E2 (Dong *et al.*, 1999; Spalholz *et al.*, 1985; Spalholz *et al.*, 1988). The LCR also contains the viral origin of replication (ORI) and has binding sites for the viral replication initiator E1 as well as several cellular proteins (Frattini *et al.*, 1994; Waldeck *et al.*, 1984). Viral LCR's vary in length and may play a role in the tissue selectivity of some papillomaviruses (Sailaja *et al.*, 1999). Experiments have also been able to demonstrate the transcriptional activity of transcription factors present in keratinocytes but not fibroblasts, supporting the hypothesis that events down stream of viral adsorption are responsible for tissue selectivity (Offord *et al.*, 1990).

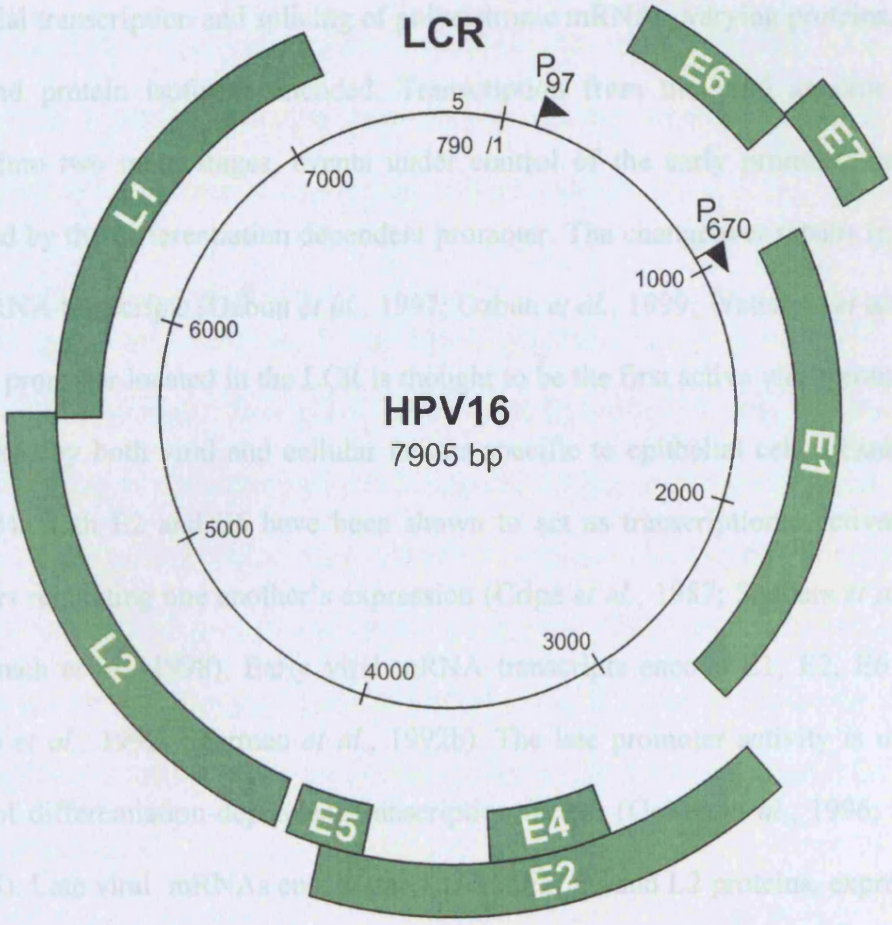

Figure 1.5 The HPV 16 Genome
The HPV 16 genome consists of a molecule of double stranded DNA approximately 8kb in size. Eight genes are encoded and are located on the same strand, in some cases, open reading frames partially overlap. The genome contains two main promoters the early promoter P97, and the late promoter P 670. The LCR is a non coding region and contains sequences involved in the regulation of viral gene transcription.

1.6.3 Control of viral genome transcription

Control of viral protein expression is regulated by several mechanisms these include differential transcription and splicing of polycistronic mRNAs, varying proteins, protein levels and protein isoforms encoded. Transcription from the viral genome can be divided into two main stages, events under control of the early promoter and those controlled by the differentiation dependent promoter. The changeover results in a major shift in RNA transcripts (Ozbun *et al.*, 1997; Ozbun *et al.*, 1999; Wettstein *et al.*, 1987). The P97 promoter located in the LCR is thought to be the first active viral promoter and is regulated by both viral and cellular factors specific to epithelial cells (Taniguchi *et al.*, 1993). Both E2 and E6 have been shown to act as transcriptional activators and repressors regulating one another's expression (Cripe *et al.*, 1987; Sanders *et al.*, 1994; Stubenrauch *et al.*, 1998). Early viral mRNA transcripts encode E1, E2, E6 and E7 (Higgins *et al.*, 1992; Sherman *et al.*, 1992b). The late promoter activity is under the control of differentiation-dependent transcription factors (Geisen *et al.*, 1996; Spink *et al.*, 2005). Late viral mRNAs encode the E1^E4, E5, L1 and L2 proteins, expression of which is heavily influenced by differential splicing of transcripts (Barksdale *et al.*, 1995; Danos *et al.*, 1985; Doorbar *et al.*, 1990a; Hummel *et al.*, 1995; Sherman *et al.*, 1992a).

1.7 Papillomavirus proteins

Papillomaviruses express relatively few proteins (usually 8 although isoforms increase this), with expression profiles following a differentiation-dependent sequence. Recent research suggests that L1, L2, E1 and E2 are the core ancestral proteins with the other viral proteins being acquired at different stages from different sources through history (Garcia-Vallve *et al.*, 2005). As well as controlling protein expression, protein functions is also believed to be modulated in a differentiation-dependent manner by multimerisation, phosphorylation, proteolyitic cleavage, altered cellular localisation and

the expression of splice variants (Grand *et al.*, 1989; Knight *et al.*, 2004; Vaeteewoottacharn *et al.*, 2005). This modulation allows single proteins to perform multiple functions at varying stages throughout the virus life cycle. The current understanding of papillomavirus proteins suggest that they are multifunctional, existing in a complex dynamic state of equilibrium with one another.

1.7.1 Early gene expression

The early genes are expressed in the basal, parabasal and mid layers of infected epithelium. Expression of these genes results in the forced proliferation of infected cells and the blocking of apoptotic pathways triggered by host cell responses. Early genes also regulate the transcription of viral and cellular genes, as well as the maintenance and replication of the viral genome (reviewed in (Doorbar, 2005). In addition to this early genes have been shown to play a role in immune evasion by down regulation and miss-localising cellular systems involved in immune surveillance (reviewed in (O'Brien *et al.*, 2002; Zhang *et al.*, 2003).

1.7.2 The Role of the E7 in the papillomavirus lifecycle

Papillomavirus genomes do not encode any polymerase enzymes and so viruses need to hijack the host cells replication machinery for viral genome replication to occur (Melendy *et al.*, 1995). The primary role of the E7 protein is to force quiescent cells back into cell cycle which increases the multiplicity of infected cells and allows viral genome amplification to occur at the required region of infected epithelium.

1.7.3 E7 overrides tumour suppressor pathways

Early work using the animal model system CRPV showed that the E7 gene is required for papilloma formation resulting from hyperproliferative growth of epithelium (Brandsma *et al.*, 1991). Expression of HPV 18 E7 has been shown to be necessary and sufficient to induce quiescent differentiated keratinocytes to re-enter the cell cycle in

raft culture, demonstrating the importance of E7 in perturbing differentiation of the inducible infected epithelium (Cheng *et al.*, 1995). Latter studies conducted in raft systems using HPV 16 E7 knockout genomes showed that E7 is required for virus genome amplification and late gene expression (Flores *et al.*, 2000). E7 mRNA transcripts and protein have been found in HPV 16 and 18 transformed cell lines and are believed to be required for the maintenance of the malignant phenotype (Smotkin *et al.*, 1986). E7 has since been shown to induce cell proliferation via an association with the tumour suppressor retinoblastoma protein (pRB) and in the case of E7s from high risk viruses this results in its degradation (Boyer *et al.*, 1996; Dyson *et al.*, 1989). A similar mechanism has also been reported to occur with the E1A SV40 protein (Chellappan *et al.*, 1992)

1.7.4 E7 and the retinoblastoma protein

E7 has been shown to associate with pRB causing the release of the transcription factor E2F resulting in initiation of S-Phase. Under normal circumstances pRB binds E2F but stimulation of mitogen activated pathways results in the phosphorylation of pRb by cyclin dependant kinases (CDK's) CDK4 and 6 leading to the release/activation of E2F (reviewed in (Dyson, 1998). Upon release E2F activates the transcription of genes required for S phase entry, including DNA polymerase α, thymidine kinase, minchromosome maintenance proteins (MCMs) and cyclins A and E (reviewed in (Herwig *et al.*, 1997). Antibodies against these proteins can be used as surrogate makers of E7 expression. E7 proteins from low risk viruses typically have a reduced in their affinity for pRb and a reduced ability to transform cells *in vivo* (Gage *et al.*, 1990; Heck *et al.*, 1992).

1.7.4.1 pRB independent effects of the E7 Protein

E7 has been demonstrated to override other pRB independent cell cycle inhibitor pathways by interacting with members of the pocket family of proteins p107 and p130. E7 associates with and induces transactivation of the AP1 transcription factors Fos and Jun (Antinore *et al.*, 1996). E7 proteins have also been shown to have the capacity to stimulate cell proliferation independently of pocket proteins by interacting with and deactivating the inhibitors of cyclins A, and E p21 and p27, which are capable of blocking PCNA mediated DNA replication (Funk *et al.*, 1997; Jones *et al.*, 1997). The ability of E7 to stimulate proliferation is supported by the finding that E2 can suppress HeLa cell growth by repressing the transcription of the constitutively active E6/E7 promoter (Nishimura *et al.*, 2000)

1.7.5 The role of the E6 protein

The main objective of the E6 protein appears to be to block apoptotic pathways activated in cell undergoing unsanctioned entrance into the cell cycle as result of the expression of E7, in order to allow viral genome replication to occur.

1.7.6 The E6 protein

The E6 protein is found in most PVs (with the exception of some ungulate and bird viruses). It is one of the two major transforming proteins and expression is maintained during neoplastic progression, E6 is expressed at low levels in during productive infections. Four different splice variants of the E6 protein are thought to exist (reviewed in (Myers, 1995) and are believed to play a role in modulating E6 function and E7 levels (Pim *et al.*, 1999; Smotkin *et al.*, 1989; Stacey *et al.*, 1995).

1.7.7 E6 prevents apoptosis by interacting with the tumour suppressor protein p53

All E6 proteins are believed to associate with and modulate the function of members of the p53 tumour suppressor protein family. p53 is a major cellular tumour suppressor

commonly referred to as the guardian of the genome, and triggers cell cycle arrest followed by apoptosis upon detection of defective or unsanctioned DNA replication (Lane, 1992). p53 acts as an upstream sensor protein and functions by modulating the transcription of other genes involved in tumour suppressor pathways (Hofseth *et al.*, 2004). E6 is able to modulate p53 activity by direct association and by inducing its degradation. Only E6 proteins from high risk viruses cause 26S -proteasome mediated degradation of p53 (Crook *et al.*, 1991; Li *et al.*, 1996; Pim *et al.*, 1994; Scheffner *et al.*, 1994).

1.7.8 E6 and the ubiquitin system

E6 has been shown to mediate p53 degradation via the E6 associated protein (E6-AP). E6-AP was found to be a member of the E3 ubiquitin ligase protein family, a domain in the C-terminus of the protein was later used to identify E3 activity in a number of seemingly unrelated proteins, now termed homologous E6AP C- terminus proteins (HECT's) (Huibregtse *et al.*, 1995). Ubiquitination is an essential cellular process affected by a multi-enzyme cascade involving classes of enzymes known as E1s (ubiquitin-activating enzymes), E2s (ubiquitin-conjugating enzymes / Ubcs), and E3s (ubiquitin-protein ligases) (Scheffner *et al.*, 1995). E6 acts as a bridging adaptor redirecting E6 AP to a substrate (p53) which under normal circumstances would have no affinity for it. This same adaptor mechanism of redirecting E3 ubiquitin ligases to target cellular proteins for degradation has since been identified in a number of other viruses including HIV and adenovirus (Margottin *et al.*, 1998; Querido *et al.*, 2001).

1.7.9 E6 can inhibit multiple apoptotic pathways

Alpha group HPV E6 proteins also have the ability to inhibit differentiation-dependent apoptosis induced by the Bcl-2 pro-death domain protein family (Magal *et al.*, 2005). As with p53, E6 has been shown to bind directly to the Bcl-2 member, Bak, resulting in

its degradation. This observation suggests that E6 proteins are able to inhibit multiple apoptotic pathways. Bak expression is abundant in normal differentiated epithelium but significantly reduced in HPV induced carcinomas. As with p53, E6 proteins from high risk viruses have an increased ability to promote ubiquitination and 26S proteasome mediated Bak degradation (Thomas *et al.*, 1999). Both p53 and Bak-induced apoptotic pathways would be activated in response to E7-induced cell proliferation; by deactivating these pathways the virus gains total control of the infected cell (Butz *et al.*, 2003; Horner *et al.*, 2004; Ilves *et al.*, 2003). Finding a novel way of knocking-out E6 activity allowing reactivation of p53 would be a very efficient way of treating HPV induced carcinomas (Cho *et al.*, 2002). This approach is currently under investigation using siRNA, peptides and intra body technology to target E6, and has been shown to induce apoptosis in the HPV transformed cell line (Griffin *et al.*, 2006; Putral *et al.*, 2005; Sterlinko Grm *et al.*, 2004).

1.7.10 The role of E6 in immune evasion

E6 has been shown to play a role in immune evasion through an ability to down regulate proteins involved in cell-cell adherens junctions. E-cadherin mediates calcium dependent cell-cell focal adhesions between keratinocytes and Langerhan cells (epithelial antigen presenting cells) (Tang *et al.*, 1993). Expression of E6 has been demonstrated to down regulate surface expression of E-cadherin. Loss of E-cadherin in turn results in decease in the number of Langerhan cells in lesions (Matthews *et al.*, 2003). Some evidence also suggests that loss of E-cadherin renders cell less susceptible to apoptosis (Ferreira *et al.*, 2005). The loss of E-cadherin also increases the risk of tumours invading the underlying tissue and has been observed in a number of cancers (Hirohashi, 1998; Oka *et al.*, 1992).

1.7.11 E6 proteins interact with and degrade PDZ domain proteins

Expression of E6 has been show to cause mislocalisation and induce proteasome mediated degradation of certain PDZ domain proteins (Kiyono *et al.*, 1997; Lee *et al.*, 2000). PDZ domains are involved in protein-protein interactions and are commonly found in trans-membrane receptors. PDZ proteins known to be affected by E6 include Dlg, MAGI 1-3 and MUPP1, which are believed to be involved in the regulation of cell growth and polarity (Gardiol *et al.*, 1999; Lee *et al.*, 2000; Thomas *et al.*, 2001). HPV genomes propagated in raft culture systems expressing mutant E6s unable to interact with PDZs show a reduction in viral genome copy number and in the growth of cells. Interestingly no change was detected in the expression level of PDZ domain proteins (Lee *et al.*, 2004).

1.7.12 The HPV E5 protein

E5 is a hydrophobic, membrane-bound protein, with weak transforming properties (DiMaio *et al.*, 2001; Horwitz *et al.*, 1988). E5 is primarily localised to the endoplasmic reticulum (ER) but can also be found in the Golgi apparatus and plasma membrane (Conrad *et al.*, 1993; Disbrow *et al.*, 2005). Despite sharing the same name and general hydrophobicity, E5 gene products vary greatly between different papillomaviruses groups (Garcia-Vallve *et al.*, 2005). Interestingly 4 different isoforms of E5 exist in A group viruses, with the α-isoform being found in all viruses associated with cervical cancer (Bravo *et al.*, 2004). The position of the E5 ORF within the genome also varies between viruses, suggesting that the virus may have acquired "E5" genes from different sources at different times throughout history (Garcia-Vallve *et al.*, 2005).

1.7.13 The functions of the E5 protein

The transforming properties of the E5 protein vary dramatically between viruses; the E5 protein of BPV1 is a true oncogene and serves as the major viral transforming protein

(DiMaio *et al.*, 1986). In contrast transformation of cells by HPV16 E5 requires the presence of E7 and expression of E5 is not maintained in HPV 16 transformed cancers. E5 is encoded in all polycistronic viral mRNA transcripts except those encoding the capsid proteins, suggesting it is required throughout the virus lifecycle (Baker *et al.*, 1996; Fehrmann *et al.*, 2003).

1.7.14 The role of E5 in immune evasion

Low levels of E5 expressed in the basal layer of infected epithelium are thought to enable the virus to shield infected cells from the immune-system. Immune evasion is thought to be achieved by reducing detection of infected cells from cytotoxic T lymphocyte (CTL)-mediated clearance by reducing surface expression of major histocompatibility class I complexes, HLA-A and HLA-B (Ashrafi *et al.*, 2002; Ashrafi *et al.*, 2005; Marchetti *et al.*, 2002; Zhang *et al.*, 2003). MHC proteins cycle to and from the cell surface allowing them to pick up/bind foreign (viral) antigens which can then be presented to the immune system. Infected cells displaying viral antigens on their surface alert the immune system to the presence of a pathogen and are stimulated to induce apoptosis by T-cells, thus preventing the spread of the infection. Viruses that establish long-term infections in their hosts have evolved a number of methods to interfere with MHC activities (Lilley *et al.*, 2005). The E5 protein has been shown to affect the maturation process of MHC proteins which are retained in the Golgi apparatus (Ashrafi *et al.*, 2005; Marchetti *et al.*, 2002).

1.7.15 The E5 protein plays a role in preventing apoptosis

The expression of the viral proteins E2 and E7 can promote apoptosis preventing the virus from completing its lifecycle. To combat this, the virus uses both E5 and E6 proteins. Upon discovery by the immune system, CTLs would force infected cells to undergo FAS and TRAIL (tumour necrosis related-factor apoptosis-inducing ligand)

mediated apoptosis. Studies have shown that expression of HPV 16 E5 desensitizes cells to these apoptotic pathways (Kabsch *et al.*, 2002b; Kabsch *et al.*, 2004). Interestingly HPV16 E5 was shown to sensitize cells to osmotic stress-induced apoptosis (Kabsch *et al.*, 2002a) which may aid virion release in mucosal infections.

1.7.16 E5 induces cell cycle modification

E5 is also thought to play a role in the genome amplification phase of the virus life cycle. Studies conducted on E5 knockout HPV 35 genomes in an organotypic raft culture system showed that loss of E5 resulted in a reduction of late viral gene expression, suggesting that E5 may play a role in stimulating late life cycle events. A reduction in the levels of the cell cycle regulators cyclin A and B was also observed indicating that E5 may also affect the cell cycle (Fehrmann *et al.*, 2003). HPV 16 E5 has also been shown to cooperate with E7 to stimulate cell proliferation and late gene expression (Bouvard *et al.*, 1994). A third study suggested that the HPV 16 E5 protein plays a quantitative role in the virus lifecycle with E5 knockout raft cultures having a 2 fold decrease in the number of suprabasal cells undergoing DNA synthesis (Genther *et al.*, 2003). E5 is believed to promote cell cycle progression through interactions with the epidermal growth factor (EGF) and platelet derived growth factor (PDGF) receptors. E5 has been shown to cause a 2-5 fold increase in EGF receptor density and enhance signal transduction, rendering cells hypersensitive to ligand stimulation (Straight *et al.*, 1993). Contradicting studies have suggested that receptor density is not affected and that cell proliferation is stimulated by an amplified signal cascade (Gu *et al.*, 1995; Leechanachai *et al.*, 1992; Ziegert *et al.*, 2003). Several studies have also shown that the E5 gene is dispensable and that normal productive infection can occur in its absence (Brandsma *et al.*, 1992; Genther *et al.*, 2003).

1.7.17 The E1 protein

The E1 gene sequence is highly conserved throughout papillomaviruses suggesting that its function is vital to the virus. The E1 protein consists of two globular domains separated by a linker region (Enemark *et al.*, 2000). All E1 proteins contain a nuclear localisation signal, a DNA binding domain in the N-terminus, and ATP-dependent DNA helicase activity in the C-terminus. E1 is believed to be expressed in the lower and mid levels of the epithelium at very low levels as it cannot be detected in tissue (Ozbun *et al.*, 1998b). Experiment have shown E1 to be essential for maintenance and amplification of viral genomes (reviewed in (Wilson *et al.*, 2002).

1.7.18 The role of E1 in viral genome replication

In vitro experiments have shown that E1 at high levels is capable of binding to and initiating replication of DNA (Kuo *et al.*, 1994; Santucci *et al.*, 1995; Seo *et al.*, 1993a; Seo *et al.*, 1993b). E1 binds DNA forming multiple hexameric complexes with ATP-dependant helicase activity (Yang *et al.*, 1993). *In vivo* the protein is expressed at such low levels that this is thought unlikely to occur unaided. Experiments have been able to demonstrate that in the absence of the E2 protein, E1 associates non-specifically to DNA (Sanders *et al.*, 2000). Co-expressing E1 and E2 results in the recruitment of E1 to the viral origin of replication (ORI) where it assembles into hexamers. E1 is thought to bind cooperatively with E2 to the E1 binding site, located adjacent to the E2 binding site (Mohr *et al.*, 1990). It is believed that the binding of E1 and E2 to the ORI causes the DNA to wrap which in turn allows the recruitment of a further two E1 molecules. E2 is then displaced from the complex by the competitive binding of ATP to the E1 C-terminus (Sanders *et al.*, 1998). E1 has been shown to form bi-hexameric complexes known to be required for the bidirectional DNA synthesis observed in HPV DNA replication. Interestingly E1 shares considerable homology with the SV40 large T antigen which has similar properties (Melendy *et al.*, 1995). Interestingly it has been

suggested that SV40 small T antigen may be a functional homolog of the cellular MCM proteins which form the hexameric helicase complexes required for cellular DNA replication, these finding may shed light on E1 function (Chong *et al.*, 2000; Gomez-Lorenzo *et al.*, 2003; Patel *et al.*, 2000).

1.7.19 The role of E1 in viral genome transcription

E1 has been shown to modulate the binding of the viral transcription factor E2 in a concentration dependent manner. The E1 protein of BPV has been shown to represses E2-mediated transactivation from the early promotor p89 (Ferran *et al.*, 1998; Sandler *et al.*, 1993). The equilibrium between occupancy of the E1 and E2 binding sites may switch the viral genome from a transcriptionally active state to a replicative state.

1.7.20 The E2 protein

The E2 protein is highly conserved throughout papillomaviruses and is involved in replication, genome maintenance, and in the control of viral transcription. The protein is comprised of two globular domains connected by a linker region. The N-terminus contains a trans-activating domain and the C-terminus is a DNA-binding and dimerisation domain (Giri *et al.*, 1988; McBride *et al.*, 1988). As with other papillomavirus proteins E2 protein function appears to be modulated by both proteolytic cleavage and phosphorylation (Hubbert *et al.*, 1988; McBride *et al.*, 1989).

1.7.20.1 Vegetative viral genome replication and maintenance

The E2 protein has been demonstrated to play a role in viral genome replication through an interaction with the E1 protein. Two E2 binding sites are located adjacent to the viral ORI (Sverdrup *et al.*, 1995). The loading of E2 onto these sites allows the specific recruitment of the viral helicase E1 to the viral ORI, which in turn allows genome amplification to occur (Sverdrup *et al.*, 1994; Sverdrup *et al.*, 1995). Another function

of E2 is to ensure even distribution of viral genomes into daughter cells, which is mediated by E2s ability to bind viral genomes onto the mitotic spindles (Bastien *et al.*, 2000; Ilves *et al.*, 1999).

1.7.20.2 E2 and transcription regulation

Initial transcription of the viral genes is controlled by cellular transcription factors binding the LCR, this is then modulated by E2 in a concentration-dependent manner (Sanders *et al.*, 1994; Stubenrauch *et al.*, 1994). Occupancy of the four E2 binding sites in the LCR is the principal mode of transcription modulation, although a direct interaction with other cellular protein also occurs (Li *et al.*, 1991). The significance of E2's role in transcriptional regulation is still unclear with some studies suggesting that the protein's role in transcription is only secondary to its role in genome maintenance (Bechtold *et al.*, 2003; Stubenrauch *et al.*, 1998). Truncated and modified forms of E2 have been identified in several HPVs and are believed to dimerise to full-length E2, but due to their lack of a trans-activating domain are thought to act as a repressor (Doorbar *et al.*, 1990b; Lambert *et al.*, 1987; Stubenrauch *et al.*, 2000).

1.8 Late gene expression

Late genes are involved in viral genome packaging and possibly virion release. E1^E4 is believed to play a role throughout the virus lifecycle but is only expressed at high levels at late time points. As the work in this thesis is primarily interested in these later roles of E1^E4, the description of the protein has been included in this section.

1.8.1 Papillomavirus capsid proteins

The papillomavirus expresses two capsid proteins L1 and L2. L1 and L2 expression is controlled by the late differentiation-dependent promoter. Both proteins are expressed in the upper layers of infected epithelium after viral genome amplification has occurred (Ozbun *et al.*, 1998a). L1 is the major and L2 the minor capsid protein. They combine

with a stoichiometry of 5/1 to from rosette structures, with 72 rosettes making up the viral capsid (Baker *et al.*, 1991). Both proteins have an NLS motif located in the C – terminus comprising of a cluster of basic amino acids (Zhou *et al.*, 1991a). It is thought that the NLS allows the proteins to enter the nucleus via interactions with members of the karyopherin receptor family (Fay *et al.*, 2004; Merle *et al.*, 1999).

1.8.2 Functions of the L1 and L2 proteins during early lifecycle events

L1 has been shown to associate with heparin sulphate and is involved in initial virus entry into uninfected cells (Joyce *et al.*, 1999). Once the virus has gained access to cells, L2 has been shown to facilitate transport of viral DNA to the nucleus via interaction with β-actin. Deletion of the actin binding domain (amino acids 25-45) significantly reduces the infectivity of HPV 16 pseudo virions (Yang *et al.*, 2003a).

1.8.3 Functions of the L1 and L2 proteins during late lifecycle events

L2 is synthesised prior to L1, and is transported into the nucleus where it accumulates in Promyelocytic leukaemia (PML) bodies, in which it is believed that viral genome amplification and packaging occurs (Florin *et al.*, 2002; Swindle *et al.*, 1999). L2 is known to be responsible for the recruitment of L1 and E2 to the PMLs (Day *et al.*, 1998; Florin *et al.*, 2002). It has been postulated that the recruitment of E2-bound DNA may facilitate selective packaging of the viral genome. The L1 protein associates into pentamers in the cytoplasm of infected cells, and these are recruited to the ND10s following the L2 induced release of SP100 (Florin *et al.*, 2002; Okun *et al.*, 2001). Both the N and C terminus domains of L2 interact with L1 pentamers, and are required for virus encapsulation (Okun *et al.*, 2001).

1.9 Papillomavirus E1^E4 proteins

The E1^E4 proteins are encoded by a spliced mRNA comprising the first few amino acids of the E1 ORF (5 in the case of HPV16 E1^E4) spliced onto the gene product of the E4 ORF (Doorbar *et al.*, 1987; Doorbar *et al.*, 1988a; Nasseri *et al.*, 1987). The E1^E4 ORF lies within a region of the E2 ORF that codes for the linker domain (see Fig 5.5). Analysis of viral mRNA transcripts suggests that the protein is expressed throughout the virus lifecycle, although the E1^E4 protein can only be detected by indirect immuno-fluorescence in upper layers of the epithelium (Doorbar *et al.*, 1992; Peh *et al.*, 2002). It has been suggested that build up of E1^E4 is caused by an increase in transcription from the differentiation-dependent promoter (Hummel *et al.*, 1992), although it is conceivable that protein stabilisation or reduced turnover may also be involved.

1.9.1 Characteristics of E1^E4 proteins

E1^E4 proteins are typically small proteins varying in size from 88 to 134 amino acids for HPV18 and ROPV respectively. There is very little sequence homology shared between E1^E4 proteins from different genera, suggesting that they have undergone significant evolution/mutation when compared to other papillomavirus proteins (Narechania *et al.*, 2005) (*see* Chapter 3). Despite this, some features are commonly observed. Most E1^E4 proteins contain a proline rich region and a region of charged residues and many, (specifically α-group E1^E4s) also contain a leucine cluster (reviewed in (Doorbar, 1996). Another commonly observed feature is a well conserved C-terminal region believed to be involved in self association (Ashmole *et al.*, 1998; Bryan *et al.*, 1998).

1.9.2 Multimerisation of E1^E4 proteins

HPV1 E1^E4 has been shown to from stable trimers or tetramers (Doorbar *et al.*, 1996) and the capacity of HPV16 E1^E4 to from dimers and hexamers has also been reported (Roberts *et al.*, 1997; Wang *et al.*, 2004). Mutation of a cysteine in HPV16 E1^E4 (conserved in A9 E1^ E4s) destabilised multimers, leading to dissociation following SDS gel electrophoresis. The cysteine mutation did not prevent self association suggesting that disulphide bond formation alone is not responsible for multimerisation (Ashmole *et al.*, 1998; Roberts *et al.*, 1997). The lack of cysteine residues in some E1^E4 proteins, as well as the ability of some multimers to survive treatments in strong reducing environments suggests that disulphide bonds are not essential for multimerisation.

1.9.3 Proteolytic cleavage of E1^E4

Proteolytic cleavage of E1^E4 has previously been observed resulting in an increase in truncated protein isoforms towards the surface of the epithelium (Breitburd *et al.*, 1987). The exact reason for truncation is not properly understood although to date it has been observed in HPV 1 and 16 E1^E4 proteins (Doorbar *et al.*, 1997; Rogel-Gaillard *et al.*, 1992a). The distribution of truncated E1^E4s suggests processing may be differentiation-dependent. This may provide the virus with an additional way to modulate protein function by modifying the phenotype of the infected cell to favour virus synthesis or virus release throughout the virus lifecycle.

An N-terminally truncated form of HPV 16 E1^E4 has previously been suggested from immunofluorescence studies although its precise role is still unclear (Doorbar *et al.*, 1997). A truncation of HPV 1 E1^E4 has also been reported *in vitro* and *in vivo.* Truncated isoforms of the protein also appear to be more abundant at the surface of lesions. Truncation of the protein was shown to remove the ability to associate with

cytokeratins and displays an altered cellular distribution (Doorbar *et al.*, 1988b; Roberts *et al.*, 2003; Rogel-Gaillard *et al.*, 1992b).

1.9.4 Phosphorylation of E1^E4 proteins

Phosphorylated forms of E1^E4 have been detected in HPV 1, 11 and 16 (Bryan *et al.*, 2000b; Das, 2005; Grand *et al.*, 1989; Wang *et al.*, 2004). HPV 1 E1^E4 was noted to become phosphorylated by protein kinase A (PKA) *in vivo.* In addition to this the phosphorylation state of the protein was shown to increase towards the surface of the lesion (Breitburd *et al.*, 1987). It was also reported that a second unidentified kinase was likely to be involved in the phosphorylation. HPV 11 E1^E4 has been shown to be phosphorylated *in vitro* by PKA and mitogen activated protein kinase (MAPK) at consensus kinase motifs in the central region of the protein. There is also strong evidence of phosphorylation of HPV11 occurring *in vivo.* Sequence analysis has also identified putative phosphorylation sites in other E1^E4 proteins (Peh, 2002). Computational analysis of HPV 16 E1^E4 has identified putative MAPK, CDK and PKA phosphorylation motifs and recent work has shown these sites to be phosphorylated *in vitro* as predicted (Das, 2005). As yet little is known about the role phosphorylation plays in modulating α-group E1^E4 function, although it has been suggested that it may function as a differentiation-dependent protein switch between a role in genome amplification and a role to one of viral egress (Bryan *et al.*, 2000b).

1.9.5 E1^E4 Functions

1.9.6 Genome amplification/replication

The role that E1^E4 plays in viral genome amplification was first identified in HPV1 lesions where it was noticed that high levels of E1^E4 coincided with viral genome amplification (Breitburd *et al.*, 1987). Since then studies on E1^E4 knock-out CRPV lesions have shown E1^E4 to be essential for viral genome amplification and late gene

expression (Peh *et al.*, 2004). The role of HPV 16 and 31 E1^E4 in genome amplification have also been demonstrated in organotypic raft cultures suggesting this function is conserved to varying degrees in E1^E4 proteins from unrelated HPV types (Nakahara *et al.*, 2005; Wilson *et al.*, 2005). Interestingly, the study investigating HPV 16 E1^E4 suggested that it was also required for genome maintenance in addition to amplification, suggesting that the protein may play a role in early life cycle events. HPV 1, 16 and 18 E1^E4 proteins have been shown to cause G2/M cell cycle arrest when expressed at high levels in epithelial cells (Davy *et al.*, 2002; Nakahara *et al.*, 2002). The purpose of E1^E4-induced cell cycle arrest is believed to be to produce a favourable environment for virus genome amplification in which the virus hijacks active cellular replication machinery. The presence of the viral proteins E1 and E2, probably allows the virus to circumvent the cellular DNA replication licensing system (Madine *et al.*, 1995) allowing multiple rounds of viral genome replication to occur in the absence of cellular DNA replication. Two threonine residues located in the proline rich domain of HPV 16 E1^E4 have been shown to be essential for mediating cell cycle arrest (Davy *et al.*, 2002). E1^E4 was shown to associate with, and cause the retention of, the active cyclin B1/CDK1 complex in the cytoplasm (Davy *et al.*, 2005). Interestingly mutation of a single threonine in a similar region of HPV1 E1^E4 also prevents cell cycle arrest from occurring. Cyclin B1 was not observed in HPV1 E1^E4 expressing-cells and it was suggested that the protein induce G2/S phase arrest by preventing the accumulation of the complex (Knight *et al.*, 2004). Interestingly Cyclin B is abundant in E1^E4 expressing cells *in vivo* (Davy *et al.*, 2005).

1.9.7 HPV 16 E1^E4 interacts with a putative RNA helicase

E1^E4 may also have a putative role in the regulation of gene expression, as a yeast two-hybrid screen demonstrated that HPV 16 E1^E4 has the ability to interact with a

novel DEAD box protein, E4-DEAD box binding protein, (E4-DBP) (Doorbar *et al.*, 2000). E4-DBP is predominantly located in the nucleus but has also been demonstrated to shuttle between the nucleus and cytoplasm. Although no role has been attributed to E4-DBP, DEAD box proteins are known to be involved in the processing, stability and transport of RNA molecules (Tanner *et al.*, 2001). Papillomaviruses are heavily dependent on RNA processing for regulation of gene expression and the virus is also believed to be able to alter host cell transcription (Baker *et al.*, 1996; Lehr *et al.*, 2002). It has been speculated that E1^E4 interactions with E4-DBP may allow the virus to control both processes (Doorbar *et al.*, 2000).

1.9.8 E1^E4's role in virion release

The exact role E1^E4 plays in virion release is unclear. The expression time frame and location of abundant E1^E4 strongly suggests that it may be involved in virion release. This hypothesis is supported by a number of studies into the function of the protein which have shown that the ability of HPV 1, 11, 16 and 31 E1^E4's to associate with and in some cases disrupt components of the cell cytoskeleton and CCE that form the mechanical barrier of the skin (Brown *et al.*, 2000; Doorbar, 1991; Pray *et al.*, 1995a; Roberts *et al.*, 1993; Wang *et al.*, 2004)

1.9.9 E1^E4 interacts with the cytokeratin network

The cytokeratins found in differentiated keratinocytes in the upper layers of the epithelium provide a tough mechanical barrier which protects the underlying tissue from desiccation and external insult. As well as providing a protective barrier for host tissue they also present the virus with an obstacle through which newly made virions must pass if they are to infect new hosts. Keratin filaments are composed of type 1 (acidic) and type 2 (basic) keratins that polymerise with specific partners at a stochometry of 1/1 (discussed in more depth in Chapter 4) (reviewed in (Coulombe *et al.*, 2002). HPV 1, 2

and 16 E1^E4 proteins have been shown to associate with keratins, HPV 2 and 16 E1^E4's association causes keratin filament network to collapse. HPV 16 E1^E4 contains an N-terminal leucine cluster (YPLLXLL) that is highly conserved through α-group E1^E4 proteins and is known to be involved in keratin association (Roberts *et al.*, 1994; Roberts *et al.*, 1997). Experiments have demonstrated that a heavily truncated N-terminal 16 E1^E4 peptide containing the leucine cluster is sufficient to localise GFP to keratin filaments (Wang *et al.*, 2004). Later experiments showed that HPV 16 E1^E4 was able to bind directly to keratin 18 (a type 1 keratin) but not its type 2 partner keratin 8 (Wang *et al.*, 2004). The ability of HPV 16 to cause cytokeratin network collapse is also affected by the E1^E4 C-terminus, which is involved in multimerisation. It has been suggested that multimerisation of E1^E4 may cause filament collapse through cross linking, although this model is brought into question when it is considered that monovalent Fab antibody fragments are also able to induce similar network collapse (Waseem *et al.*, 2004).

1.9.10 E1^E4 disrupts the cornified cell envelope

As well as associating to keratins HPV 11 and 59 E4 have been demonstrated to associate with and disrupt the cornified cell envelope (CCE) (Brown *et al.*, 2004; Bryan *et al.*, 2000a). The CCE forms a robust shell of proteins around cells in the upper layers of cornified epithelium providing mechanical strength and resistance to desiccation. The CCE is composed of proteins such as loricrin , involucrin, keratins and small proline rich proteins, cross-linked by N-(γ glutamyl) lysine isopeptide bonds, created by transglutaminase (Kalinin *et al.*, 2001). Transglutaminase is activated by the high calcium environments encountered towards the surface of differentiated epithelium (Agardh *et al.*, 2005). Interestingly activation of calcium-dependent PKC is required for late viral gene expression in organotypic raft cultures, suggesting that the formation of

the CCE and E1^E4 expression are dependent on the same differentiation signal (Pray *et al.*, 1995a). Immuno-fluorescence analysis showed cells expressing HPV 11 E1^E4 lack detectable loricrin and keratin 10. EM data also demonstrated that CCEs were up to 65% thinner and displayed morphological aberrations in the presence of HPV11 E1^E4. HPV 11 infected, E1^E4 positive cells were also shown to be more fragile. HPV11 E1^E4 could be co-purified with the CCE. Experiments showed E1^E4 to be disulphide bonded to components of the CCE (Brown *et al.*, 2000; Bryan *et al.*, 2000a; Bryan *et al.*, 2001). Further experiments demonstrated that levels of loricrin mRNA transcripts were reduced suggesting that cell reinforcement systems may be affected by protein-protein interactions and at a transcriptional level (Lehr *et al.*, 2002). In natural HPV 1 lesions, cells expressing E1^E4 also showed lower levels of loricrin and filaggrin, indicating that the CCE may be targeted by diverse papillomaviruses (Doorbar *et al.*, 1996).

1.9.11 HPV 16 E1^E4 interacts with mitochondria inducing apoptosis

HPV 16 E1^E4 has been shown to associate with mitochondria when expressed at high levels *in vitro*. Mitochondrial association was seen to occur after association with, and collapse of the cytokeratin network. Association of E1^E4-with mitochondria resulted in the formation of perinuclear aggregates, loss of membrane potential and apoptosis. It was suggested that E1^E4-induced apoptosis in the terminally differentiated layers of the epithelium may facilitate virion release (Raj *et al.*, 2004).

1.10 Papillomaviruses and cancer

The link between cervical cancer and papillomavirus infections was first made in the early 80's(Reid *et al.*, 1982). Why only a few papillomaviruses have the ability to cause malignancies is still not understood clearly. Cervical neoplasias are graded using the cervical intraepithelial neoplasia (CIN) scale ranging from CIN I to CIN III. As tissue

progresses to CIN I a slight thickening of the mitotically active compartment occurs and by CIN III, differentiation in the tissue is lost and the entire epithelium can be mitotically active. Invasive cancer begins when transformed cells breakthrough into the dermis and invade the underlying tissue. Typically only 10% of CIN I lesions will progress to CIN II with the rest spontaneously regressing. A significant percentage of CIN III lesions may progress to invasive cancers. Lesions typically take years to progress from CIN I through to invasive cancers, suggesting there are a series of stages that cells go through before cancers develop (Arends *et al.*, 1998; Murthy *et al.*, 2000).

1.10.1 HPV genome integration

One factor found to significantly increase the chances of neoplastic progression is viral genome integration into the host cell DNA (Vernon *et al.*, 1997). In productive viral infections, the viral genome is maintained as an episome. Although integration can occur at various sites in the host cells DNA, the integration site in the viral genome remains relatively well conserved and results in the disruption of the of E1^E4 and E2 ORF. While integrating viral DNA stands a chance of disrupting cellular oncogene and does sometimes occur, the effect of restructuring viral DNA is well understood. Disrupting E1^E4 expression may prevent cyclin B1 mediated arrest from occurring. Loss of E2 expression results in the up-regulation of the HPV early promoter resulting in higher expression of the viral oncogenes E6 and E7 (Jeon *et al.*, 1995a; Jeon *et al.*, 1995b). Integration events appear to occur more frequently, with high risk viruses suggesting that certain DNA sequences may be partly responsible for their high risk status (Kessis *et al.*, 1996). The discovery of invasive cancers with exclusively episomal viral DNA shows that although integration plays a role in neoplastic progression it is not a prerequisite (Matsukura *et al.*, 1989). The finding of integrated

genomes in low grade lesions also suggests that secondary factors are important in malignant progression.

1.10.1.1 The role of HPV proteins in neoplastic progression

The HPV E6 protein is expressed in all cervical carcinomas and HPV transformed cell lines. Loss of E6 expression is sufficient to reactivate dormant tumour suppressor pathways inducing apoptosis in HeLa cells (Goodwin *et al.*, 2000). E6 proteins disrupt p53 function that normally guards cells against acquiring genetic mutations by arresting mitotic cells and/or activating apoptotic pathways following the detection of DNA damage. Prolonged expression of E6 can allow cells to accumulate genetic damage, which would not otherwise be permitted. Cells expressing E6 have been shown to withstand irradiation without undergoing cell cycle arrest or apoptosis (Kessis *et al.*, 1993; Storey, 2002). Resistance to apoptotic stimulation also makes cells more susceptible to genetic damage induced by exposure to environmental carcinogens (Kjellberg *et al.*, 2000).

A further function seemingly unique to high risk viruses is their ability to target cellular proteins for degradation. Interactions between high risk E6 and E7s with their target proteins result in the degradation of RB and p53. This process is tightly regulated in normal viral infections, and the upregulation of these proteins as a result of genome integration accentuates this affect resulting in a higher risk of cancer (Sherman *et al.*, 1996).

As with E6 and E7, the HPV E5 protein has transforming properties and is commonly referred to as an oncogene (DiMaio *et al.*, 2001), although the exact extent of its involvement in neoplastic progression is unclear. E5 is known to have oncogenic

properties such as the ability to stimulate anchorage independent growth of cells *in vitro* via its interaction with growth receptors (Leechanachai *et al.*, 1992). Unlike E6 and E7, E5 is rarely detected in invasive cancers and this gene is commonly lost during the integration process (Stoler *et al.*, 1992).

1.10.2 Other risk factors linked to cervical cancer

Although the presence of high risk viral DNA is though to be essential for the development of squamous cell carcinoma (SCC), it is clear that other factors play a significant role. Additional risk factors include duration between puberty and menopause (oestrogen exposure), use of the contraceptive pill, genetic predisposition, immuno-suppression (especially after organ transplants), smoking, obesity, exposure to environmental carcinogens and secondary infection such as HIV and chlamydia (Brisson *et al.*, 1994; Daling *et al.*, 1992; Kjellberg *et al.*, 2000; Lacey *et al.*, 2003; Luesley *et al.*, 1994; Moreno *et al.*, 2002; Munoz *et al.*, 1997; Peng *et al.*, 1991).

1.11 HPV management

1.11.1 Cervical screening

Cervical cancer is the second most prominent female cancer (after breast cancer) globally responsible for >250,000 deaths annually (Parkin *et al.*, 2005). In some western nations it has dropped to one of the most common female cancers due to the success of screening programs (Boyle *et al.*, 2005). The relatively long period between hyperplasia and invasive cancer (~4 years) means that potentially problematic lesions can be detected and destroyed before they progress. The current cervical screening program is based on the Papanicolaou staining technique and involves the detection of abnormal cells based on their morphology alone (Warner *et al.*, 1989). The introduction of cell proliferations markers such as PCNA, Ki67, MCM, and p16 may revolutionise

screening in the next couple of years (Doorbar *et al.*, 2005; Dray *et al.*, 2005; Freeman *et al.*, 1999; Keating *et al.*, 2001; Nieh *et al.*, 2005; Williams *et al.*, 1998).

1.12 Papillomavirus vaccines

There are currently two different lines of vaccine research; these can be described as prophylactic and therapeutic. Prophylactic vaccines generate neutralising antibodies to virus capsid proteins preventing infections from occurring, whereas therapeutic vaccines work by stimulating the adaptive immune system in order to clear existing infections.

Recent research has demonstrated that papilloma vaccines are highly subtype specific and provide little if any protection against closely related viruses making a comprehensive cervical cancer vaccine unlikely in the near future (Giroglou *et al.*, 2001b). The most promising line of research into a prophylactic vaccine using VLP's consisting of L1 and L2 from both HPV 6, 11, 16 and18 (Stanley, 2005; Yang *et al.*, 2005; Zhou *et al.*, 1991b). A recent breakthrough was made when large scale clinical trials results showed it to provide 100% protection against acquiring new infections (Harper *et al.*, 2006; Koutsky *et al.*, 2002; Mao *et al.*, 2006; Villa *et al.*, 2005) and the vaccine is now considered ready for FDA approval. Although the target groups is currently undecided, it has been suggested that the vaccine should be targeted at young girls between the ages of 11-13 before they become sexually active, as will provide less protection to those already infected with high risk viruses (Short *et al.*, 2006; Soubeyrand *et al.*, 2005). Despite this success, many questions are left unanswered. The vaccine is still relatively expensive to manufacture and it is not known how long protection lasts so its economic viability remains to be seen (Garnett *et al.*, 2000). Another unknown factor is whether infections by other high risk viruses will become

more prevalent if HPV 16 and 18 infections are eradicated. The ability of the virus to evolve when placed under selective pressure also remains to be seen.

Work on therapeutic vaccines has looked at the early virus proteins E1, E2, E5, E6 & E7. E6 and E7 based vaccines have been shown to provide some protection against subcutaneously seeded tumour cells (Meneguzzi *et al.*, 1991). The holy grail of research, a vaccine that could not only prevent infection but also treat lesions as well as associated tumours is still some way off.

1.12.1 Papillomavirus therapies

Despite the recent success of the new vaccine much remains to be done to find new therapies to treat pre-existing papilloma infections. At present there are very few therapeutic options available for the treatment of lesions and these are relatively primitive. The most commonly used treatment involves removal or destruction of infected tissue. Salicylic acid is currently used to burn away HPV 2 infected tissue in verrucas. Persistent cervical lesions can be ablated using cryotherapy, loop electrosurgical excision procedure or surgical excision. More recently some new products such as imiquimod cream have come onto the market. Imiquimod is a immunomodulatory cream that induces the production of cytokines increasing lesion clearance times (Beutner *et al.*, 1998). Although primarily intended for use on genital warts, Imiquimod has recently been trialled against other cutaneous papilloma infections with some success (Harwood *et al.*, 2005).

1.13 Virus release mechanisms

Viruses have evolved many mechanisms to identify, access and replicate inside specific host cells and numerous mechanisms have also developed to allow progeny virions to escape infected cells. The mechanism by which viruses exit their host cells depends on

the final configuration of the mature virion, intended route of viral transmission and the intended duration of virus infection. Enveloped viruses must pass through a host cell membrane to acquire their lipid coats, whereas non-enveloped viruses have evolved different exit strategies. Virus release mechanisms can be divided into three main categories; budding, exit via secretory pathways, and cell lysis. Cell lysis should not be confused with cytopathic effect (CPE), which is commonly observed during viral egress from infected cells and is induced by a build up of toxic viral proteins and disruption of normal cell function.

1.13.1 Lytic exit strategies

The T4 bacteria phage has a simple exit strategy using the viral enzyme lysozyme to cleave open cell walls and membranes of infected cells, allowing new virions to be released into the environment (Fischetti, 2005). Viruses of eukaryotic hosts have to control virion release more carefully, depending on whether chronic or transient infections are to be established. Viruses intent on establishing chronic infections control virion release and CPE-induced cell lyses so as minimise detection by the immune system and excessive damage to host tissue. Transient infections such as with influenza tend to use more explosive infection strategies resulting in significant CPE and tissue damage. The high rate of virion release enables such viruses to out pace host immune responses (Smith *et al.*, 2002).

1.13.2 Exit through secretary pathways

Simian virus 40 (SV40) belongs to the Polyomaviridae family of non enveloped viruses which escape from cells without inducing cell lysis. Newly made virions are concentrated in intracellular vesicles, from where they are transported to the cell surface and released by membrane fusion event. Release of SV40 can be blocked by treating cells with the inhibitor of intracellular vesicular transport monensin (Clayson *et al.*,

1989). Vaccinia virions are shed by endocytosis and CPE induced lysis, and virions shed by different methods are distinct with the exocytosis-released virions being membrane bound and more infectious.

1.13.3 Lytic viral egress

Adenovirus is also a non-enveloped virus whose release is generally believed to require host cell lysis (Zhang *et al.*, 1994). Infection results in disruption of vimentin prior to viral gene expression by rapid reaction to viral adsorption (Belin *et al.*, 1987). The adenovirus E1B protein also disrupts the vimentin filament network. Collapse of vimentin filaments results in the formation of perinuclear bundles (Janoff *et al.*, 1991). The adenovirus also has the ability to disrupt keratin filaments using the adenovirus protease (AVP). Unlike the papillomavirus this is caused by enzymatic cleavage of keratin 18 at amino acid 74 resulting in headless keratin molecules unable to polymerise (Chen *et al.*, 1993) AVP requires actin as a co factor for proteolytic cleavage of keratins (Brown *et al.*, 2002). In addition to disrupting the cell cytoskeleton, adenovirus structural proteins are also toxic to cells enhancing CPE and possibly aiding virion release (Pettersson *et al.*, 1969). Adenoviruses appear to use CPE as a mechanism of virion release although CPE is aided by specific proteins which purposefully disrupt host cell systems that may interfere with virion release.

1.13.4 Papillomavirus virion release ??

To date very little is known about the papillomavirus release mechanisms. Egress of mature papillomavirus virions occurs at the surface off terminally differentiated epithelium and so is not directly linked to viral pathology. It has been assumed that virions are released into the environment as terminally differentiated cell slough off from the surface. This model may be true to a certain extent but it is probable that keratinized cells with cornified envelopes would not provide a good vehicle for virion

distribution and would more likely function to encapsulate virions (Luby-Phelps, 1994; Seksek *et al.*, 1997). It has previously been shown that the E1^E4 protein associates with and disrupts keratin filaments *in vitro* and *in vivo* (Doorbar *et al.*, 1991; Roberts *et al.*, 1994; Sterling *et al.*, 1993a; Wang *et al.*, 2004). HPV 11 E1^E4 has also been shown to disrupt and weaken cornified cell envelopes (Brown *et al.*, 2004; Bryan *et al.*, 2000a; Bryan *et al.*, 2000b). The dramatic upregulation of E1^E4 towards the cell surface also points to it playing a role in virus egress. By disrupting and degrading the cytokeratin network the virus is likely to increase cell fragility, allowing fragmentation of terminally differentiated keratinocytes and the release of virus particles. This effect would likely be enhanced by direct physical contact.

1.14 Aims

The aims of this thesis are threefold.

1. To examine the mechanism by which HPV 16 E1^E4 induces keratin filament collapse in undifferentiated cells grown in monolayer culture (*in vitro*), and to determine the fate of affected keratins.

2. To relate these findings to the events which follow E1^E4 binding to keratins *in vivo* during natural infections in differentiated epithelium.

3. To establish the extent to which E1^E4-keratin interactions persist amongst HPV's of distinct evolutionary origin, in an attempt to provide an insight into the role of the E1^E4 proteins during productive HPV infections.

2 Materials and Methods

2.1 Materials

2.1.1 Suppliers of reagents

Except where specified, or in the exceptions given below, reagents were obtained from Sigma-Aldrich Company Ltd. (Poole, UK) or VWR International Ltd. (Lutterworth, UK).

Agarose, ammonium persulfate (APS), ethidium bromide (EtBr), sodium dodecyl sulfate (SDS) and N, N, N', N'-tetramethylethylenediamine (TEMED) were obtained from Bio-Rad Laboratories Ltd. (Hemel Hempstead, UK). Foetal calf serum (FCS) was obtained from Perbio Science UK Ltd. (Cramlington, UK). EMPIGEN BB ™ was obtained from Calbiochem, VWR International Ltd. ECL reagents, rainbow molecular weight markers, glutathione sepharose 4B and protein G sepharose beads were obtained from Amersham Pharmacia Biotech UK Ltd. (Little Chalfont, UK). Ultra Pure ProtoGel® acrylamide was obtained from National Diagnostics Ltd. (Hull, UK). Restriction endonucleases and Complete Protease Inhibitor Cocktail Tablets were obtained from Roche Diagnostics Ltd. (Lewes, UK). Phospho-specific keratin antibodies (8250, 3055, LJ4 and 2D6) were kindly provided by Bishr Omary.

2.1.2 Media and buffers

Name	Components
1 x Phosphate buffered saline (PBS)	1 % (w/v) NaCl, 0.025 % (w/v) KCl, 0.14 % (w/v) Na_2HPO_4, 0.025 % (w/v) KH_2 PO_4. The pH was adjusted to 7.4 with concentrated HCl.
1 x Tris-borate-EDTA (TBE)	1.21 % (w/v) Tris base, 0.62 % (w/v) boric acid, 0.19 % (w/v) EDTA. pH 8.0.
2 x Laemmli buffer	4% (w/v) SDS, 20 % (v/v) glycerol, 0.12M Tris, 1mM DTT PH 8, containing a trace of bromophenol blue

Table 2.1 General buffers

Name	Components
Luria-Bertani (LB) medium	1 % (w/v) Tryptone, 0.5 % (w/v) yeast extract, 1% (w/v) NaCl. The pH was adjusted to 7.0 with 5 N NaOH.
LB agar	LB medium containing 2% Bacto agar (Difco Laboratories Ltd., Detroit, USA).
Selective LB media	LB medium or LB agar containing antibiotics [50 mg/l ampicillin (Amp) or kanamycin (Kan)].
2 x TY medium	1.6 % (w/v) Tryptone, 1 % (w/v) yeast extract, 0.5 % (w/v) NaCl. The pH was adjusted to 7.0 with 5 N NaOH.

Table 2.2 *E. coli* growth media

Name	Components
Trypsin-Versene	0.8 % (w/v) NaCl, 0.02 % (w/v) KCl, 0.12 % (w/v) NA_2HPO_4, 0.02 % (w/v) KH_2PO_4, 0.01 % (w/v) EDTA, 0.01 % (w/v) trypsin, 0.001 % (w/v) phenol red.
Medium A	DMEM (Sigma) containing 10 % (v/v) FCS (unless otherwise indicated), 0.01 % (w/v) streptomycin and 0.006 % (w/v) penicillin.
Time-lapse medium	CO_2 Independent Medium (Gibco) containing 10 % (v/v) FCS, 0.01 % (w/v) streptomycin, 0.006 % (w/v) penicillin and 10 mM ascorbic acid.
Cell freezing solution	FCS containing 10% (v/v) dimethyl sulfoxide (DMSO).

Table 2.3 Cell culture media and reagents

2.2 Molecular biology techniques

2.2.1 DNA constructs used

In cell culture wild type HPV 16E1^E4 was expressed by transfection of the pMV11.16E1^E4 construct (Davy *et al.*, 2002) and by infection with recombinant adenovirus containing the rAD16E1^E4 construct (Doorbar *et al.*, 2000). M2 E1^E4 was expressed by infection with recombinant adenovirus containing the e M2 rAdM2 construct (Wang *et al.*, 2004). The T22A, T23A mutant of E1^E4 was expressed by transfection of the pMV11 E1^E4 T22A, T23A expression vector (Davy *et al.*, 2002). βgal was expressed by infection of recombinant adenovirus containing the rAD β–gal construct (fournier1999). HPV 2, 4, 18 31, 35, 45 and 65 E1^E4 proteins were expressed by the transfection of the pcDNA 3 expression vectors kindly provided by Dr Heather Griffin, National institute for medical research, London. pYFP-E1^E4 was produced by cloning wild type E1^E4 into the pEYFP-C1 (Clonetech).

2.2.2 Details of the *E. coli* strain used

Strain	Genotype	Supplier
DH5α	deoR end A1, gyrA96, hsdR17(r_k- m_k+), recA1, relA1, supE44, thi-1, Δ(lacZYA-argFV169) ϕ80δλacZΔM15, F-, λ-	Clontech (Basingstoke, UK)

2.2.3 Culture of *E. coli*

Cells were grown in LB medium containing suitable selective antibiotics to prevent loss of plasmids. Cultures were incubated at 37 °C either on agar plates or in liquid medium with 200 rpm shaking.

2.2.4 Long term storage of *E. coli* cultures

E.coli cultures were stored for prolonged periods as glycerol stocks. Glycerol stocks were prepared by mixing equal volumes of mid-log cultures with 50 % (v/v) sterile glycerol. Solutions were mixed by inversion and stored at -70 °C.

2.2.5 Preparation of electrocompetent *E. coli*

E. coli cells (DH5α) were grown in LB medium at 37 °C with vigorous shaking to an A_{600} value of 0.5. All subsequent steps were carried out at 4 °C. Cells from 200 ml of culture were harvested by centrifugation at 4000g for 10 min in 250 ml centrifuge tubes (Corning, UK) using a J6 centrifuge (Beckman Coulter UK Ltd.). Cells were resuspended in 200 ml ice-cold ddH_2O. Cells were then centrifuged and resuspended three more times as above, but resuspension was performed sequentially in ddH_2O (100 ml), then 10 % glycerol (4 ml) and then 10 % glycerol (200 µl). The final cell suspension was stored in aliquots at -70 °C.

2.2.6 Transformation of *E. coli* by plasmid DNA

Approximately 100 ng of DNA was used to transform 40 µl of electrocompetent *E. coli* cells in a 0.2 cm cuvette using a Gene Pulser (Bio-Rad Laboratories Ltd., Hemel Hempstead, UK) with the following settings: 1.5 kV, 25 µF, 200 Ω. Cells were recovered by suspension in 1 ml of S.O.C. medium (Invitrogen Ltd., Paisley, UK) and incubation at rt. in the absence of an antibiotic. Cell suspension (100 µl) was then spread onto an LB agar plate containing a suitable selective antibiotic and incubated overnight at 37 °C.

2.2.7 Purification of plasmid DNA using commercially available kits

Plasmid DNA was purified from *E. coli* using the Wizard® Plus Miniprep DNA Purification System (Promega UK Ltd., Southampton) or a Plasmid Maxi Kit (QIAGEN Ltd., Crawley, UK), in accordance with the manufacturer's instructions.

2.2.8 Purification of DNA on a CsCl gradient

Plasmid DNA that was prepared as described above and which gave poor results following transfection was purified on a CsCl gradient as follows. Bacteria containing plasmid DNA were streaked onto a suitable selective LB agar plate. A single colony

was transferred into 5 ml of selective LB medium and incubated overnight at 37 °C with shaking. A 1:1000 dilution of this was used to inoculate 400 ml of selective LB medium. Following incubation as above, cells were harvested by centrifugation as described in Section 1.2.4. The cell pellet was suspended in 4 ml of Buffer 1 (50 mM glucose, 25 mM Tris base, 10 mM EDTA, pH 8). Lysozyme solution (1 ml) was added to a final concentration of 5 mg/ml and the suspension was incubated for 5 min at r.t. Buffer 2 (0.2 M NaOH, 1 % SDS; 10 ml) was added and the lysate was incubated for 5 min on ice. Buffer 3 (3 M potassium acetate, 11.5 % (v/v) acetic acid; 7.5 ml) was added and the solution mixed immediately and incubated for 5 min on ice. The solution was cleared by centrifugation at 10000g for 15 min at 4 °C in a JA20 rotor using a J25 centrifuge (Beckman Coulter UK Ltd.). Propan-2-ol (13.5 ml) was added to the cleared supernatant, which was incubated for 5 min at r.t and centrifuged again as before. The nucleic acid pellet was washed with 70 % ethanol, air dried, resuspended in 4.95 ml of TE buffer (10 mM Tris, 1 mM EDTA, pH 8.0) and incubated at 60 °C until pellet dissolved. This DNA solution was added to a tube containing 5.25 g of CsCl and 50 µl of 10 mg/ml EtBr. The solution was added to a 5.1 cm Quick-Seal® ultracentrifuge tube (Beckman Coulter UK Ltd.) and centrifuged in a VTi 65.2 rotor using a Beckman L-90K ultracentrifuge at 200,000 g overnight at 20 °C. The DNA band was collected using a syringe and needle. EtBr was removed by washing repeatedly with CsCl saturated propan-2-ol. Absolute ethanol was added to a final concentration of 75 % (v/v) and the DNA was precipitated by centrifugation 10000g for 15 min at 4 °C in a JA20 rotor using a J25 centrifuge. The pellet was washed in 70 % (v/v) ethanol, air-dried and resuspended in 0.5 ml TE buffer. An equal volume of equilibrated phenol chloroform was added, to obtain an aqueous phase the samples were vortexed for 10 s and centrifuged (10000 g, 2 min). The upper layer was removed into an equal volume of

phenol:chloroform:isoamylalcohol (24:24:1) and an aqueous phase obtained as before. To remove traces of phenol a final extraction was performed with an equal volume of chloroform. The aqueous phase was collected and ethanol precipitated and the DNA pellet dissolved in 500 µl endonuclease-free water.

2.2.9 Quantification of DNA

DNA concentrations were assayed using an Ultrospec™ 3300 pro UV/Visible Spectrophotometer (GE Healthcare UK Ltd., Chalfont St.Giles, UK). DNA solutions were diluted 1:500 and their A_{260} value measured. It was assumed that an A_{260} of 1.0 was equal to a DNA concentration of 50 µg/ml.

2.2.10 Agarose gel electrophoresis

PCR products and plasmids were separated on 1.5 % or 1 % agarose gels, respectively. Gels were buffered with 1 x TAE and contained 1 mg/ml EtBr. Samples were mixed with 1/10 volume their volume of 10 x loading buffer (50 % glycerol, 0.5 % bromophenol blue and 0.4 % (w/v) xylene cyanol). Electrophoresis was carried out at a constant voltage of 80 V, limiting to 200 mA. DNA bands were visualised using transmitted UV illumination and compared to DNA markers (New England Biolabs Ltd., Hitchin, UK) of known molecular mass. Images were captured using a Kodak Image station 440 and digital science software 1D software (Perkin Elmer Life sciences, Ltd., Cambridge)

2.2.11 Digestion of DNA with restriction endonucleases

DNA was digested with the appropriate restriction endonuclease in 1 x reaction buffer (according to the manufacturer's recommendation); BSA was added when required. DNA (0.05-5 µg) was digested with 5 U of enzyme in a total volume of 40 µl for 1 h at 37 °C. Enzyme was heat inactivated at 60 °C for 5 min.

2.2.12 Treatment of plasmid DNA with alkaline phosphatase

To prevent self-ligation of endonuclease-digested plasmid DNA, the linearized vectors were dephosphorylated at their 5' ends. Approximately 5 μg of vector was incubated with 5 U of calf intestinal alkaline phosphatase (Roche Diagnostics Ltd., Lewes, UK) in a total volume of 80 μl buffer for 1 h at 37 °C.

2.2.13 Polymerase chain reaction (PCR)

2.2.13.1 Primer design

A set of forward and reverse primers was designed to be complementary to the E1^E4 target gene sequence. Additional nucleotide sequences were added in order to encode a Kozak start site (Alberts, 2002) (forward primer only) and to incorporate restriction sites (Hind III, BamH I). PrimerSelect software (DNASTAR Inc., Madison, USA) was used to predict and minimize the formation of primer dimers and hairpin loops. Primers were obtained from Oswel Research Products Ltd. (Romsey, UK).

AAG AAG G /AA GCT T /AC CAT GGC TGA TCC TGC AGC -forward
Hind III E4

ATC ATT GTG ATG TGG GTA TC /CCTAGG/ TGG TGG -reverse
E4 BamH I

2.2.13.2 PCR reaction mix

Reagents used per 25μl reaction:

Template DNA	100 ng
Deoxyribonucleotides (dNTPs)	2.5 mM each
10 x PCR buffer (ABgene)	2.5 μl
$MgCl_2$ (ABgene)	2.5 mM
Forward primer	10 pmol
Reverse primer	10 pmol
Taq Gold polymerase (ABgene)	1μl

The total volume was made up with ddH_20.

2.2.13.3 PCR conditions

PCR was performed on a PTC-200 DNA Engine Thermal Cycler (MJ Research, GRI, Braintree, UK) using the following program: 1 min at 94 °C (DNA denaturation) followed by 1 min at 54 °C (primer annealing) followed by 1 min at 72 °C (DNA elongation). This cycle was repeated 30 times and followed by a final DNA elongation step of 10 min at 72 °C. A heated lid was used throughout.

2.2.13.4 Purification of PCR product

Following separation on a 1% agarose gel, the PCR reaction products were purified using the QIAquick Gel Extraction Kit (QIAGEN Ltd., Crawley, UK) in accordance with the manufacturer's instructions.

2.2.14 Ligation of insert into vector

Following restriction endonuclease digestion, the concentrations of the insert and vector were determined by gel quantification on a 1 % agarose gel using a low DNA mass ladder (Invitrogen Ltd., Paisley, UK). The insert was ligated with 0.5 μg of vector at a 6:1 molar ratio, using 40 U of T4 DNA ligase (New England Biolabs Ltd., Hitchin, UK) in a total volume of 20 μl, and by incubation at 4 °C for 16 h, according to the manufacturer's instructions

2.2.15 Colony selection following ligation

Ligation reactions were used to transform *E.coli* as described in Section 2.2.6. To select colonies containing a correctly orientated insert, individual colonies were picked and used to inoculate 2.5 ml of LB, containing a suitable selective antibiotic. Overnight cultures were subsequently screened by PCR and restriction digest to assays. A PCR reaction was then carried out to determine the presence of an insert; reactions were carried out as described in Section 2.2.12. Reaction products were run on a 1% agarose gel. Reactions resulting in a 300 bp band in the gel indicated the presence of insert in

the culture. The plasmid was prepared by miniprep as described in Section 2.2.7. Plasmid was digested as described in Section 2.2.11 and the reactions run on a 1% agarose gel to check for the presence of insert. Colonies with a positive result in both these assays were selected. DNA was prepared from these colonies as described in Section 2.2.7.

2.3 Cell culture techniques

2.3.1 Cell lines

2.3.1.1 SiHa cells

SiHa cells (Friedl et al., 1970) are a transformed cervical epithelial cell line derived from a tumour containing integrated HPV16 genomes. SiHa cells constitutively express E6/E7 but lack E1^E4 expression due to loss of the E1^E4 ORF caused by integration of the viral genome. This cell type gives high efficiency infection with recombinant adenoviruses (rAd).

2.3.1.2 AK8 & AK13 cells

Both cell lines were derived from a vulva carcinoma cell line and were kindly provided by Rudolph Leube (Windoffer *et al.*, 1999); (Strnad *et al.*, 2001). AK8 cells were stably transfected with ECFP-human keratin 8 plasmid and express a ECFP-tagged 8/18 keratin network. AK13 cells were stably transfected with an EGFP-human keratin 13 plasmid. Both cell lines are grown in 1 μg/ml geneticin every fourth passage to maintain expression levels.

2.3.1.3 HaCaT cells

HaCaT cells are a human keratinocyte cell line which was obtained following the transformation of normal skin cells by culturing in calcium-rich medium (Boukamp *et*

al., 1988). HaCaT cells express numerous keratin subtypes, including K8/18 and K5/14, and also K1/10 and K5/13, which are differentiation-dependent.

2.3.1.4 SW13 C2 and T7K cells

The SW13 C2 cell line was derived from a human adrenal tumour (Hedberg *et al.*, 1986). This cell line lacks expression of any intermediate filament networks but contains intact microtubule and actin cytoskeleton networks. The SW13 T7K cell line also expresses a functional keratin 8/18 network. These cell lines could be transfected and rAd infected.

2.3.2 Routine cell culture

Unless otherwise stated, cells were grown in medium A in flasks of surface area 75 cm^2 at 37 °C and 5 % (v/v) CO_2. Cells were grown to 80 % confluence before being subcultured. To do this, cells were washed in 2 ml trypsin/versene then 2 ml fresh trypsin/versene was applied to the cells for approximately 5 min at 37°C until they became detached from the flask. Trypsin was quenched by the addition of 5 ml of medium. Cells were routinely split 1/20 into a new flask containing 10 ml of medium.

2.3.3 Long term storage of cells

Cells were detached from the flask as described above and harvested by centrifugation at 2500 g for 5 min at r.t. Cells were suspended in 5 ml cell freezing solution (FCS containing 10 % DMSO) and divided into 1 ml aliquots which were then wrapped in 5 layers of paper tissue. Tubes were then transferred to a -70 °C freezer for 16 – 24 h. After freezing, cells were transferred to liquid nitrogen for long term storage.

2.4 Cell transfection and infection techniques

2.4.1 DNA transfection

Cells were seeded onto glass cover slips in the wells of a 24 well plate at a density of $3x10^4$ cells in 0.5 ml medium per well and grown for 24 h as described in Section 2.3.2. Cells were then transfected using GeneJuice® transfection reagent (Novagen, Nottingham, UK) in accordance with the manufacturer's instructions using vectors prepared as described in section 2.2.1.

2.4.2 Infection of cells with adenovirus

2.4.2.1 G1/S phase synchronization of SiHa cells

To arrest SiHa cells at the G1/S phase boundary prior to rAd infection, 70% confluent flasks of SiHa cells were grown in low-serum medium (medium A containing 0.5% (v/v) FCS) for 48 h. Cells were then treated with trypsin (Section 2.3.2) and grown in 90 mm dishes at a density of $5x10^5$ cells per dish in 5 ml medium A containing 2 μg/ml aphidicolin. Cells were released from this block after 24 h by washing 3 x in 5 ml of sterile PBS and incubation in medium A.

2.4.2.2 Adenovirus infection of SiHa cells

Adenovirus was applied to SiHa cells at a multiplicity of infection of 100 virus particles per cell in 5 ml of medium A for 24 h medium was then removed and the cells were washed twice with 5 ml PBS and incubated in fresh medium A. Time points were measured from the point of rAd addition to cells.

2.5 Biochemical and cell biology techniques

2.5.1 Antibody techniques

2.5.1.1 Preparation of phage antibody

The B11 Fab antibody was purified from the periplasmic space of *E. coli* as follows. An overnight culture of *E. coli*, transformed with pUC119His.6myc containing an HPV 16

immunoglobulin gene (Doorbar *et al.*, 1997), was set up in 10 ml 2 x TY medium containing 1 % glucose. This was used to inoculate two flasks each containing 1.5 l TY medium and 0.1 % glucose. Cells were grown at 37 °C to an A_{600} value of 0.8, induced with 1 mM IPTG and grown for 3 h at 30 °C. Cells were harvested by centrifugation in a Beckman J6 centrifuge at 2000 g for 15 min at 4 °C. They were gently suspended in ice-cold resuspension buffer (0.6 M sucrose, 1 mM EDTA, 30 mM Tris, pH7.9) and left for 20 min on ice. Cells were then centrifuged in a Beckman JA20 rotor at 5000 x g for 10 min at 4 °C and the supernatant was reserved on ice. The pellet was resuspended in ice-cold 5 mM $MgSO_4$ and incubated for 20 min on ice. Cells were centrifuged once more as before, the supernatant was combined with the previous one and this preparation (termed the "periplasmic prep") was stored at -20 °C. If either supernatant was cloudy then it was centrifuged at 5000 g as above until all particulate material had been removed. Ni-NTA Agarose resin (QIAGEN) was centrifuged at 200 g for 5 min at 4 °C in a bench top centrifuge. The ethanol was removed and discarded and the beads were washed in 10 ml of binding buffer (0.5 M NaCl, 5 mM imidazole, 20 mM Tris, pH7.9) by centrifugation as before. Washed beads were added to the periplasmic prep and put on an end over end rotator at 4 °C for 1 h to allow binding. Beads were centrifuged as before and the supernatant discarded. The beads were resuspended in 80 ml of binding buffer and placed on the end over end rotor for a further 10 min followed by centrifugation as before. The resin was then washed twice more in 30 ml binding buffer by resuspension and centrifugation as before. Beads were resuspended in 30 ml of binding buffer and then transferred to a Poly-Prep column (Bio-Rad Laboratories Ltd.). The excess buffer was allowed to run through and the column was washed with a further 5 ml buffer. The antibody was eluted with 6 ml of elution buffer (0.5 M NaCl, 1 M imidazole, 20 mM Tris, pH7.9), immediately transferred to prepared dialysis tubing

(Pierce SnakeSkin™, 7000Da cut-off, Perbio Science UK Ltd.) and dialysed overnight against 3 l of PBS at 4 °C. The PBS was changed for another 3 l and dialyzed for a further 3 h. The final solution was snap frozen and stored at -20 °C.

2.5.1.2 Conjugation of phage antibody to Alexa Fluor® 488

The protein concentration in the antibody preparation was determined by taking the A_{280} value as described in Section 2.2.9. The solution was then concentrated in an Amicon® Ultra-15 Centrifugal Filter Device (Millipore Ltd., Watford, UK; MWCO 10000) to a concentration of 2 mg/ml. The protein was then labelled using the Molecular Probes™ Alexa Fluor® 488 Labelling Kit (Invitrogen Ltd.) in accordance with the manufacturer's instructions.

2.5.2 Sample preparation from cells prior to immunoprecipitation and/or gel electrophoresis

2.5.2.1 Treatment of cells with proteasome inhibitors

Cells were infected with 16E4 or β–gal rAd as described in Section 2.4.2.2. Cells were treated with either 10 μM ALLN (Calbiochem, VWR International Ltd.), 10 μM of MG132 (Sigma-Aldrich Company Ltd.) or 5 μl of vehicle (DMSO) 18 h prior to harvesting.

2.5.2.2 Harvesting cells treated with proteasome inhibitors

Cells were washed twice in PBS and the plates were inverted and blotted dry on clean tissue. Lysis buffer (1 % (w/v) SDS/PBS 150 μl per plate) was added and the cells scraped off with a cell scraper. Genomic DNA was digested from lysate by the addition of Benzonase (125 U/Plate) Novagen, Merck Biosciences Ltd., Nottingham, UK).

2.5.2.3 Treatment of cell lysate with isopeptidase

SiHa cells were seeded in a 90 mm dish at a density of 5 x 10^5 cells/dish. Cells were infected with rAd as described in Section 2.4.2.2 24 h after seeding. Cells were

harvested 48 h post infection by incubation in 1 mM EDTA in PBS followed by cell scraping and centrifugation at 2500 g for 5 min at r.t. The pellet was suspended in 400 µl of reaction buffer (25 mM HEPES pH 7.5, 10 mM DTT, 0.5 % NP40 (v/v)) and the resulting cell lysate was treated with 0.5 µl Benzonase (125U) and placed on ice for 30 min, mixing every 10 min during the incubation. Isopeptidase (4 U, Calbiochem) was added to 5 µl of reaction buffer and incubated at r.t. for 15 min. Cell lysate (2 µl) was added and the mixture incubated at r.t. for 20 min. The mixture was boiled for 5 min in Laemmli buffer and the proteins were separated on a 12 % SDS-PAGE gel and visualized by western blot (Section 2.5.5). To determine the extent of the reaction treated and untreated control samples were probed with a ubiquitin antibody. Successful reactions were determined by significant redistribution of ubiquitin bands.

2.5.2.4 Cell fractionation

SiHa cells were fractionated according to solubility in different detergents. Following rAd infection and harvesting (see Section 2.5.2.2) the cell pellet was suspended in 200 µl of lysis buffer (1 % (v/v) NP40, 0.5 µl Benzonase (125U) and 25 mM Complete Protease Inhibitor Cocktail in PBS). The cell lysate was incubated with rotation for 1 h at 4 °C and then centrifuged at 10000 g for 10 min at 4 °C. The supernatant (the "NP-40 fraction") was reserved. The pellet was suspended in 200 µl PBS containing 1% EMPIGEN BB™ (v/v) and 25 mM Complete Protease Inhibitor Cocktail by vigorous pipetting, and incubated with rotation as before. The extract was centrifuged as before and the supernatant (the "Empigen fraction") was reserved. The remaining protein pellet was suspended in 200 µl of 9 M urea (the "urea fraction"). All fractions were stored at – 20 °C.

2.5.3 Sample preparation from tissue sections prior to immunoprecipitation and/or gel electrophoresis

2.5.3.1 Sectioning lesions using a cryostat

HPV lesions stored under liquid nitrogen were defrosted and fixed in acetone for 3 min at -20 °C. Following 5 min rehydration in 20 ml distilled water they were placed in a plastic mould and covered in OCT compound (VWR International Ltd.). OCT compound was solidified by dipping the mould into absolute ethanol cooled to -78 °C with solid CO_2. The block was then crudely trimmed using a razor blade and left a further 10 min in the cryostat (Leica JUNG CM3000). A piece of moistened filter paper was attached to a cryostat chuck by immersion in chilled ethanol, OCT compound was applied to this and the lesion attached by solidifying the OCT compound in chilled ethanol. The chuck was mounted into the cryostat and excess OCT compound was removed with a razor blade. Slices (20 μm) were taken through each lesion from top to bottom. Sections were collected in pairs using forceps pre-cooled on dry ice; each pair was stored at -80 °C in a 1.5 ml microcentrifuge tube.

2.5.3.2 Protein extraction from lesions

Sectioned lesions were defrosted and 40 μl of protein extraction buffer (1 mM DTT, 10 % (w/v) SDS in PBS) added to each tube. Following 2 min incubation with 0.5 μl Benzonase (125U) at 4 °C, the protein was solubilized vigorously using a pipette. Samples were boiled for 20 min before SDS-PAGE (Section 2.5.5).

2.5.4 Immunoprecipitation techniques

2.5.4.1 Covalent coupling of antibody to protein G sepharose beads

Protein G sepharose beads (50 μl) were equilibrated by washing in binding buffer (1 % NP-40 / PBS) and centrifuged 3000 g for 5min to remove ethanol (two washes were performed). For antibody coupling, equilibrated beads were suspended in 1 ml of binding buffer and antibody was added. The mixture was rotated for 1 h at 4 °C to allow

antibodies to bind. Beads were washed twice in 1 ml 0.2 M sodium borate (pH 9.0) by centrifugation as before. Beads were suspended in 1 ml of this buffer and 20 µl were taken for analysis. Solid dimethyl pimelimidate (DMP) was added to a concentration to 20 mM. The mixture was rotated for 30 min at r.t. and 20 µl were taken for analysis. The reaction was stopped by washing the beads once in 1 ml of 0.2 M ethanolamine (pH 8.0) by centrifugation as before followed by suspension in 1 ml fresh ethanolamine buffer and rotation for 2 h at 4 °C. Beads were then washed twice in 1 ml PBS by centrifugation as before, suspended in 1 ml of PBS containing 0.01 % (w/v) sodium azide and stored at 4 °C.

2.5.4.2 Analysis of antibody coupling efficiency

Beads were removed prior to and after the addition of the covalent cross linking agent DMP, as described above. They were boiled for 5 min in 2 volumes of Laemmli buffer, and separated by SDS-PAGE and stained with Coomassie Brilliant Blue R-250 as described in Section 2.5.5. Coupling was deemed successful if antibody heavy chains could not be detected after the addition of DMP.

2.5.4.3 Immunoprecipitation

SiHa cells were grown in 90 mm dishes and infected with rAd as described in Section 2.4.3. They were harvested 24 h post infection in 200 µl of lysis buffer (1 % (w/v) SDS in PBS), treated with 0.5 µl Benzonase (125 U) and centrifuged at 13000 g for 10 min. Supernatant (50 µl) was mixed with 950 µl binding buffer (1 % (v/v) NP-40 in PBS), incubated at 4 °C on an end over end rotator for 1 h and centrifuged at 13000 g for 10 min at 4 °C to remove any precipitated protein. The supernatant (950 µl) was mixed with 5 µg antibody and allowed to bind on an end over end rotator as before. Equilibrated protein G sepharose beads (Section 2.5.4.1; 50 µl) were added to the mixture, which was rotated for 1 h at 4 °C. Following centrifugation at 1000 g for 2 min

at r.t. beads were suspended in 1 ml of binding buffer, this wash was repeated 4 times. The proteins were eluted by boiling in 20 µl Laemmli buffer (-DTT) for 5 min at 95 °C and visualised by SDS-PAGE and western blot (Section 2.5.5).

2.5.4.4 Immunoprecipitation using antibodies coupled to protein G sepharose beads

Beads that had been coupled to antibodies were washed 3 times in binding buffer and suspended in 1 ml of binding buffer as described in Section 2.5.4.1. Cell lysates and beads were incubated with rotation for 3 h at 4°C. Beads were then washed and treated as described in the previous section.

2.5.5 Gel electrophoresis and protein analysis

2.5.5.1 SDS polyacrylamide gel electrophoresis (SDS-PAGE)

Gels were cast in Mini-PROTEAN® II gel apparatus (Bio-Rad Laboratories Ltd.) according to the table below. Samples were loaded onto gels and separated by electrophoresis in gel running buffer (25 mM Tris pH 8.3, 200 mM glycine, 0.1 % SDS) at 150 V and 200 mA until the dye front reached the end of the gel. Rainbow™ Molecular Weight Markers (Amersham Pharmacia Biotech UK Ltd.) were used to determine the mass of separated proteins.

	12 %	15 %	Stacking gel
Water	3.3 ml	2.3 ml	6.8 ml
ProtoGel® (30 % acrylamide, 0.8 % bis-acrylamide)	4.0 ml	5.0 ml	1.7 ml
1.5 M Tris (pH 8.8)	2.5 ml	2.5 ml	-
1.0 M Tris (pH 6.8)	-	-	1.25 ml
10 % SDS	0.1 ml	0.1 ml	0.1 ml
10 % APS	0.1 ml	0.1 ml	0.1 ml
TEMED	4 µl	4 µl	10 µl

Table 2.4 Polyacrylamide gel recipes

2.5.5.2 Silver staining of SDS-PAGE gels

Gels were fixed in 50 % (v/v) methanol for 30 min, incubated in 0.019 % (w/v) sodium thiosulfate solution for 1 min and briefly washed three times in ddH_2O. Gels were then

incubated with staining solution (0.37 % (w/v) formaldehyde, 0.26 % (w/v) silver nitrate) for 8 min and briefly washed three times with ddH_2O. Bands were visualized using developing solution (2 % (w/v) sodium carbonate, 0.016 % (w/v) formaldehyde, 0.004 % (w/v) sodium thiosulfate). The staining reaction was stopped with 1 % (v/v) acetic acid.

2.5.5.3 Coomassie blue staining of SDS-PAGE gels

SDS-PAGE gels were incubated in Coomassie blue stain (0.25 % (w/v) Coomassie Brilliant Blue R-250, 50% (v/v) methanol, 10 % (v/v) acetic acid) for 30 min with shaking. Gels were rinsed three times in ddH_2O and incubated in destain solution (50 % (v/v) methanol, 10 % (v/v) acetic acid) overnight with shaking, a tissue being placed in the container to soak up excess dye.

2.5.5.4 Transfer of proteins to membranes (western blotting)

Protein from gels was transferred to Immobilon-P membrane (Millipore Ltd.) using a Mini Trans-Blot® (Bio-Rad Laboratories Ltd.) at 150 V, 200 mA for 2 h in transfer buffer (25 mM Tris-HCl pH 8.3, 200 mM glycine, 20 % (v/v) methanol). Membranes were blocked by incubation with Marvel solution (5 % (w/v) Marvel (Premier International Foods Ltd., Spalding, UK) in PBS) overnight at 4 °C.

2.5.5.5 Detection of protein on membranes

Primary and secondary antibodies were diluted in Marvel solution before use (see antibody table "Table- 2.5"). Membranes were incubated in primary antibody for 1 h at r.t., rinsed in PBS and washed three times in PBS containing 0.1 % (v/v) TWEEN® 20 (Sigma-Aldrich Company Ltd.) for 5 min at r.t. This process was repeated using the appropriate secondary antibody. Binding of the secondary antibody was visualized using the ECL ™ Western blotting analysis system (Amersham Biosciences Ltd., Little

Chalfont, UK) followed by exposure to Kodak MXB X-ray film (Xograph Imaging Systems Ltd., Tetbury, UK).

2.6 Staining and imaging techniques

2.6.1.1 Antibody staining of cells grown on cover slips

Cells that had been grown on and either transfected or infected on cover slips (see Section 2.4) were washed twice in PBS, fixed in 100 % methanol for 2 min at -20 °C and washed twice in PBS. They were then blocked in 300 µl of blocking solution (2 % (w/v) BSA in PBS) for 1 h. Antibodies were diluted (see "Table2 5.") in staining solution (1 % (v/v) FCS in PBS). Cover slips were inverted and each was placed on a 50 µl drop of primary antibody on a sheet of sealing film and incubated in a darkened humidified chamber for 1 h at r.t. They were then washed once in PBS containing 0.1 % (v/v) TWEEN® 20 and three times in PBS. If required, cover slips were incubated in a second primary antibody and then washed as before. They were then incubated in a solution of secondary antibody(s) containing 1µg/ml DAPI as above. They were washed as before, rinsed in distilled water, blotted dry and mounted on a 5 µl drop of Citifluor™ (Agar Scientific Ltd., Stansted, UK) on a microscope slide.

2.6.1.2 MitoTracker staining of cells grown on cover slips

Cells were transfected on cover slips as described in Section 2.4.1. Medium was removed 30 min prior to fixation and replaced with 500 µl medium containing MitoTracker Red (Molecular Probes™, Invitrogen Ltd.) diluted 1/4000 from stock (1 µM in DMSO stored -20 °C). Cells were incubated in 5 % CO_2 for 30 min at 37 °C before being fixed with methanol and stained as above.

2.6.1.3 Antibody staining of formalin fixed paraffin embedded tissue sections

Formalin fixed paraffin embedded tissue sections were given three 5 min washes in xylene, rehydrated in graded ethanol (100 %, 80 %, 50 % and then 30 % (v/v), sequentially; 5 min in each) and washed in PBS. They were then heated in a microwave on high power for 18 min in phosphate citrate buffer (0.05 M sodium phosphate, 0.025 M citric acid, pH 6.0). The sections were allowed to cool on the bench for 5 min before two 5 min washes in PBS. The sections were then blocked for 2 h in 10 % (v/v) normal goat serum (Dako Ltd., Ely, UK) in PBS. Antibody solutions were prepared as in Section 2.6.1.1. Sections were wiped to remove excess blocking solution, 50-200 µl of primary antibody was applied to the tissues, and the slides were placed in a darkened humidified chamber overnight at 4 °C. They were then washed three times for 5 min in PBS containing 0.1 % (v/v) TWEEN® 20. The incubation was repeated with a second compatible (i.e. rabbit and mouse) primary antibody solution; sections were washed again and subsequently incubated, with Alexa 488 and 594 conjugated secondary antibodies containing 1 µg/ml DAPI, washing after each incubation as before. The slides were then rinsed in distilled water and mounted in Citifluor using an appropriately sized cover slip.

2.6.2 Imaging techniques

2.6.2.1 Low power microscopy

Low power images of tissue sections were acquired using a Labophot II microscope (Nikon Ltd., Kingston-upon-Thames, UK). Images were acquired using a SenSys monochrome camera using IPLab imaging software (Roper Scientific, Marlow, UK). Three colour images were produced using the software to overlay separate channels.

2.6.2.2 Confocal microscopy

Cells images were acquired using a Leica DMRXE upright microscope (Leica Microsystems Ltd., Milton Keynes, UK) and a 100 x objective lens, unless otherwise stated. Specimens were scanned using the following excitation (ex) and emission (em) wavelengths: DAPI, ex 359 nm, em 395-520 nm; Alexa-488, ex 488 nm, em 505-685 nm; Alexa-594, ex 568 nm, em 595-710 nm; Cy5, ex 647 nm, em 655-725 nm. Fluorophores were excited sequentially to reduce cross channel bleed through and to allow maximum emission detection. Specimens were scanned with 0.5 μm intervals between Z sections with 4 accumulations per frame. Images are presented as an overlay projection of all frames, resulting in a composite image, or as an individual optical section when examining fine structures.

2.6.2.3 Quantitative confocal microscopy

To quantify protein expression levels (using fluorescence), samples were stained using identical concentrations of both primary and secondary antibodies. Image colour was adjusted using the overglow-underglow function; where possible, gain and overglow were adjusted to remove all off scale pixels (green pixels have grey scale values <0, blue pixels have grey scale values >255. When this was not possible, settings were set to give the lowest fluorescence at which an image could be obtained. Fluorescence intensities were analysed using built-in software (Leica. Microsystems Ltd.).

2.6.2.4 Time-lapse microscopy

Cells were seeded at $3x10^5$ cells per dish in 60 mm glass bottom dishes (MatTek Corporation, Ashland, USA). Cells were grown for 24 h (medium A) before being transfected with EYFP16E4 using Genejuice (Section 2.4.1). Medium was replaced 12-24 h after transfection with 2 ml of warmed time-lapse medium. The cells were transferred to the chamber of a DeltaVision microscope (Olympus Ltd., London, UK)

that had been preheated to 37 °C. The cells were left to equilibrate for at least 1 h then imaged using a 100 x lens at Bin 1.

2.6.2.5 Fluorescence recovery after photobleaching (FRAP)

FRAP experiments were performed on living cells plated as described previously using a DeltaVision microscope equipped which a 488 nM Quantifiable Laser Module (QLM). The beam expander was set to position 1 and the Laser spot centred using a target cell. During centring, the laser intensity was set to 12 % for the minimum spot size. Targets were then aligned using the pre-adjusted cross hairs. Targets were bleached by a 0.05 s pulse with the laser set at 25 % power. Subsequent images were captured using softWoRx® QLM software (Applied Precision®, LLC, Marlborough, UK). Bleached targets were then tracked using a custom built patch (provided by Dan Zue NIMR) in ImageJ and then exported to and analyzed using Microsoft® Office Excel software.

Antigen	Antibody	Raised in	Supplier	Western Blot	Immunohistochemitry/ Immunocytochemitry
HPV 16E4	TVG402	Mouse	In House	1/20	1/10
High risk HPV E1^E4's	TGV405	Phage	In House	-	1/100
Pan Keratin Ab cocktail (C2562)	(C2562) C-11, PCK-26, KS-90, Ks-1A3, M20, A53-B/A2	Mouse	Sigma	1/1000	1/200
Pan Keratin	Ab8797	Rabbit	abcam	-	1/1
Keratin 5 & 8	Cam5.2	Mouse	MRC	1/100	1/10
Keratin 18	Cy-90	Mouse	Sigma	1/1000	1/200
Keratin 1	LH1	Mouse	ICRF		1/10
Keratin 1	NCL-CK1	Mouse	Novacastra	-	1/100
Keratin 4	NCL-CK4	Mouse	Novacastra	-	1/100
Keratin 5	LH8	Mouse	ICRF	-	1/10
Keratin 5	NCL-CK5	Mouse	Novacastra	-	1/100
Keratin 16	LL025	Mouse	ICRF	-	1/10
Keratin 10	NCL-CK10	Mouse	Novacastra	-	1/100
Keratin 10	K0199-12	Mouse	US Biological	1/100	-
Keratin 13	NCL-CK13	Mouse	Novacastra	-	1/100
Keratin 14	LL001	Mouse	ICRF	-	1/10
Keratin 14	NCL-ll002	Mouse	Novacastra	-	1/100
Keratin 14	C9097-14B	Mouse	US Biological.	1/200	-
LJ4	LJ4	Mouse	Omary MB.	1/1000	1/100
3055	3055	Rabbit	Omary MB.	1/2000	1/1000
2D5	2D6	Mouse	Omary MB.	1/1000	1/100
8250	8250	Rabbit	Omary MB.	1/2000	1/1000
IB4	IB4	Mouse	Omary MB	1/1000	1/100
α Tubulin	B512	Mouse	Sigma	-	1/250

α Mouse A488	A-11029	Goat	Molecular Probes	-	1/200
α Rabbit A488	A-11034	Goat	Molecular Probes	-	1/200
α Mouse A594	A-11032	Goat	Molecular Probes	-	1/200
α Rabbit A594	A-11037	Goat	Molecular Probes	-	1/200
α Goat A594	A-11058	Donkey	Molecular Probes	-	1/200
α Mouse HRP	NA931	Goat	Amersham	1/2000	-
α Rabbit HRP	NA934	Donkey	Amersham	1/2000	-
α Rat A594	A-21211	Rabbit	Molecular Probes		1-200
HPV2 E4	-	Rabbit	In House	-	1/750
HPV11 E4	-	Rabbit	In House	-	1/100
HPV1 E4	-	Rat	In House	-	1/500
HPV1 E4	-	Rabbit	In House	-	1/?
HPV18 E4	-	Rabbit	In House	-	1/500
HPV 4 E4	-	Rabbit	In House		1/750
HPV65 E4	-	Rabbit	In House		1/750
Mitochondria	Mtco2	Mouse	RDI	-	1/100
Cyclin B	GNS11	Mouse	Neomarkers	-	1/200
MCM7	47DC141	Mouse	Neomarkers	-	1/150
GAPDH	MAB374	Mouse	Chemicon	1/2000	-
Ubiquitin	Sc-8017	Mouse	Santa cruze	1/200	1/100
Ubiquitin	Z0458	Rabbit	DAKO	1/2000	1/500

Table 2.5 Antibodies

3 Conservation of function between E1^E4 proteins

3.1 Aims

The E1^E4 protein is a complex protein with multiple and varying functions, the purposes of which are not yet fully understood. The aim of this study was to use immunofluorescent staining to determine whether the known functions of the HPV 16 E1^E4 protein (mitochondrial, keratin and cyclin B binding) are conserved in other high risk α-group E1^E4 proteins. The properties of HPV 2 E1^E4, and α-group virus that causes benign cutaneous infections, was also investigated to determine if viruses with mucosal and cutaneous tropism from the same genera behave in the same fashion. In addition to these viruses, it was decided to investigate whether the E1^E4 proteins from an evolutionary distant branch of the phylogenetic tree share functions with α-group E1^E4 proteins. The closely related HPV types 4 and 65 γ-group viruses, which cause benign cutaneous infections, were included in the study in order to determine whether they shared any functions with each other, the cutaneous HPV2 E1^E4 protein or other α-group E1^E4 proteins. It is hoped that the finding of this study will help to better understand the role of the E1^E4 protein in the virus lifecycle.

3.2 Introduction

3.2.1 Methods used to classify papillomaviruses

Initial attempts to classify papillomaviruses have investigated tissue tropism, hybridisation and restriction enzyme mapping in order to characterise different isolates (O'Banion *et al.*, 1987). More accurate classifications were achieved using DNA sequence data (Cole *et al.*, 1987). The first comprehensive papillomavirus classification was achieved by amplifying a fragment of the L1 open reading frame of different papillomaviruses and comparing the DNA sequences (Chan *et al.*, 1995b). Several classifications have since followed, resulting in papillomaviridae phylogenetic trees

with similar topologies. The currently recognised classification system includes 118 papillomavirus types which have been classed into genera (de Villiers *et al.*, 2004) (see Fig 1.1). In addition to this, resent classification strategies have investigated whole genome alignments, which have suggested that genomes may have evolved in a modular fashion and that the high risk papillomaviruses may be more closely related than previously thought (Garcia-Vallve *et al.*, 2005).

3.2.2 Virus evolution

Papillomaviruses have been detected in both mammals and birds, (Chan *et al.*, 1992; de Villiers *et al.*, 2004) and appear extremely species specific. This suggests that papillomaviruses arose in an ancestor common to mammals and birds, suggesting that these viruses are approximately 200 million years old (Chan *et al.*, 1995b) (Fig 3.1). Since their emergence, papillomaviruses appear to have mutated remarkably slowly, making them a valuable tool for tracking animal evolution and population migration (Ho *et al.*, 1993; Ong *et al.*, 1993; Scherneck *et al.*, 1983). Although modern papillomaviruses display very limited abilities to jump species (productive infections were achieved from chimp to pigmy-chimp cross infections and non-productive cross infections from cow to horse (Lancaster *et al.*, 1977; Van Ranst *et al.*, 1992)), papillomaviruses appear not to have truly co-evolved with their hosts for two reasons. Virus phylogeny does not mirror host phylogeny accurately, breaking with Fahrenholz's rule[1], and therefore indicating that cross infections may have occurred though history (Chan *et al.*, 1995a), although re-classifications may change this. Selection pressure exerted on a host by a parasite is negligible when compared to the selective pressure exerted on the parasite by the host (Jermy, 1984). Therefore viral evolution should be

[1] Cospeciation is the process whereby one population speciates in response to and in concert with another, and is a consequence of the associates dependence on its host for its survival.

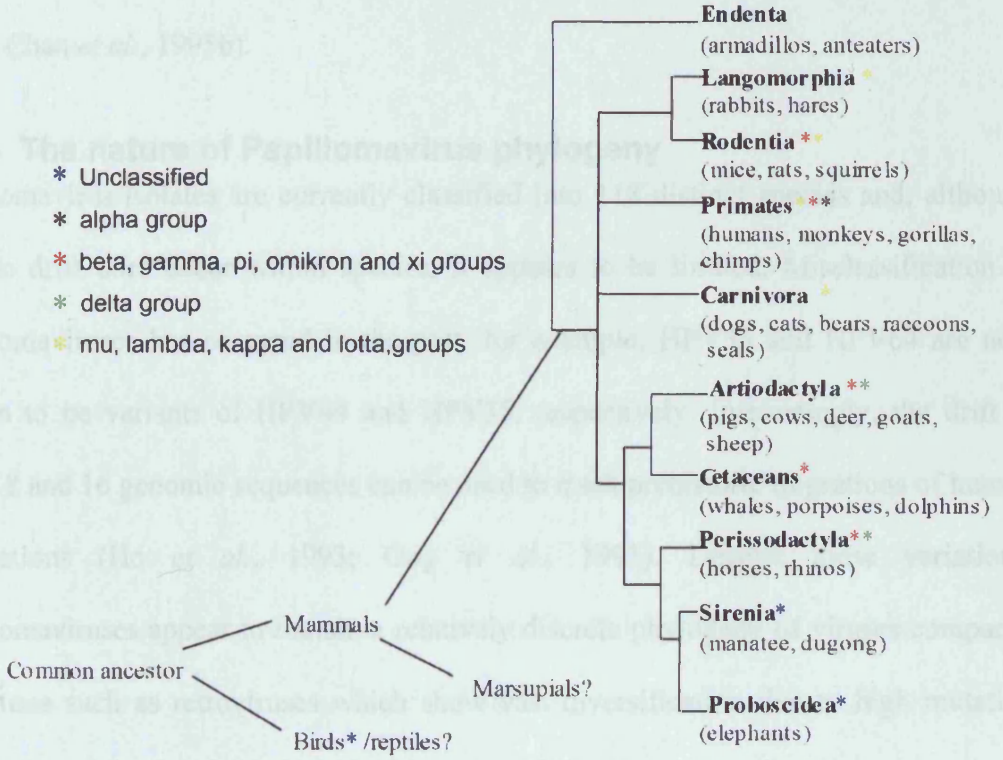

Figure 3.1 Mammalian evolution
Diagram shows the evolution of mammals and birds from a common ancestor over 200 million years ago. The spread of closely related papillomaviruses (see Fig 1.1) identified throughout the animal kingdom is shown. The branch containing the gamma, pi, omikron and xi viruses is the most divergent throughout the animal kingdom indicating that they may be the most ancient groups. The distribution of viruses in the branch containing the mu, lambda, kappa and lotta group viruses makes it possible to speculate an age of approximately 110 million years when hosts last shared a common ancestor (Benton and Ayala, 2003). Alpha group virus distribution is limited to primates, hinting at a more recent emergence. Data from (Antonsson and Hansson, 2002; Bossart et al., 2002; de Villiers et al., 2004; Jacobson et al., 1982; Tachezy et al., 2002; Villiers de, 2001).

described as sequential evolution with the virus being forced to evolve to accommodate modifications in biochemical mechanisms in the host (Bernard *et al.*, 1994; Chan *et al.*, 1997; Chan *et al.*, 1995b).

3.2.3 The nature of Papillomavirus phylogeny

Papillomavirus isolates are currently classified into 118 distinct species and, although genetic drift does occur within species, it appears to be limited. Misclassification of papillomaviruses has occurred in the past, for example, HPV55 and HPV64 are now known to be variants of HPV44 and HPV35, respectively. Interestingly, the drift in HPV18 and 16 genomic sequences can be used to track prehistoric migrations of human populations (Ho *et al.*, 1993; Ong *et al.*, 1993). Despite these variations, papillomaviruses appear to remain a relatively discrete phylogeny of viruses compared to viruses such as retroviruses which show vast diversification due to high mutation rates (Alberdi Leniz *et al.*, 2004; Bartolo *et al.*, 2005; Ciccozzi *et al.*, 2005).

3.2.3.1 Papillomavirus mutation rates

The discrete nature of papillomavirus phylogeny is likely due to them having a mutation rate comparable to that of their hosts, (1bp/several thousand years (de Villiers *et al.*, 2004)). This low mutation rate is partly due to papillomaviruses lacking any viral polymerase enzymes, which makes them reliant on high fidelity host cell DNA polymerases. The slow mutation rate is surprising considering that viral DNA replication occurs in cells expressing E6 and E7, which are usually associated with genetic instability (Banks *et al.*, 1987; Bedell *et al.*, 1989; Brusa *et al.*, 2003; Hawley-Nelson *et al.*, 1989). This may suggest that viruses are under constant selective pressure from sources such as the host immune responses. Various attempts to classify papillomaviruses in the past have used genes which show comparatively high levels of homology. The E4 gene sequence is of little use to taxonomists due to the lack of

homology shared between different virus subtypes. This suggests that the E4 gene may be a hotspot for the accumulation of mutations in the papillomavirus genome (Narechania *et al.*, 2005).

This work is part of an ongoing collaboration with other lab members (Woei Peh and Heather Griffin) whose aim is to characterise the function of the E1^E4 proteins from phylogenetically diverse papillomaviruses. Protein sequences were analysed and compared using a protein alignment tool and by observing immunostaining patterns in cell culture. HPV 16, 18, 31, 35 and 45 are all high risk mucosal tropic α-group viruses and were detected with the TVG405 antibody. HPV 2 is a cutaneous tropic α-group virus detected using a specific polyclonal antibody, and HPV 4 and 65 are both cutaneous tropic γ-group viruses, also detected using specific polyclonal antibodies.

3.3 Results

3.3.1 E1^E4 protein sequence alignments

E1^E4 gene sequences for HPV 1, 2, 4, 16,18, 31, 35, 45 and 65 were obtained from the HPV sequence website (http://hpv_web.lanl.gov/), and analysed using the Edit sequence program (DNASTAR incorporated, USA) and MultAlin sequence alignment software (http://prodes.toulouse.inra.fr/multalin/multalin.html.). Alignments were performed using the E1^E4 protein sequences from the α or γ genus alone, and also from the μ genus sequence (Fig 3.2)

All α-group E1^E4 proteins investigated appear to share an N-Terminal leucine cluster (LLXLL) (Fig 3.2 A and C red arrows), which was previously shown to be required for cytokeratin association (Roberts *et al.*, 1997; Wang *et al.*, 2004). α-group proteins also

Figure 3.2 Sequence alignments of HPV E1^E4 proteins
HPV E1^E4 sequences aligned using MultAlin software. (A.) α group sequence alignments. Note islands of sequence homology at the C and N terminus (black arrows) and the YPLLXLL domain (red arrows) as well as a proline rich region (blue arrows). (B) γ group sequence alignments show very high sequence homology throughout the entire protein length. The red arrows indicate the region used in the charge distribution table. (C) There is considerable heterogeneity between the α, γ and μ group E1^E4 proteins. The green arrows indicate the leucine cluster in HPV1 E1^E4.

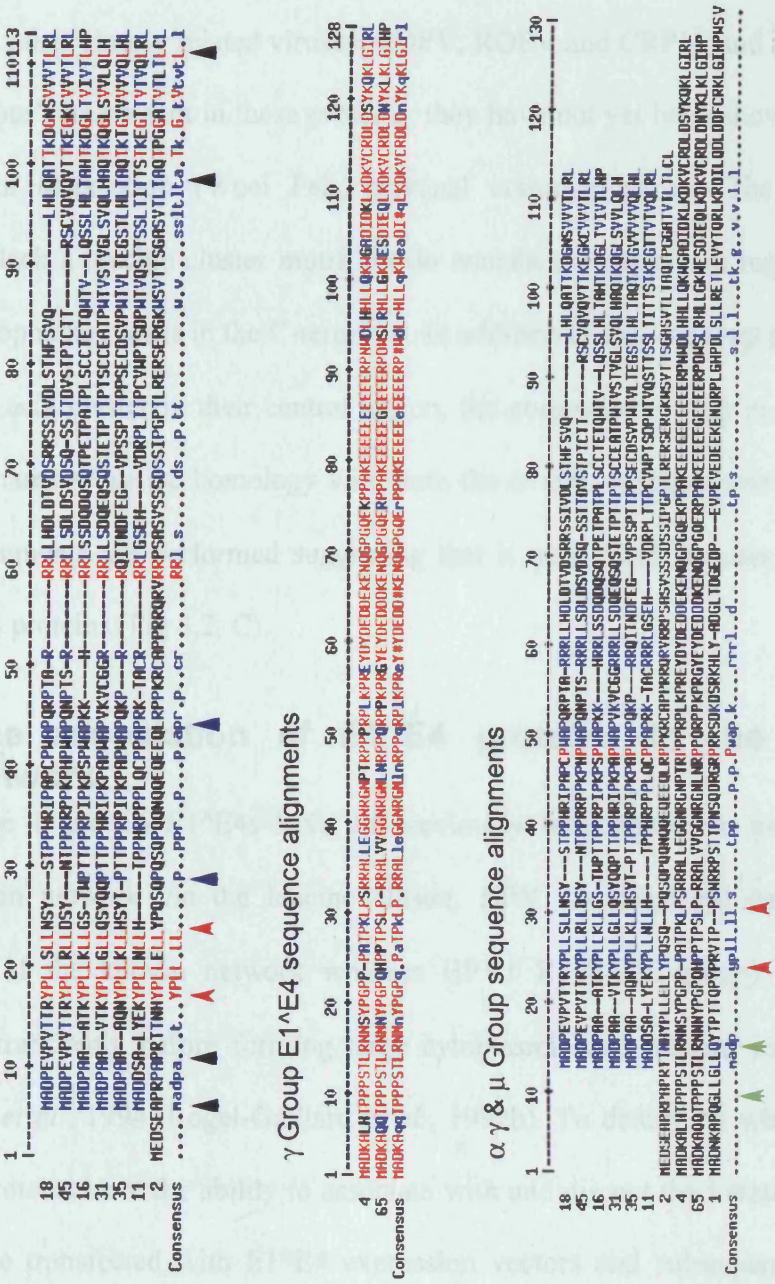
A.
α Group seqence alignments
B.
γ Group E1^E4 sequence alignments
C.
α γ & μ Group sequence alignments

share a proline rich region and a hydrophobic C-Terminal region thought to be involved in multimerisation (Bryan *et al.*, 1998; Wang *et al.*, 2004). A leucine cluster (Fig 3.2 C, green arrows) can also be seen in HPV 1 E1^E4, which has also been demonstrated to bind keratin (Roberts *et al.*, 1994). Interestingly, the leucine cluster is absent in other closely related viruses, COPV, ROPV and CRPV, and although "leucine rich regions" are present in these proteins, they have not yet been shown to be involved in keratin association (Woei Peh, personal communication). The γ-group E1^E4 proteins lack a leucine cluster motif but do contain a proline rich region in the centre and hydrophobic motifs in the C-terminus. In addition to this, γ-group proteins contain a glutamic acid cluster in their central region, the purpose of which is unknown. HPV1 E1^E4 shares sequence homology with both the α and γ-group proteins depending on how alignments are performed suggesting that it may share features with both types of E1^E4 proteins (Fig 3.2, C).

3.4 The association of E1^E4 proteins to the cytokeratin network

HPV type 1 and 16 E1^E4s have all previously been shown to associate with the cytokeratin network via the leucine cluster. HPV 16 (α-group) cause an apparent collapse of the keratin network whereas HPV1 E1^E4 (μ-group) appears to bind keratins transiently before forming large cytoplasmic and nuclear inclusion granules (Roberts *et al.*, 1994; Rogel-Gaillard *et al.*, 1992b). To determine whether other HPV E1^E4 proteins have the ability to associate with and disrupt the keratin network, SiHa cells were transfected with E1^E4 expression vectors and subsequently analysed by immunostaining. SiHa cells are a cervical cancer cell line and so were considered to be a suitable model for investigating the properties of the high risk α-group E1^E4 proteins. It is notable that the cutaneous tropic types 2, 4 and 65 may behave differently

when expressed in differentiated cutaneous keratinocytes. Attempts to express the proteins in HaCat cells failed due to the difficulties encountered in transfecting the cells.

3.4.1 The effect of fixation on E1^E4 and cytoskeletal filament networks

To determine the optimum fixation conditions for visualising E1^E4 and cytoskeletal filament, SiHa cells were fixed with either ice cold methanol (2 min) or 5 % (w/v) paraformaldehyde (5 min). Cells were subsequently stained for keratins (C2562 pan-keratin antibody) or microtubules (B512) and DNA (DAPI) and analysed by confocal microscopy. Cells fixed with methanol contained sharp and clearly defined keratin filaments and microtubules (Fig 3.3 B, D and F). No clear keratin filaments or microtubules could be observed in cells fixed with paraformaldehyde, suggesting that this fixation process destroys filaments (Fig 3.3 A, C and E). Transfected SiHa cells revealed that all the α-group proteins tested were able to produce sharp filamentous staining patterns when fixed with both methanol and paraformaldehyde (see Fig 6.14). Because of the differences observed in keratin and microtubule staining patterns, α-group E1^E4's were fixed with methanol in all experiments. Fixation protocols had a significant effect on the staining patterns observed for γ type E1^E4 proteins. Paraformaldehyde fixation resulted in a sharp E1^E4 filamentous staining pattern. Filaments could also be observed after methanol fixation but were significantly less apparent (compare Fig 3.4 D, (methanol) with Fig 3.7 S, (paraformaldehyde)). As a result of this finding, cells transfected with γ-group proteins were fixed using both methods and the findings are discussed in the following sections.

3.4.2 Association of E1^E4 proteins to the cytokeratin network

SiHa cell transfected with α-group E1^E4 expression vectors were fixed with methanol

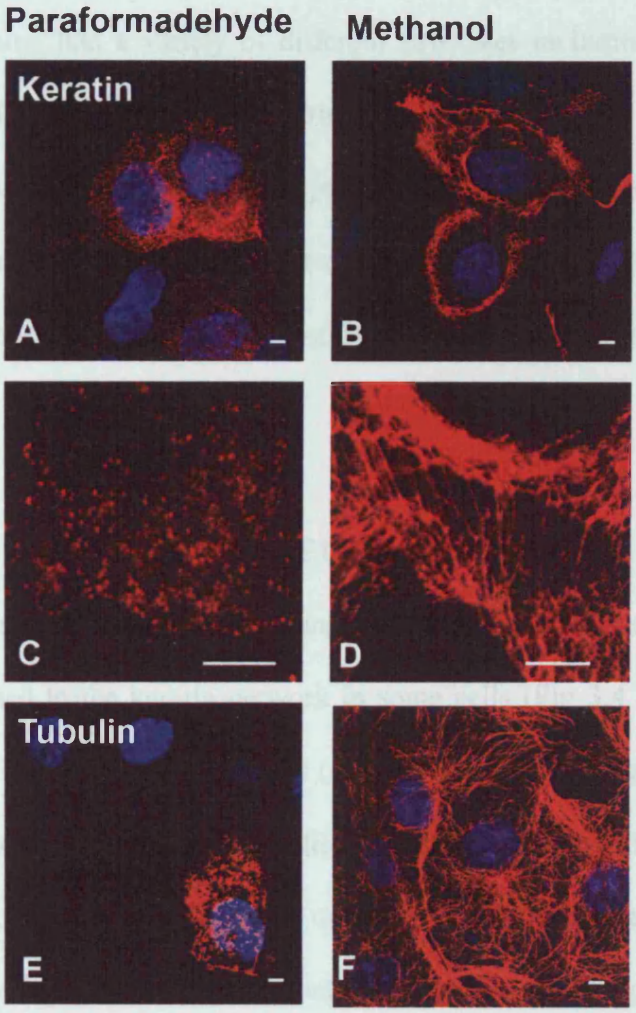

Figure 3.3 The effect of methanol and paraformaldehyde fixation on keratin and microtubules
SiHa cells were fixed with either methanol (-22 ^{0}C, 2 min) or paraformaldehyde (rt, 5 min) and subsequently stained for keratins or microtubules (red) and DNA (DAPI, blue). Paraformaldehyde fixation disrupted the filamentous appearance of both keratins and microtubules (A, C, E). Both microtubules and keratin filaments remained intact after methanol fixation (B, D, F). Scale bars denote 5 μm.

and stained for E1^E4, keratin (C2562) and DNA (DAPI). All α-group E1^E4 proteins investigated were shown to associate with the cytokeratin network in SiHa cells (Fig 3.4). E1^E4 staining had a variety of different structures including filaments bundles and aggregates. The majority of these structures colocalised with keratins suggesting that the association of α-group E1^E4 proteins to the keratin network induces the collapse of the affected network. This may suggest that a similar keratin bundling mechanism is conserved throughout α-group E1^E4 proteins regardless of tissue tropism.

Cells transfected with HPV 4 or 65 E1^E4 were fixed with either methanol or paraformaldehyde. Cells fixed with methanol contained weakly filamentous E1^E4 that partially colocalised to the keratin network in some cells (Fig 3.4 D-F, W-Y). Not all E1^E4 filaments co-stained with keratins (arrow Fig 3.4D-F), suggesting that γ-group E1^E4 proteins associated with a second filament network. Perinuclear keratin filament collapse was not observed to occur with 4 or 65 E1^E4. Cells transfected with HPV 4 or 65 E1^E4 fixed with paraformaldehyde contained significantly sharper E1^E4 filaments (see Fig 3.5) that did not colocalise with keratins filaments (data not shown), which were destroyed during the fixation process (see Fig 3.3). This finding suggests that keratin association may be a feature common to α-group E1^E4 proteins but not necessarily γ-group E1^E4's.

3.4.3 The association of E1^E4 proteins to microtubules

Having determined that γ-group E1^E4 proteins may be associated with cytoskeletal filaments other than keratin, the association of E1^E4 filaments to actin and microtubules was investigated (for further information on both see section 4.2.1).

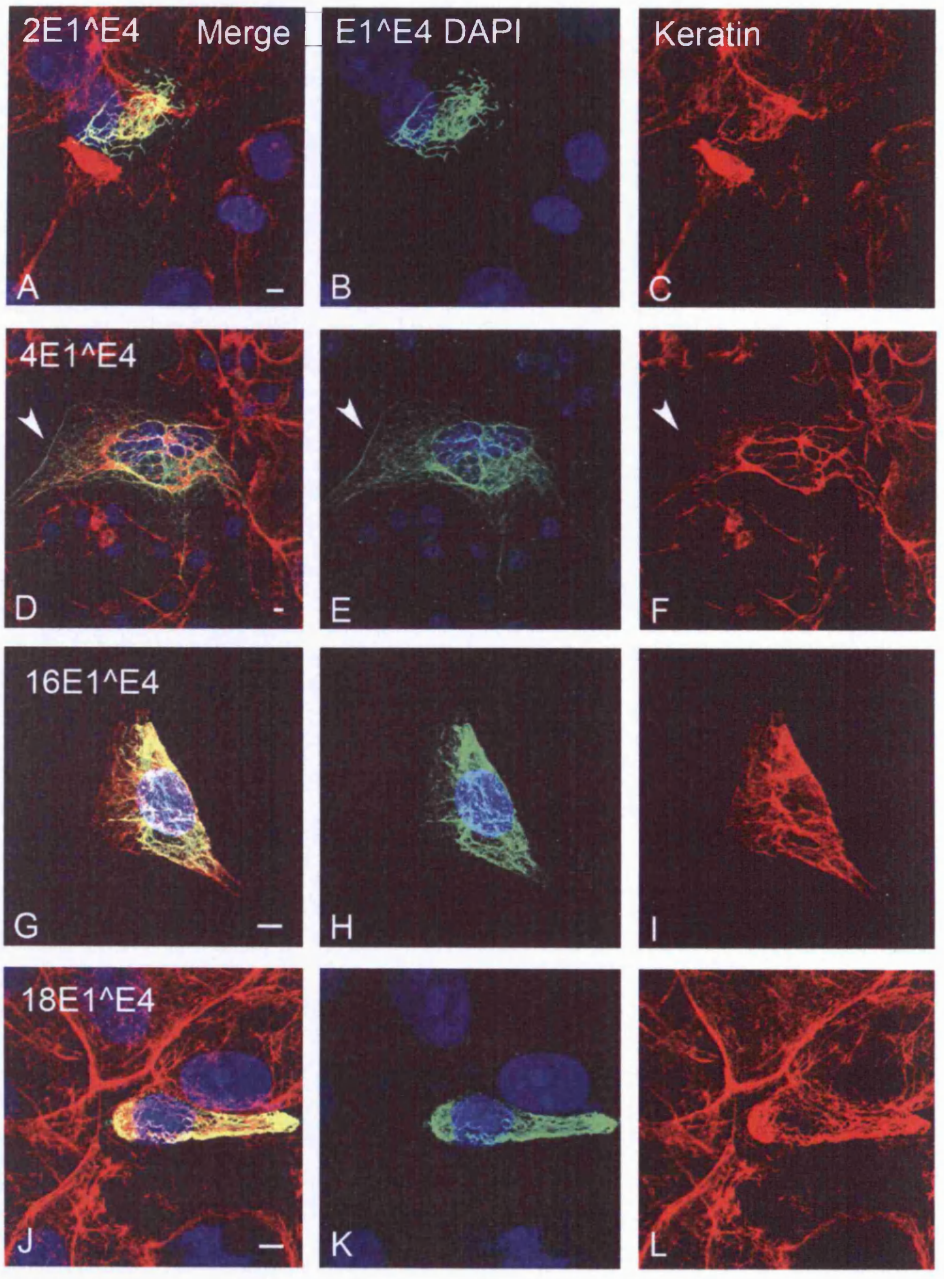
2E1^E4
Merge
E1^E4 DAPI
Keratin
A
B
C
4E1^E4
D
E
F
16E1^E4
G
H
I
18E1^E4
J
K
L

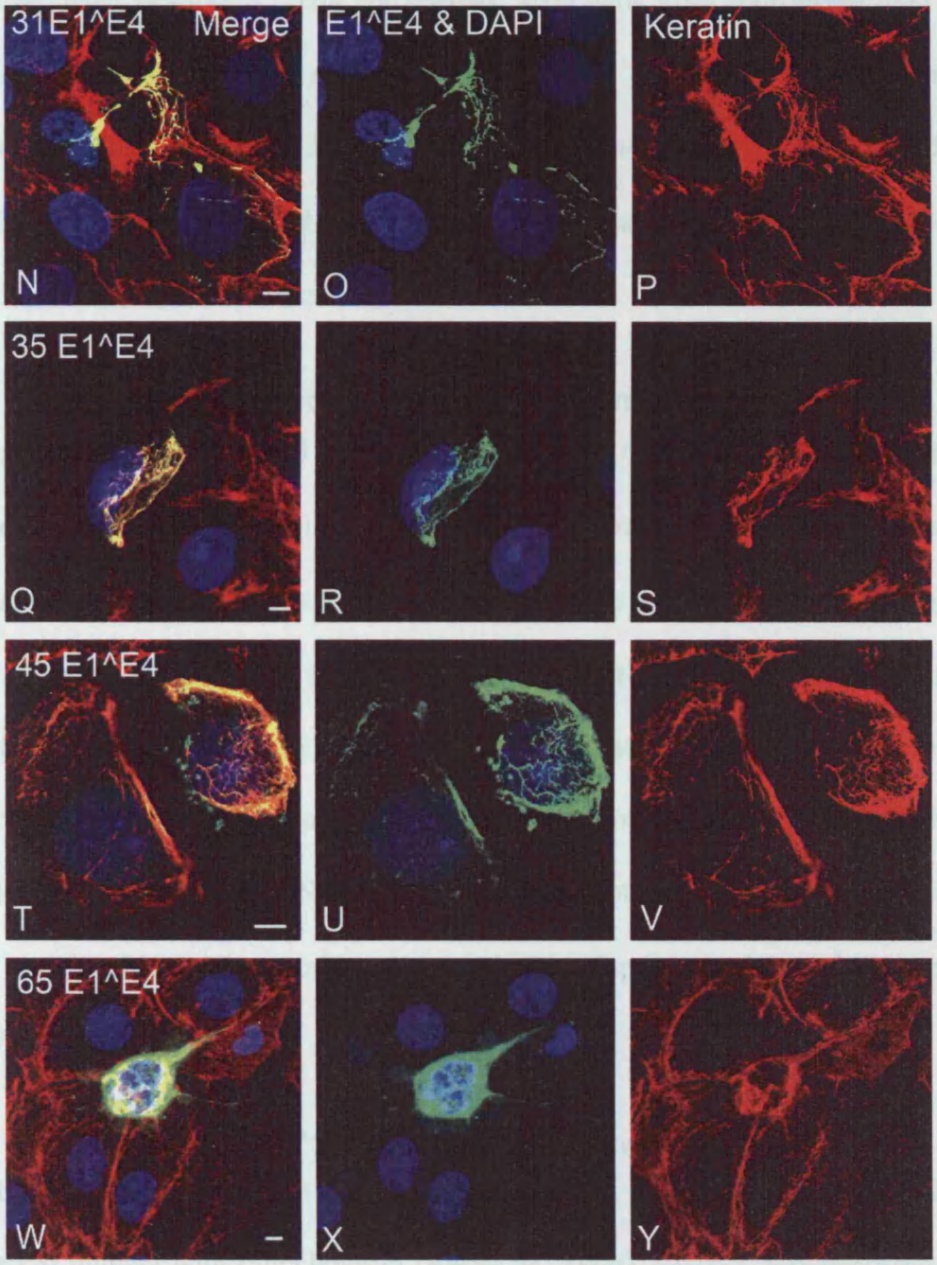

Figure 3.4 HPV E1^E4 proteins have the capacity to associate with and disrupt keratin filament networks.
SiHa cells transfected with HPV E1^E4 expression vectors and stained for keratin (red), E1^E4 (TVG405, green) and DNA (DAPI, blue). All α-group E1^E4 proteins demonstrated the ability to associate to and disrupt cytokeratin filament networks. HPV 4 and 65 E1^E4's colocalised to keratin but to a lesser existent than the α-group. Non keratin-associated E1^E4 filaments were visible with HPV 4 (arrow D-F). Scale bars denote 5 μm.

Neither α nor γ-group proteins were found to associate with actin filaments, which were visualised using phalloidin (Data not shown). SiHa cells were transfected with E1^E4 expression vectors and fixed as described in section 3.4.1 before being stained for E1^E4 and α-tubulin (B512). High power confocal images were taken and individual optical slices closely examined. α-group E1^E4 proteins did not show any evidence of colocalisation with microtubules (Fig 3.5).

3.4.4 γ-group proteins colocalise well with microtubules.

The γ-group HPV 4 and 65 E1^E4 proteins were both observed to colocalise perfectly with microtubules. In addition to colocalisation, γ-group E1^E4 proteins appeared to cause an increase in microtubule filament thickness (up to 300 nm compared to 23 nm in the absence of E1^E4). γ-group E1^E4 association also appeared to prevent disruption of microtubules by paraformaldehyde fixation, since intact microtubules were observed in E1^E4-containing cells but were not detected in the neighbouring E1^E4-negative cells (Fig 3.5 S-X). Unlike α-group proteins, which caused the collapse of the associated keratin network, no microtubule collapse was observed at time points up to 72 hours.

3.4.5 Association of E1^E4 proteins to mitochondria

In addition to associating with the cytoskeleton, HPV 16 E1^E4 has previously been reported to interact with mitochondria (Raj *et al.*, 2004). Healthy mitochondria appear as punctate structures in the cytoplasm, possessing either a concave shape or appearing as long interconnected tube-like structures. Mitochondria are highly dynamic organelles capable of undergoing both fusion and fission events in response to changing intracellular environments (Otsuga *et al.*, 1998; Yaffe, 1999). It was reported that mitochondria in HPV 16 E1^E4-expressing cells reorganise into a large perinuclear

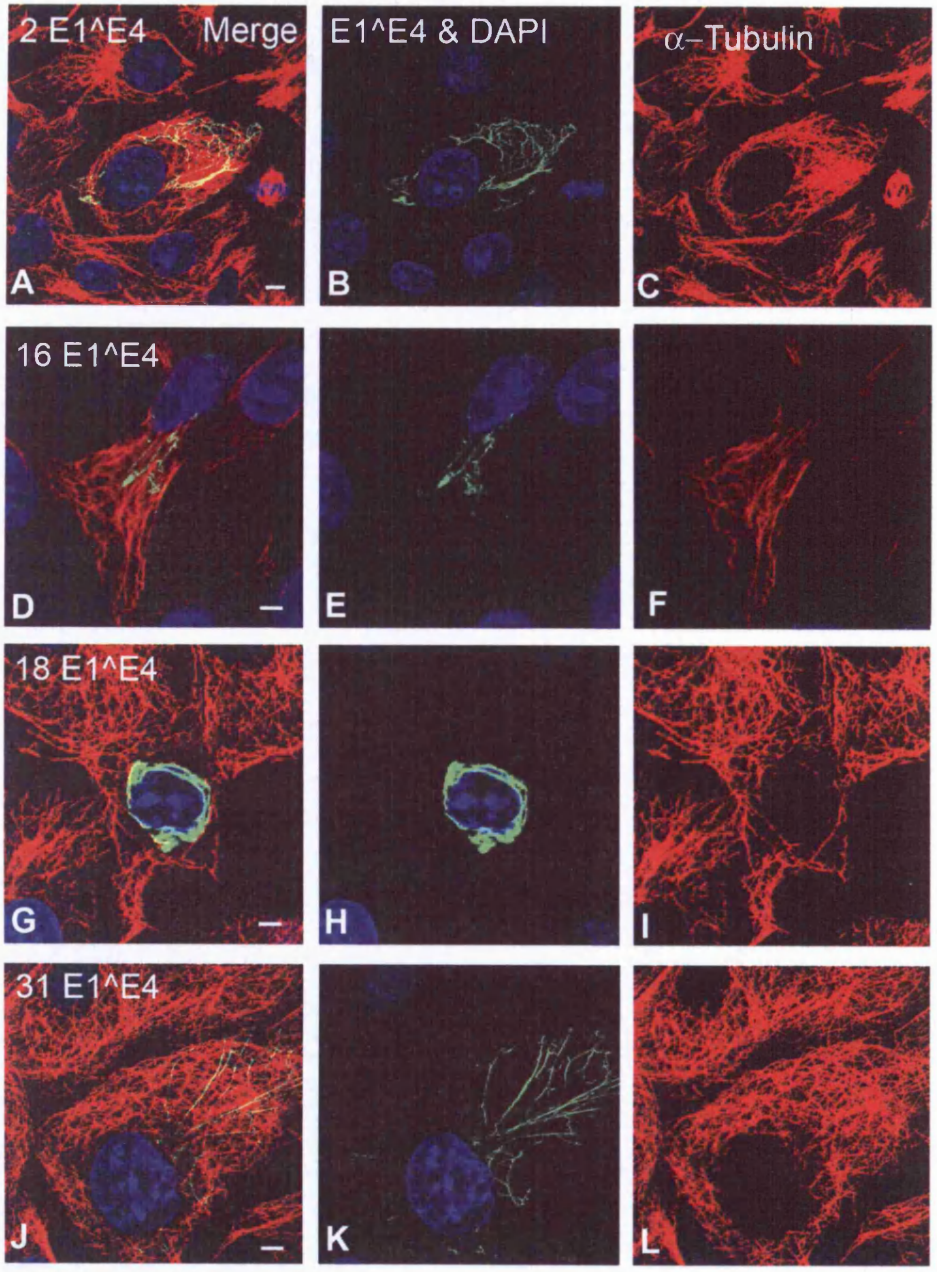
2 E1^E4 Merge
E1^E4 & DAPI
α–Tubulin
A
B
C
16 E1^E4
D
E
F
18 E1^E4
G
H
I
31 E1^E4
J
K
L

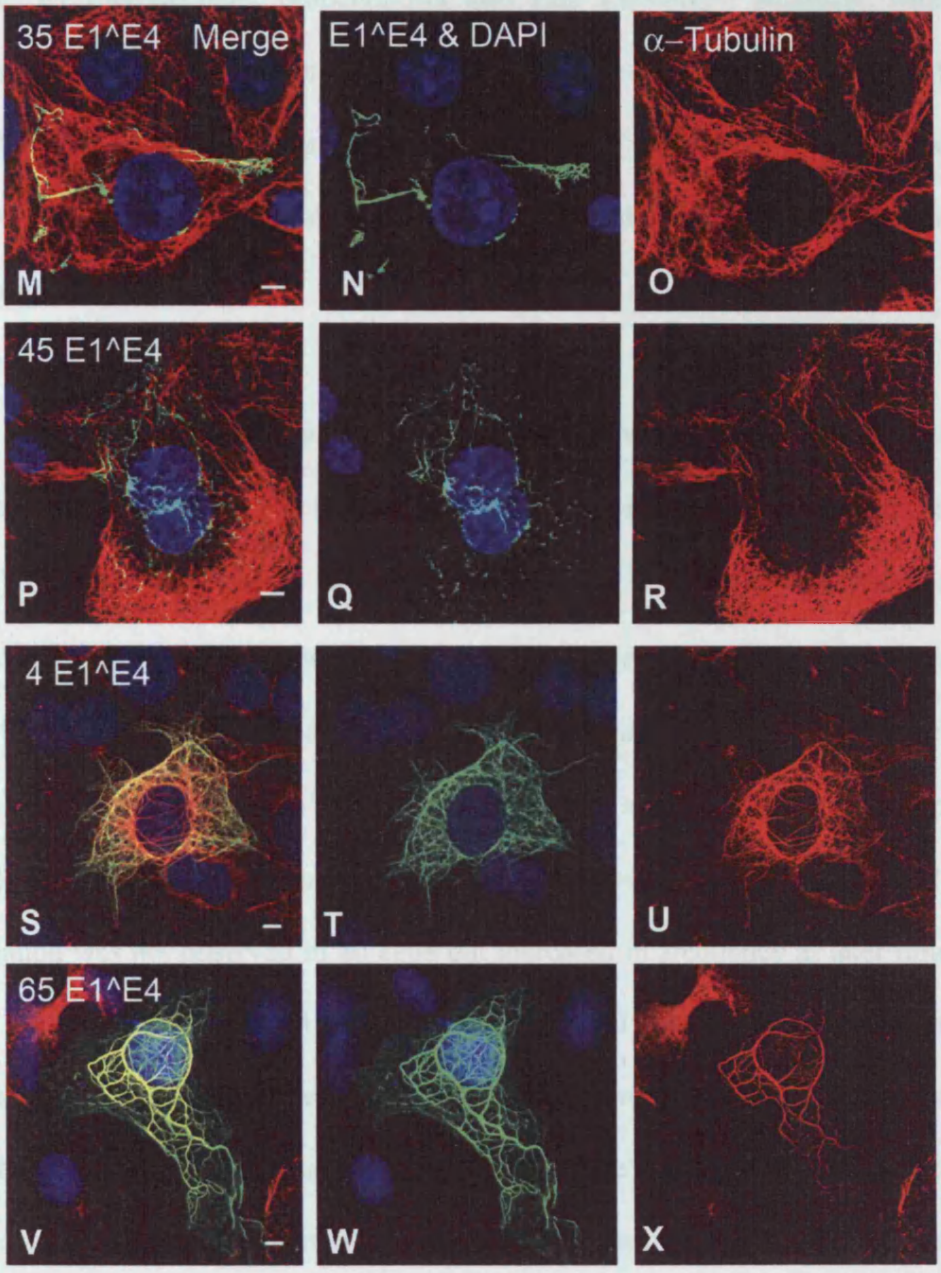

Figure 3.5 The association of E1^E4 proteins with microtubules
SiHa cells transfected with α-group HPV E1^E4 expression vectors fixed with methanol and stained for α-tubulin (red), E1^E4 (TVG405, green) and DNA (DAPI, blue). Images of α-group E1^E4 proteins with a filamentous appearance show that filaments do not colocalize (A-R). Microtubules are unaffected by the expression of γ-group E1^E4 proteins. SiHa cells transfected with γ-group E1^E4 proteins were fixed with paraformaldehyde (S-X), γ-group E1^E4 proteins colocalised with and protect microtubules against paraformaldehyde mediated disruption (note, no microtubules are observed in neighbouring cells). Microtubule filament morphology is also altered by 4 and 65 E1^E4 expressions. Scale bars denote 5 μm.

bundle. E1^E4-associated mitochondria also lose membrane potential, which may induce apoptosis. It was also shown that the leucine cluster is essential for mitochondrial association. As the leucine cluster is conserved throughout α-group E1^E4 proteins, it was decided to investigate whether other E1^E4 proteins also colocalise with mitochondria.

SiHa cells were transfected with E1^E4 expression vectors, and mitochondria were labelled with mitotracker red (Molecular Probes) prior to fixation with methanol (α-group) or paraformaldehyde (γ-group), and staining for E1^E4 (different fixation procedures did not affect mitochondrial staining patterns). At 24 hours all α–group E1^E4 proteins were observed to localise with and cause disruption of mitochondria (Fig 3.6). All α–group E1^E4's appeared to behave in a similar fashion and displayed a mixed population of filamentous, bundled and speckled patterns. Mitochondrial association was not observed in all cells but increased in frequency at later time points (Data not shown). Both small punctate (mitochondrial shaped) and larger perinuclear (presumably keratin associated) E1^E4 structures were observed to co-stain with mitochondria. This finding may suggest that on some occasions E1^E4 associates to individual mitochondria, whereas on other occasions mitochondria become associated to the collapsed keratin bundles. γ-group E1^E4 proteins did not display any detectable mitochondria associations, suggesting that these proteins lack the ability to associate with mitochondria.

3.4.6 The association of E1^E4 with Cyclin B

HPV 16 E1^E4 has previously been reported to induce cell cycle arrest (G2) by sequestration of the cyclin B CDK 1 complex into the cell cytoplasm (Davy *et al.*,

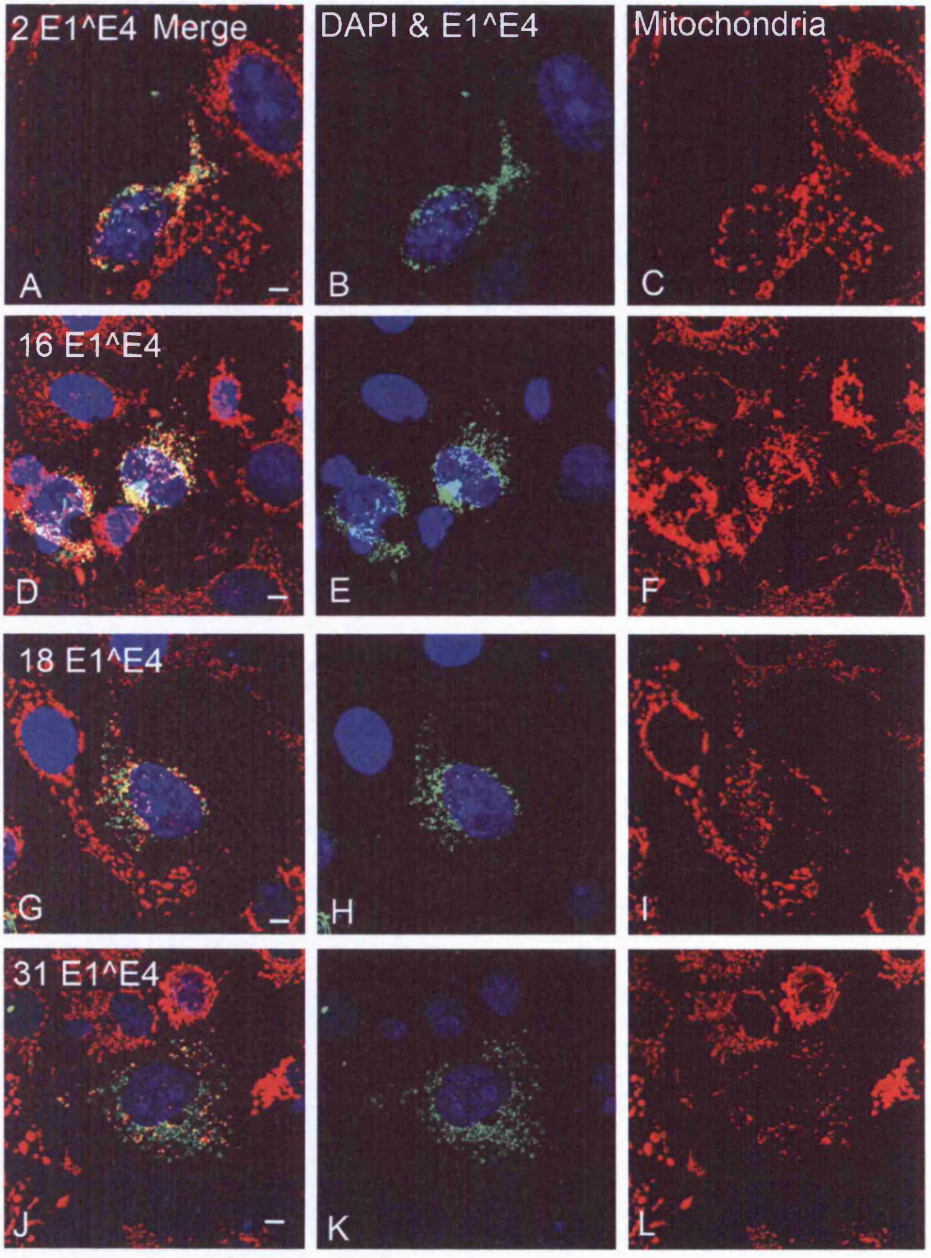
2 E1^E4 Merge
DAPI & E1^E4
Mitochondria
A
B
C
16 E1^E4
D
E
F
18 E1^E4
G
H
I
31 E1^E4
J
K
L

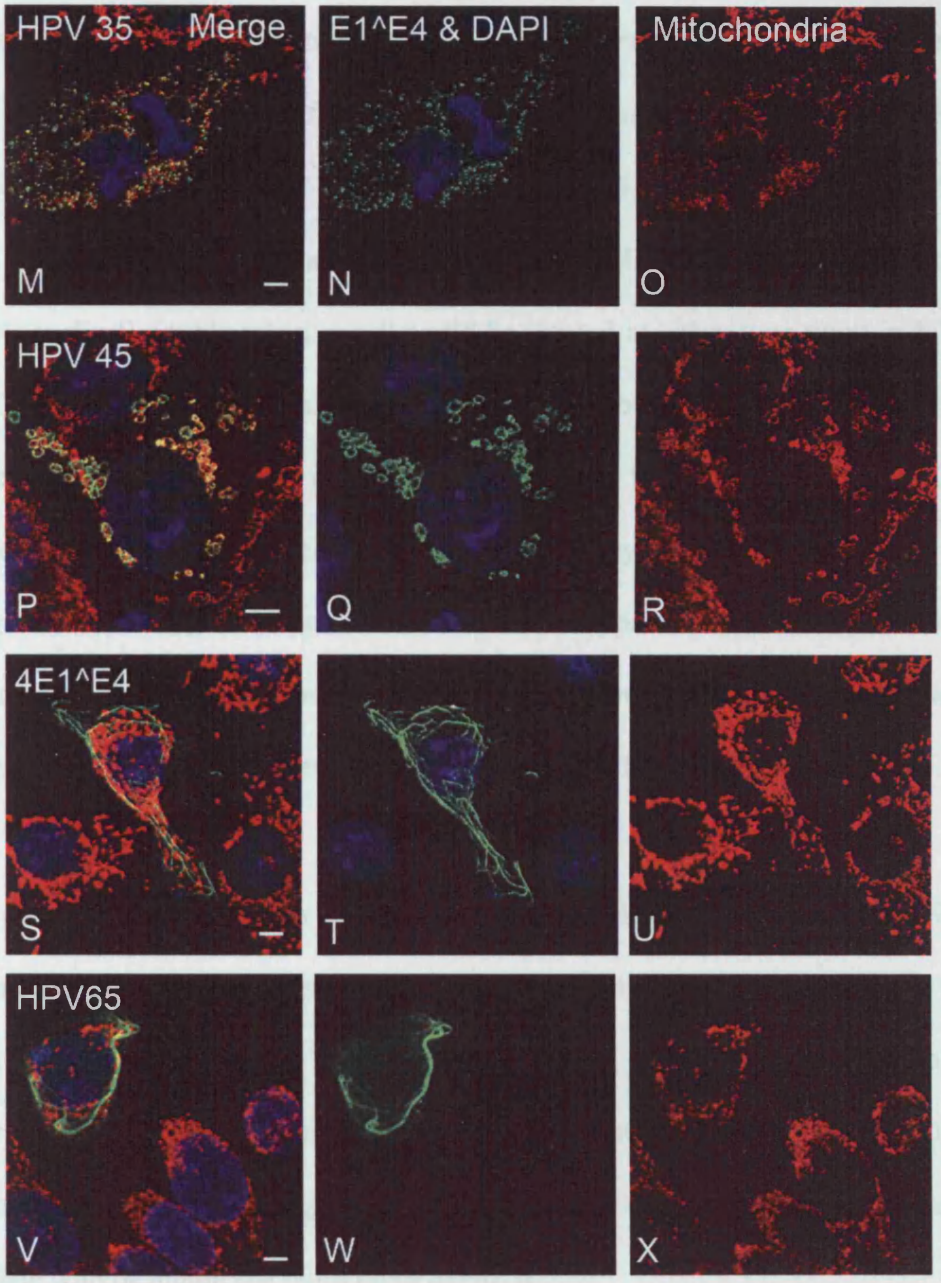

Figure 3.6 The association of E1^E4 proteins with mitochondria
SiHa cells were transfected with α-group E1^E4 expression vectors and stained with mitotracker red (Molecular Probes, red) before being fixed with methanol and stained for E1^E4 (TGV405, green) and DNA (DAPI, blue). All α-group E1^E4 proteins were seen to colocalize with mitochondria (A-R). SiHa cells transfected with γ-group E1^E4 expression vectors were treated in the same way but fixed with paraformaldehyde (S-X). Differential fixation procedures did not affect mitochondria staining (compare A-R with S-X). No co-localization was seen to occur between 4 or 65 E1^E4 and mitochondria. Scale bars denote 5 μm.

2005). The ability of the α and γ–group E1^E4 proteins to associate with cyclin B was investigated. SiHa cells were transfected with E1^E4 expression vectors, and cells were fixed at 24 or 48 h post-transfection with methanol (α-group) or paraformaldehyde (γ-group), and stained for E1^E4 and cyclin B (GNS11). HPV 16, 18, 31 35 and 45 E1^E4 could all be observed to colocalise with cyclin B in SiHa cells (Fig 3.7 D-R). No HPV 2 E1^E4 /cyclin B double positive cell could be located at either time point in SiHa cells (Fig 3.7 A-C). This result may suggest that the association with HPV 2 E1^E4 is weaker or that HPV 2 E1^E4 may behave in a similar fashion to HPV 1 E1^E4 which has been reported to block cell cycle by preventing cyclin B accumulation in the cell (Knight *et al.*, 2004). Although the association of type 16 E1^E4 to cyclin B is well characterised further studies using synchronised cells may be required to determine the existence of the interaction between other α-group E1^E4 proteins and cyclin B.

HPV 4 and 65 E1^E4 proteins were not observed to colocalise with cyclin B (Fig 3.7 S-X). In cells that stained positive for both proteins, cyclin B accumulated in the nucleus. Weak colocalisation between cyclin B and 4 E1^E4 was observed in apoptotic cells (determined by fragmented nuclei, observed in DAPI stain (see inlay Fig 3.7 T)). These results suggest that unlike α-group proteins, γ-group E1^E4 proteins lack the ability to associate with or inhibit the build up of cyclin B.

3.5 Discussion

All HPV E1^E4 proteins investigated in this study were shown to have a conserved ability to associate with and disrupt the components of the cell cytoskeleton. Whereas α-group proteins associated with the cytokeratin network, γ-group proteins appeared to preferentially associate with microtubules although some evidence of partial keratin

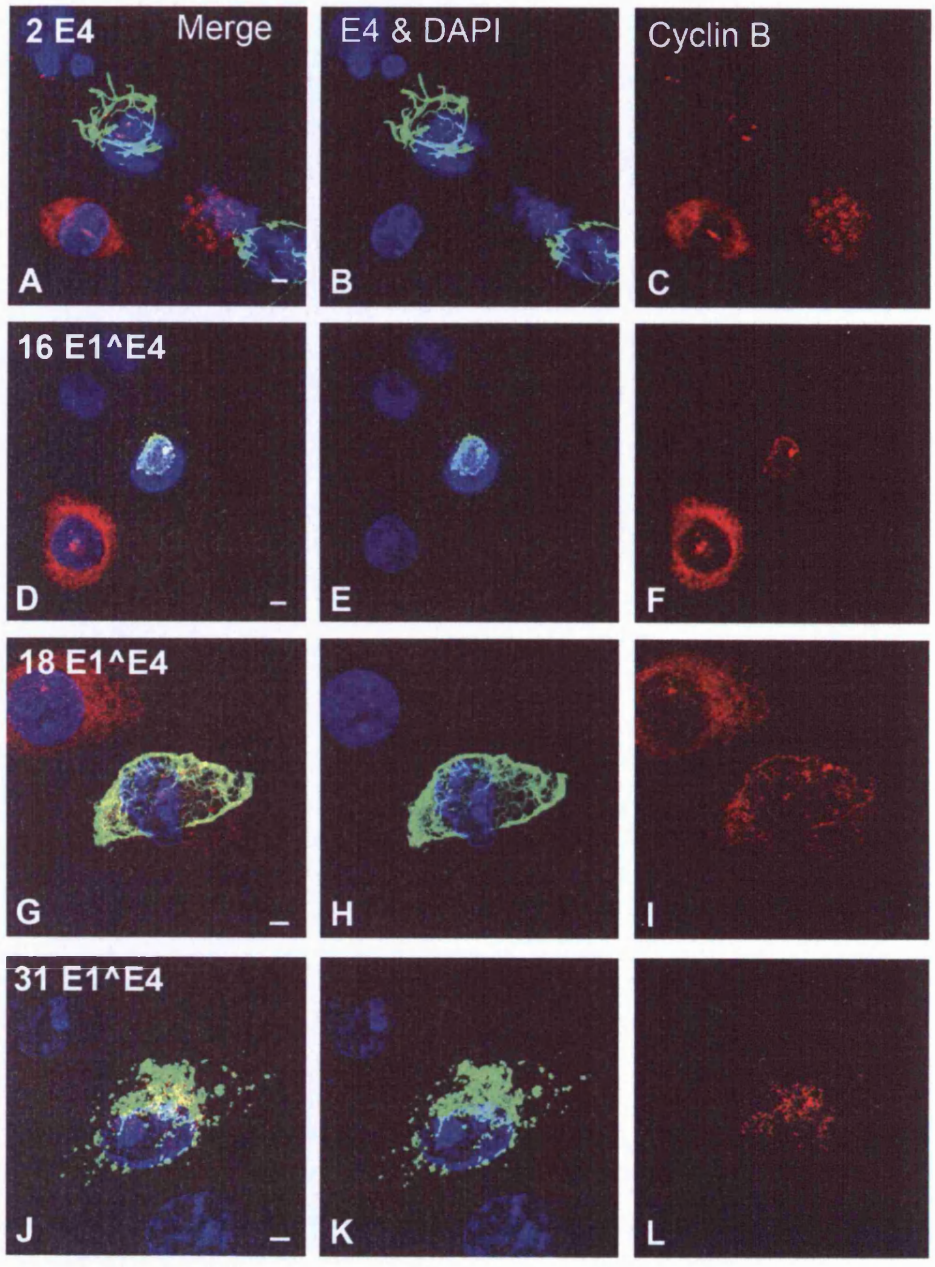
2 E4
Merge
A
E4 & DAPI
B
Cyclin B
C
16 E1^E4
D
E
F
18 E1^E4
G
H
I
31 E1^E4
J
K
L

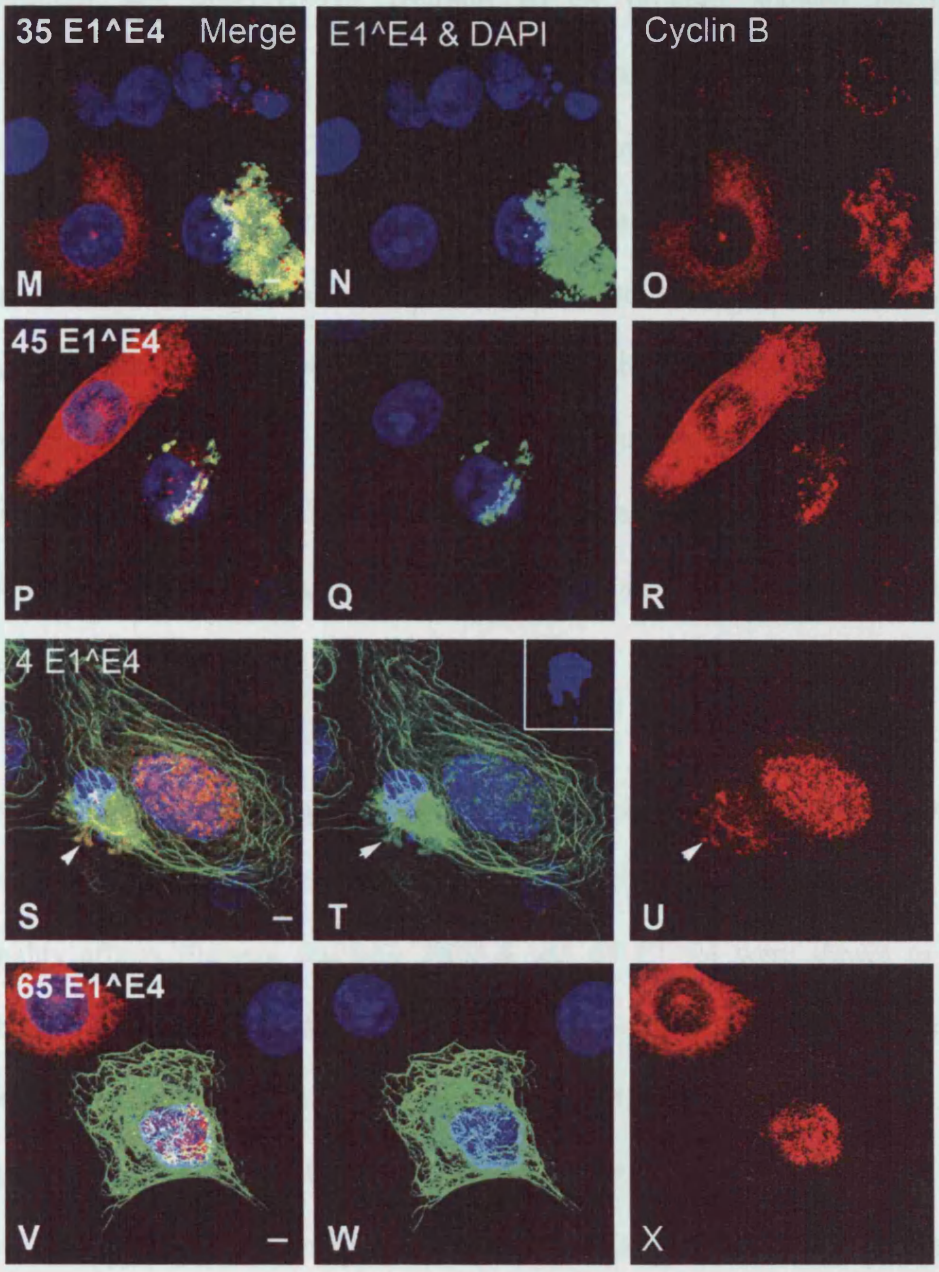

Figure 3.7 Association of E1^E4 proteins to cyclin B
SiHa cells transfected with α-group E1^E4 expression vectors were fixed with methanol and stained for cyclin B (GNS-11, red) E1^E4 (green) and DNA (DAPI, blue). Cyclin B colocalisation could be seen with HPV 16, 18, 31, 35 and 45 (D-R). HPV 2 E1^E4 was not observed to colocalize with cyclin B and double positive cells could not be found (A-C). SiHa cells transfected with γ-group E1^E4 expression vectors were treated in the same way but fixed with paraformaldehyde. No colocalisation between 4 or 65 E1^E4 was observed (except in apoptotic cells arrow S-T (inlay shows cells nucleus T)), cyclin B could be seen to accumulate in the nucleus of some cells HPV 4 or 65 E1^E4 indicating that nuclear import was unaffected. Scale bars denote 5 μm.

colocalisation was observed.The α-group E1^E4 proteins showed no sign of colocalising to microtubules in SiHa cells, whereas γ-group proteins showed preferential colocalisation to microtubules. It has since been discovered that when expressed in the NIKS cell line, (containing keratins 5, 14, 13), HPV 4 and 65 E1^E4 can associate with keratins in addition to microtubules (personal communication, woei Peh). These findings mean that cellular factors (most probably the expression of native keratin subtypes) influence the ability of the γ-group E1^E4 proteins to associate with different components of the cell cytoskeleton. The α group viruses are found in both mucosal and cutaneous sites, γ-types only infect cutaneous sites, so *in vivo* are perhaps more likely to behave as they do in NIKS.

E1^E4 proteins from both groups caused the disruption of affected cytoskeletal filaments, and to filament collapse in the case of the α-group proteins, which presumably affects filament function. HPV 4 and 65 E1^E4 were shown to protect microtubules from paraformaldehyde induced disruption whereas 16 E1^E4 was able to protect keratin filaments against paraformaldehyde diruption (see Fig 6.14). These findings may suggest some form of stabilisation or cross-linking between E1^E4 proteins and cytoskeletal components. Both α and μ–group E1^E4 proteins (HPV 1,11,16) have previously been shown to have the ability to multimerise via a C-terminal motif (Ashmole *et al.*, 1998; Bryan *et al.*, 1998; Roberts *et al.*, 1997; Wang *et al.*, 2004). In the case of HPV16 E1^E4 multimerisation is believed to aid filament reorganisation (Wang *et al.*, 2004) and it is tempting to speculate that HPV 4 and 65 E1^E4 proteins may cause microtubules stabilisation by a similar process.

All the α-group proteins investigated have demonstrated the ability to associate with and aggregate mitochondria whereas γ-group E1^E4 proteins did not. To determine whether this ability is unique to all α–group viruses and absent in all γ group proteins would require the investigation of additional virus subtypes. Although the purpose of this function remains unclear, it has been reported to induce apoptosis, which may aid virus release (Raj *et al.*, 2004). α-group viruses are only found in primates suggesting that they may be a more recently evolved group. If this is the case then mitochondrial association may be a more recently evolved function that offers an evolutionary advantage to this group of viruses.

HPV 16 is known to induce cell cycle arrest via its ability to sequester active cyclin B into the cytoplasm (Davy *et al.*, 2000; Davy *et al.*, 2005). This is the likely mechanism for E1^E4 induced cell cycle arrest, since active cyclin B/CDK complexes are required to enter the nuclease for cell cycle progression. In this chapter it has been shown that HPV 18, 31, 35, and 45 E1^E4 proteins also colocalise with cyclin B in the cytoplasm. This observation suggests that these proteins may be able to induce cell cycle arrest by a similar mechanism. This was not apparent in cells expressing the other α E1^E4 protein HPV 2 E1^E4. Instead HPV 2 E1^E4 expressing cells contained low levels of cyclin B. It is therefore possible that HPV 2 E1^E4 inhibits the build up of cyclin B in the absence of colocalisation as has been reported for the μ-group HPV1 E1^E4 protein (Knight *et al.*, 2004).

HPV 4 and 65 do not appear to colocalise with cyclin B. Cells that contain both E1^E4 and cyclin B showed cyclin B accumulation in the nucleus, suggesting that these proteins did not inhibit cyclin B build up or cause cytoplasmic sequestration. It is not

known whether HPV4 and 65 E1^E4 cause cell cycle arrest, however, both proteins were shown to affect microtubules, which in itself may disrupt the cell cycle. Cells arrested in this way by inhibitors such as taxol usually contain restructured chromatin (Barboule *et al.*, 1997; Jordan *et al.*, 1996). Condensed chromatin could not be observed in cell expressing HPV 4 and 65 E1^E4, indicating that if cell cycle arrest has occurred, it may be through some other pathway.

In summary, these data suggest that ability to disrupt elements of the cytoskeleton is a conserved function that is common to all the E1^E4 proteins investigated. The α-group proteins were shown to localise selectively to the cytokeratin network, which is believed to affect cell integrity and aid virion release. The γ-group protein have the ability to affect both keratin and microtubules depending on the environment in which they are expressed, which gives them the potential to affect both the cell cycle and the cell integrity. These findings suggest that although E1^E4 functions appear to vary between different virus subtypes, the ability to interact and disrupt the cell cytoskeleton is highly conserved in distantly related viruses.

4 The effect of 16 E1^E4 on keratins in SiHa cells

4.1 Aims

Although the association between the HPV E1^E4 proteins and keratins has been known for some time, the purpose and outcome of the interaction is still not clearly understood. This work follows on from the study in Chapter 3, and aims to gain a better understanding and significance of the interaction between E1^E4 and keratins.

4.2 Introduction

4.2.1 The cell cytoskeleton

To understand the purpose of the E1^E4-keratins interaction, it is necessary to understand how the cell cytoskeleton functions in order to comprehend how the systems are being targeted by the virus. Due to the complex way in which the different components of the cytoskeleton interact, a brief overview of cytoskeletal structures has been included. The cytoskeleton is composed of a series of filament networks that are responsible for intracellular transport, cell motility and protection against mechanical damage. The cytoskeleton is composed of three distinct filament networks, the macro filaments (microtubules), micro-filaments (actin) and intermediate filaments (keratins and others), each of which has distinct properties and perform a variety of different functions. Microtubules are composed of 2 subunits, α and β tubulins, that polymerise into hollow, cylindrical, polar filaments, 24 nm in diameter (Fig 4.1A). Microtubules originate from a single point in the cell referred to as the microtubule organising centre (MTOC), which is located in the centrosome, and are involved in intracellular transport. Microtubules exist in a state of flux referred to as dynamic instability, and can polymerise from one end whilst depolymerising from the other, producing an effect referred to as treadmilling, which can facilitate intracellular transport. Micro-filaments are formed from actin homo-polymers, and form polar filaments 5-7 nm

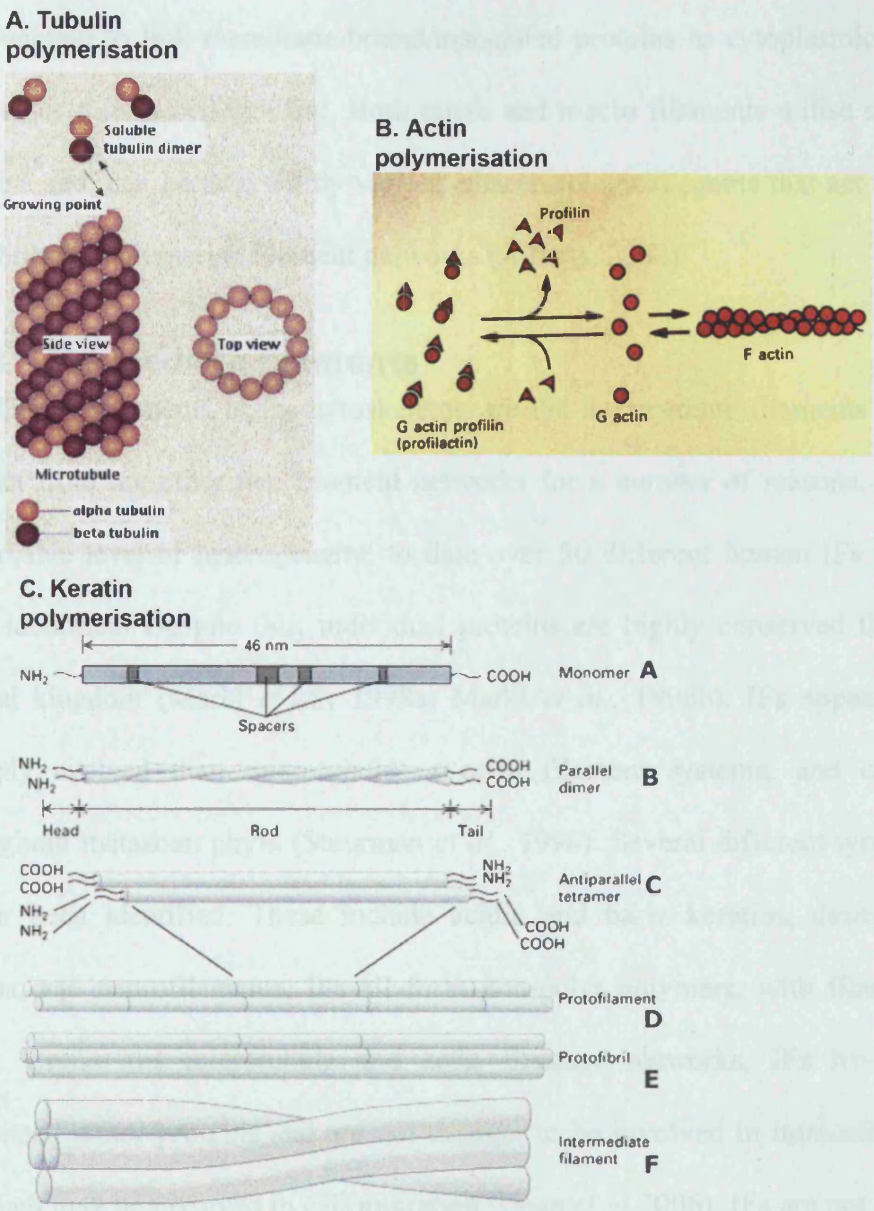

Figure 4.1 Polymerisation of cytoskeletal filament networks
Figure shows the polymerisation of microtubules, actin and keratin filaments. Microtubules dimerise before polymerising to form hollow polar filaments ~24 nm in diameter (A), image taken from (www.cellbio.utmb.edu). Actin monomers form polar homopolymers after shedding profilin (B) image taken from (www.academic.brooklyn.cuny.edu). Keratin filaments form non polar filaments by the dimerisation of type I and type II subunits. Type I and type II keratin rod domains twist round one another to from dimers which spontaneously assemble into staggered tetramers. Protofibrils are 4 tetramers thick, four protofibils assemble into an intermediate filament (C). Image taken from (www.biology.iupui.edu).

in diameter (Fig 4.1). Actin filaments form a network beneath the plasma membrane and function to link membrane-bound/associated proteins to cytoplasmic proteins and play a key role in cell motility. Both micro and macro filaments utilise specific motor proteins and can be targeted by various pharmacological agents that act to stabilise or destabilise/depolymerise filament networks (Alberts, 2002).

4.3 Intermediate filaments

The final components of the cytoskeleton are the intermediate filaments (IFs). IFs are distinct from the other two filament networks for a number of reasons. IFs display a remarkable level of heterogeneity; to date over 50 different human IFs proteins have been identified. Despite this, individual proteins are highly conserved throughout the animal kingdom (Markl *et al.*, 1998a; Markl *et al.*, 1998b). IFs appear to be more recently evolved than microtubule or actin filament systems, and can be found throughout metazoan phyla (Stuurman *et al.*, 1998). Several different types of IF have so far been identified. These include acidic and basic keratins, desmin, vimentin, lamins, and neurofilaments. IFs all form non-polar polymers, with filaments ~10nm thick. Unlike the microtubule and actin filament networks, IFs have no known associated motor proteins and are not thought to be involved in intracellular transport although may be involved in cell migration (Long *et al* 2006). IFs are not housekeeping proteins and genes encoding cytoplasmic IFs are expressed in a cell type specific or differentiation-dependent fashion (Coulombe *et al.*, 2000). IFs are significantly more stable than microtubules and actin, forming insoluble networks. Cells lacking IFs are more likely to undergo apoptosis or rupture when exposed to mechanical stress (Takahashi *et al.*, 1999)

4.3.1 Keratin polymerisation

All keratins contain head and tail domains connected by a long α-helical rod domain, ~310 amino acids in length, comprised of long heptad repeats containing leucine or hydrophobic residues at positions "a" and "d" of the helix. Keratins form stable, non-covalent, obligate heteropolymers with specific binding partners. The type II keratin, K8, forms a network with its type I binding partner, keratin 18 in hepatocytes and simple epithelium. Keratins K5 and 14 form a network in undifferentiated basal epithelial cells, K4/13 in differentiated mucosal epithelium and K1/10 in differentiated cutaneous epithelium (reviewed in (Coulombe *et al.*, 2002). Polymers are formed when the rod domain of types I and II keratins twist round one another to form parallel coiled-coil dimers. Dimers assemble into staggered tetramers, which form the basic building blocks of filaments. Keratin intermediate filaments are composed of blocks of tetramers, 8 units thick, forming filaments ~10nm in diameter (Fig 4.1C). The keratin polymerisation process results in a very flexible fibre, which has tremendous tensile strength, giving cells the ability to resist damage. Experimental evidence suggests that head and tail domains do not play a part in the polymerisation process (reviewed in (Fuchs, 1994)). Various conserved phosphorylation sites have been identified in both domains. It has been suggested that the tail domain may make a significant contribution to the elasticity of keratin filaments (Coulombe *et al.*, 2000).

4.3.2 Keratin filament organisation

The properties of the keratin filament network, is thought to be regulated in a number of different ways. Rheological studies investigating the mechanical properties of keratin filament suspensions have provided some interesting information about the nature with which keratin filaments interact with one another. The elastic properties of keratin IF suspensions cannot be entirely explained by steric forces (a simple solution of tangled/overlapping filaments in solution would not behave in such a way).

Interestingly the properties of keratin IF suspensions are very comparable to those of F-actin filaments in the presence of exogenous cross-linking proteins. This finding suggests that keratins filaments may be able to interact (cross-link) with one another in the absence of other proteins (Ma *et al.*, 1999). An innate cross linking ability would significantly increase the mechanical strength of the network formed. Expression of different keratin monomers also alters keratin filament network architecture (Coulombe *et al.*, 1989). Keratin networks have demonstrated the ability to relocate and reorganise in cells during processes such as wound healing, cell migration and mitosis (Paladini *et al.*, 1996).

4.3.3 Keratin-associated proteins

Unlike other filament networks, keratins appear to have no associated motor proteins. To date only three cellular keratin-specific binding proteins have been identified (Coulombe *et al.*, 2000). These are filaggrin and trichohyalin, both of which are found in differentiated epithelium. These proteins are believed to play a role in altering keratin network architecture as cells differentiate, in order to increase their mechanical strength (Hamilton *et al.*, 1991). The keratin network is reorganised during mitosis, the process is regulated by phosphorylation and the 14.3.3 protein is though to bind phosphorylated keratins modulateting their solubility (Liao *et al.*, 1996). Another keratin-associated protein is plectin, which acts as a cytoskeletal cross-linking protein that attaches the keratin network to microtubules and actin filaments (Seifert *et al.*, 1992). As well as associating with structural proteins, keratins have been reported to associate with a number of signalling proteins (reviewed in (Paramio *et al.*, 2002)).

4.4 Biochemical modifications to keratins

Keratins are known to undergo a number of different biochemical modifications including phosphorylation, glycosylation and ubiquitination. These modifications are

involved in reorganising the keratin network and are invoked by mitosis, apoptosis, stress and differentiation-dependant stimuli. Although 20 different keratins have been identified to date, the majority of research has focused on keratins 8 and 18 which are simple epithelial types.

4.4.1 Mitotic reorganisation of the keratin network

The phosphorylation of keratins was first shown by 2D gel electrophoresis (Gilmartin *et al.*, 1980). Mitotic arrest has been demonstrated to induce phosphorylation and glycosylation of keratin 8 and 18 in hepatocyes, during which time keratin filaments depolymerise and form numerous small inclusion bodies (Chou *et al.*, 1993a). Type II keratins become phosphorylated during mitosis at the highly conserved motif Ser-73 residue by p38 mitogen-activated protein kinase (MAPK) in tissues and cultured cells (Ku *et al.*, 2002a; Liao *et al.*, 1997; Toivola *et al.*, 2002). Phosphorylation of keratin 8 at Ser 23 and 431 appears to occur upon stimulation of the EGF receptor and during mitotic arrest, and is thought to be facilitated by mitogen activated protein kinase (MAPK), and CDC2 kinase (Ku *et al.*, 1997b). A major physiological phosphorylation site on the type 1 keratin K18, Ser 52, is part of a consensus site for cyclic AMP-dependent protein kinase, calmodulin-dependent protein kinase, S6 kinase and PKC and becomes phosphorylated during interphase thereby facilitating filament reorganisation (Ku *et al.*, 1994). The soluble pool of keratin is not differentially phosphorylated, suggesting that interaction with other cellular factors is responsible for the inhibition of keratin polymerisation in the cytosol (Chou *et al.*, 1993b). It has since been discovered that the 14-3-3 protein bind to keratin 18 upon phosphorylation at Ser-33, and act as solubilzation co-factor (Ku *et al.*, 1998; Liao *et al.*, 1996). The binding of 14-3-3 to the cytokeratin network has been demonstrated to modulate keratin filament solubility and mitogenic progression (Ku *et al.*, 2002b).

4.4.2 Keratin modifications during apoptosis

Phosphorylation of Keratin 18 at Ser- 53 precedes cleavage by caspases 3, 6 and 7 in a conserved, non-alpha-helical region. The caspase recognition site in keratins is conserved in lamins and other IF proteins, but interestingly, type II keratins seem to be remarkably resistant to apoptosis induced proteolysis (Caulin *et al.*, 1997). The M30 epitope of keratin 18 becomes exposed upon caspase cleavage resulting in a 26kDa fragment becoming apparent in apoptotic cell lysates (Leers *et al.*, 1999). Caspase cleavage of keratin 14 and 19 also produces low molecular weight fragments (Ku *et al.*, 2001). Keratin 10 appears to lack a caspase cleavage site, which may reflect its role in terminally differentiated epithelia where the integrity of the K1/10 network is important. Despite being degraded during apoptosis, keratins have been shown to play a vital role in regulating cellular responses to pro-apoptotic signals. Studies have shown that cells expressing a keratin 8/18 network are more resistant to TNF and Fas-mediated apoptosis than those that lack keratins. Resistance is thought to occur by the binding of downstream signalling molecules such as TRADD and Raf-1 (Inada *et al.*, 2001; Ku *et al.*, 2004). Knock out/in studies have demonstrated that cells show greater sensitivity to pro-apoptotic signalling in the absence of keratins (Marceau *et al* 2004). This suggests that as well as providing mechanical strength to cells, keratins also allow the cell to survive in stressful environments in which it would normally undergo apoptosis.

4.4.3 Keratin turnover and ubiquitination

The ubiquitination of keratins was first identified in Mallory bodies (see section 4.5.2) formed in mice (Ohta *et al.*, 1988). Since then it has been demonstrated that keratins are ubiquitinated and then degraded via the proteasome as part of keratin network turnover. The ubiquitination of keratins is thought to be regulated in part via phosphorylation. The phosphorylation of K8 at Ser-23, 73 and 431 protects against, but does not prevent, ubiquitination whereas the link between phosphorylation of K18 and ubiquitination,

remains unclear (Ku *et al.*, 2000). Interestingly, herpes simplex virus type 2 (HSV 2), which also infects epithelial tissue, is believed to trigger the degradation of cytokeratins with a viral kinase US3. This kinase has been demonstrated to induce phosphorylation of keratin 17, which in turn leads to its ubiquitination and degradation. Knock out studies have demonstrated a difference in cytopathic effects in the absence of the kinase (Murata *et al.*, 2002).

4.5 Keratins and disease

Keratins are known to play a role in a number of diseases, with mutations in keratins causing skin and liver pathology. Studies of these conditions have lead to a much better understanding of overall keratin function.

4.5.1 Stress-stimulated phosphorylation of the keratin network

It has long been evident that the phosphorylation state of keratins can modulate keratin function and may be involved in keratin associated diseases. An early study was able to show the dephosphorylation of keratins in cells stressed by culturing them in the presence of acrylamide (Eckert *et al.*, 1988). Since then further studies appear to suggest that the opposite is true and that keratins become increasingly phosphorylated in stressed cells. Experiments in mice investigating liver damage resulting from the ingestion of the hepatotoxin griseofulvin, have shown that under these circumstances, keratins become hyper-phosphorylated and form Mallory bodies (Cadrin *et al.*, 1995; Chou *et al.*, 1993b). Stress-mediated phosphorylation of Ser-73 on keratin 8 byPKC delta has been shown to regulate disassembly of keratin intermediate filaments. Keratins have also been shown to be phosphorylated in cells that have been exposed to shear and hypoxic stresses, resulting in the collapse of the affected network (Omary *et al.*, 1998; Ridge, 2004; Ridge *et al.*, 2005).

4.5.2 Mallory bodies

A number of different stresses can lead to the formation of perinuclear keratin aggregates referred to as Mallory bodies (keratin aggresomes). Mallory bodies are characterised by the presence of hyperphosphorylated and ubiquitinated keratins that can be visualised as high molecular weight keratin "smears" following SDS gel electrophoresis (Bardag-Gorce *et al.*, 2002; Ohta *et al.*, 1988); (Fausther *et al.*, 2004; Nakamichi *et al.*, 2005). A number of proteins that associate with the mis-folded or collapsed keratin networks in Mallory bodies have also been identified, including Hsp70, Hsp25 and p62 (Fausther *et al.*, 2004; Janig *et al.*, 2005; Zatloukal *et al.*, 2002). Mallory body formation can be mimicked by feeding mice the phosphatase inhibitor, okadaic acid, which causes keratin networks to collapse into perinuclear aggregates that contain multiple phospho-keratin species. Mallory body formation can also be induced in other ways, e.g. by feeding mice griseofulvin, treating cells with proteasome inhibitors and over-expressing a single keratin species (Bardag-Gorce *et al.*, 2004; Cadrin *et al.*, 1995; Nakamichi *et al.*, 2002). Mallory bodies are believed to form in order to clear misfolded and/or hyperphosphorylated, ubiquitinated keratins when the proteasome system becomes overloaded (Riley *et al.*, 2003). As part of this process, cells use microtubules to sweep up keratins into perinuclear aggregates located at the microtubule organising centres (Riley *et al.*, 2003). Aggresome formation has also been reported to result in proteasome inhibition (Bence *et al.*, 2001; Bennett *et al.*, 2005).

4.5.3 Keratin mutations linked to disease

Mutations in specific keratins have been linked to a number of clinical conditions. Transgenic mice over-expressing a human keratin 18 with a mutation in the highly conserved arginine 89, develop chronic hepatitis and show a predisposition to drug-induced liver damage (Ku *et al.*, 1995; Ku *et al.*, 1996). The phosphorylation of keratins is believed to protect against hepatotoxicity hence mutations in keratins may render

some individuals more susceptible to liver damage induced by toxic stress (e.g. binge drinking) (Ku *et al.*, 1996; Ku *et al.*, 2005; Stumptner *et al.*, 2000). The disfiguring skin disease epidermolysis bullosa simplex (EBS), is an inherited disease caused by a mutations in either keratin 5 or 14 (Coulombe *et al.*, 1991; Lane *et al.*, 1992). The mutations prevent correct keratin polymerisation resulting in a fragile epidermis that is prone to blistering and damage. EBS may provide some insight as to why the papilloma viruses have evolved to target keratins at a specific point in the virus life cycle (discussed later).

4.6 The association of E1^E4 with keratin

The association between keratin and the E1^E4 protein was first observed in keratinocytes expressing HPV16 E1^E4, where it was noticed that the E1^E4 protein had a filamentous staining pattern. E1^E4s were shown to colocalize with keratin filaments but not actin, microtubules or nuclear lamins (Doorbar *et al.*, 1991). Later work showed that HPV1 and 31 E1^E4 proteins also had the capacity to associate with cytokeratins (Pray *et al.*, 1995b; Roberts *et al.*, 1994). Whereas HPV 16 and 31 appear to be capable of binding to and collapsing the cytokeratin network, HPV 1 E1^E4 appears to associate transiently with keratins before forming large cytoplasmic inclusion bodies with no resulting disruption of keratin networks (Rogel-Gaillard *et al.*, 1993). Mutational analysis was able to demonstrate that the conserved N-terminal YPLLXLL motif present in HPV 16 and other α-group viruses (see Fig 3.2) is responsible for its association with keratins (Roberts *et al.*, 1997). HPV 1 contains an N-terminal LLGLL motif which can be lost due to N-terminal processing (Doorbar *et al.*, 1996; Roberts *et al.*, 1994; Roberts *et al.*, 1997; Roberts *et al.*, 2003). The ability of HPV 16 to colocalize directly to keratin filaments has also been observed by immunoelectron microscopy (Sterling *et al.*, 1993b). More recent work has demonstrated that a region at the C-

terminus of 16E1^E4 may be responsible for modulating cytokeratin collapse (Roberts *et al.*, 1997; Wang *et al.*, 2004). Coimmuno-precipitation studies have demonstrated that HPV 16 has the capacity to bind directly to keratin 18 but not its type II binding partner keratin 8. It has also been shown that the E1^E4-keratin association is not just an *in vitro* phenomenon but it also occurs *in vivo* (Doorbar *et al.*, 1997; Wang *et al.*, 2004). From this data it has been hypothesised that E1^E4 may induce keratin filament disruption *in vivo* by multimerising on keratin filaments in order to aid viral egress.

4.7 Results

4.7.1 Keratin association with E1^E4 in SiHa cells

E1^E4 has previously been reported to associate with keratin networks in cells. To observe this, SiHa cells were infected using the recombinant adenovirus (rAD) HPV 16 E1^E4 expression system (Doorbar *et al.*, 2000) before the cells were fixed and stained with antibodies raised against keratins (C2562) and E1^E4 (TVG405) at 12, 24 and 48 h post transfection. The staining patterns observed varied in appearance depending on the time after infection, and could be divided into 3 distinct groups. At 12 h post infection most cells showed a distinct filamentous pattern that colocalised almost exclusively with keratin filaments (Fig 4.2 A-C). At 24 h E1^E4 is observed to colocalise with keratins in a filamentous pattern in various states of collapse, (Fig 4.2 D-F). E1^E4 association caused the keratin filaments to appear bundled together into thicker filaments, an event that presumably precedes their collapse. When collapse occurred, keratins were found to form perinuclear bundles or cage-like structures that can wrap around the nucleus. A third punctate staining pattern was manifested as multiple E1^E4

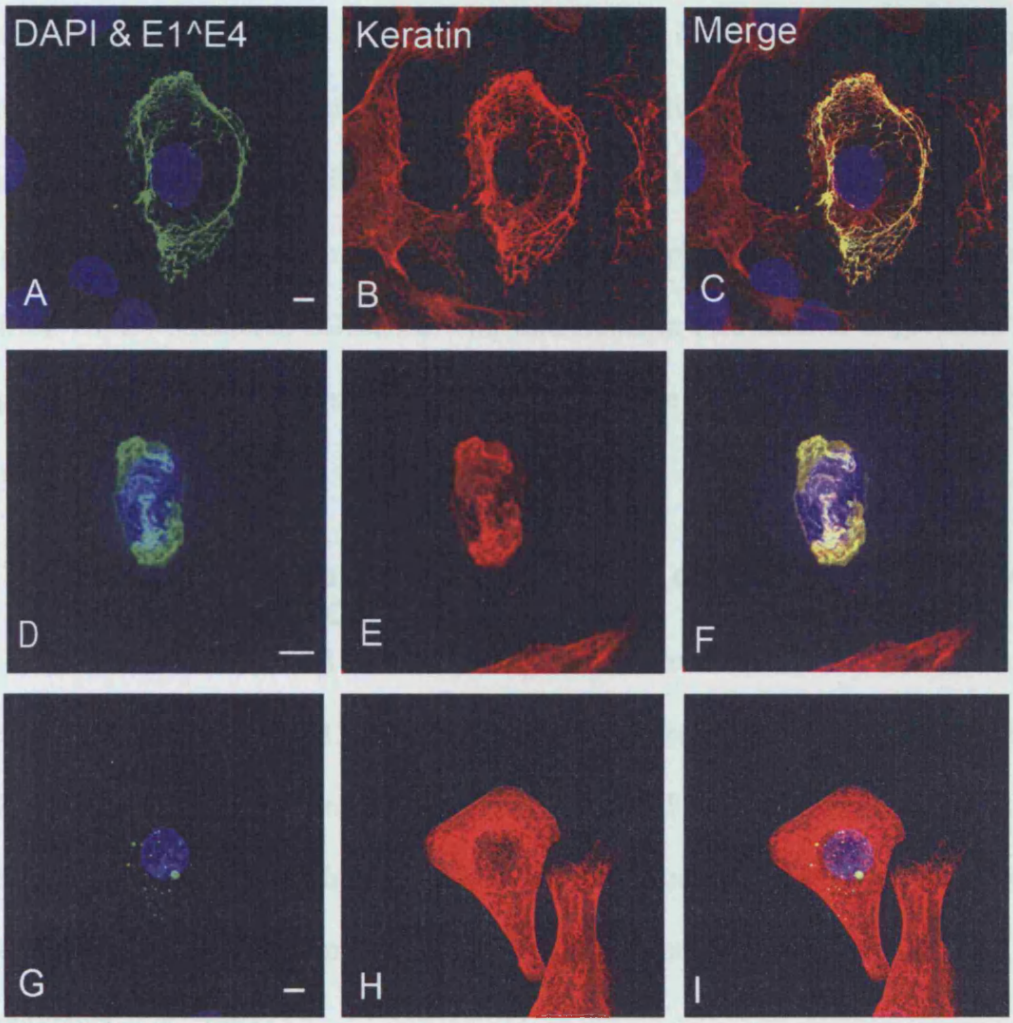

Figure 4.2 Effect of E1^E4 on keratin networks
Images show SiHa cells infected with the rAD E1^E4 expression system, fixed 24 h post infection and stained for DNA (DAPI-blue), keratin (C2562-red) and E1^E4 (TVG405-green). E1^E4 displays three different staining patterns. E1^E4 is commonly filamentous in appearance and colocalises with keratin filaments (A-C). E1^E4 expression leads to the collapse of associated keratin networks into perinuclear bundles (D-F). Cells also commonly contain non filamentous E1^E4 bodies which are not always keratin associated, keratin networks appear intact in some of these cells (G-I). Scale bars denote 5 μm.

structures, including condensed perinuclear aggregates as well as more discreet cytoplasmic structures. This staining pattern increased in frequency at later time points (Fig 4.2 G-I). The perinuclear E1^E4 structures always co-stained with keratins, whereas the smaller more diffuse structures did not. It is known that E1^E4 has the capacity to associate with mitochondria so it was decided to investigate whether the diffuse E1^E4 structures colocalise with mitochondria (see section 4.8). When taken together, these data suggest that E1^E4 is capable of forming multiple keratin-associated structures, not all of them being filamentous.

4.7.2 E1^E4 can collapse multiple types of keratin network when expressed in HaCat cells.

It is not known whether E1^E4 can disrupt or induce modifications to other keratin networks such as 5/14 or 4/13, which are encountered *in vivo*. To determine whether 16 E1^E4 could interact with and disrupt these keratins E1^E4 was expressed HaCat cells. HaCat cells express a keratin network that contains keratins 5, 14 8, and 18, as well as the differentiation-dependent 4, 13, 1 and 10 keratins (Breitkreutz *et al.*, 1991; Breitkreutz *et al.*, 1993).

HaCat and SiHa cells were infected with rAD E1^E4, fixed and stained for E1^E4 (TVG405) and specific keratins (antibodies from Novocastra). SiHa cells stained positive for keratin 8 and 18; were negative for keratins 4, 5, 10 and 14; approximately 10% of SiHa cells were found to express keratins 4 and 13 (not shown); and HaCat cells stained positively for keratins 4, 5, 8, 10, 13, 14 and 18. All keratins in HaCat cells appear to colocalize with E1^E4 and be remodelled in the same fashion following E1^E4 association (Fig 4.3). This data must not however be over-interpreted as the different keratins form a single inter-connected network. In addition to this, the differentiation-dependent keratins 4, 13, 1 and 10 may not be modified in the same way

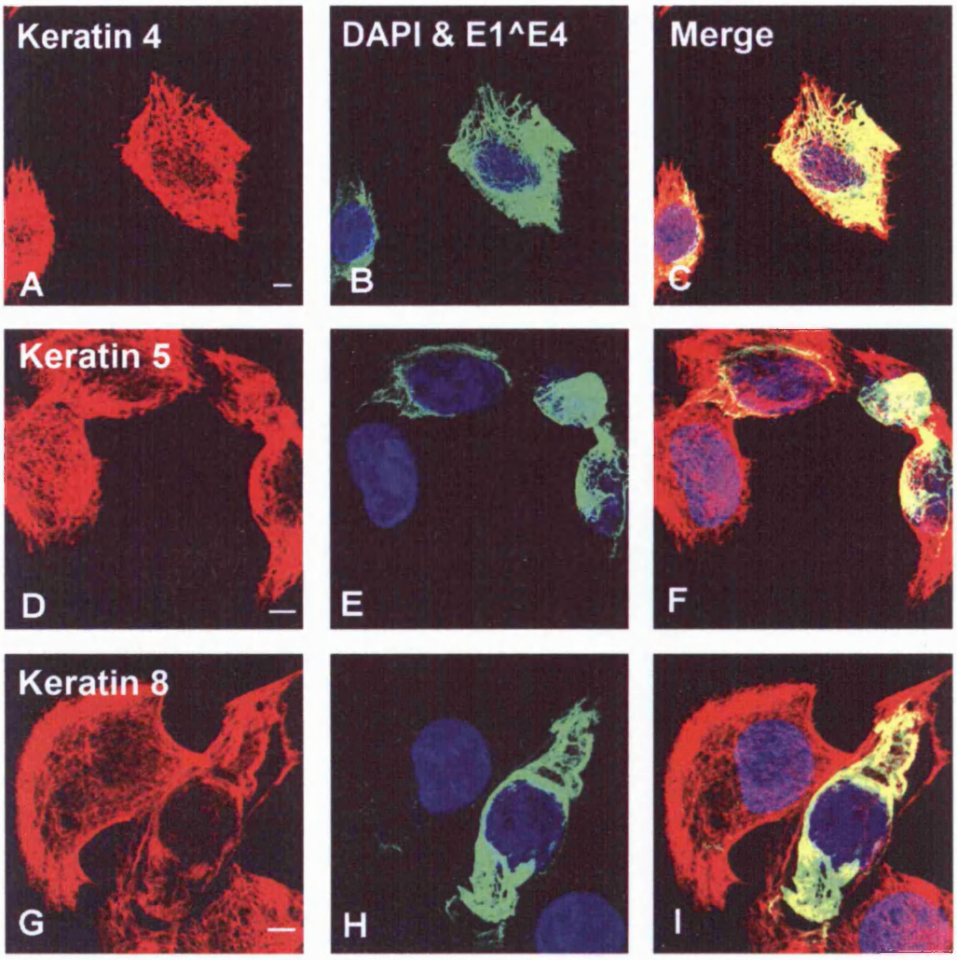

Figure 4.3 E1^E4 expression in HaCat cells
HaCat cells infected with rAD E1^E4, were fixed 24 h after infection and stained for E1^E4 (TVG405-Green), keratin specific antibodies (Novacastra, red) and DNA (DAPI-Blue). Keratin staining shows that E1^E4 appears to have the capacity to associate with and disrupt keratins 4, 5, 8,10,13,14 and 18 (A-U). Scale bars denote 5 μm.

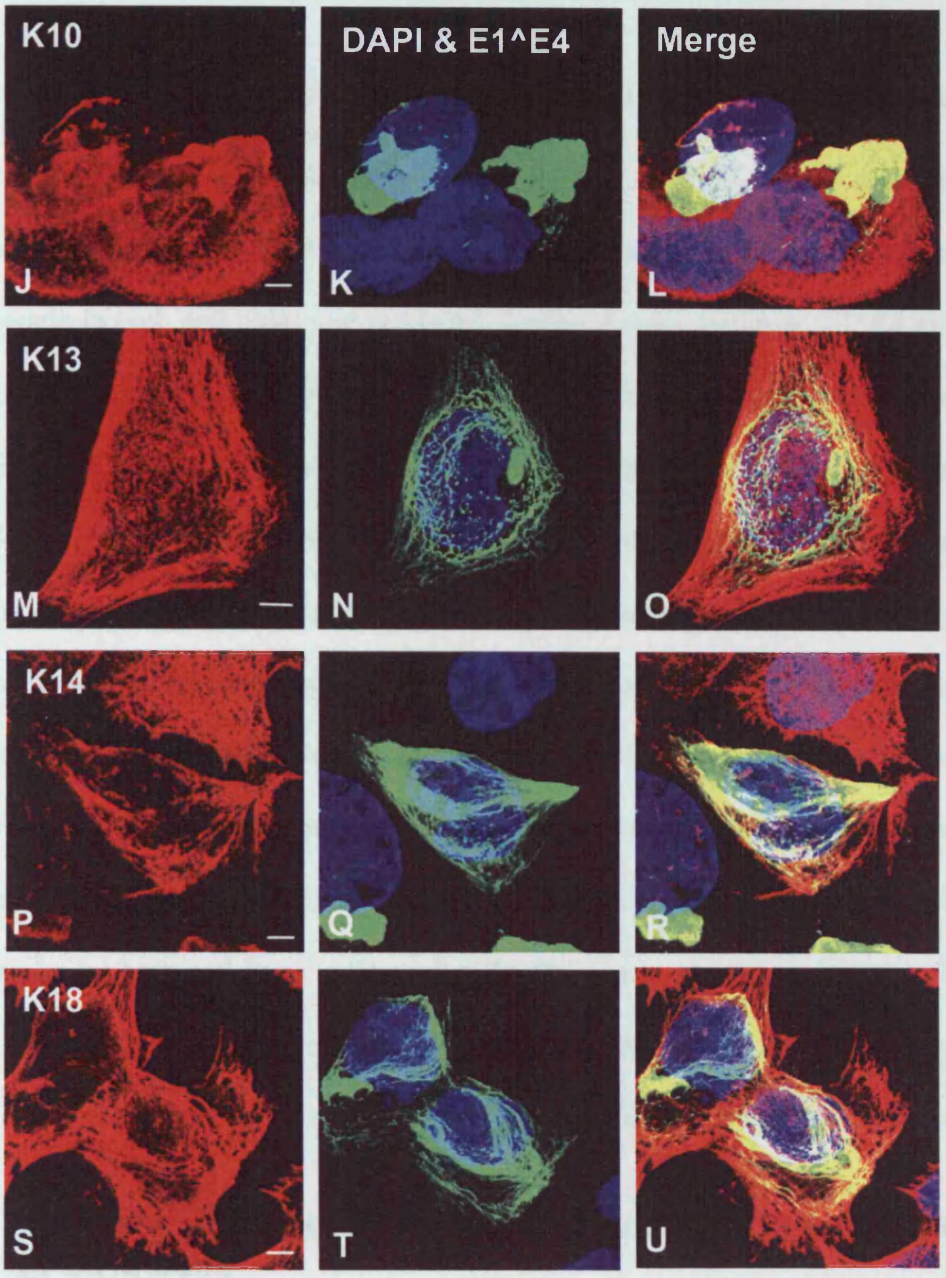
K10
DAPI & E1^E4
Merge
J
K
L
K13
M
N
O
K14
P
Q
R
K18
S
T
U

as networks at the surface of terminally differentiated epithelium. These observations suggest that 16 E1^E4 may associate with multiple keratin subtypes.

4.7.3 E1^E4 expression patterns in the presence of multiple different keratin polypeptides

HaCat and SiHa cells were infected with rAD E1^E4, fixed 12, 24, 48, and 72 h post infection and stained for E1^E4 (TVG405) and keratin (C2562). E1^E4 co-localised with keratin in both cell types and produced similar staining patterns. E1^E4 expressed in SiHa cells induced keratin 8/18 networks to collapse rapidly, leading to the formation of perinuclear bundles by 24 h. This is apparent from the rapid decrease in filamentous E1^E4 staining and the corresponding rapid increase in collapsed and aggregate staining patterns observed at 24 h (Fig 4.4 A). HaCat cells appear to be significantly more resistant to keratin network collapse due to the expression of greater keratin levels or different keratin subtypes. Unlike SiHa cells, intact filament networks could be observed in HaCat cells 72 h post infection (~35% of cells) (Fig 4.4 B). Both cell lines contained keratin-associated E1^E4 aggregates that increased in frequency with time. The graphs for both cell lines indicate that the frequency of collapsed keratin bundles levels off with time, whereas aggregates continue to increase in frequency suggesting that they may be at the end point for the collapsed structures (Fig 4.4).

4.8 The association of E1^E4 with mitochondria and keratin in SiHa cells

HPV 16 E1^E4 has previously been shown to associate with mitochondria, although the purpose of the E1^E4 mitochondrial interaction is as yet unknown (Raj *et al.*, 2004). Using keratin and E1^E4 antibodies in conjunction with a mitochondrial stain the relationship between E1^E4 aggregates, keratin and mitochondria was investigated. SiHa cells were infected with rAD E1^E4 or rAD β-gal, treated with mito-tracker (Molecular Probes), fixed with methanol 24 h post infection, and stained for E1^E4

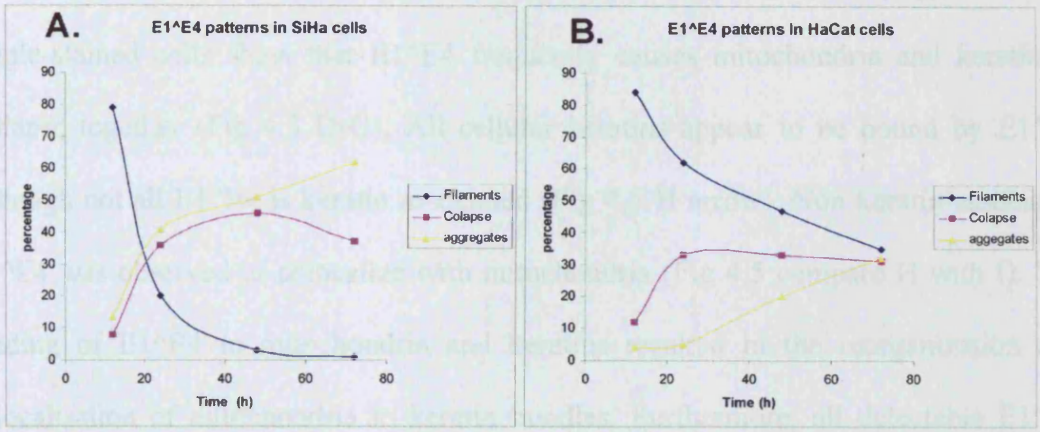

Figure 4.4 The temporal distribution of different E1^E4 structures in HaCat and SiHa cells.
Cell count data for SiHa and HaCat cells infected with rAD E1^E4 and stained for E1^E4 and keratin (100 cells counted / time point) for filaments, bundles and aggregates for examples refer to Fig 4.2. Graph A shows a decrease in the number of SiHa cell with filamentous E1^E4 over time, cells with filamentous E1^E4 drop to 2% by 72 h. In contrast 30% of HaCat cells maintain filamentous E1^E4 at 72% indicating a greater resistance to network collapse. Both populations show and increase in collapsed keratin bundles at later time points with curves flattening at ~48 h, with SiHa cells peaking at 50 % and with HaCat only 36% (A-B). Cells containing E1^E4 associated keratin aggregates continue to increase up to 72 h indicating E1^E4 aggregates to be at an end point.

(TVG405) and keratin (C2562). Cells were examined using high power confocal microscopy. In the absence of E1^E4, keratins form a filamentous network throughout the cytoplasm, with mitochondria existing as punctate structures (Fig 4.5 A-C). Triple-stained cells show that E1^E4 frequently causes mitochondria and keratin to collapse together (Fig 4.5 D-G), All cellular keratins appear to be bound by E1^E4 although not all E1^E4 is keratin associated (Fig 4.5 H arrow). Non keratin-associated E1^E4 was observed to colocalize with mitochondria (Fig 4.5 compare H with I). The binding of E1^E4 to mitochondria and keratins resulted in the reorganization and colocalisation of mitochondria to keratin bundles. Furthermore, all detectable E1^E4 was observed to localise to either mitochondria or keratin, with very little unbound protein being present.The examination of SiHa cells containing filamentous E1^E4 showed that E1^E4 can selectively bind to keratins without affecting mitochondria (Fig 4.6 A-D) as previously reported (Raj *et al.*, 2004). Conversely in cells containing E1^E4 aggregates (Fig 4.6 E-K), E1^E4 associates with both keratin and mitochondria and in some cases these aggregates can be observed in the absence of keratin network saturation or collapse. It is thought likely that keratin saturation and network collapse occur prior to aggregate formation allowing E1^E4 to associate with mitochondria. E1^E4 production may possibly cease allowing keratin networks to reform. The higher frequency of cells exhibiting aggregate staining at later time points makes this seem probable (see Fig 4.4).

4.9 E1^E4 association induces the phosphorylation of keratins

Keratin networks become highly phosphorylated as a result of normal cell cycle progression during mitosis and apoptosis, and reorganise into multiple aggregate like structures (Ku *et al.*, 1994; Ku *et al.*, 1998; Ku *et al.*, 2002b). The observation of similar structures in E1^E4-expressing cells prompted us to investigate the

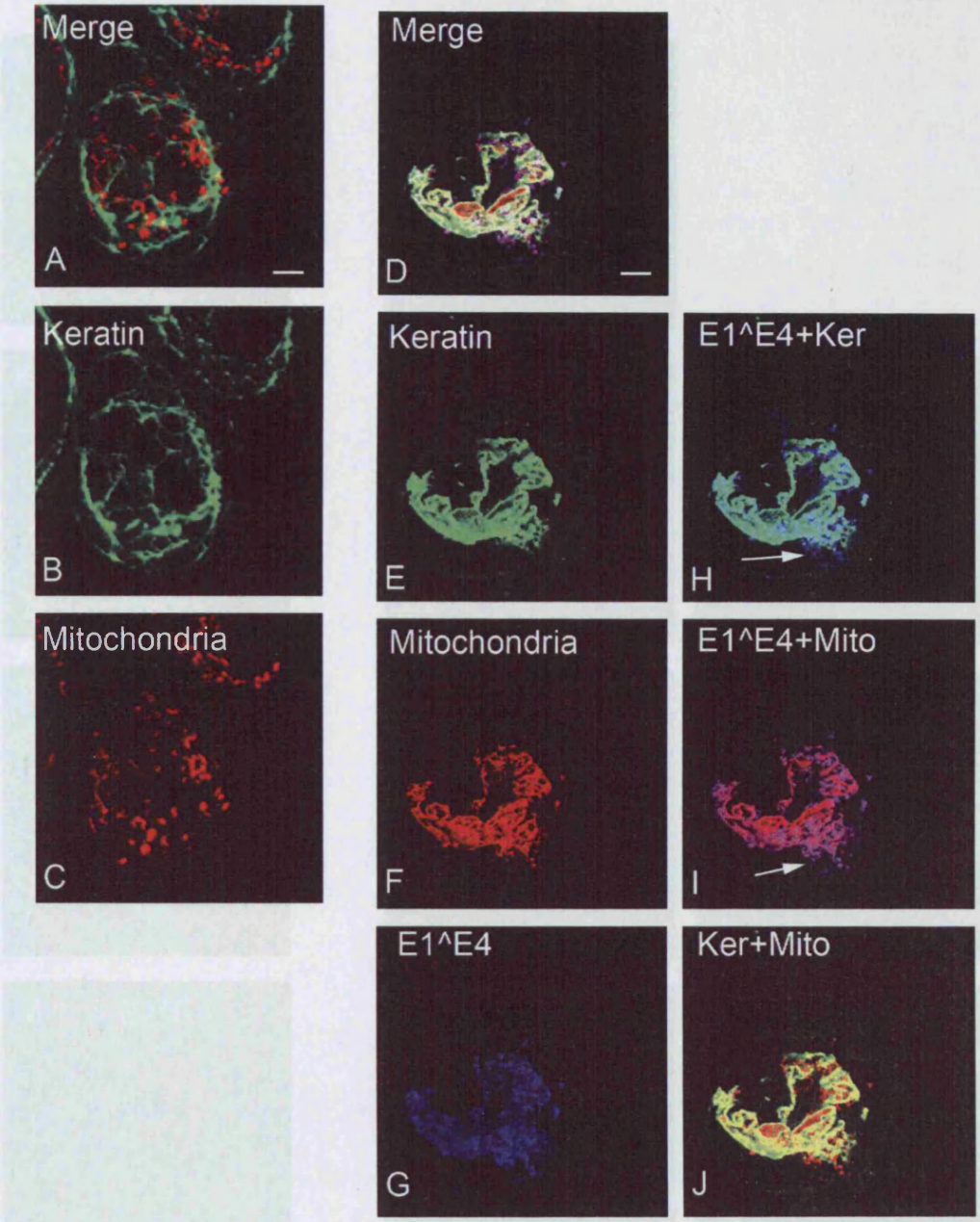

Figure 4.5 The association of E1^E4 to keratin and mitochondria
Example of a SiHa cell stained for keratin (C2562) and mitochondria (Mitotracker-red), the two systems do not colocalize, keratins form cytoplasmic filament networks and mitochondria exist as punctuate structures (A-C). In the presence of E1^E4 (TVG402-blue) mitochondria and keratin collapse together, (D and J). All keratin is bound by E1^E4 although not all E1^E4 is keratin associated (H arrow). E1^E4 not associated to keratin is be bound to mitochondria (I arrow). Scale bars denote 5 μm.

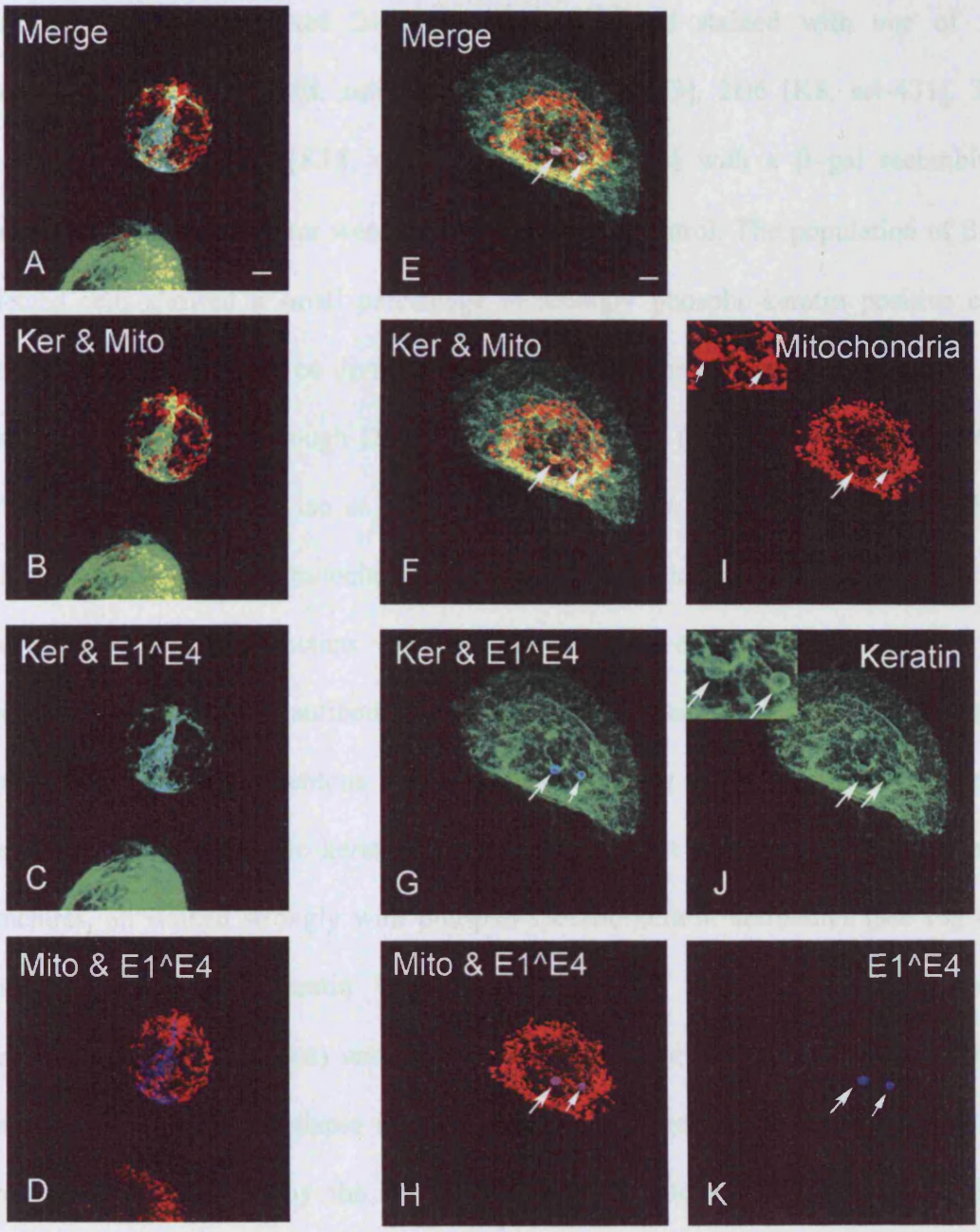

Figure 4.6 E1^E4 associated to keratin and mitochondria selectively
SiHa cells infected with rAD E1^E4, fixed 24 h after infection and stained for keratin (C2562-green), mitochondria (Mitotracker-red) and E1^E4 (DAPI-blue). E1^E4 can be seen to associate to keratin without affecting mitochondria (A-D). Cells containing E1^E4 aggregate structures (E-K) E1^E4 can be observed to associate to both keratin (inlay J) and mitochondria simultaneously (arrows E-K) in the absence of keratin network saturation or collapse (E-K). Scale bars denote 5 μm.

phosphorylation state of keratins in the presence of E1^E4. SiHa cells were infected with rAD 16 E1^E4, fixed 24 h after infection and stained with one of four phospho-specific anti-keratin antibodies (LJ4 [K8, ser-73], 2D6 [K8, ser-431], 3055 [K18, ser-52] and 8250 [K18, ser-33]). Cells infected with a β–gal recombinant adenovirus expression vector were used as a negative control. The population of β–gal infected cells showed a small percentage of strongly phospho-keratin positive cells. This subset of cells could be divided into two populations consisting of apoptotic and mitotic cells (identified though DAPI staining) (Fig 4.7) (Ku *et al.*, 1997b; Ku *et al.*, 1998; Ku *et al.*, 2002a; Liao *et al.*, 1997; Toivola *et al.*, 2002). The 3055 antibody exhibited a low level of mitochondrial background staining in SiHa cells (data not shown). At 24 h post infection ~ 50% of E1^E4-positive cells reacted strongly with phosphor-specific keratin antibodies (Fig 4.8). E1^E4 associated with both collapsed keratin bundles and filamentous keratin but the majority of these cells did not cross react with phospho-specific keratin antibodies. Cells that contained E1^E4 aggregate structures, all stained strongly with phospho-specific keratin antibodies (see Fig 4.9). The observation that keratin bundle formation can occur in the absence of phosphorylation (not shown) and that filament phosphorylation is not necessarily a consequence of keratin collapse (see Fig 4.8), may suggest that phosphorylation is a stress response induced by the association of E1^E4 to filaments. These findings suggest that the formation of keratin associated E1^E4 aggregates may occur as a direct result of keratin phosphorylation.

4.9.1 E1^E4 and Cyclin B1 colocalise in aggregates

It is known that HPV16 E1^E4 has the ability to sequester the cyclin B/CDK 1 complex into the cytoplasm (Davy *et al.*, 2005). It is also know that the cyclin B/CDK 1 complex can phosphorylate keratin 18 (K18-Ser33) during M phase (Zhou *et al.*, 1999). In

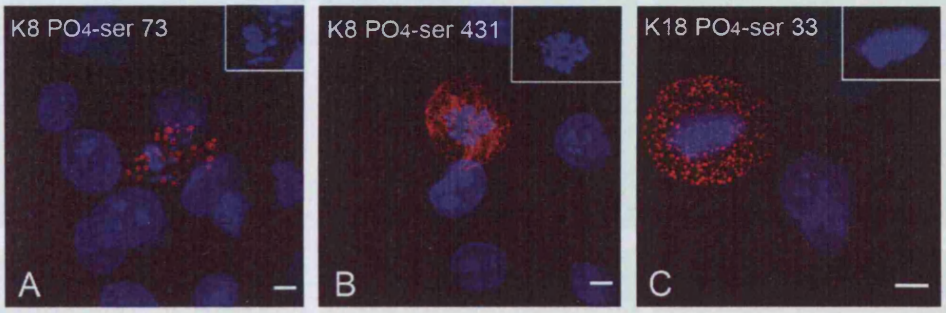

Figure 4.7 Phospho-specific keratin antibodies react with mitotic and apoptotic SiHa cells

SiHa cells infected with β-gal rAD were stained for phosphorylated keratin, (K8 PO4 ser-431(2D6), PO4 ser-73 (LJ4), or K18 PO4 ser- 33 (8250) (red) and DNA (DAPI-blue). Apoptotic/mitotic status of cells was determined by DAPI stain (see inlays A-C). (A-B) LJ4 and 2D6 reacted strongly with cytoplasmic structures in both mitotic and apoptotic cells. (C) 8250 produced strong cytoplasmic staining in mitotic cells. Cells with normal nuclei showed little reactivity with the phospho-specific keratin antibodies. Scale bars denote 5 μm.

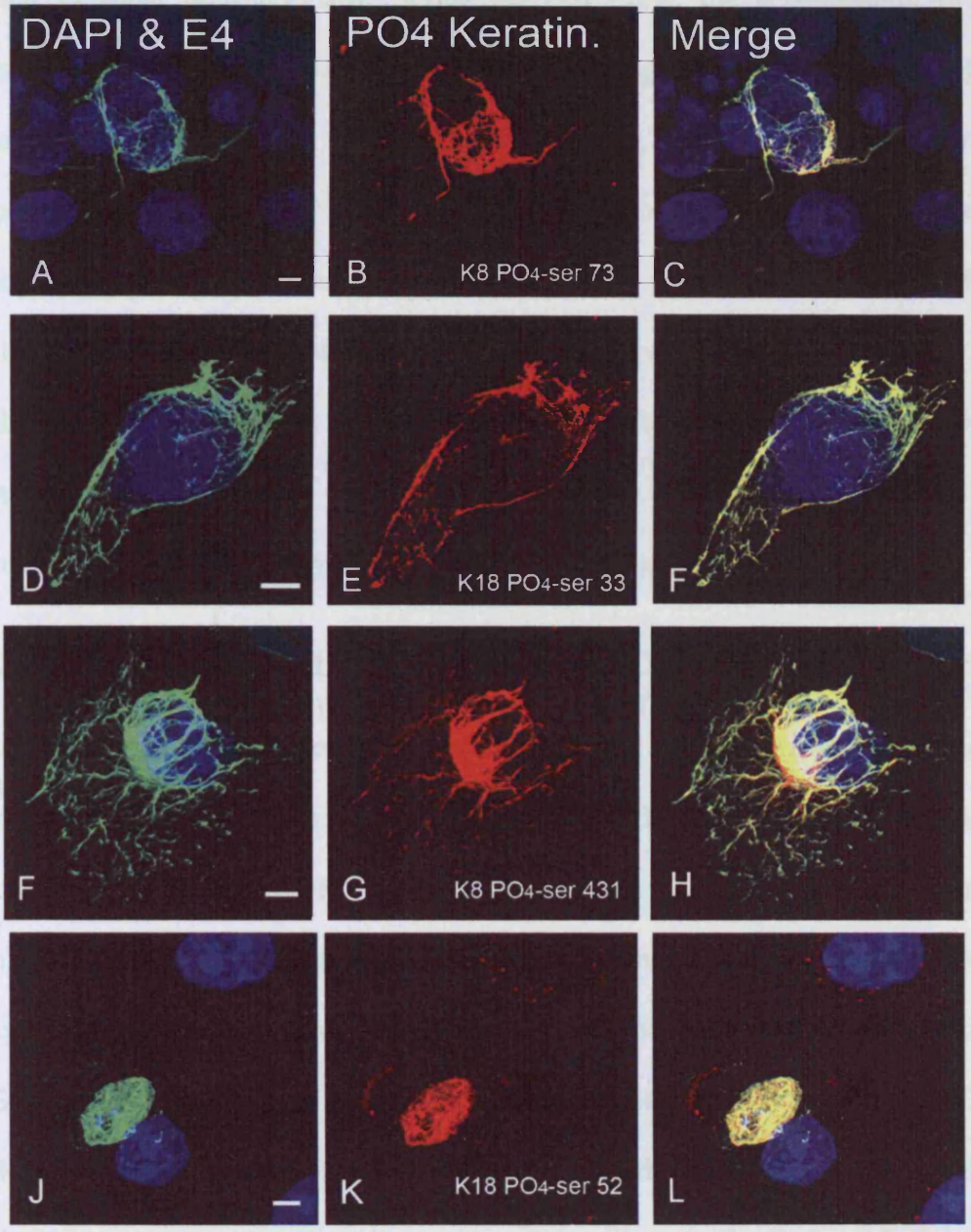

Figure 4.8 E1^E4 binding induces multi-site phosphorylation of type I and II keratins

SiHa cells infected with rAD E1^E4 were fixed 24 h post infection and stained for E1^E4 (TVG405-green), phospho specific keratin antibodies (K8 PO_4 ser-431 (2D6), PO_4 ser-73 (LJ4), K18 PO_4 ser- 33 (8250) PO_4 ser-52 (3055)) (red) and DNA (DAPI-Blue). The keratin 18 PO_4 ser-52 antibody (3055) appeared to cross react with mitochondria (J-L). The association of E1^E4 to keratin filaments resulted in the phosphorylation of affected keratin structures. Scale bars denote 5 μm.

addition to being phosphorylated during the cell cycle, the accumulation of this phospho-keratin isoforms has also been observed during toxin induced Mallory body formation (Fausther *et al.*, 2004). Double staining for E1^E4 and cyclin B, demonstrated that less than10 % of cells with filamentous E1^E4 showed visible co-localization (not shown). By contrast, cyclin B could be seen to colocalize with ~90 % of E1^E4 aggregates. These structures were also observed to contain phosphorylated keratin (Fig 4.9). The collapse of keratins may concentrate cyclin B staining making it easier to visualise. Conversely sequestration of cyclin B to keratin filaments by E1^E4 may result in keratin phosphorylation promoting aggregate formation.

4.9.2 Is the recruitment of the cyclin B/CDK1 complex to keratin responsible for keratin phosphorylation?

Having established that both keratin phosphorylation and cyclin B-E1^E4 colocalisation predominate on E1^E4-keratin aggregates, it was decided to investigate whether the association of the cyclin B/CDK1 complex was involved in keratin phosphorylation. To examine this, a mutant E1^E4 (T22A, T23A) which is unable to sequester cyclin B into the cytoplasm was utilised. This mutation is not predicted to affect the association of E1^E4 with keratins (Davy *et al.*, 2002). It was hypothesized that if cyclin B/CDK 1 was involved in the phosphorylation of E1^E4-associated keratin, this mutant would be unable to sequester cyclin B and may therefore affect cyclin B-dependent keratin phosphorylation. Immunostaining using the panel of phospho-specific keratin antibodies revealed that all four keratin sites still underwent phosphorylation including keratin 18 ser-33, which is a known *in vitro* substrate of the cyclin B/CDK 1 complex (Ku *et al.*, 1998). These data indicate that recruitment of the cyclin B/CDK1 complex by E1^E4 is not essential for the phosphorylation of these sites in the E1^E4-associated keratin networks (Fig 4.10).

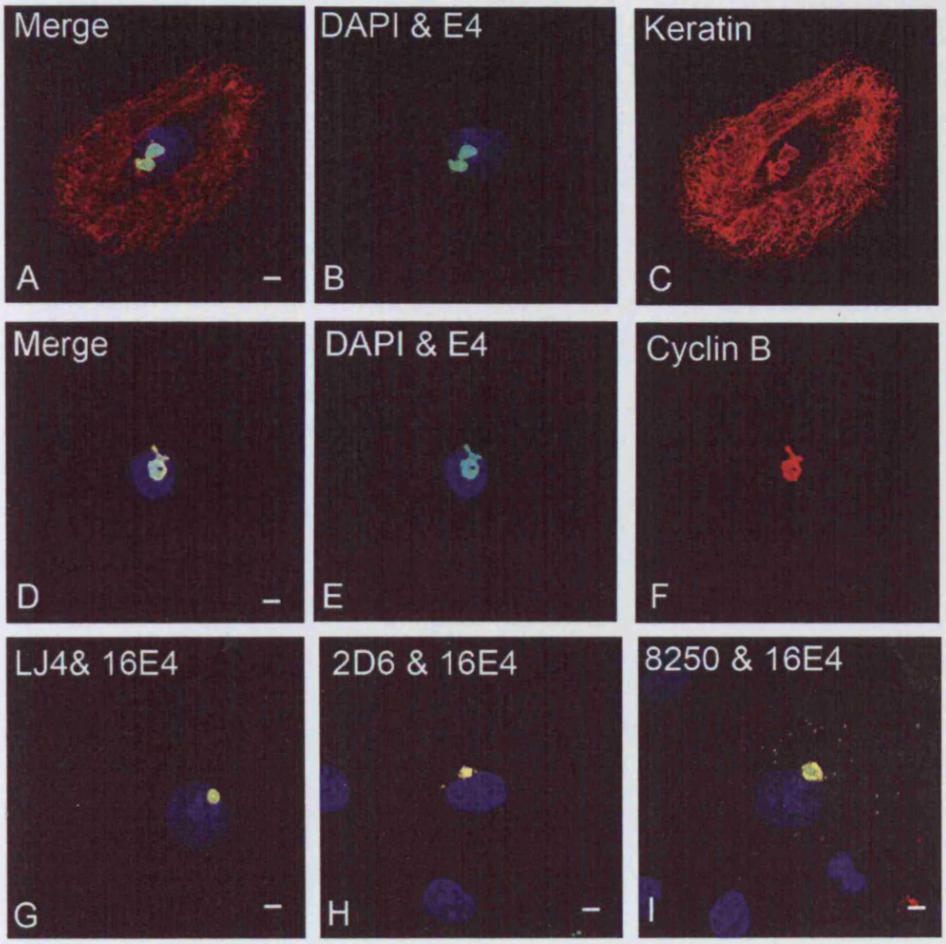

Figure 4.9 E1^E4 aggregates contain highly phosphorylated keratin and Cyclin B
SiHa cells infected with rAD E1^E4 were fixed 24 h post infection and stained for E1^E4 (TVG405, green) keratin (C2562, red) and DNA (DAPI, blue). E1^E4 aggregates contain keratin (A-C). Cells stained for Cyclin B (GNS11-red) reveal that almost 100 % of E1^E4 aggregates also contain Cyclin B (D-F). E1^E4 aggregates also react strongly with phospho-specific keratin antibodies (K8 PO_4 ser-431 (2D6), PO_4ser-73 (LJ4), and K18 PO_4 ser-33 (8250), (red) (G-I). scale bars denote 5 μm.

Figure 4.10 An E1^E4 mutant with a reduced affinity for Cyclin B maintains the ability to induce keratin phosphorylation

SiHa cells transfected with a mutant (T22A, T23A) E1^E4 expression vector were fixed 24 h post transfection and stained for E1^E4 (TVG405-green), keratin (C2562-red) and DNA (DAPI-Blue). The mutant E1^E4 maintained its ability to bind and disrupt keratin filament networks as previously reported (A-C). Staining with phospho specific keratin antibodies (K8 PO4 ser-431 (2D6), PO4 ser-73 (LJ4), K18 PO4 ser- 33 (8250) PO4 ser-52 (3055)-(red)) showed that (T22A, T23A) E1^E4 maintained the ability to induce multiple keratin phosphorylation events (D-O). 3055 produces background mitochondrial staining (M-O). Scale bars denote 5 μm.

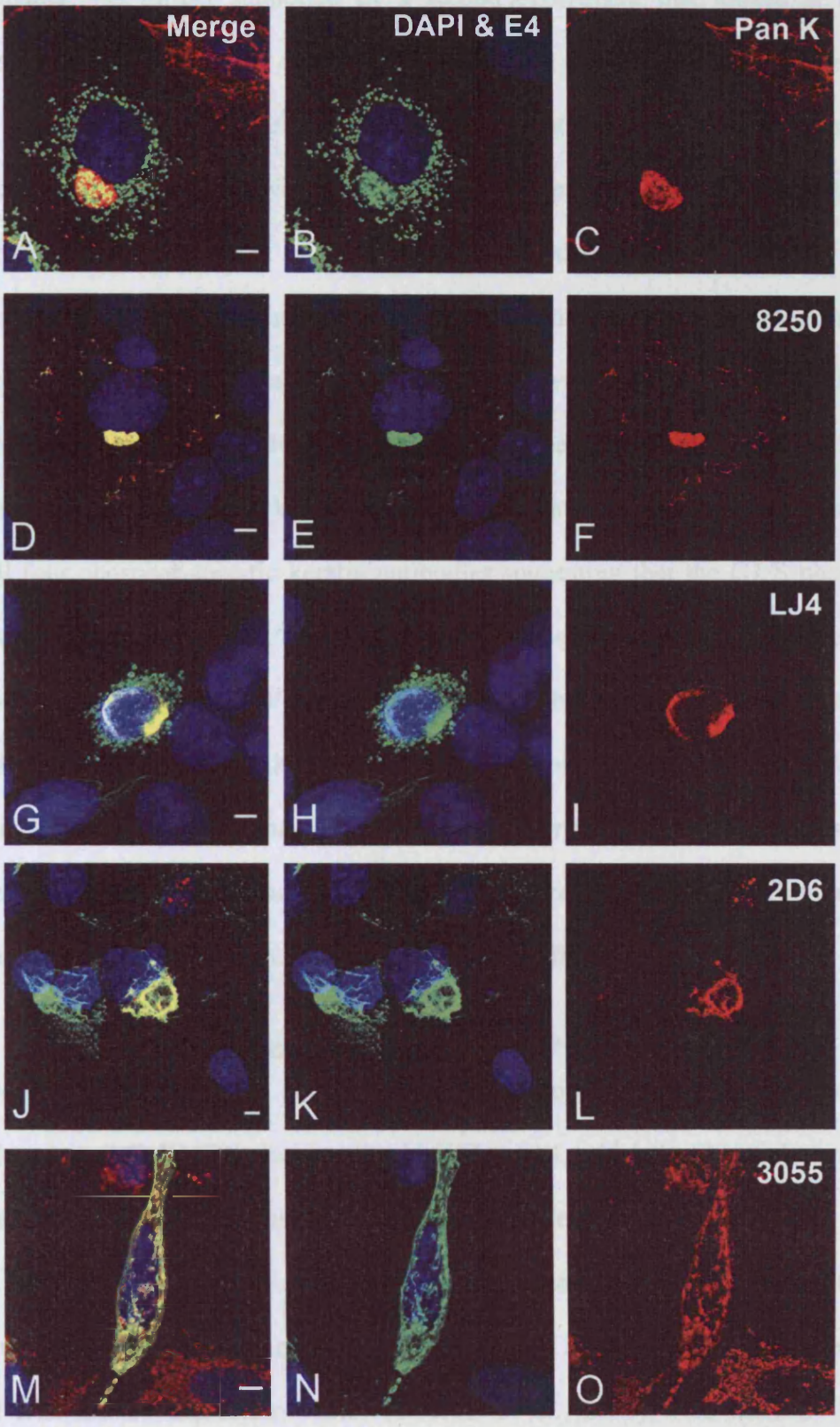
Merge
DAPI & E4
Pan K
A
B
C
8250
D
E
F
LJ4
G
H
I
2D6
J
K
L
3055
M
N
O

This finding was further supported by a second experiment that looked at E1^E4 expression in SiHa cells held under aphidicolin block using an established protocol (Davy *et al.*, 2005). SiHa cell were synchronised at G1/S using low serum and aphidicolin and then infected with rAD E1^E4. One population was then released from the aphidicolin block 6 h post infection whereas the other remained under the block. The cells were fixed and stained for E1^E4 and keratin, at 24 h post infection. The population released from the aphidicolin block had twice as many of E1^E4/keratin aggregates when compared to the blocked population. Despite the difference in E1^E4's appearance, E1^E4-associated keratin structures in both populations stained positively with all four phosphor-specific keratin antibodies suggesting that the G1/S phase cell cycle arrest did not prevent E1^E4-induced keratin phosphorylation of these sites. The increased frequency of E1^E4/Keratin aggregates in the released population may be attributable to higher levels of kinase activity at later points in the cell cycle (reviewed in (Stark *et al.*, 2004), which may promote aggregate formation. These findings suggest that keratin phosphorylation may be a stress induced response to E1^E4 binding and that it is not necessarily linked to the proteins ability to disrupt the cell cycle.

4.9.3 Linking keratin Phosphorylation to E1^E4 binding

To investigate the relationship between keratin phosphorylation and E1^E4 binding, a second mutant (M2 E1^E4), lacking the LLKLL motif, which has been shown to be involved in E1^E4 binding keratin, was utilised (Roberts *et al.*, 1994; Wang *et al.*, 2004). M2 E1^E4 has a greatly reduced ability to bind to and collapse keratin networks and is unable to associate with mitochondria (Raj *et al.*, 2004). SiHa cells infected with an M2 rAD E1^E4 expression vector (Doorbar *et al.*, 2000) were fixed 24 h post infection and stained for E1^E4 and Keratin. M2 E1^E4 formed large irregular condensed structures that showed almost no keratin (Fig 4.11 A-C) (see next section).

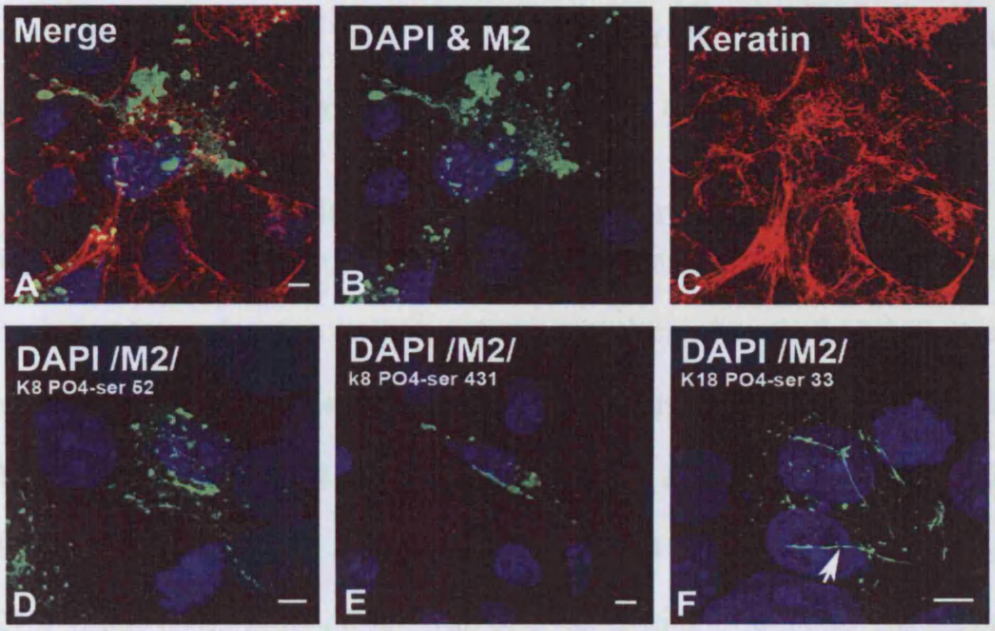

Figure 4.11 M2 E1^E4 a keratin binding mutant show very little keratin phosphorylation.
SiHa cells infected with rAD M2 E1^E4 were fixed 24 h post infection and stained for E1^E4 (TVG405-green) keratin (C2562-red) and DNA (DAPI-blue). M2 E1^E4 did not form filamentous structure commonly observed with wild type E1^E4 although, a few partially filamentous globules were observed (arrow F). No keratin reorganisation was observed to occur in cell expressing M2 E1^E4 at 24 h (A-C). Staining of cells with TVG405 (Green) and phospho specific keratin antibodies (K8 PO_4 ser-431 (2D6), PO_4 ser-73 (LJ4) and K18 PO_4 ser- 33 (8250) red) overlay images show that expression of M2 E1^E4 did not induce phosphorylation of cytokeratin networks (D-F). Scale bars denote 5 μm.

Phosphorylated keratin was not observed using any of the four phospho-specific antibodies in cells expressing M2 E1^E4 (Fig 4.11 D-F). These data indicate that a direct interaction between keratin and E1^E4, or that the resultant network reorganisation is required for keratin phosphorylation to occur.

4.9.4 M2 E1^E4 maintains a weak affinity for keratin network

Having noticed during the earlier experiment that M2 appeared to have a very limited ability to localise to keratins in SiHa cells, it was decided to perform a time course experiment to see if the association altered over time. SiHa cells were infected with rAD M2 E1^E4, fixed at 12, 24, 48, 72 h after infection and stained for keratin (C2562) and E1^E4 (TVG405) (Fig 4.12). At 12 h very little M2 E1^E4 could be seen in the cells. By 24 h visible levels had built up, with cells comprising of a mixed population that showed both diffuse and condensed staining patterns (Fig 4.12 A-C). Interestingly a few stretched-globular structures that weakly colocalize with keratin were also observed (Fig 4.12 D-F). Between 48-72 h keratin colocalisation increased resulting in disruption and bundling of keratins (Fig 12 G-I). Unlike wild type E1^E4, M2 never displays a purely filamentous pattern and forms condensed structures which displays weak keratin colocalisation which increases over time, eventually resulting in network disruption only at late time points.

4.10 Characterisation of E1^E4 and keratin complexes

4.10.1 Western blot analysis of the wild type and mutant 2 E1^E4

SiHa cells were infected with rAD β-gal, wild type or M2 E1^E4 expression vector and harvested at 12, 24 or 48 h post infection. The lysates were separated on a 15% SDS/PAGE gel and transferred to a nitrocellulose membrane then probed for E1^E4 and glyceraldehhyde-3-phosphate dehydrogenase (GAPDH) (used as loading control) (Fig 4.13). β-gal infected extracts did not contain E1^E4-reactive bands. Wild type E1^E4

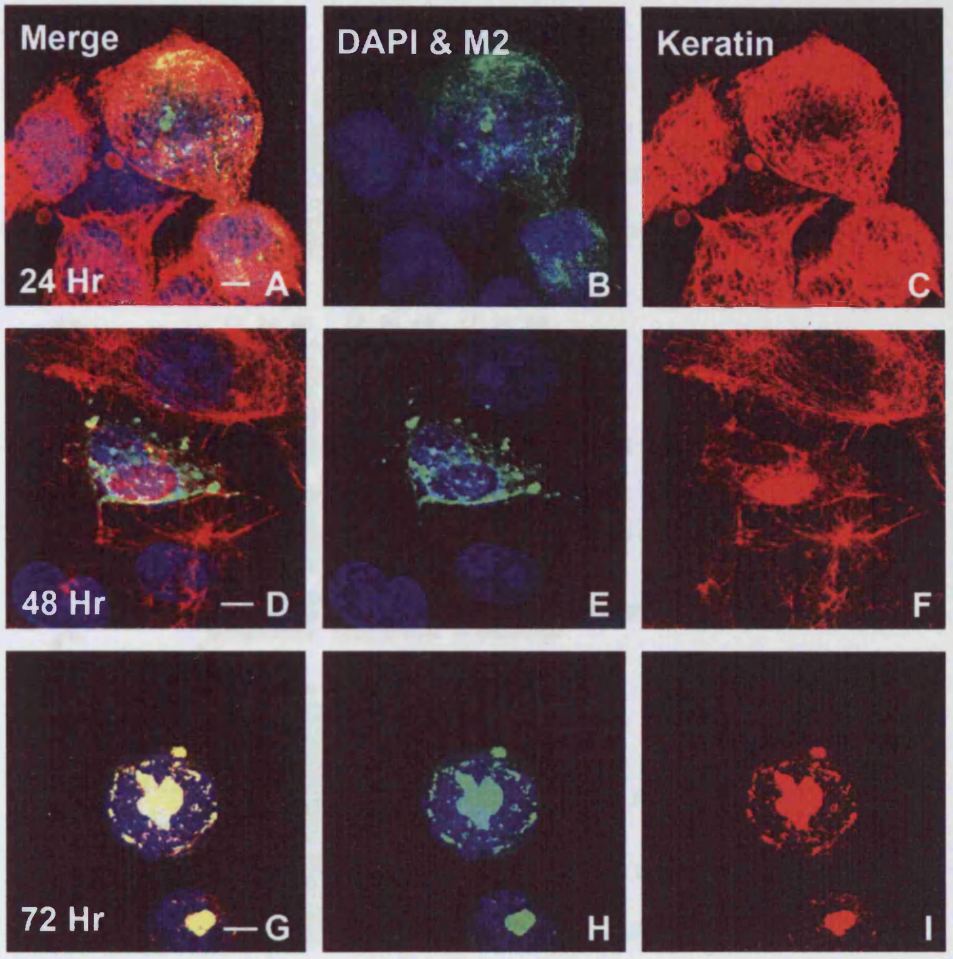

Figure 4.12 Build up of M2 E1^E4 in SiHa cells results in keratin filament disruption

SiHa cells infected with rAD M2 E1^E4 were fixed 24, 48, and 72 h after infection and stained for E1^E4 (TVG405-Green), keratin (C2562-red) and DNA (DAPI-Blue). M2 E1^E4 displays a variety of different patterns. At early time points cells contain both diffuse and globular M2 E1^E4 with few filamentous structures and little keratin colocalisation (A-F). Keratin staining builds up in M2 E1^E4 structures and by 72 h M2 E1^E4 the majority of cellular keratin is found to localise with M2 E1^E4 resulting in the disruption of networks (G-I). Scale bars denote 5 μm

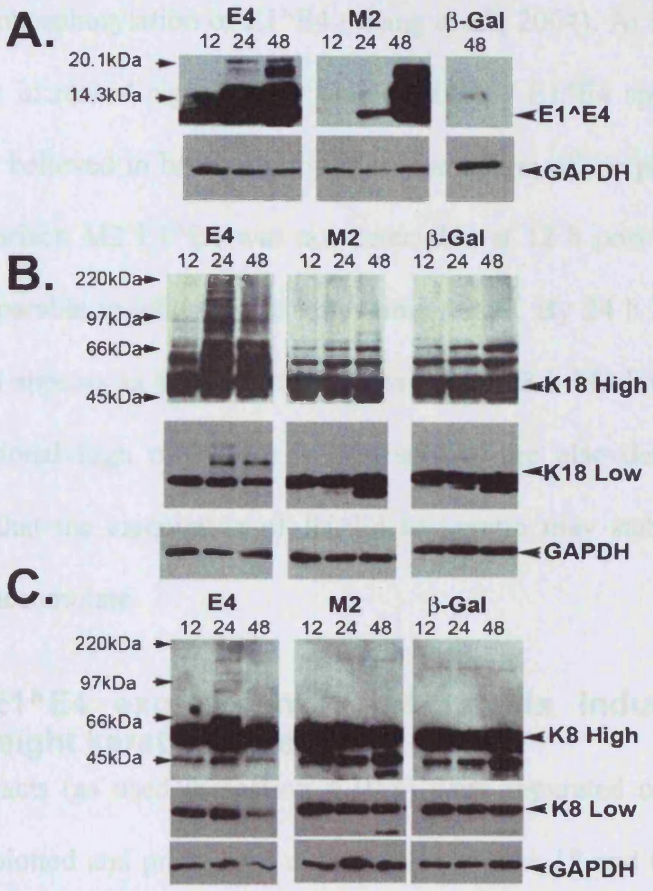

Figure 4.13 Western blot characterisation of wild type and M2 E1^E4 expression and keratin species in SiHa cells over a 48 h time course

A shows the build up of wild type and M2, E1^E4 in rAD infected SiHa cells 12, 24 and 48 h post infection (probed with TVG402). Wild type E1^E4 expression can be detected 12 h post infection and continues to build up between 24 and 48 h. M2 expression cannot be detected at 12 h, but by 48 h expression has dramatically increased and is approximately comparable to that of wild type protein. The right most lane contains β-gal infected SiHa extract and demonstrates that TVG402 does not react with other cellular proteins. Blot **B** shows extracts probed for keratin 18 (CY-90). Low exposures show high molecular weight keratin 18 species in the wt E1^E4 lanes, higher exposures reveal the presence of keratin ladders. At 48 h, high levels of M2 E1^E4 expression do not result in the formation of keratin ladders, and are comparable to the β-gal population. **C** shows extracts of SiHa cells infected with wt or M2 E1^E4 or β-gal rAD at 12, 24 and 48 h post infection probed for keratin 8 (Cam 5.2). Low exposures of the blot reveal little difference between the three groups. Higher exposures show high molecular weight keratin 8 species present in the wt-E1^E4 lanes. Keratin 8 and 18 blots of extracts from M2 and β-gal infected cells appear comparable at all time points. All blots were re-probed with GAPDH as a loading control.

could be detected at 12 h and ran as 2 bands. The top band has been shown to result from the phosphorylation of E1^E4 (Wang *et al.*, 2004). At later time points, the levels of protein increased significantly with additional E1^E4 species also being observed. These are believed to be caused by multimerisation of the protein (Wang *et al.*, 2004). By comparison M2 E1^E4 was not detectable at 12 h post infection, and levels were only comparable to wild type at latter time points. By 24 h M2 can be detected at low levels and appears as a single band, however by 48 h M2 levels have increased greatly and additional high molecular weight species are also detectable. This observation suggests that the association of E1^E4 to keratin may stabilise the protein allowing levels to accumulate.

4.10.2 E1^E4 expression in SiHa cells induces high molecular weight keratin ladders

SiHa extracts (as used in section 4.10.1) were separated on a 10% SDS/PAGE gel, Western blotted and probed for either a keratin 8 or 18 and GAPDH. The keratin blots showed that all three cells extracts were comparable at 12 h (Fig 4.13 B and C). At later time points additional high molecular weight keratin 18 species are clearly visible in the E1^E4 extracts (Fig 4.13 B) as previously reported (Wang *et al.*, 2004). No increase in high molecular weight keratin 18 species is observed in the M2 E1^E4 or β-gal extracts at these time-points. The emergence of high molecular weight keratin 18 species coincided with an increase in E1^E4 levels (Fig 4.13A), suggesting that the two are linked. Despite high expression levels at 48 h (Fig 4.13 A) abundant M2 E1^E4 does not result in the formation of keratin ladders. Extracts were also probed for keratin 8 (Fig 4.13 C). High molecular weight keratin 8 species were also observed in wild type E1^E4 extracts at 24 h but not β-gal or M2 E1^E4 extracts. However, they were much less intense than the keratin 18 species and could not be detected at 48 h due to loss of cells (Fig 4.13 C).

A build up of low molecular weight keratin 8 and 18 species was observed in both M2 and β-gal extracts over this time period. These species were less intense in E1^E4 extracts. At late time points wild type E1^E4-expressing cells undergo keratin collapse and apoptosis both of which cause cells to float off the plate (the extent of cell loss can be determined by strength of GAPDH bands) (also see Fig 4.18). Low molecular weight keratins bands observed in M2 E1^E4 and β-gal at late time points may be caused by caspase cleavage of keratin (Caulin *et al.*, 1997; Ku *et al.*, 1997a; Oshima, 2002; Schutte *et al.*, 2004). The lack of low molecular weight keratins (see arrows Fig 4.13 B and C) may indicate that E1^E4 expressing cells detach from the plate prior to the initiation of apoptosis. Alternatively apoptosis may only be initiated in cells which have lost their keratins as mitochondrial association (previously linked to apoptosis (Raj *et al.*, 2004)) is usually observed after keratin collapse. High molecular weight keratin species may be induced by glycosylation or ubiquitination.

4.10.3 Keratin specific western blots of HaCat cell lysate

To examine whether E1^E4-association could induce biochemical modifications to keratins other than K18/8, HaCat cells were infected with either wild type or M2 E1^E4 rAD. Cells were harvested 12, 24, 48, 72 and 96 h post infection. Expression of wild type and M2 E1^E4 in HaCat cells was comparable to SiHa cells with M2 levels building up more slowly over time (Fig 4.14 A). Lysates were separated on a 10% SDS/PAGE gel and probed with keratin specific antibodies. Keratin 8 and 18 blots were comparable to those from SiHa cells with high molecular weight species being observed in both (Fig 4.14 B). Keratin 10 blots were weak and it is possible that this keratin species is not abundant in HaCat (data not shown). No high molecular weight keratin species could be observed in keratin 13 blots. Weak high molecular weight keratins 4

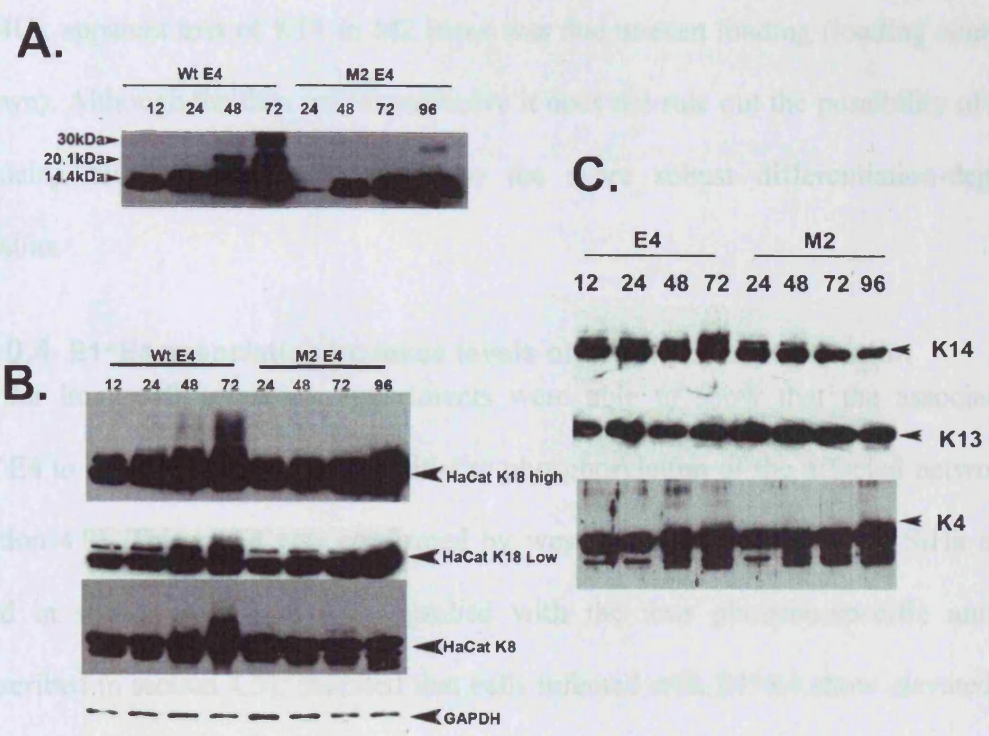

Figure 4.14 Affect of wild type and M2 E1^E4 or different keratin subtypes in HaCat cells

HaCat cell infected with wild type or M2 E1^E4 rAD were harvested 12, 24,48 and 72 h (24,48, 72 and 96 h for M2) post infection. Extracts were separated on a 10% SDS PAGE gel probed for E1^E4 (TVG402). Blots revealed that M2 builds up more slowly than wild type protein. Extracts separated on 10% SDS/Page gels were probed with subtype specific keratin antibodies (K8 cam5.2, K18 Cy-90, K14-LL001, K13-NCLCK13. An increase in high molecular weight keratin 8 and 18 species was observed in E1^E4 extracts. Levels of M2 E1^E4 are low at 24 h time points but greatly increase by 48 hr (A). M2 E1^E4 does not cause an increase in keratin high molecular weight keratins species (B). Keratin 13 blots revealed no, differences between wild type and M2 E1^E4 extracts with not detectable high molecular weight keratin. Both the keratin 4 and 14 blots showed some evidence of additional high molecular weight species by 72 hr in the E1^E4 lanes.

and 14 bands could be detected at late time points in wild type E1^E4 extracts (Fig 4.14C), apparent loss of K14 in M2 lanes was due uneven loading (loading control not shown). Although the data are inconclusive it does not rule out the possibility of E1^E4 inducing biochemical modifications to the more robust differentiation-dependent keratins.

4.10.4 E1^E4 association increase levels of keratin phosphorylation

Earlier immunofluorescence experiments were able to show that the association of E1^E4 to keratin resulted in the multi-site phosphorylation of the affected network (see section 4.9). This result was confirmed by western blot analysis of the SiHa extracts used in section 4.10.1. Extracts probed with the four phospho-specific antibodies (described in section 4.9), revealed that cells infected with E1^E4 show elevated levels of keratin phosphorylation at 24 h (Fig 4.15). At 24 h post infection M2 expressing cells did not show elevated levels of keratin phosphorylation and were comparable to the β-gal population. By 48 h post-infection phosphorylation levels in all populations were elevated (data not shown). This may be due to apoptosis/cell stress associated with adenovirus infection. These data confirm that the association of E1^E4 with keratin facilitates keratin phosphorylation.

4.10.5 The effect of E1^E4 keratin-binding on the solubility of both proteins

We have shown that M2 maintains an ability to associate with and disrupt keratin filaments although the rate of disruption was significantly reduced. In addition to this its expression does not induce biochemical modification to keratins. Fractionation experiments were conducted to determine whether M2 had the capacity to affect keratin solubility as has previously been reported for wild type E1^E4 (Wang *et al.*, 2004). Wild type E1^E4, M2 and β-gal infected SiHa cells were harvested from the plate using

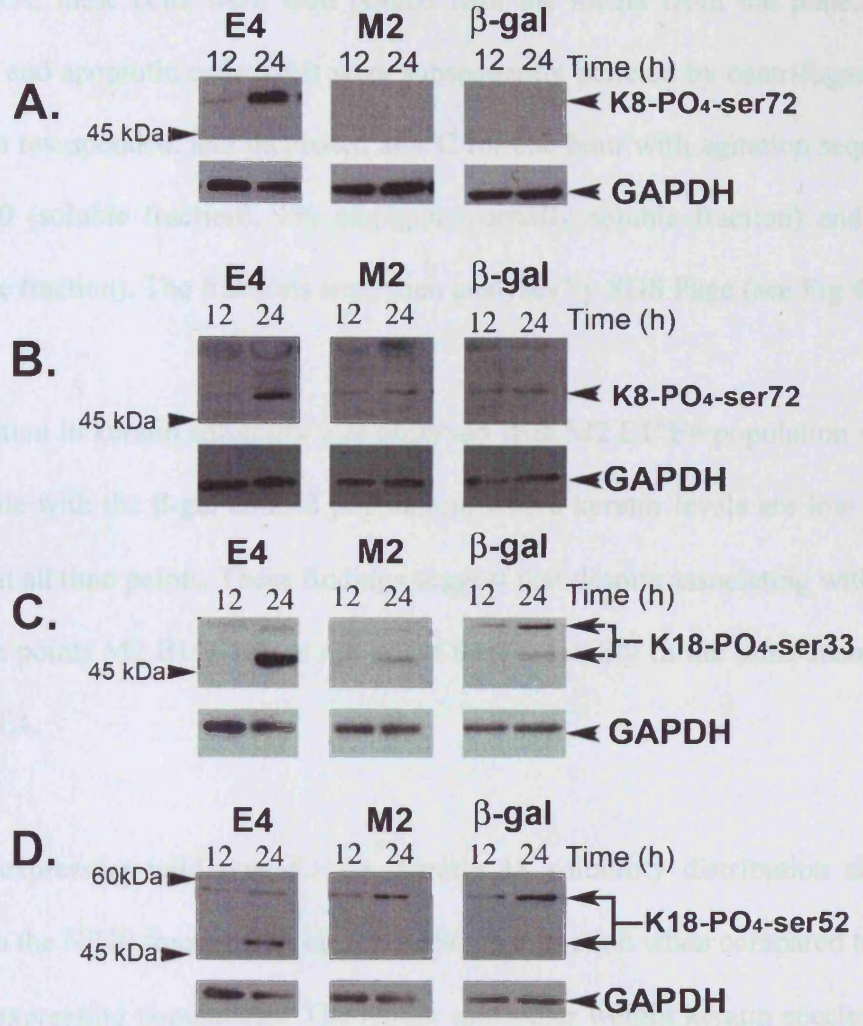

Figure 4.15 E1^E4 expression increases levels of phosphorylated keratin 8 and 18
SiHa cells infected with β-gal, wild type or M2 E1^E4 rAD were harvested at 12 and 24 h post infection (same extracts used in fig 4.13). Extracts were probed with phospho specific keratin antibodies IB4 [K18, PO4 ser 33], 3055 [K18, PO4 ser 52], LJ4 [K8, PO4 ser 73] and 2D6 [K8, PO4 ser 431]. Blot A shows extracts probed for K8, PO4 ser 73 the antibody reacts with E1^E4 extracts at 12 h the signal increases at 24 h, M2 and β-gal extracts are negative. Blot B shows E1^E4 extracts contain significantly more K8, PO4 ser 431 at 24 h than β-gal or M2 extracts. Blot C shows extracts probed for K18, PO4 ser 33 the lower band which corresponds to keratin 18 is significantly stronger in E1^E4 extracts. Blot D shows extracts probed for K18, PO4 ser 52 two bands are detected the lower band corresponding to keratin 18 is only present in the E1^E4 extracts (upper bands in C and D may be antibody reacting with an unidentified cellular protein).

PBS/EDTA, these cells were then pooled with the media from the plate, containing detached and apoptotic cells, cells were subsequently pelleted by centrifugation. Pellets were then resuspended, and incubated at 4°C for one hour with agitation sequentially in 1% NP40 (soluble fraction), 1% empigen (partially soluble fraction) and 9 M urea (insoluble fraction). The fractions were then analyses by SDS Page (see Fig 4.16)

No reduction in keratin solubility was observed with M2 E1^E4 population which were comparible with the β-gal control population, where keratin levels are low in the urea fraction at all time points. These findings suggest that despite associating with keratins a later time points M2 E1^E4 does not effect their solubility in the same manner as wild type E1^E4.

In cells expressing wild type E1^E4, keratin 18 solubility distribution shifts, being weaker in the NP40 fraction and higher in the urea fraction when compared to the β-Gal and M2 expressing populations. The higher molecular weight keratin species are found exclusively in the insoluble (urea) fraction (Fig 4.16.B).

The way in which the experiments were conducted (1 h incubations) may have exaggerated the solubility of each fraction, as keratin is usually seen predominantly in the empigen fractionation. This data show that keratin solubility is reduced, in E1^E4 epressing cells but is not affected by M2 E1^E4.

Wild type E1^E4 fractionates predominantly to the empigen fraction (Fig 4.16 A). At early time points the phosphorylated form of the proteins is present exclusively in the empigen fraction however at later time points it is also observed in the urea fraction.

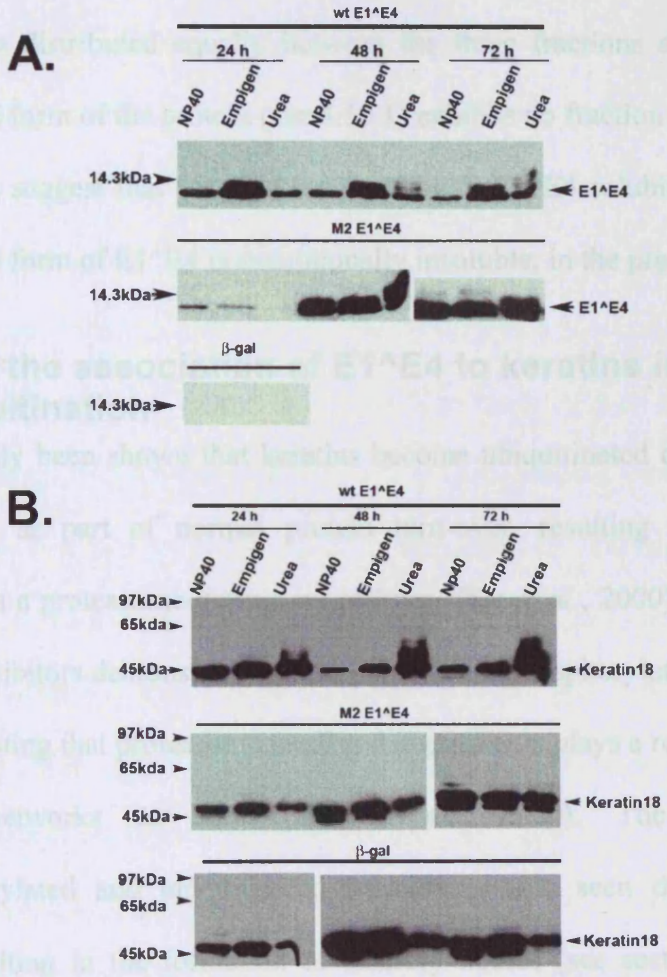

Figure 4.16 Fractionation of E1^E4, M2 and keratins from SiHa cells
SiHa cells infected with wild type and M2 E1^E4 or β-gal were harvested. Proteins was extracted sequentially in 1%NP40, 1% empigen and 9 M urea and probed for keratin 18 or E1^E4. E1^E4 is predominantly found in the empigen fraction. High molecular weight (phosphorylated) E1^E4 is predominantly found in the empigen fraction. M2 E1^E4 is more soluble and expressed at very low levels at 24 h, at later time points M2 is evenly distributed through the three fractions (A). Wild type E1^E4 expression induces a solubility shift in keratin causing a decrease in the NP40 fraction and a significant increase in the urea fraction. High molecular weight keratin species are only found in the urea fraction. M2 E1^E4 does not cause a shift in keratin solubility and is comparable to the β-gal fractionation (B.).

This distribution contrasts dramatically with M2 E1^E4. At 72 h despite associating to keratins, M2 is distributed equally between the three fractions and significantly the phosphorylated form of the protein (see 4.10.1) exhibits no fraction preference (Fig 4.16 A). These data suggest that keratin binding reduces E1^E4 solubility, furthermore the phosphorylated form of E1^E4 is exceptionally insoluble, in the presence of keratin.

4.11 Does the association of E1^E4 to keratins induce their ubiquitination

It has previously been shown that keratins become ubiquitinated during Mallory body formation and as part of normal protein turn-over, resulting in their subsequent degradation via a proteasome-dependent pathway (Ku *et al.*, 2000). Experiments using proteasome inhibitors demonstrated a build up of both phosphorylated and ubiquitinated keratins suggesting that proteasome mediated degradation plays a role in the turnover of cytokeratin networks *in vivo* (Ku *et al.*, 2000). The accumulation of hyperphosphorylated and ubiquitinated keratins is also seen during some disease processes resulting in the formation of Mallory bodies (see section 4.5.2). Previous experiments have shown that expression of E1^E4 induces keratin phosphorylation (Fig 4.8) and the formation of multiple high molecular weight keratin species (Fig 4.13). A series of experiments were carried out to determine whether E1^E4 induces the ubiquitination of keratins in a manner similar to that seen during Mallory body formation.

4.11.1 The ubiquitin- proteasome system

The proteasome is a large cytosolic proteolytic complex that is involved in the selective degradation of proteins which are selectively targeted for degradation by the covalent conjugations of multiple ubiquitin molecules. Proteasome-mediated degradation is involved in multiple cellular processes including protein turnover as well as the

degradation of cell cycle regulators and misfolded proteins. The ubiquitin proteasome system is commonly subverted by viruses, which override cellular processes by targeting specific proteins for proteasome mediated degradation (reviewed in (Shackelford *et al.*, 2005). To target a substrate for degradation, an activating enzyme, E1, transfers ubiquitin to a carrier E2 enzyme, and this in turn tags ubiquitin on to the targeted substrate with the help of E3 enzymes. Substrate recognition is primarily carried out by E3 enzymes. Ubiquitin is usually conjugated onto a lysine on the target protein and can perform several different functions depending on the manner in which the poly-ubiquitin chain is constructed. Conjugation of ubiquitin molecules to an existing ubiquitin chain at lysine 48 or 29 signals degradation (a minimum chain length of four is required for proteasome mediated degradation) whereas the addition to ubiquitin lysine 64 on certain proteins has been demonstrated to trigger DNA repair and transcription factor activation (reviewed in (Pickart, 2001). Mono-ubiquitination of proteins has been linked to endocytosis, histone regulation and virus budding (reviewed in (Hicke, 2001). The ubiquitination of misfolded proteins can serve to recruit chaperones in an attempt to rescue them. If proteins are successfully refolded ubiquitin chains are removed by the enzyme isopeptidase, but if unsuccessful, proteins are degraded, and it has been suggested that ubiquitinated keratins may undergo this process (Janig *et al.*, 2005).

The proteasome is composed of 2 separate components, a 19S regulatory domain, and the 20S proteolytic domain. The 19S regulatory domain consists of a base and a lid domain and is located at either one or both ends of the 20S proteolytic complex producing the 26 or 30S proteasome, respectively. The 19S regulatory domain recognises target proteins by way of their poly ubiquitin chains, which it removes

before unfolding proteins and directing them to the pore of the 20S subunit where proteolysis occurs. The proteolytically active sites are located within the lumen of the cylindrical 20S complex to (reviewed in (Dahlmann, 2005)).

4.12 E1^E4 aggregates colocalize with ubiquitin.

The first experiment was designed to determine whether any E1^E4 structures colocalised with ubiquitin. SiHa cells infected with E1^E4 were double stained for E1^E4 and ubiquitin. In cells containing E1^E4 with a filamentous pattern, ubiquitin staining was diffuse and did not colocalize with E1^E4 (Fig 4.17 A-C). This staining pattern was also observed in neighbouring E1^E4 negative cells (Fig 4.17 D-G). Cells containing E1^E4 collapsed keratin bundles/aggregates contained diffuse ubiquitin staining, however, the dense E1^E4 structures reacted strongly with ubiquitin antibodies (Fig 4.17 D-J). Interestingly this pattern is similar to that observed in figure 4.9 where dense E1^E4 structures also reacted strongly with phospho-specific keratin antibodies (Fig 4.6). This observation suggests that dense E1^E4/keratin structures may have characteristics in common with Mallory bodies, which also contain hyperphosphorylated and ubiquitinated keratins (Cadrin *et al.*, 1995; Ohta *et al.*, 1988; Stumptner *et al.*, 2000)

4.13 Proteasome inhibitors enhance E1^E4 induced keratin laddering

To establish whether high molecular weigh keratin species were indeed ubiquitinated experiments were conducted with a proteasome inhibitor which prevented the degradation of ubiquitinated proteins. SiHa cells were treated overnight with either ALLN (an inhibitor of the chymotryptic-like activity of the proteasome) (10 μM in 5 μl of DMSO) or with vehicle (5 μl DMSO). Cells were harvested and lysate separated on a 12% SDS/PAGE gel western blotted and probed for ubiquitin (Sc-8017) (Fig 4.18). The

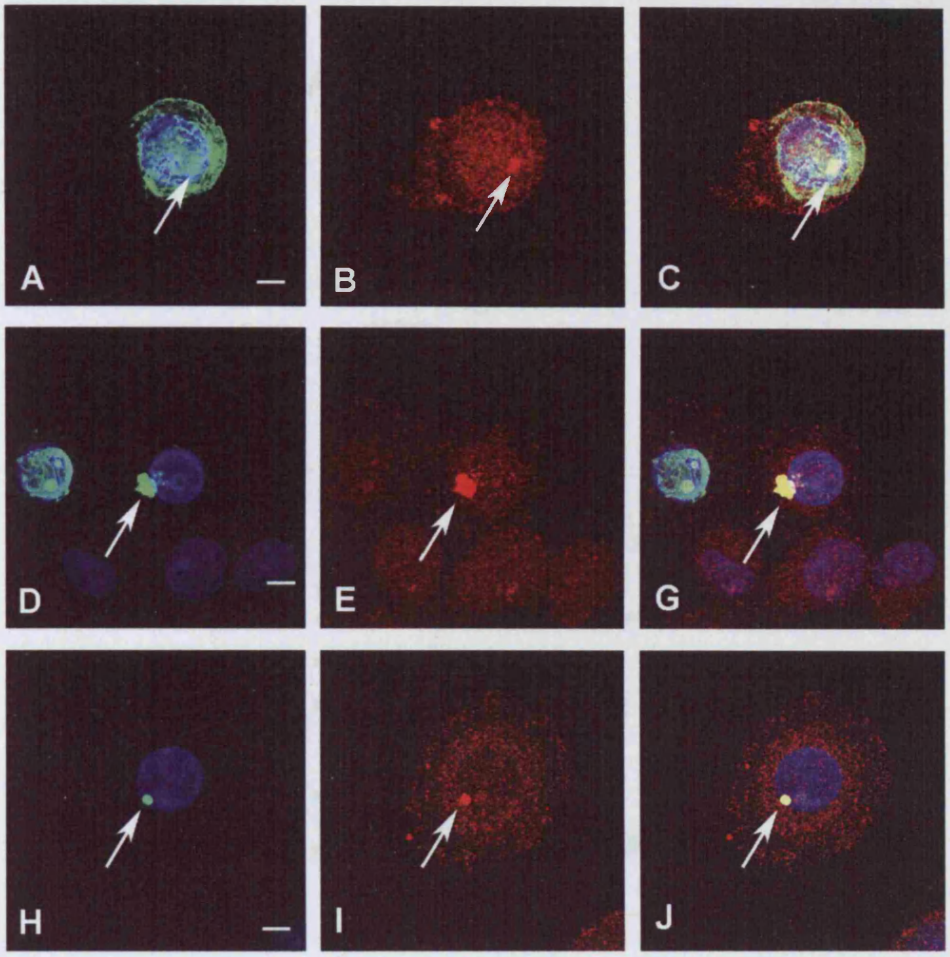

Figure 4.17 Dense E1^E4 structures colocalise with ubiquitin
SiHa cells infected with rAD E1^E4 were stained for E1^E4 (TVG405-green), ubiquitin (Z0458- red) and DNA (DAPI-Blue). E1^E4 with a filamentous staining patterns does not colocalise well with ubiquitin (A-C), in contrast dense bundles and E1^E4 aggregates react strongly with ubiquitin antibodies (D-J). Neighbouring E1^E4 negative cells show a diffuse ubiquitin staining pattern (D-G). Scale bars denote 5 μm.

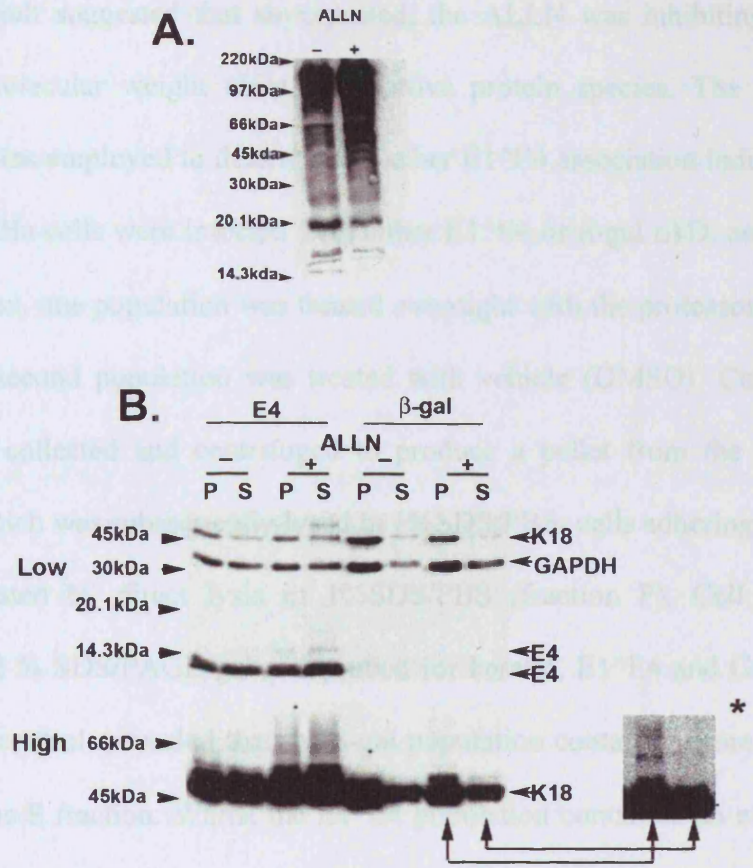

Figure 4.18 Affects of proteasome inhibitors on E1^E4 and Keratin
SiHa cells treated overnight with the proteasome inhibitor ALLN, or vehicle (DMSO) overnight extracts were probed for ubiquitin (Sc-8017). Blot A shows an increase in high molecular weigh ubiquitin species in the treated population, suggesting inhibition of the proteasome. SiHa cells infected with E1^E4 or β-gal and treated with ALLN or vehicle were harvested by collecting supernatant (S) and plate (P) fractions and SDS lysates were probed for keratin 18 (CY-90), E1^E4 (TVG402) and GAPDH (loading control). High molecular weight keratin species were significantly enhanced by the addition of proteasome inhibitors in both P and S E1^E4 fractions. Higher exposures of the blots also revealed the presence of high molecular weight keratin species in the ALLN treated P fraction of β-gal cells (photoshop enhanced panel B*). Treatment of cells with ALLN was also observed to increases high molecular weight E1^E4 species although no laddering was observed (top panel B).

treated lysate showed an increase in high molecular weight ubiquitinated species (Fig 4.18 A). This result suggested that as expected, the ALLN was inhibiting the break down of high molecular weight ubiquitin reactive protein species. The proteasome inhibitor ALLN was employed to determine whether E1^E4 association induced keratin ubiquitination. SiHa cells were infected with either E1^E4 or β-gal rAD, and harvested 24 h after infection, one population was treated overnight with the proteasome inhibitor ALLN, and the second population was treated with vehicle (DMSO). Culture media from plates was collected and centrifuged to produce a pellet from the supernatant population (S) which was subsequently lysed in 1%SDS/PBS; cells adhering to the plate were then harvested by direct lysis in 1%SDS/PBS (fraction P). Cell lysate was separated on a 12 % SDS/PAGE gel and probed for keratin, E1^E4 and GAPDH (Fig 4.18B). Loading controls revealed that the β-gal population contained more cells in the P fraction than the S fraction. Whilst the E1^E4 population contained an even number of cells in the P and S fractions due to the properties of E1^E4 (apoptosis induction and keratin disruption) which can cause cells to float off. The blots revealed a significant increase in high molecular weight keratin. Species in both ALLN treated E1^E4 fractions. The emergence of a weak high molecular weight keratin species can also be seen in the ALLN treated β-gal P population (Fig 4.18.B*). Due to the large number of ubiquitin reactive species, in these cell extracts (Fig 4.18A) it was not possible to use ubiquitin blots to identify different ubiquitin reactive bands in E1^E4 and β-gal samples (see Fig 4.21). These experiments were repeated using a second proteasome inhibitor MG132, and similar results were observed (data not shown).

It has previously been reported that treatment with proteasome inhibitors induces the formation of high molecular weight keratin 18 species formed by ubiquitination (Ku *et*

al., 2000). This data supports the hypothesis that the E1^E4-induced keratin ladders are caused by ubiquitination. In addition to seeing an increase in high molecular weight keratin species, both of the ALLN-treated fractions contain an additional E1^E4 band pointing to the stabilisation/reduced turnover of E1^E4 multimers. These high molecular weight species have previously been demonstrated to be caused by multimerisation (Wang *et al.*, 2004), although the possibility of E1^E4 ubiquitination cannot be ruled out.

4.13.1 Immunoprecipitation of keratin, ubiquitin and E1^E4

To determine if any of the high molecular weight E1^E4 or keratin species enhanced by the addition of proteasome inhibitor were ubiquitinated; immuno-precipitation experiments were conducted. The aim was to determine if any immuno-precipitated E1^E4 or keratin bands reacted with ubiquitin or whether ubiquitin immuno-precipitations could pull down any E1^E4 or keratin species. Initial experiments failed to pull down anything due to excessive levels of SDS, and it was also noticed that heavy and light chain antibody contamination in the regions of interest could hinder the identification of ubiquitinated proteins. Samples lysed in 1% SDS or 9 M urea/ 0.1% NP40 contained insoluble species of interest (data not shown), without inhibiting antibody binding (Fig 4.19.A). To reduce antibody contamination, antibodies were covalently cross-linked to beads using dimethyl pimelimidate (DMP). Cross-linking antibodies to beads significantly reduced heavy and light chain contamination making IP blots easier to interpret (Fig 4.19.B). Using samples lysed in 1 % SDS and cross-linked antibodies, it was possible to successfully IP E1^E4, keratin 18 and ubiquitin from E1^E4 infected SiHa cell lysates (Fig 4.19 see below).

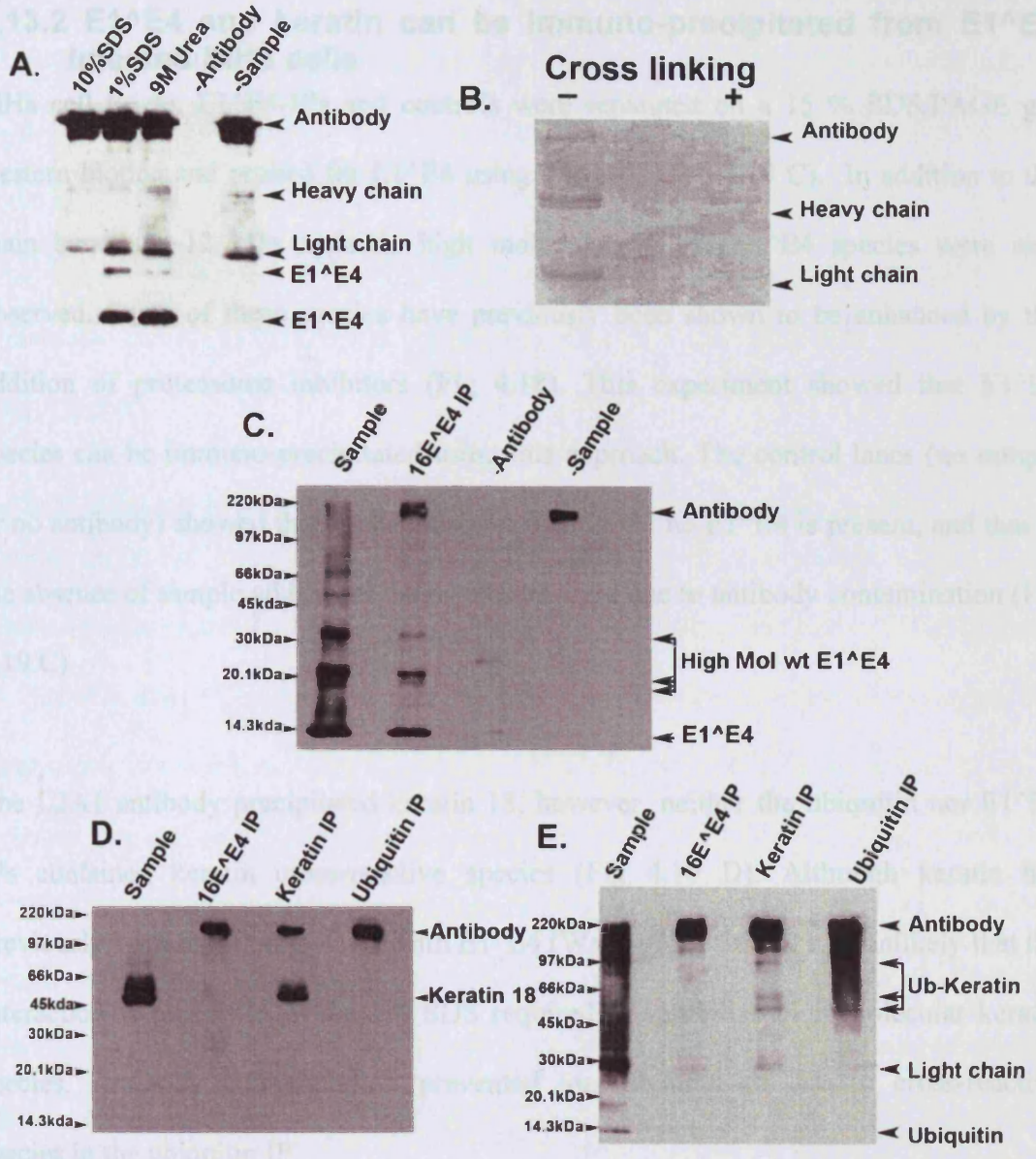

Figure 4.19 Immunoprecipitation of E1^E4, ubiquitin and keratin
E1^E4-infected SiHa cell were harvested in 10% SDS, 1% SDS or 9M urea. Proteins could be IP'ed from 1% SDS or urea extracts but contained significant heavy and light chain antibody contamination when probed for E1^E4 (A). Cross-linking antibodies to beads with DMP resulted in a significant decrease in the presence of heavy and light chain released from beads as shown by coomassie stain (B). E1^E4-probed E1^E4 IP shows that 4 species were pulled down. In the absence of antibody no E1^E4 was present, whereas in the absence of sample, only antibody contamination is observed (C). E1^E4, keratin and ubiquitin IP's probed for keratin 18, demonstrate that keratin 18 was only present in keratin IP lane (D.). E1^E4, keratin and ubiquitin IP's probed for ubiquitin showed ubiquitin IP's capture multiple high molecular weight ubiquitin species (E.). The E1^E4 IP lanes does not contain any ubiquitin cross reactive bands. The keratin IP lane contains high molecular weight ubiquitin cross reactive bands (keratin IP E).

4.13.2 E1^E4 and keratin can be immuno-precipitated from E1^E4 infected SiHa cells

SiHa cell lysate, E1^E4-IPs and controls were separated on a 15 % SDS/PAGE gel western blotted and probed for E1^E4 using TVG402 (Fig 4.19 C). In addition to the main band at ~12 kDa multiple high molecular weight E1^E4 species were also observed. Some of these species have previously been shown to be enhanced by the addition of proteasome inhibitors (Fig 4.18). This experiment showed that E1^E4 species can be immuno-precipitated using this approach. The control lanes (no sample or no antibody) showed that in the absence of antibody no E1^E4 is present, and that in the absence of sample additional bands present were due to antibody contamination (Fig 4.19.C).

The L2A1 antibody precipitated keratin 18, however, neither the ubiquitin nor E1^E4 IPs contained keratin cross-reactive species (Fig 4.19 D). Although keratin has previously been reported to co-IP with E1^E4 (Wang *et al.*, 2004), it is unlikely that the interaction is preserved in the 1% SDS required to solubilise high molecular keratin species. Antibody contamination prevented identification of keratin cross-reactive species in the ubiquitin IP.

4.13.3 Ubiquitin probed IPs

To establish if any E1^E4 or keratin species were ubiquitinated, E1^E4 and keratin IPs were probed with a ubiquitin antibody. The ubiquitin blot demonstrates that the ubiquitin IP was successful and had pulled down multiple high molecular weight ubiquitin-reactive proteins. No clear ubiquitin reactive species was identified in the E1^E4 IP lane. The high molecular weight E1^E4 species present in the E1^E4-probed E1^E4 IP (Fig 4.19C) were not detected by the ubiquitin antibody, confirming that they are probably caused by multimerisation as previously suggested (Wang *et al.*, 2004) and

not E1^E4 ubiquitination. Several ubiquitin reactive bands were detected in the keratin IP lanes. This result strongly suggested that ubiquitinated keratin species were present in E1^E4 expressing SiHa cell lysate. High molecular weight keratin species have previously been demonstrated to be induced by wild type but not M2 E1^E4 (Fig 4.13).Furthermore, high molecular weight species were enhanced by the addition of proteasome inhibitors (Fig 4.18). These data suggested that they may be induced by ubiquitination.

4.13.4 Keratin IPs from E1^E4 and β-Gal infected SiHa cells

Having generated evidence to suggest that the high molecular weight keratin bands induced by the expression of E1^E4 are caused by ubiquitination (Fig-4.19E), the extent of ubiquitination of both K8 and 18 was further investigated using ubiquitin probed keratin IPs. Extracts from both β-gal and E1^E4 infected SiHa cells harvested 48 h post infection were immuno-precipitated using both L1A2 and the pan keratin antibody (C2562). Due to the problems encountered in earlier experiments with high molecular weight antibody contamination, the amount of antibody used for each immuno-precipitation was further reduced. Lanes containing antibody and no sample showed that antibody contamination had been virtually eliminated. IPs were probed for ubiquitin (Fig 4.20 A and C) and then re-probed for keratin 18 (Fig 4.20 B and D). Control lanes revealed a number of low molecular weight ubiquitin species adhering to the beads (Fig 4.20 C). These ubiquitin contamination bands were of lower molecular weight than those observed in the keratin immuno-precipitations. In addition to this, low molecular weight ubiquitin bands were not present in the keratin immuno-precipitation lanes suggesting that the coupling of antibodies to beads reduced this background.

GAPDH blots of extracts showed that comparable amounts of proteins had been used in each IP (Fig 4.20B). Keratin blots of extracts showed that comparable amounts of

Figure 4.20 E1^E4 and β-gal Keratin IP's
Extracts from SiHa cells infected with β-gal and E1^E4 rAD and harvested 24 h post infection were IP'ed for keratin (C2562 (A) and L2A1 (C)) and probed for ubiquitin (A and C). Blots were then re-probed for keratin 18 (B and D). The lane containing antibodies and no sample shows negligible heavy and light chain antibody contamination. Only the E1^E4 keratin IP lane contains detectable ubiquitin reactive species (3 min exposure). E1^E4 and β-gal extracts were also probed for keratin 8 and 18 species (A). The same membrane was re-probed for keratin 18 demonstrating keratin IP's were successful but that only the E1^E4 IP lane contained high molecular weight keratin species (10 s exposure). Keratin 8 and 18 blots were also re-probed for GAPDH to demonstrate sample equal loading (B). A second keratin IP was performed on the same extracts using the L2A1 keratin antibody and probed for Ubiquitin. The lane containing no sample showed little, heavy or light chain antibody contamination. IP's preformed without antibodies produced weak low molecular weight background bands but were clear in the region of interest. Ubiquitin reactive keratin species were only present in the E1^E4 keratin IP lane and not the β-gal lane (3 min exposure). E1^E4 sample was also run on the same gel and probed for keratin 8 and 18 to aid the identification of bands (C). The membrane was re-probed for keratin 18 which was only present in IP lanes not the control lanes (10 s exposure). High molecular weight keratin 18 species were only present in the E1^E4 lane with bands matching some ubiquitin reactive species (D). Ubiquitin blots (3 min exposure) were aligned with keratin 18 re-probes (10 s exposure) preformed on the same membrane, some bands aligning perfectly (arrows). E1^E4 samples probed for keratin 8 and 18 are included for reference (E).

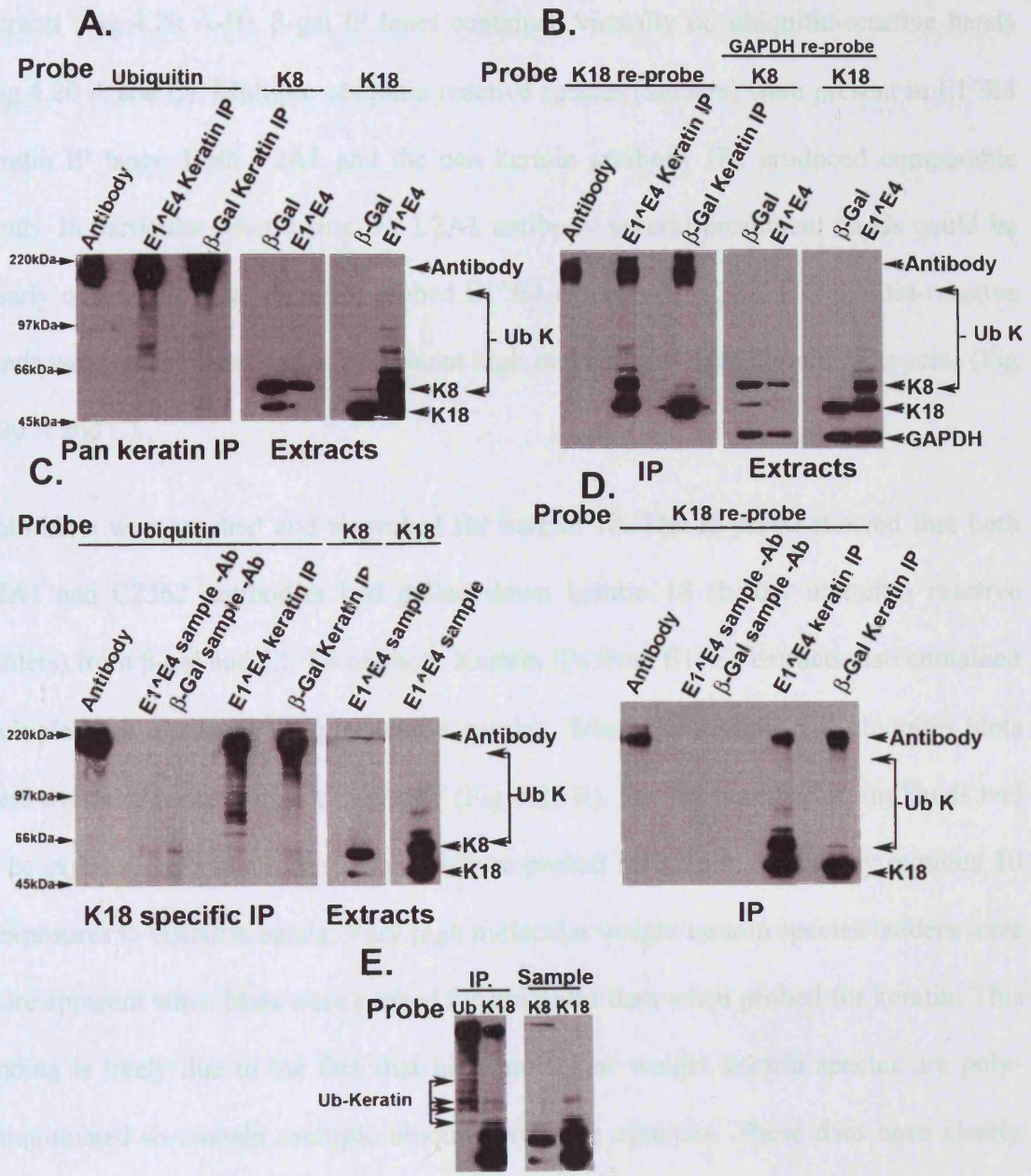
A.
Probe
Ubiquitin
K8
K18
Antibody
E1^E4 Keratin IP
β-Gal Keratin IP
β-Gal E1^E4
β-Gal E1^E4
220kDa
97kDa
66kDa
45kDa
Antibody
Ub K
K8
K18
Pan keratin IP
Extracts
B.
Probe
K18 re-probe
GAPDH re-probe
K8
K18
Antibody
E1^E4 Keratin IP
β-Gal Keratin IP
β-Gal E1^E4
β-Gal E1^E4
Antibody
Ub K
K8
K18
GAPDH
IP
Extracts
C.
Probe
Ubiquitin
K8
K18
Antibody
E1^E4 sample -Ab
β-Gal sample -Ab
E1^E4 keratin IP
β-Gal Keratin IP
E1^E4 sample
E1^E4 sample
220kDa
97kDa
66kDa
45kDa
Antibody
Ub K
K8
K18
K18 specific IP
Extracts
D.
Probe
K18 re-probe
Antibody
E1^E4 sample -Ab
β-Gal sample -Ab
E1^E4 keratin IP
β-Gal Keratin IP
Antibody
Ub K
K18
IP
E.
IP.
Sample
Probe
Ub K18
K8 K18
Ub-Keratin

keratin were present in each IP and that keratin ladders were only present in E1^E4 extracts (Fig 4.20 A-B). β-gal IP lanes contained virtually no ubiquitin-reactive bands (Fig 4.20 A and C). Multiple ubiquitin reactive species (ladders) were present in E1^E4 keratin IP lanes. Both L2A1 and the pan keratin antibody IPs produced comparable bands. In particular when using the L2A1 antibody several prominent bands could be clearly observed in the ubiquitin-probed E1^E4 extracts (Fig 20 C). Ubiquitin-reactive bands were an identical size as prominent high molecular weight keratin 18 species (Fig 4.20 A and C).

Both blots were washed and re-probed for keratin 18. The re-probe showed that both L2A1 and C2562 antibodies had pulled down keratin 18 (below ubiquitin reactive ladders) from β-gal and E1^E4 extracts. Keratin IPs from E1^E4 extracts also contained multiple high molecular weight keratin species. When the keratin and ubiquitin blots were overlaid, bands matched perfectly (Fig 4.20 E). Furthermore, ubiquitin bands had to be exposed for 3 min to visualise, when re-probed for keratin, blots only required 10 s exposures to visualise bands. Very high molecular weight keratin species/ladders were more apparent when blots were probed for ubiquitin than when probed for keratin. This finding is likely due to the fact that high molecular weight keratin species are poly-ubiquitinated so contain multiple ubiquitin reactive epitopes. These data have clearly identified a number of keratin species present only in E1^E4 expressing cells, suggesting that keratin 18 may be significantly more ubiquitinated than its type 2 binding partner keratin 8. This finding is interesting when it is considered that HPV 16 E1^E4 has been shown to bind specificity to keratin 18 (Wang *et al.*, 2004).

4.13.5 Cleavage of ubiquitin chains by isopeptidase

Having identified ubiquitinated keratin species by immuno-precipitation, we decided to confirm the result using an alternative approach. Instead of purifying the species of interest it was decided to try and deplete them using the enzyme isopeptidase. The enzyme cleaves isopeptide bonds and liberates ubiquitin chains from proteins, so rescuing them from proteolysis (see section 4.11.1). SiHa cell were infected with wild type E1^E4 rAD and treated for 12 h with the proteasome inhibitor, ALLN, in order to prevent turnover of ubiquitinated species prior to harvesting with PBS/EDTA. Cell pellets were resuspended in 200 µl of isopeptidase buffer and gently lysed using 0.5 % (v/v) NP40 and 1 µl of benzonase. To determine the activity of the isopeptidase, 2 µl of sample was treated with vehicle (buffer), or 1 or 2 µl of activated isopeptidase, with sample volumes being adjusted using isopeptidase buffer, prior to incubation at room temperature for 20 min. Samples were mixed with loading buffer, separated on a 10 % SDS/PAGE gel and probed for ubiquitin (Fig 4.21A). The blot showed that 1 µl of enzyme had very little effect on the sample, whereas 2 µl appeared to cause a significant reduction in the number of high molecular weight ubiquitin species suggesting that the enzyme had cleaved ubiquitin chains from proteins (Fig 4.21). To probe the keratin species of interest present in E1^E4 expressing cells, 2 µl of lysate was incubated with 3 µl of enzyme or buffer and treated as previously described. Membranes were then probed for keratin 18. Low exposures of the blot revealed that keratin loading was comparable for both samples. Higher overnight exposures were required to show a detectable reduction in high molecular weight keratin species in the treated sample. This result shows that the treatment of cellular extracts with the ubiquitin cleaving enzyme isopeptidase removes high molecular weight keratin bands produced in the presence of

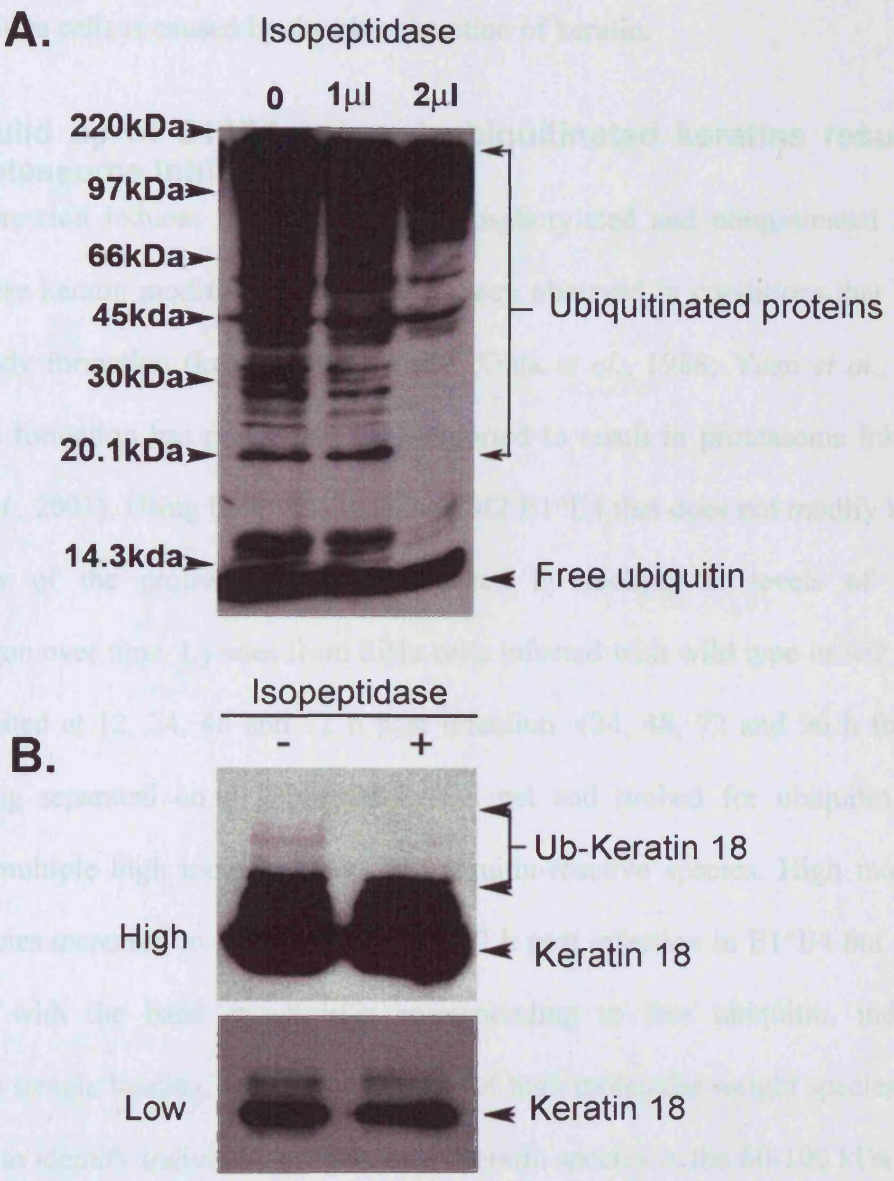

Figure 4.21 Isopeptidase cleavage of ubiquitin from keratin
SiHa cells were infected with E1^E4 rAD, harvested in isopeptidase buffer and treated with vehicle (buffer), 1 or 2 µl of isopeptidase, and probed for ubiquitin. Lysate treated with 2 µl of enzyme show reduced high molecular weight ubiquitin species (A). Lysate treated with vehicle (-) or 3 µl isopeptidase (+) and probed from keratin 18 revealed that treated extract contain fewer high molecular weight keratin species (B top panel), short exposure demonstrated comparable keratin loading (B lower panel).

E1^E4. This result further supports the argument that the keratin laddering observed in E1^E4 positive cells is caused by the ubiquitination of keratin.

4.13.6 Build up of E1^E4 induced ubiquitinated keratins results in proteasome inhibition

E1^E4 expression induces the build up of phosphorylated and ubiquitinated keratin species, these keratin modifications have also been observed in conditions that lead to Mallory body formation (keratin aggresomes) (Ohta *et al.*, 1988; Yuan *et al.*, 1998). Aggresome formation has previously been reported to result in proteasome inhibition (Bence *et al.*, 2001). Using both wild type, and M2 E1^E4 that does not modify keratin, the activity of the proteasome was monitored by looking at levels of protein ubiquitination over time. Lysates from SiHa cells infected with wild type or M2 E1^E4 were harvested at 12, 24, 48 and 72 h post infection (24, 48, 72 and 96 h for M2), before being separated on a 12% SDS/PAGE gel and probed for ubiquitin. Blots contained multiple high molecular weight ubiquitin-reactive species. High molecular weight species increased in strength at 48 and 72 h post infection in E1^E4 but not the M2 lanes, with the band at ~8 kDa corresponding to free ubiquitin, indicating comparable sample loading. Due to the number of high molecular weight species it was impossible to identify individual ubiquitinated keratin species in the 60-100 kDa region of interest (Fig 4.22 C). The dramatic increase in the number of high molecular weight ubiquitin species is comparable to what is observed after the addition of proteasome inhibitors (see Fig 4.18). The data presented here suggests that E1^E4 expression may cause the build up of ubiquitinated keratins and result in the formation of keratin aggresomes.

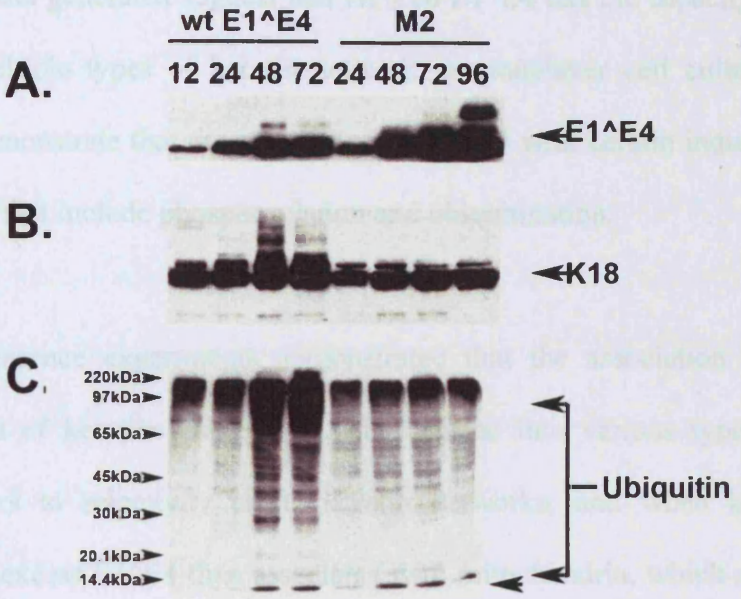

Figure 4.22 E1^E4 induced ubiquitinated keratin accumulation results in Proteasome inhibition.
Blots of extracts from wild type and M2 E1^E4 rAD infected SiHa cells harvested 12 24 48 and 72 h post infection (24, 48, 72 and 96 h in the case of M2). Blots show that both E1^E4 and ubiquitinated keratin species increase with time blots A and B. The same extracts probed for ubiquitin reveal an increase in high molecular weight ubiquitin species 48 and 72 h post infection in wild type E1^E4 lanes C.

4.14 Discussion

The aim of this study was to determine the effect of the E1^E4 keratin interaction on keratin. The data generated suggest that HPV16 E1^E4 has the capacity to bind to and reorganise multiple types of keratin network in monolayer cell culture. It was also possible to demonstrate that the association of E1^E4 with keratin induces biochemical modifications that include phosphorylation and ubiquitination.

Immunofluorescence experiments demonstrated that the association of E1^E4 with multiple types of keratins can cause their collapse into various types of structures. E1^E4 appears to selectivity target keratin networks, and when keratins become saturated, the excess E1^E4 then associates with mitochondria, which appears to result in their colocalisation with keratin bundles as previously reported (Raj *et al.*, 2004). In addition to bundles, E1^E4 formed aggregates that interacted simultaneously with both keratin and mitochondria in some cases in the absence of keratin network collapse. This may be explained by the hypothesis that keratin networks have collapsed and then reformed, and that E1^E4 expression may have ceased. This is supported by the finding that E1^E4 aggregates are observed more frequently at later time points. In addition to this, E1^E4 aggregates were shown to contain Cyclin B, hyperphosphorylated keratin and ubiquitin.

Phosphorylation of keratin filaments is known to promote the formation of keratin aggregates and it was hypothesised that the recruitment of the cyclin B/CDK1 complex by E1^E4 may be partly responsible for keratin phosphorylation. Experiments with mutant E1^E4s demonstrated that phosphorylation of keratin required a direct association with E1^E4 but was not necessarily dependent on the ability of E1^E4 to

sequester cyclin B to keratins. E1^E4 aggregates were observed less frequently in cells arrested at G1/S with aphidicolin, suggesting that their formation may be promoted by S-G2 progression through cell cycle, this may be due to a elevated kinase activity later in the cell cycle (reviewed in (Stark *et al.*, 2004).

Western blot analysis confirmed the presence of highly phosphorylated keratins and the formation of high molecular weight keratin ladders. Keratin laddering has previously been shown to be caused by ubiquitination (Ku *et al.*, 2000). Attempts to observe biochemical modifications to keratins 1/10, 5/14 and 4/13 were only partially successful with possible modification observed in K4 and K14. This may not be a significant finding as relative levels of keratins were not determined. HaCat cells are known to down regulate keratin 10 when grown in low calcium media (Kee *et al.*, 2001). Keratin 10 is known to induce cell cycle arrest (Paramio *et al.*, 1999), so it is possible that cells down-regulate other differentiation dependant keratins making it hard to identify modified species.

Fractionation experiments showed that E1^E4 expression decreases the solubility of keratin and demonstrated that high molecular weight keratin species are very insoluble. Furthermore, it was noticed that there may be a connection between the increase in high molecular weight keratin species and a depletion of soluble keratins: it still remains to be determined which is the cause and which is the effect.

Several different approaches were taken to identify E1^E4-induced ubiquitination of keratins. Immuno-staining demonstrated that ubiquitin colocalises with E1^E4 aggregates. Treatment of E1^E4-infected cells with proteasome inhibitors caused a

significant build up of high molecular weight keratin species. Proteasome inhibition has previously been shown to induce a build up of ubiquitinated keratins (Ku *et al.*, 2000). In addition to this, proteasome inhibition induced a build up of high molecular weigh (presumably multimeric) E1^E4 species, suggesting that the two may connected.

Immuno-precipitation of ubiquitin and E1^E4 was able to show that the E1^E4 protein itself appears not to be targeted by the ubiquitin system whereas keratin is. Keratin immuno-precipitation demonstrated that significantly higher levels of ubiquitinated keratins were present in E1^E4 cells than β-gal infected control cells. The identification of ubiquitinated keratin was further supported by the finding that keratin ladders could be depleted by enzymatic cleavage of ubiquitin chains by isopeptidase.

The previously identified, highly conserved LLXLL domain that has been reported to be essential for keratin association appears to have a more complex function (Roberts *et al.*, 1994; Wang *et al.*, 2004). Experiments showed that E1^E4 has a reduced affinity for keratin in the absence of this domain, but still maintains a limited ability to bind to and reorganise keratin networks. Interestingly, in the absence of the LLXLL motif, the E1^E4 protein loses its ability to induce a keratin solubility shift, or biochemical modifications. The finding that M2 E1^E4 had little effect on keratin has additional significance as it demonstrates that biochemical modifications to keratin are induced by E1^E4 as a result of the direct association of the protein to keratin. The M2 protein is predicted to maintain its cell cycle arrest ability (Nakahara *et al.*, 2005) for which keratin association is not required (Davy *et al.*, 2005), suggesting that E1^E4-induced cell cycle arrest is not responsible for the observed modifications to keratin. This

finding suggests that the mechanisms for targeting keratin networks may be highly conserved though out α-group E1^E4 papillomavirus proteins.

These data when combined, suggest that E1^E4 expression in monolayer cells induces the formation of keratin aggresomes, with proteasome inhibition appearing to occur as a result of accumulation of ubiquitinated keratin. Protein aggresome formation has previously been reported to induce proteasome inhibition (Bence *et al.*, 2001; Bennett *et al.*, 2005), although this has not been experimentally demonstrated for Mallory bodies. The mechanism by which E1^E4 induces biochemical modifications of keratin still remains to be identified. Some evidence suggests that E1^E4 multimerises on keratin filaments (Wang *et al.*, 2004). Although E1^E4 multimerisation has been linked to keratin network collapse (Wang *et al.*, 2004) it has been previously demonstrated that monomeric Fab antibodies can associate with keratins and also induce network collapse (Waseem *et al.*, 2004), suggesting that other mechanisms cannot be ruled out. In addition to this, it is known that a variety of non-specific cell stress events can collapse keratins inducing the formation of Mallory bodies (Cadrin *et al.*, 1995; Nakamichi *et al.*, 2002; Yuan *et al.*, 1998). Because of this it is important to further understand the mechanisms behind E1^E4-induced keratin aggresome formation, in order to better understand how the protein affects keratin networks *in vivo*. It remains to be seen whether keratin network collapse/reorganisation, phosphorylation and subsequent ubiquitination, observed in undifferentiated cells grown in monolayer culture can be observed *in vivo*.

5 The association of E1^E4 with keratin *in vivo*

5.1 Aims

Previous work has shown that the expression of E1^E4 in undifferentiated cells grown in monolayer culture results in its association to the cytokeratin network, which in turn causes the reorganisation and collapse of the affected network (Doorbar *et al.*, 1991). Work presented in the previous chapter was able to show that E1^E4-induced keratin collapse causes the phosphorylation and ubiquitination of keratins resulting in formation of Mallory body-like aggregates. Keratins expressed at the surface of terminally differentiated epithelium are already highly modified and so it remains to be seen whether any of these E1^E4-induced effects can be observed *in vivo*. This chapter aims to identify the effects of E1^E4 on keratin *in vivo* and to determine whether E1^E4 maintains the capacity to associate with and disrupt keratins networks. It also aims to establish whether E1^E4 can induce biochemical modifications such as the phosphorylation and ubiquitination of native keratins.

5.2 Introduction

5.2.1 Effects of epithelial differentiation on keratins networks

As cells move up the epithelium they undergo the process of terminal differentiation, during which time keratins are modified in several ways. Keratin 5/14 networks expressed in basal cells are down-regulated, and the differentiation-dependent keratins, 4/13 in mucosal epithelium, or 1/10 in cutaneous epithelium are expressed. Towards the surface of the tissue, keratins undergo additional modifications which make the networks even more robust. These form a mechanical barrier which protects the underlying tissue from external insult. Keratin filaments have been shown to become disulphide bonded to one another in the upper layers of the epithelial tissue as it undergoes terminal differentiation (Sun *et al.*, 1978). Another differentiation dependent

protein, filaggrin, exists as a polyprotein precursor and is activated by proteolytic cleavage. The filaggrin monomers bind and cross-link keratin filaments thus forming aggregated keratin fibres that provide additional strength to the networks (reviewed in (Presland *et al.*, 2000)).

5.2.2 Reasons for studying HPV2 and HPV16 in parallel

Due to the small size of HPV 16 lesions, their limited E1^E4 expression, and the difficulty in acquiring frozen HPV 16 lesions that are required for later experiments, HPV 2 (verrucas) and HPV 16 lesions have been examined in parallel. HPV 2 lesions are considerably larger, and express significantly more E1^E4, making them easier to work with. Frozen HPV 2 lesions (obtained from Northampton chiropody school) were used for western blot analysis, as formalin-fixed proteins cannot be resolved by SDS/PAGE (due to the covalent bonds that result from formalin treatment). Both type 2 and type 16 are α-group papillomaviruses, whose E1^E4 proteins contain the LLXLL motif required for keratin targeting. In Chapter 3 the proteins were shown to behave in a broadly similar fashion, both disrupting keratin networks and so HPV2 E1^E4 was predicted to be a suitable substitute model for HPV 16E1^E4 *in vivo*.

5.3 Results

5.3.1 Types 2 and 16 E1^E4 can be seen to colocalize with keratins *in vivo*

It was decided to investigate whether type 2 E1^E4 associates with keratins *in vivo* as has previously been reported to occur for type 16 (Doorbar *et al.*, 1997; Wang *et al.*, 2004). Types 2 and 16 lesions were triple stained for DNA, E1^E4 and keratin. The association of both HPV 16 (Fig 5.1) and 2 E1^E4 (Fig 5.2) with keratin filaments was observed in a sub-set of cells in lesions. Furthermore this ability of keratin antibodies to recognise E1^E4-associated keratin filaments suggests that E1^E4 association does not

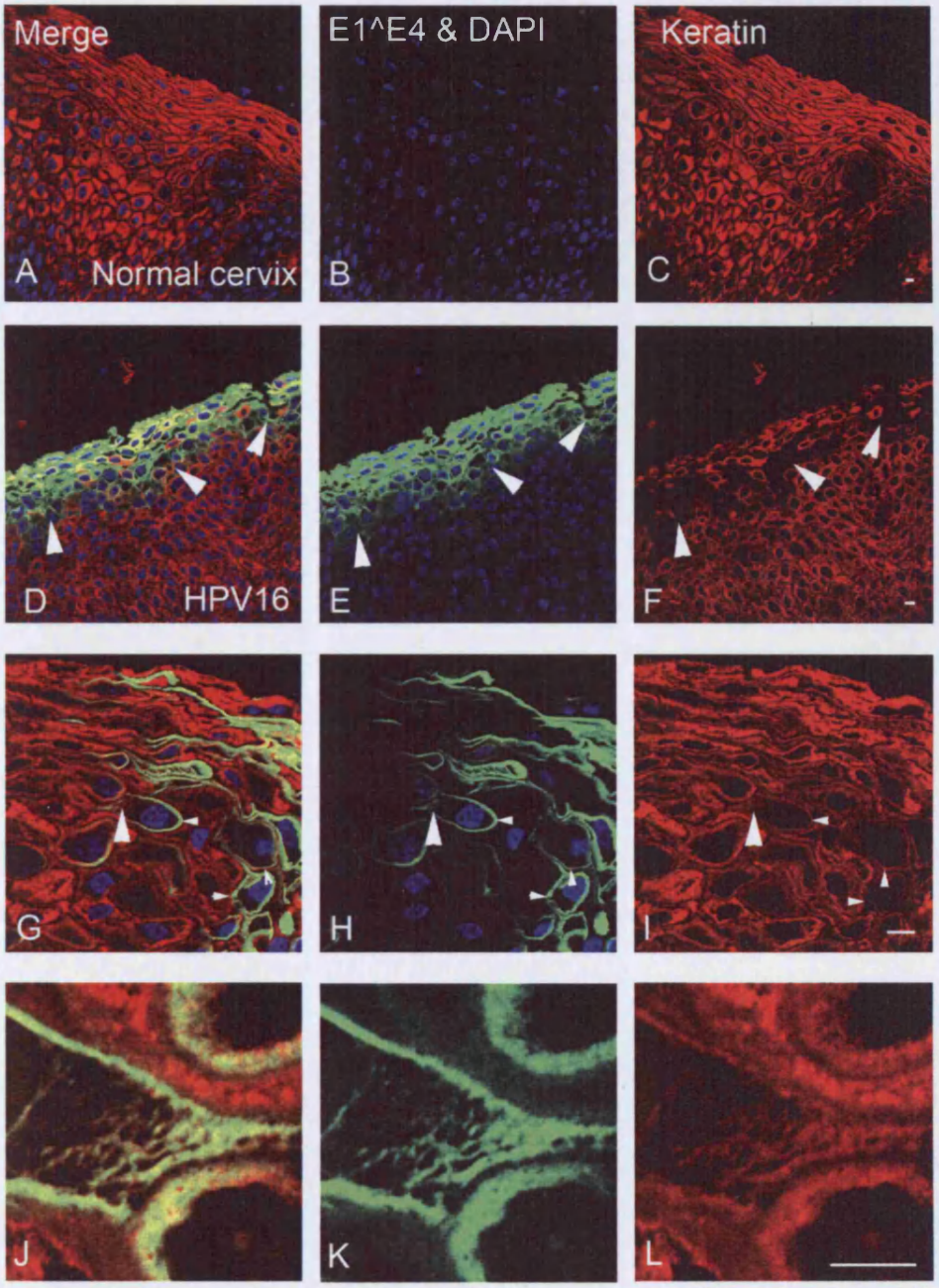

Figure 5.1 HPV 16E1^E4 and keratin colocalisation can result in the disruption of keratin networks in cervical epithilium.
Paraffin-embedded, formalin-fixed, normal (A-C) and HPV 16-infected (D-F) cervical epithelia, were stained for keratin (C2562, red), DNA (DAPI, blue) and HPV16 E1^E4 (TVG405, green). (A-C) Normal cervical epithelium does not cross-react with E1^E4-specific antibodies and contains a solid, unbroken keratin stain in the upper layers of the tissue. (D-F) Infected tissue expressing E1^E4 displays a damaged keratin stain (see arrows in D-F). (G-I) Cells expressing filamentous E1^E4 could be found as previously reported (Wang et al., 2004). High magnification images (J-L) of cells containing filamentous E1^E4 (large arrow in G-I) reveals that individual E1^E4-associated keratin filaments can be identified, showing that E1^E4 association to filaments does not mask keratin antibody epitopes. Reorganisation of keratins to the edge of the cells can also be observed in some cells (small arrows G-I). Scale bars denote 5 μm.

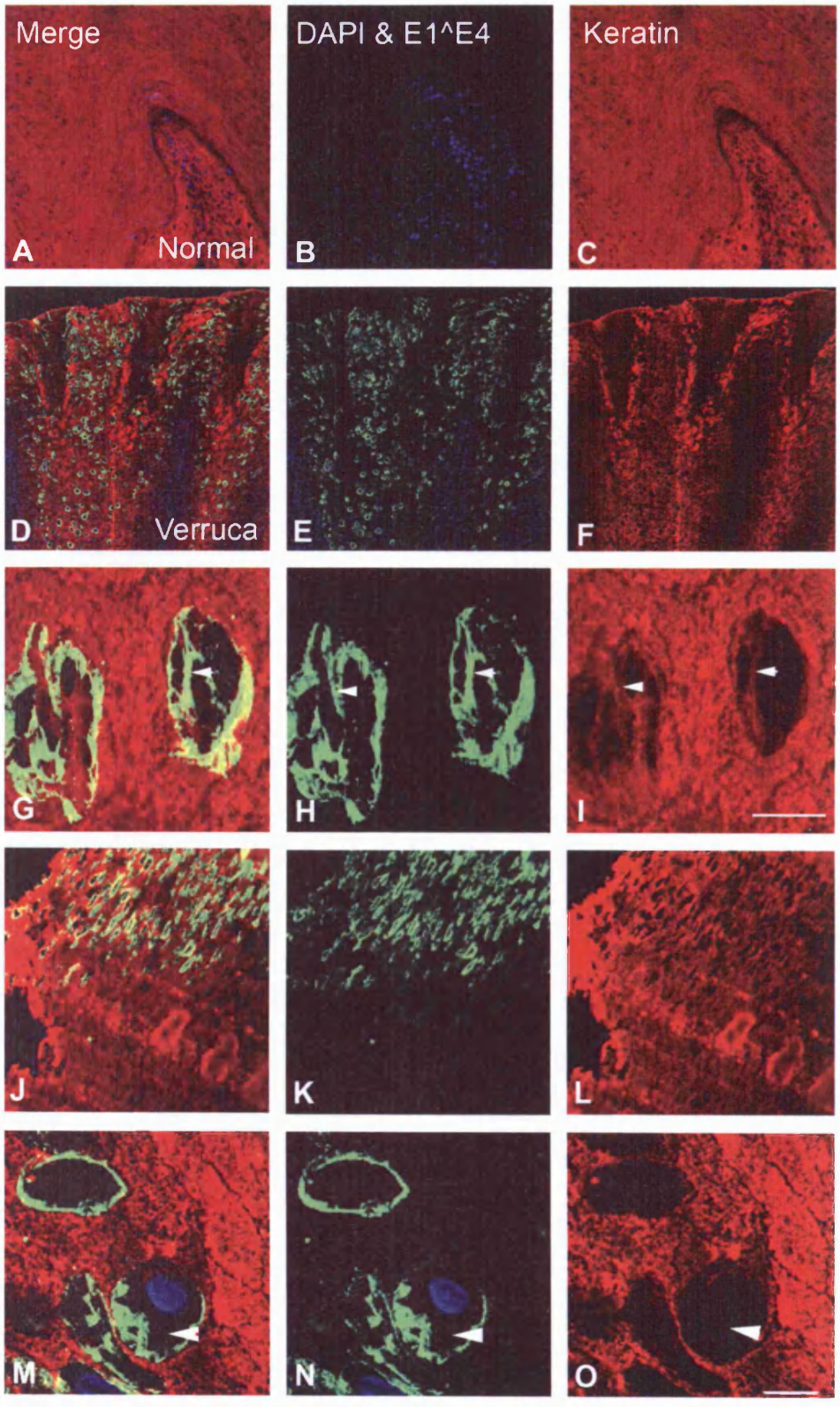
Merge
DAPI & E1^E4
Keratin
A
Normal
B
C
D
Verruca
E
F
G
H
I
J
K
L
M
N
O

Figure 5.2 HPV 2E1^E4 and keratin colocalisation results in the disruption of keratin networks in cornified tissue.
Paraffin-embedded, formalin fixed, normal (A-C) and HPV 2-infected (D-R) foot skin, was stained for keratin (C2562, red), DNA (DAPI, blue) and HPV2 E1^E4 (rabbit polyclonal, green). (A-C) Normal cornified foot skin (20 X objective) does not react with HPV2 E1^E4 antibodies and contains an unbroken keratin stain throughout the tissue. (D-F) Image of HPV 2-infected skin shows E1^E4 expression in an HPV2 lesion. Image produced by stitching together multiple images (using 20 x objective). (G-I) High power images reveal that HPV 2 can be observed to associate with keratin filaments in tissue, without masking keratin antibody epitopes (arrows G-I). The cornified layer of an HPV 2 lesion (40 x objective) displays perforated keratin staining in regions expressing E1^E4. (J-L) E1^E4 colocalises with keratin "holes". Neighbouring regions lacking E1^E4 expression display a solid unbroken keratin stain. (G-I) Keratin staining is commonly found to be reduced in intensity and reorganised to the edge of the cell in E1^E4-positive cells. Note that E1^E4-negative regions of the cell do not stain with keratin (arrows M-O). (P-R) Regions towards the surface of infected tissue appeared to be torn and damaged, which frequently contain high levels of E1^E4 (arrows, P-R). Scale bars denote 5 μm.

necessarily mask keratin antibody epitopes (see Fig 5.1G-L). These data indicate that keratin association is a strategy employed by both mucosal-and cutaneous-tropic α–group papillomaviruses. Although it was possible to identify cells in which E1^E4 and keratin colocalised, there was little evidence of cytokeratin collapse occurring, in contrast to the situation found *in vitro*. A few cells lower down in the epithelium of some lesions could be found showing some signs of partial reorganisation (not shown)(Doorbar *et al.*, 1997; Wang *et al.*, 2004) but no keratin aggregates were observed. A sub-population of both HPV 2 and 16 cells appeared to show relatively bright fluorescent ring-like keratin structures, suggesting that the keratins have partly reorganised to the edge of cells (see Fig 5.1 G-I, 5.2 M-O). Unlike cells *in vitro,* no E1^E4 aggregate structures were observed in tissue. These data suggest that although keratin collapse may occur infrequently, its rarity suggests that it is unlikely to be E1^E4's primary mode of action.

5.3.2 Types 2 and 16 E1^E4 proteins may reduce levels of keratin *in vivo*

Although type 2 and 16 E1^E4 proteins could be observed to localise with keratin in some cells, the absence of strong keratin staining in cells expressing abundant E1^E4 was observed significantly more frequently. HPV 16 lesions with gaps in the keratin staining were frequently observed. Keratin "holes" colocalised with areas of high E1^E4 expression (Fig 5.1 D-F). Normal cervical epithelium did not react with 16 E1^E4 antibodies and displayed solid keratin staining throughout (see Fig 5.1 A-C). The same was observed in HPV 2-infected E1^E4 positive tissue where keratin staining appears to be reduced or absent from the tissue in regions with high levels of E1^E4 expression (Fig 5.2 J-O) (also see Appendix I). In a region of cornified tissue expressing a well defined column of E1^E4, the E1^E4-positive region appears as holes in the

keratin stain (Fig 5.2 J-O). In the adjacent E1^E4-negative region the keratin staining is continuous and unbroken. These data show that in regions with high levels of E1^E4 expression, keratins appears to be reorganised giving the tissue a perforated appearance, suggesting an E1^E4 induced effect on the keratin integrity. It is conceivable that the apparent reduction in keratin is caused by E1^E4 masking of keratin epitopes. Although this theory cannot be ruled out, the same reduction is observed in HPV 16 tissue when a rabbit polyclonal pan-keratin antibody (Novocastra) was used (data not shown). Furthermore, the C2562 pan keratin antibody contains a cocktail of pan-specific monoclonal antibodies and should be able to recognise multiple keratin epitopes. That E1^E4-associated keratin filaments can be observed in some cells in lesions, suggests that binding does not result in keratin epitope masking. In addition to this observation, E1^E4 association to keratin filaments *in vitro* does not result in keratin epitope masking *(see* Fig 4.2 J-L and 4.3 G-I). It was also observed that nucleated cells containing E1^E4 structures at the periphery of cells did not contain keratin staining in E1^E4-negative regions towards the centre of the cell as observed in the neighbouring tissue, (see Fig 5.2 M-O). In addition to these observations, expression of HPV16 E1^E4 was shown to be able to induce polyubiqutination of keratins (see Chapter 4), which is known to promote their degradation (Ku *et al.*, 2000). When combined these data suggest that the observed E1^E4 effect on keratin staining is caused primarily by the reorganisation and/or loss of keratin rather than epitope masking.

5.3.3 E1^E4 may induce keratin phosphorylation *in vivo*

Although E1^E4 could be seen to induce keratin phosphorylation *in vitro,* it is not possible to say for certain if this is not a stress response that results from E1^E4 build-up, or whether it is in some other way related to keratin collapse or reorganisation. To determine if E1^E4 association induced phosphorylation of keratins *in vivo*, normal and

infected cervical epithelium was stained with the panel of phospho-specific antibodies (described in section 4.9).

The phospho-specific antibodies used in earlier experiments were raised against keratins 8 and 18 , not keratins 4 and 13 that are expressed at the surface of cervical epithelium, and so it was not certain that they would react with tissue. However both the 8250 [K18 PO4 ser-33] and 2D6 [K8 PO4 ser-431] antibodies did react with 16 E1^E4 -positive sections of infected epithelium (Fig 5.3 and 5.4). The 3055 [K8 PO4 ser-52] and LJ4 [K8 PO4 ser-73] antibodies did not react with proteins in formalin fixed cervical tissue (data not shown). Neither of the antibodies reacted with normal, uninfected cervical epithelium (Fig 5.3 and 5.4 A-C). A subset of cells containing high level E1^E4 reacted with the phospho-specific antibodies (Fig 5.3 and 5.4, D-F). Furthermore, phospho-specific antibody staining was observed to colocalise with E1^E4 (Fig 5.3 and 5.4, G-I) as previously reported to occur *in vitro* (see section 4.9). These data suggest that E1^E4 association with keratin networks in infected epithelium may result in the phosphorylation of keratins in a subset of cells *in vivo*. These data must not be over interpreted as it has not yet been proven that these antibodies will react with keratin 13. Despite this it is thought that the staining may be genuine as sections were restained and found to express keratins 8 and 18 (not shown). Keratin 8 /18 network has been reported to be expressed in cervical tissue, with increasing frequency as tissue differentiation is lost during neoplastic progression, and are commonly found in cervical tumours (Martens *et al.*, 1999; Smedts *et al.*, 1990).

5.3.4 E1^E4 expression induces altered ubiquitin localization *in vivo*

The association of HPV 16 E1^E4 to the keratin network in SiHa cells causes affected keratin network to become highly phosphorylated and ubiquitinated (see Chapter 4). At

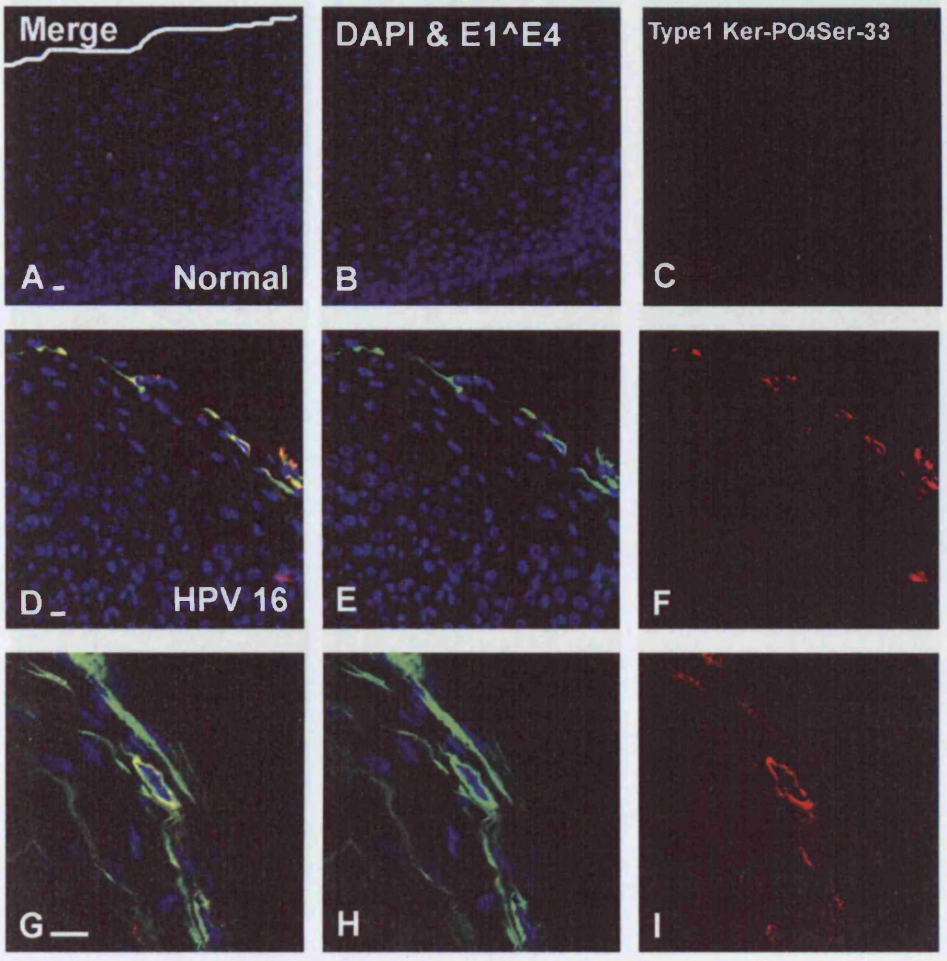

Figure 5.3 HPV 16 E1^E4 expression may induce type 1 keratin phosphorylation in cervical epithelium

Normal or HPV 16-infected, cervical epithelium was stained for 16 E1^E4 (TVG405, green) and DNA (DAPI, blue) type 1 keratin phospho Ser-33 (8250, red). Normal cervix did not react with TVG405 or 8250 (A-C) (tissue surface marked by line). 8250 (K18-PO4ser 33) reacted with a subset of E1^E4-positive cells towards the surface of infected tissue (D-F). High magnification images taken on a confocal microscope showed that 8250 staining colocalises with E1^E4 (G-I). Scale bars denote 20μm

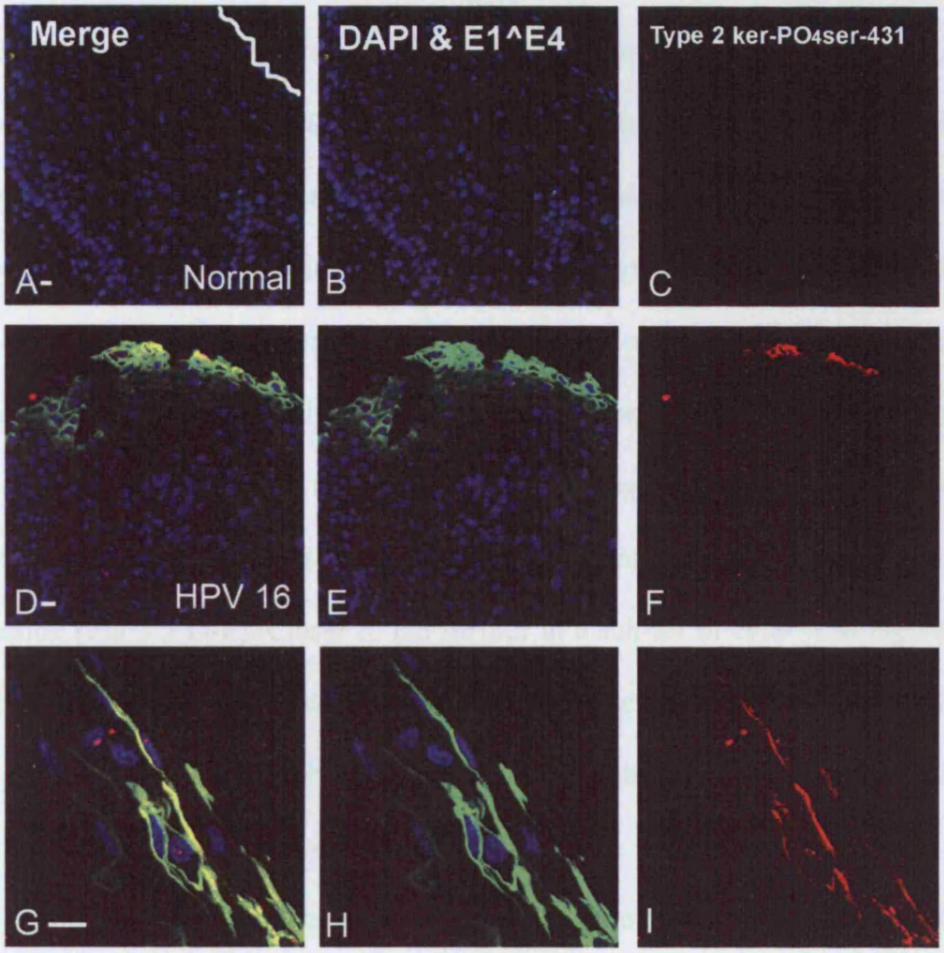

Figure 5.4 HPV 16 E1^E4 expression may induce type 2 keratin phosphorylation in cervical epithelium
Normal or HPV 16-infected, cervical epithelium was stained for 16 E1^E4 (TVG405, green) and DNA (DAPI, blue) type 2 keratin phospho-Ser-431(2D6, red). Normal cervix did not react with either TVG405 or 2D6 (A-C) (tissue surface marked by line). 2D6 (K8- PO4ser-431) reacted with a subset of E1^E4 positive cells towards the surface of infected tissue (D-F). High magnification images taken on a confocal microscope showed that 2D6 staining colocalises with E1^E4 (G-I). Scale bars denote 20μm

present it is unclear whether these biochemical modifications are linked to keratin network collapse, which is rarely observed *in vivo*. It was decided to investigate whether E1^E4 disruption of keratins *in vivo* results in their subsequent ubiquitination, as a first step lesions were double stained for E1^E4 and ubiquitin. Previous studies investigating the location of ubiquitin in epithelia have shown that mitotically active cells in the basal layer are strongly immunopositive for ubiquitin, (Sato *et al.*, 1997). Immunostaining of normal cervical epithelium with ubiquitin antibodies produced a discreet pattern which reduced in intensity towards the surface of tissue (Fig 5.5 A-C). In HPV 16-positive cervical tissue this pattern is also observed and continues during low level E1^E4 expression (Fig 5.5 D-F). Closer to the surface in a sub-set of cells with high levels of 16 E1^E4, a cytoplasmic build up of ubiquitin was observed (Fig 5.5 D-F). Furthermore some ubiquitin staining was observed to colocalize with E1^E4 (Fig 5.5 G-I). The same pattern was observed with two ubiquitin antibodies; a polyclonal (DAKO, not shown) and a monoclonal (Santa-Cruz, used in Fig 5.5). Sections were also stained with rabbit serum, and no staining was observed (data not shown). This finding supports the hypothesis that E1^E4-expression induces increased ubiquitination of certain cytoplasmic proteins or a relocation of certain nuclear proteins.

HPV 2 E1^E4 expression was also observed to alter ubiquitin expression *in vivo*. In normal tissue ubiquitin staining was predominantly nuclear but could be detected in the cytoplasm of cells in the basal layer. Cytoplasmic ubiquitin staining is lost in the mid-layers of the epithelium (Fig 5.6 A-C), and staining could not be detected in E1^E4-negative regions of the cornified layer (Fig 5.6 O-R, see phase image(P) for tissue borders) as has been reported previously (Sahin., 2001). E1^E4 expressed in the mid and lower layers coincided with a cytoplasmic build up of ubiquitin in a sub-set of cells,

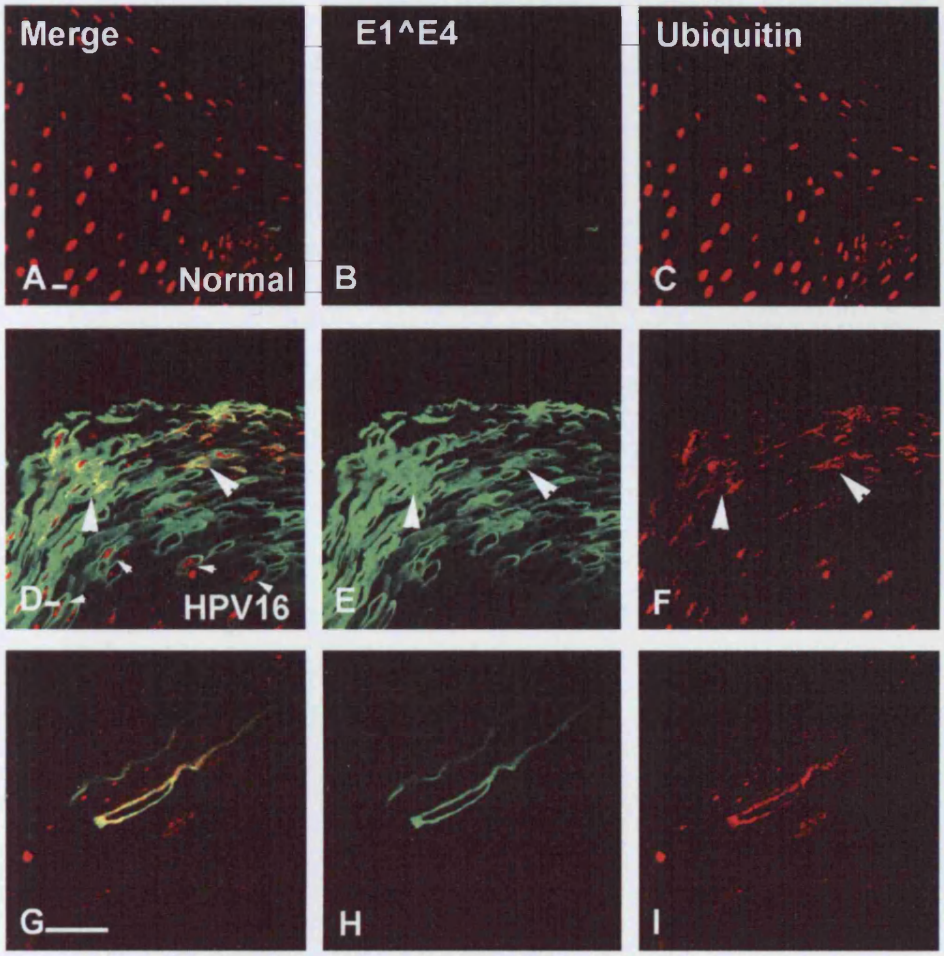

Figure 5.5 16 E1^E4 expression induces a build up of cytoplasmic ubiquitin
In normal cervical epithelium stained for 16 E1^E4 (TVG405, green) and ubiquitin (Sc-8017, red) (A-C), ubiquitin has a discreet staining pattern, reducing towards the surface of the tissue. In infected tissue ubiquitin staining is initially nuclear (small arrows). Towards the surface in regions expressing high levels of E1^E4, ubiquitin staining appears in the cytoplasm of a sub-population of cells (big arrows D-F). Higher magnification images reveal that the cytoplasmic ubiquitin colocalises with E1^E4 staining (G-I). Scale bars denote 20μm

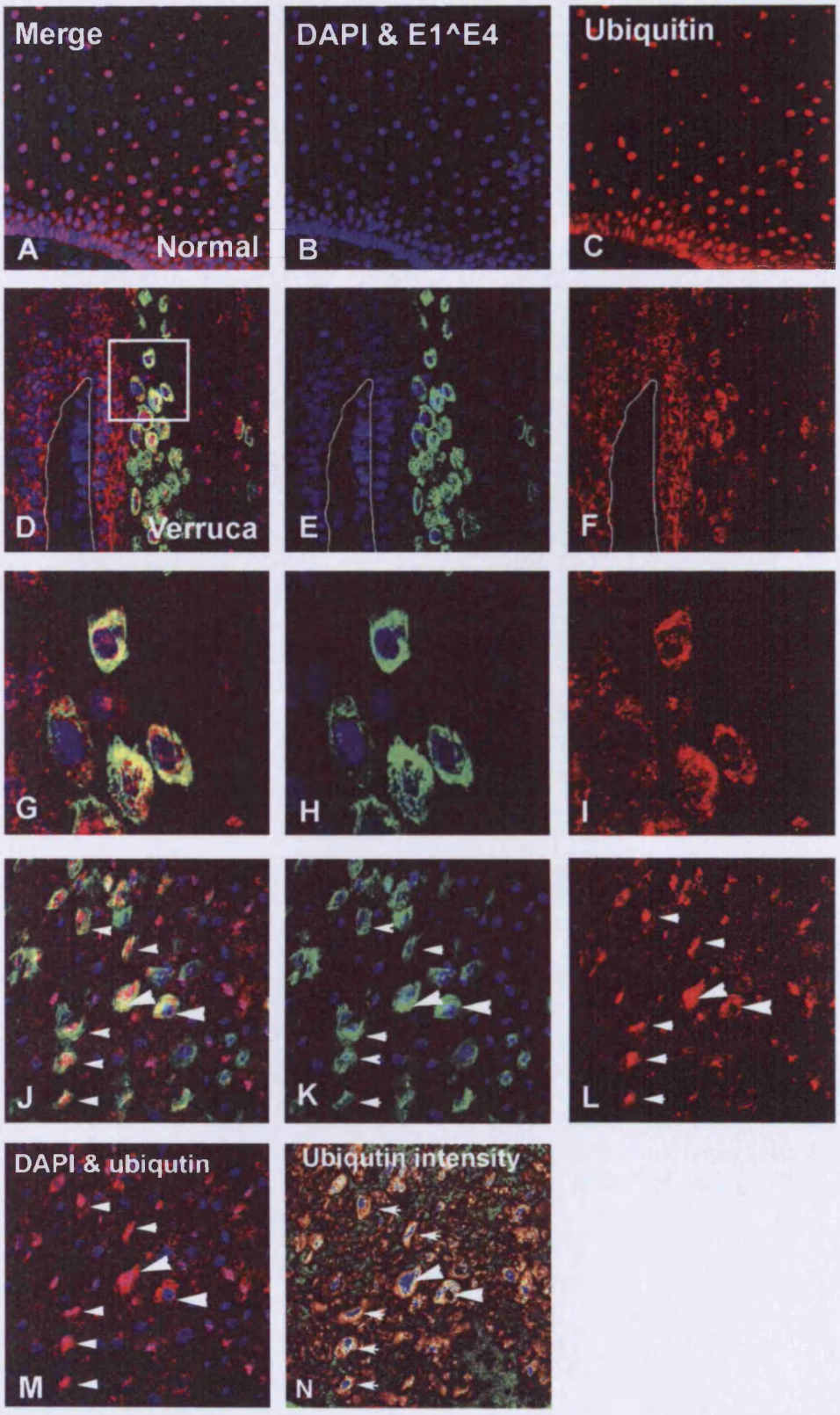
Merge
DAPI & E1^E4
Ubiquitin
A
Normal
B
C
D
Verruca
E
F
G
H
I
J
K
L
DAPI & ubiqutin
Ubiqutin intensity
M
N

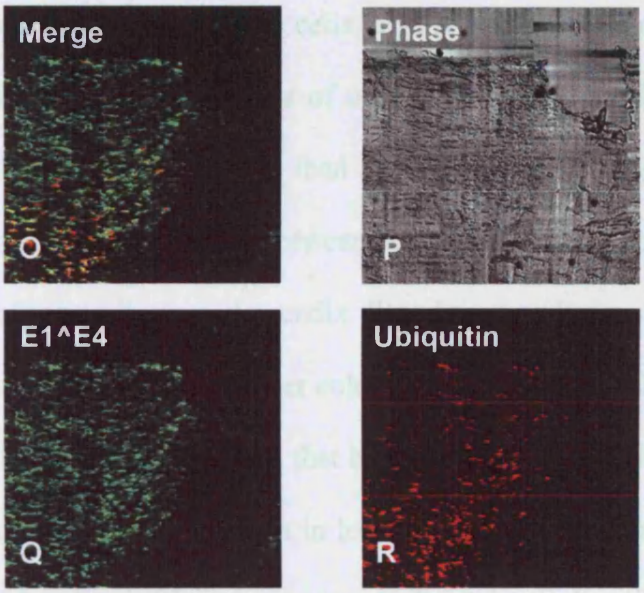

Figure 5.6 Type 2 E1^E4 expression induces ectopic ubiquitin expression
Normal and HPV2-infected foot skin was stained for E1^E4 (green), ubiquitin (Sc-8017, red) and DNA (DAPI, blue). (A-C) Nuclear and cytoplasmic ubiquitin staining is seen in mitotically active cells towards the basal layer. (D-I) Cells expressing E1^E4 in the lower layers also contain cytoplasmic ubiquitin which colocalises with E1^E4 in some cells (white line indicates basal layer D-F). (J-N) In the mid layers ubiquitin staining decreases and becomes nuclear, but some E1^E4-positive cells maintain elevated levels of cytoplasmic ubiquitin. (N) A quantitative image (blue pixels denote region of greatest intensity, green the lowest) shows E1^E4 positive cells contain higher levels of ubiquitin than surrounding cells. (O-R) Multiple 20 x images were stitched together to produce a composite image of the cornified layer of an HPV 2 lesion. Ubiquitin staining is normally absent from the cornified layer but is maintained in some regions when E1^E4 is present.

with E1^E4 and ubiquitin colocalising in most but not all of these cells (Fig 5.6 D-N). E1^E4 induced cytoplasmic build up of ubiquitin did not inhibit nuclear ubiquitin staining, but could also be detected in cells lacking nuclear staining (large arrows Fig 5.6 J-N). Quantitative confocal images of ubiquitin showed that E1^E4-positive cells generally had higher ubiquitin levels than surrounding cells (Fig 5.6 N). Ubiquitin staining in the cornified layer varied between lesions, with some containing few E1^E4 and ubiquitin-positive cells (see Appendix II). In some lesions however, ubiquitin staining extended into the cornified layer colocalised strongly with E1^E4-positive cells (Fig 5.4 O-R). These findings suggest that both HPV 2 and 16 E1^E4 expression may induce ectopic localisation of ubiquitin in lesions. This may be due to E1^E4 induced ubiquitination of keratins, although this is not the only explanation. Virus infections commonly subvert the ubiquitin system (reviewed in (Shackelford *et al.*, 2005), with the E6 protein being a good example, and it may be that other HPV proteins are involved. In addition to this, events such as wound healing (due to infiltration of immune cells) (Kondo *et al.*, 2002) and UV stress (Sahin., 2001) can alter the ubiquitin reactivity of the epithelium, indicating that there may be several explanations other than the ubiquitination of keratins that may be the cause of these observations.

5.4 E1^E4 induced effects on keratin and ubiquitin in the virus life cycle

So far this work has been able to show an apparent loss or redistribution of keratin which coincides with E1^E4 expression (section 5.3.2). Furthermore, it has been possible to show an altered ubiquitin staining pattern in lesions, which suggest that E1^E4 expression may be inducing the ubiquitination of cytoplasmic proteins. It was decided to use other markers of virus-life cycle progression in order to determine at what stage these events were occurring. Loss of the proliferation marker, mini chromosome maintenance 7 (MCM-7), was used to identify the end of early life-cycle

events (Middleton, 2003), and an L1 antibody was to used identify the cells that have established capsid protein production (Doorbar *et al.*, 1997; Peh *et al.*, 2002). The objective of this was to determine the point in the virus life-cycle where the high-level expression of E1^E4 that is necessary for keratin reorganization occurs.

5.4.1 Elevated levels of E1^E4 coincide with the loss of MCM staining and the onset of L1 expression

The onset of E1^E4 staining has previously been reported to coincide with the loss of MCM staining. The overlapping layers containing E1^E4-MCM double positive cells is believed to be where viral genome amplification occurs (Middleton, 2003; Peh *et al.*, 2004). HPV 16 lesions stained with MCM and E1^E4 at low exposures show a few double positive cells at the lowest points of E1^E4 expression (Fig 5.7 A-D). Over-exposing the images (E1^E4 sill does not appear in adjacent regions (Fig 5.7E)) reveals low-levels of E1^E4 penetrating deeper into the tissue and shows a significant number of double positive cells (Fig 5.7 F). MCM-E1^E4 double positive cells generally contain lower levels of E1^E4 than those with keratin loss and altered ubiquitin distribution, suggesting that these events may occur after viral DNA amplification has occurred.

To determine at what point in the epithelium the viral capsid proteins are expressed, tissue sections were stained for L1. The antibody produced clean staining and did not react with normal tissue (data not shown). In HPV 16 lesions, L1 expression could be detected in the upper layers of the tissue, with the exact location depending on the timing of E1^E4 expression, which typically preceded L1 expression by a few cell layers as previously reported (Doorbar *et al.*, 1997; Peh *et al.*, 2002). L1 expression begins in cells with moderate levels of E1^E4 and was confined to the nucleus (Fig 5.8 A-F). Towards the surface of the tissue, coinciding with high levels of E1^E4, L1 can

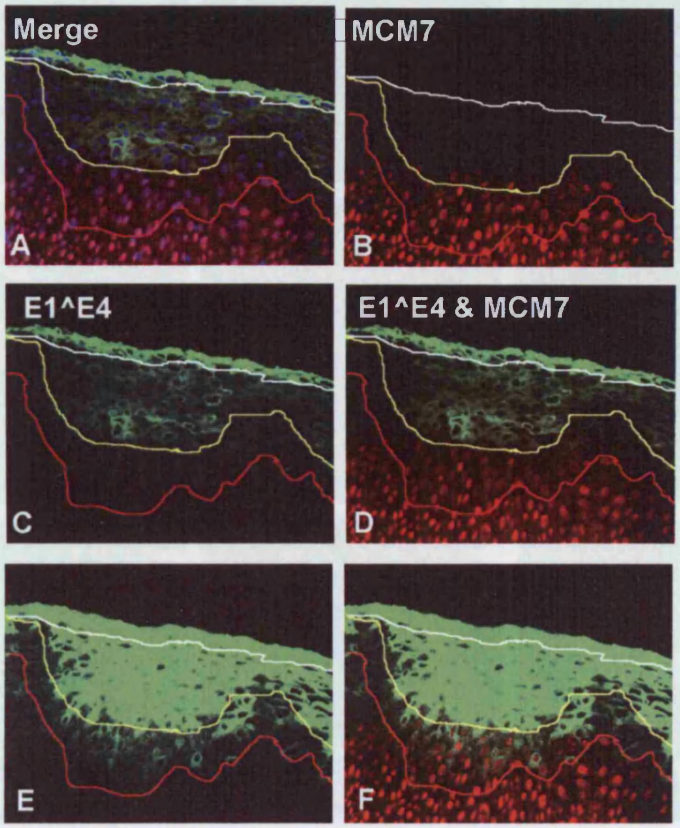

Figure 5.7 Low levels of E1^E4 can be detected extending well into MCM positive regions, whereas very high levels are expressed at the surface of the tissue. HPV16-positive cervical lesions were stained for DNA (DAPI, blue) E1^E4, (TVG405, green) and MCM7 (47DC141, red). (A-B) MCM staining is nuclear; expression is lost towards the middle of the lesion. (C-D) Low exposures suggest E1^E4 and MCM double positive cells are rare, with only a few cells being visible. (E-F) However longer exposures of the image suggest that E1^E4 may be expressed closer to the basal layer and may extend several layers into the MCM-positive region. Very high levels of E1^E4 are expressed at the surface of the tissue (above the white line) moderate levels extend deeper into the tissue (between the white and yellow lines) and very low levels are detectable deeper in the tissue and extend several cell layers into MCM positive regions (between the yellow and red lines).

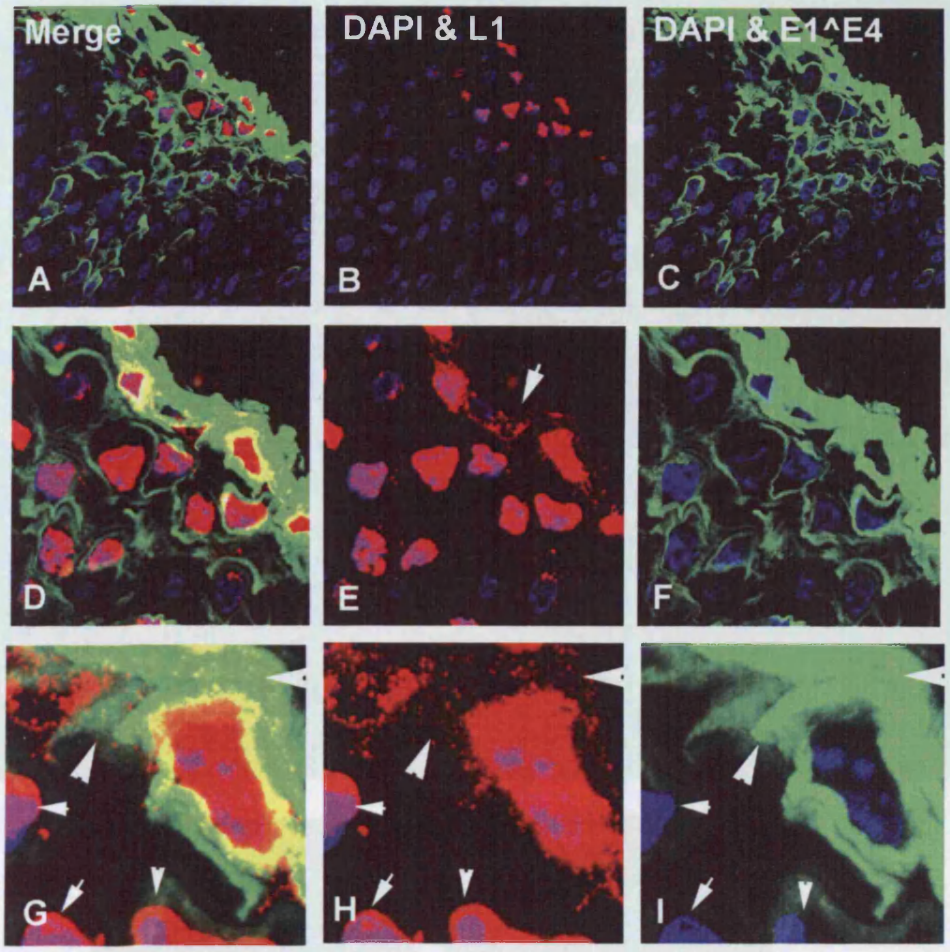

Figure 5.8 HPV 16 E1^E4 expression precedes L1 staining, and very high levels of E1^E4 coincide with cytoplasmic build up of L1

HPV 16-positive Cervical lesions were stained for E1^E4 (TVG405, green) and L1 (CamVir1, red) and DNA (DAPI, blue). Images show that E1^E4 staining is exclusively cytoplasmic (A & D) and precedes L1 expression by several cell layers (A-C). L1 staining is initially nuclear but becomes increasingly cytoplasmic in the final few layers of the tissue, coinciding with elevated levels of E1^E4 (D-F). Close up of area shown by box in E (G-I) clearly shows particulate L1 staining in cytoplasm (large arrows, G-I) at the cell surface whereas L1 is located in the nucleus in underlying cells (small arrow G-I).

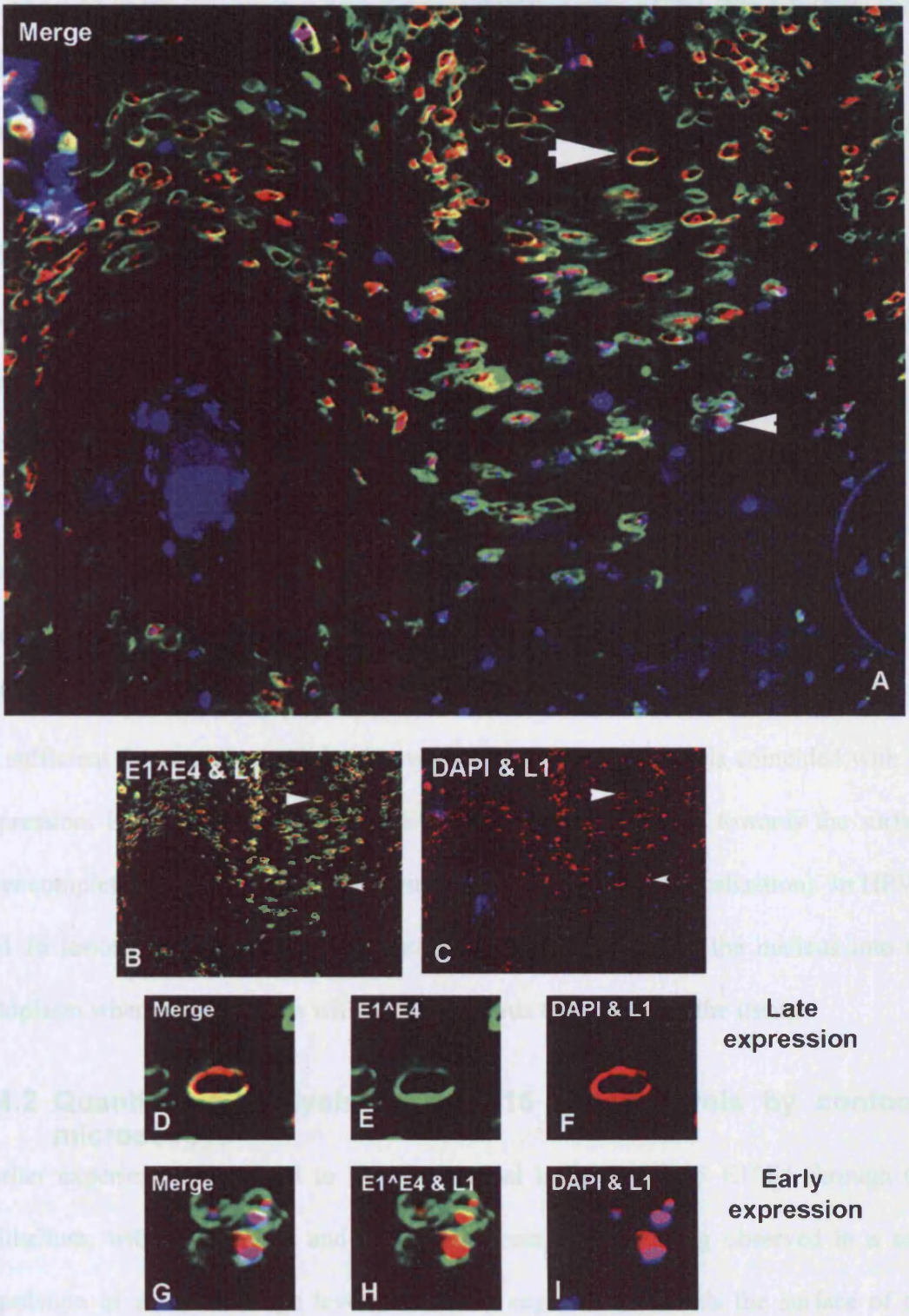

Figure 5.9 HPV2 E1^E4 staining precedes L1 expression
HPV 2 lesions were stained for HPV2 E1^E4 (polyclonal, green), L1 (Cam Vir 1, red) and DNA (DAPI, blue). E1^E4 expression preceded L1 expression by several layers (A-C). High magnification images of cells in the lower layers (small arrow A-C) reveal that L1 expression was initially nuclear (G-I). In cells towards the surface of the tissue (big arrow A-C), L1 expression becomes cytoplasmic and can be observed to colocalize with E1^E4 (D-F).

be observed in the cytoplasm where it may colocalize with E1^E4 (Fig 5.8 D-I). These data suggest that very high levels of E1^E4 are only initiated when virion assembly is complete and mature virions are released from the nucleus ready for release. As with HPV 16, HPV2 tissue stained for L1 indicated that E1^E4 expression precedes L1 (Fig 5.9 A-C) (also see Appendix III) as previously reported (Peh *et al.*, 2002). In the lower regions of the HPV2 lesion L1 is expressed in the nucleus and does not localise with E1^E4 (Fig 5.9 G-I). In higher layers of HPV2 lesions, L1 can be observed to localize with E1^E4 in the cytoplasm (see Fig 5.9 D-F).

The observations made in this section suggest that in HPV 16 lesions, E1^E4 expression levels are altered towards the surface of the tissue, allowing the protein to perform different tasks at specific points of the virus lifecycle. Low level expression appears to be sufficient for genome amplification whereas higher E1^E4 levels coincided with L1 expression. Interestingly, type 16 E1^E4 levels appear to elevate towards the surface after completion of virion assembly (coinciding with altered L1 localisation). In HPV 2 and 16 lesions, L1 expression was also observed to move from the nucleus into the cytoplasm where it colocalises with E1^E4 towards the surface of the tissue.

5.4.2 Quantitative analysis of HPV 16 E1^E4 levels by confocal microscopy

Earlier experiments appeared to show a gradual build up of 16 E1^E4 through the epithelium, with keratin loss and ubiquitin relocation only being observed in a sub-population of cells with high levels of E1^E4 expression towards the surface of the infected tissue. In order to quantify levels of E1^E4 expression, confocal images of lesions double stained for E1^E4 and keratin, ubiquitin or L1 were analysed using a quantitative function in the Leica confocal software. Lines starting at, and perpendicular to, the surface of the tissue were drawn across each image; the fluorescence intensity for

each channel was then plotted along the line (Fig 5.10). Plots revealed significant increase in E1^E4 levels close to the surface of the tissue. The point at which the fluorescence increase occurred depended on the depth of E1^E4 expression in the tissue and varied in thickness. In addition to this, a decrease in keratin levels was observed to coincide with the elevation of E1^E4 levels (Fig 5.10 A) no such decrease was observed in normal tissue (Fig 5.10 B). Furthermore, an increase in ubiquitin also coincide with elevated levels of E1^E4 (Fig 5.10 C). L1 staining showed that L1 expression precedes the elevation in E1^E4 levels and that the relocation of L1 appears to coincide with a further increase in E1^E4 (Fig 5.10 E). These data suggest that a significant increase in E1^E4 levels may be linked to the reorganisation of keratin, ectopic ubiquitin expression and relocation of the L1 viral capsid protein in the upper regions of lesions. These data add weight to the hypothesis that E1^E4 expression is not just a simple on or off process, but that expression is purposefully regulated by the virus as it approaches the surface of infected tissue, and that this follows viral genome amplification and virion production. If these findings are correct then this indicates that E1^E4 may perform a final function in the terminal phase of viral life cycle following virion assembly to aid virion release.

5.5 Western Blot analysis of HPV2 lesions

In order to determine whether E1^E4 induces biochemical modifications to cytokeratins *in vivo,* proteins extracts from HPV2 infected and normal foot tissue were analysed by western blot. Frozen, HPV2-infected tissue (verrucas), surgically removed from patients with problematic lesions, was used for the study. Frozen, normal skin taken from patients post-mortem, was used as a negative control. Frozen tissue was sectioned from top to bottom using a cryostat. Proteins extracted from the sections were probed for E1^E4, keratins 10 and 14, and ubiquitin. Eighteen lanes of verruca tissue were loaded

Figure 5.10 Quantitative analysis of E1^E4 levels reveals that high levels of expression coincide with specific events in the virus lifecycle.
Confocal images of HPV 16 lesions stained for E1^E4 (TVG405, green), DNA (DAPI, blue) and either keratin (C2562, A and B), ubiquitin (Sc-8017, C and D) or L1 (camvir 1, E) (red), were analysed quantitatively using the area quantitate function in the Leica confocal software. Eight lines were drawn from the surface of the tissue to the lowest point and the fluorescence intensity measured (on a 250-point grey scale) of the green (graphs A1-E1) and red (graphs A2-E2) channels along the lines. Graphs A1, C1, and E1 show levels of E1^E4 increasing towards the surface of the tissue, before spiking at the surface (E1^E4 spikes denoted by black arrows). Graph B1 and D1 show very low levels of florescence in E1^E4 negative tissue with no increase in fluorescence towards the surface (note y-axis scale bar max of 30). A reduction in keratin fluorescence coincides with the onset of high levels of E1^E4 (A1-A2). No decrease in keratin levels is observed towards the surface in normal tissue (B2). A peak in ubiquitin fluorescence is observed towards the surface and coincides with the elevated E1^E4 levels (C1,-C2). No surface increase in ubiquitin is observed in E1^E4 negative tissue (D1-D2). E1^E4 expression precedes L1 expression (E1-E2), but L1 expression (*) precedes the elevation in E1^E4 levels (**).

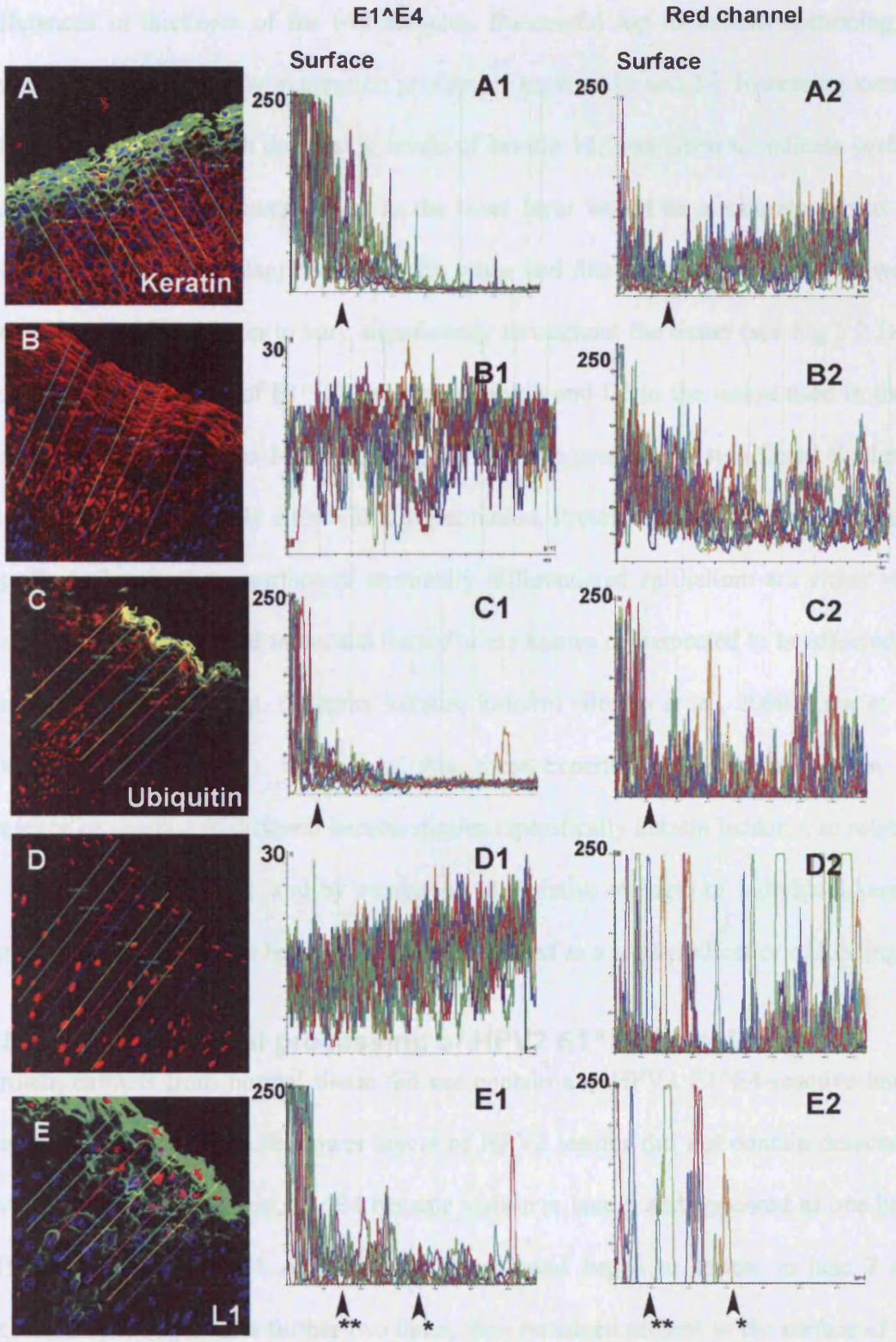
E1^E4
Red channel
Surface
Surface
A
A1
A2
250
250
Keratin
B
B1
B2
30
250
C
C1
C2
250
250
Ubiquitin
D
D1
D2
30
250
E
E1
E2
250
250
L1
**
*
**
*

(from lowest layer to surface) whilst just 9 lanes of normal skin were loaded, due to the differences in thickness of the two samples. Successful top to bottom sectioning of lesions was determined by expression profiles of keratins 10 and 14. Increasing keratin 10, which coincided with decreasing levels of keratin 14, was taken to indicate surface tissue. To refer to the lowest layers as the basal layer would be inaccurate due to the folds in the tissue (papillae) caused by the virus, and this causes the distance between the surface and basal layer to vary significantly throughout the tissue (see Fig 5.2 D-F) (for expression profiles of E1^E4, keratin, ubiquitin and L1 in the lesion used in these experiments see Appendix I-III). Loading controls also presented a significant challenge as protein levels generally alter with differentiation. Proteins known to be expressed at significant levels at the surface of terminally differentiated epithelium are either viral (and hence cannot be used in normal tissue) or are known or suspected to be affected by viral gene expression (e.g. filaggrin, keratin, loricrin) (Brown *et al.*, 2000; Lehr *et al.*, 2002; Lehr *et al.*, 2003). Because of this, these experiments aimed to look at the presence or absence of different keratin species (specifically keratin ladders), in relation to the presence of E1^E4, and by comparing the relative strength of individual keratin bands to the major keratin band which, would be used as a crude indicatior of loading.

5.5.1 The differential processing of HPV2 E1^E4 in lesions

Protein extracts from normal tissue did not contain any HPV2 E1^E4-reactive bands (not shown). Slices from the lower layers of HPV2 lesions did not contain detectable levels of the E1^E4 protein. E1^E4 became visible in lane 5 and appeared as one band ~15kDa in size (Fig 5.11 A). A second lower band began to appear in lane 7 and increased in strength for a further two lanes, then remained present to the surface of the tissue. Lane 10 contained a further band ~28kDa in size, which also appeared to continue to be present to the surface of the tissue. A possible fourth band ~17 kDa in

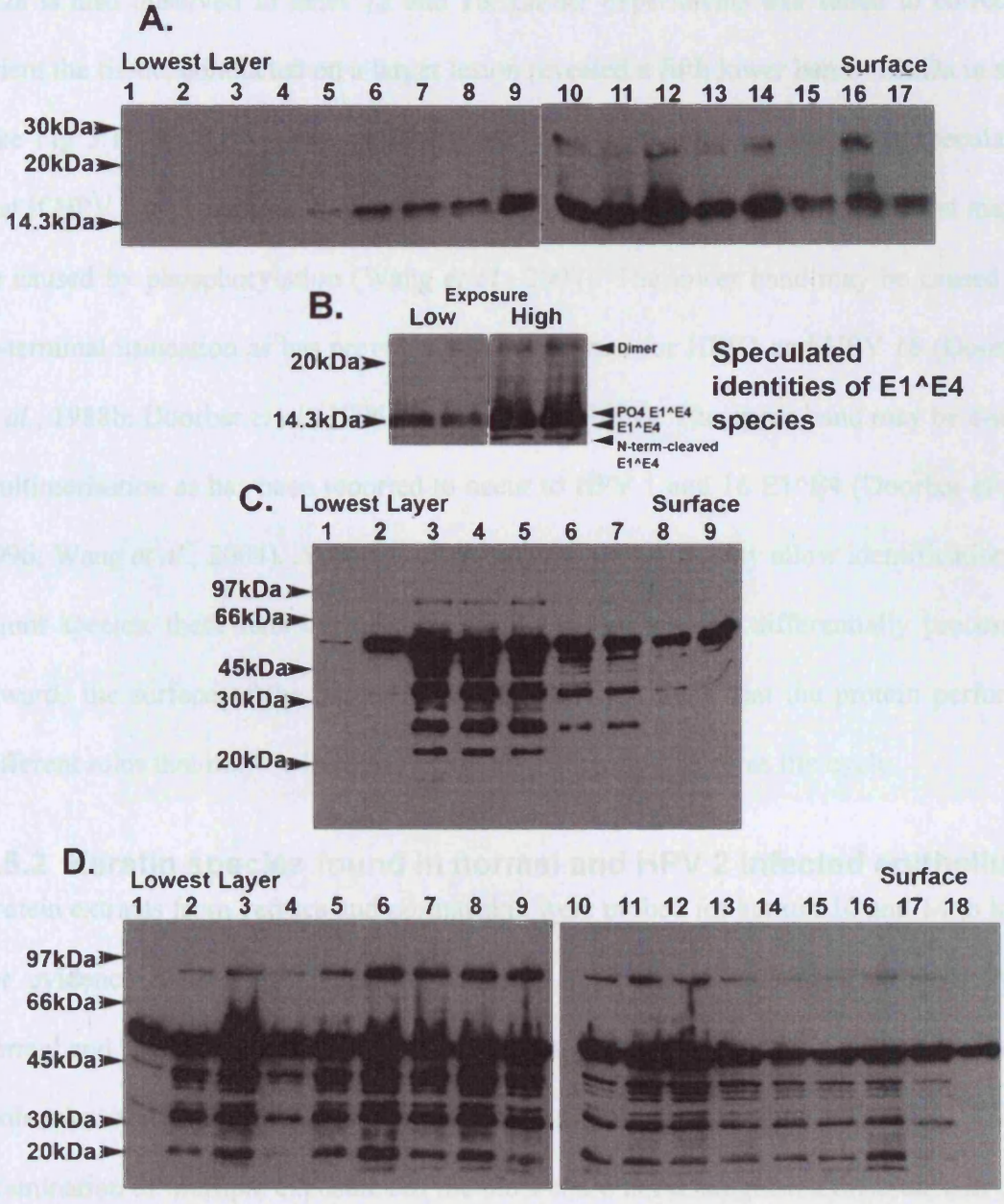

Figure 5.11 E1^E4 expression in tissue coincides with altered keratin 14 species
A top-to-bottom sectioned HPV2-lesion was analysed by western blot for expression of HPV 2 E1^E4 and keratin species. (A) E1^E4 cannot be detected in the lowest layers, but is initially expressed as a single band in lane 5. A second lower band appears in lane 7, a third band ~28kDa in size becomes visible in the middle of the tissue in lane 10. (B) Blots performed on lysates of a second lesion suggest the presence of a fourth lower molecular weight E1^E4 species ~10 kDa in size. (C-D) Keratin 14 (C9097-14B) blots show multiple bands in both normal (C) and infected tissue (D). Little variation in low molecular weight (less than 51 kDa) keratin species was observed between normal and infected tissue. A high molecular weight band (~88 kDa) is observed in both normal and infected tissue and appears to increase in strength relative to total keratin in lanes 6-13 coinciding with the build up of E1^E4 levels (see blot A).

size is also observed in lanes 12 and 16. Earlier experiments that failed to correctly orient the tissue, conducted on a larger lesion revealed a fifth lower band ~10kDa in size (see Fig 5.11 B). Although specific E1^E4 bands were not identified, it is speculated that if HPV 2 processing is similar to HPV 16 it is possible that the major doublet may be caused by phosphorylation (Wang *et al.*, 2004). The lower band may be caused by N-terminal truncation as has previously been reported for HPV1 and HPV 16 (Doorbar *et al.*, 1988b; Doorbar *et al.*, 1996; Doorbar *et al.*, 1997). The upper band may be due to multimerisation as has been reported to occur to HPV 1 and 16 E1^E4 (Doorbar *et al.*, 1996; Wang *et al.*, 2004). Although increasing E1^E4 levels may allow identification of minor species, these data indicate that HPV2 E1^E4 may be differentially processed towards the surface of the tissue, supporting the hypothesis that the protein performs different roles that may be linked to the various stages of the virus life cycle.

5.5.2 Keratin species found in normal and HPV 2 infected epithelium

Protein extracts from verruca and normal skin were probed for keratin 10 and 14 to look for evidence of E1^E4-induced biochemical modifications. Keratin 14 blots from normal and infected tissue show a major band at ~51kDa. A number of additional lower molecular weight bands were also found in normal and infected tissue. Close examination of multiple exposures of the blots could not distinguish a difference in low molecular weight species between normal and infected tissue. Keratin 14 expression weakened towards the surface of the tissue indicating top-bottom sectioning was successful. Two high molecular weight species ~61 and ~88 kDa in size were observed in infected and normal tissue (Fig 5.11C-D). A 92 kDa species (possibly a type I and II keratin dimer), was also observed in keratin 10 blots (Fig 5.12 C), the band was stronger in relation to the main (51 or 58 kDa) band in infected tissue. Interestingly the observed increase in strength of this band in lane 5 coincided with the onset of E1^E4 expression

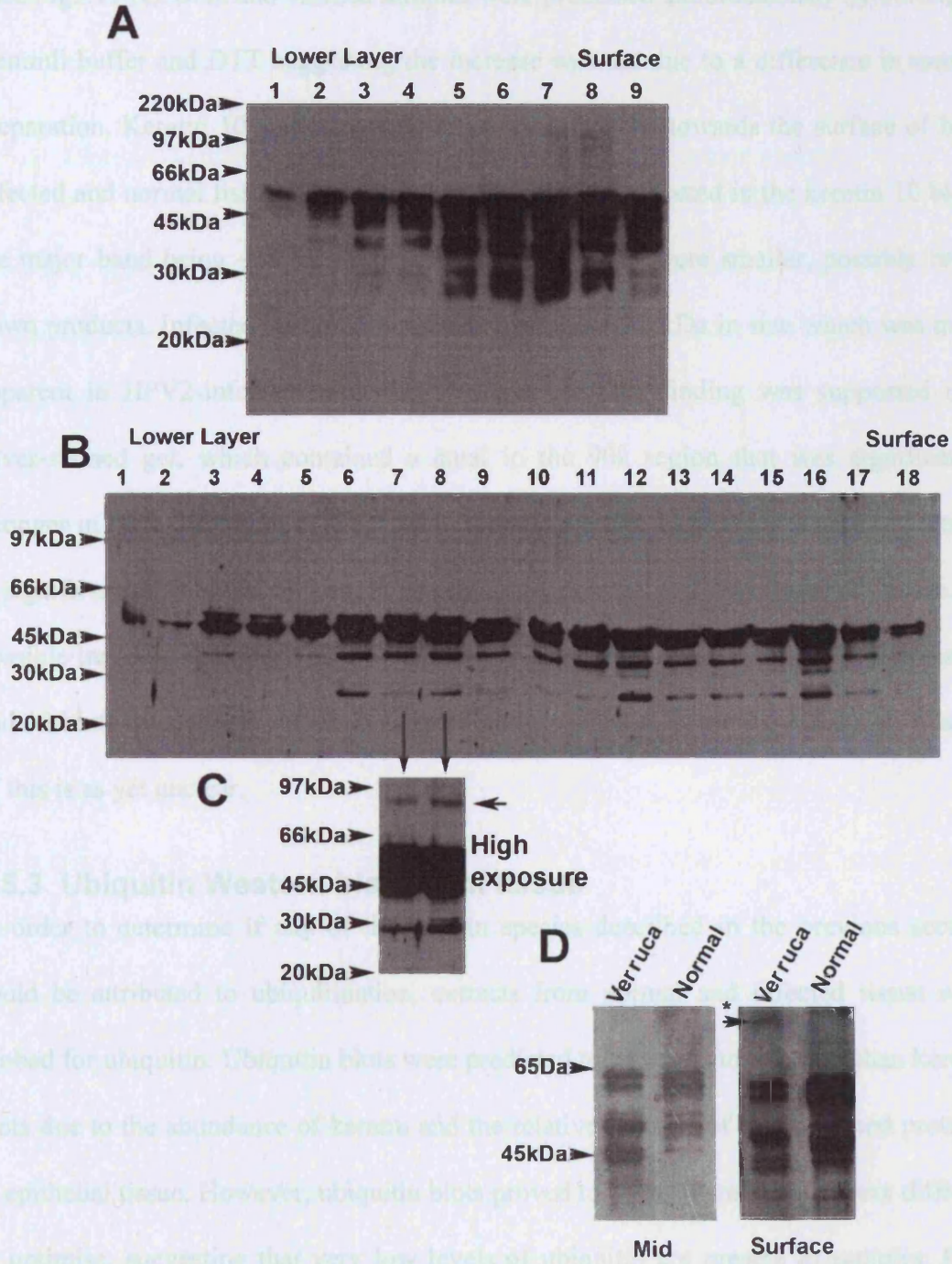

Figure 5.12 Keratin 10 and silver stain analysis of HPV 2-infected and normal skin
Top to bottom sectioning was performed on normal (A) and HPV 2-infected (B) skin, and extracts were probed for keratin 10 (K0199-12). Keratin levels increase towards the surface of normal tissue. An increase was less apparent in the infected issue due to folds in the tissue (A-B). Multiple low molecular weight keratin10 species were detected in both normal and infected tissue. Higher exposures of the blots show a ~92 kDa band (arrow C) present in infected tissue, which could not be detected in normal tissue. Silver-stained gels of mid and surface regions from normal and infected tissue shows a 90kDa band (D*) is picked up in verruca but is absent from normal tissue, despite more tissue being loaded in the normal lane (D).

(see Fig5.11 A). Skin and verruca samples were processed simultaneously by boiling in laemmli buffer and DTT suggesting the increase was not due to a difference in sample preparation. Keratin 10 was expressed at increasing levels towards the surface of both infected and normal tissue. Three major bands could be detected in the keratin 10 blots, the major band being ~58 kDa in size the weaker bands were smaller, possibly break down products. Infected tissue also contained a band ~ 92 kDa in size which was more apparent in HPV2-infected tissue (Fig 5.12 A-C). This finding was supported in a silver-stained gel, which contained a band in the 90k region that was significantly stronger in HPV 2 samples (Fig 5.12 D). Keratin western blots were unable to identify a significant difference in keratin species between normal and infected tissue. A possible increase in strength of the ~88 and 92 kDa bands was observed in keratins 14 and 10 blots respectively, between infected and normal tissue, although the significance of this is as yet unclear.

5.5.3 Ubiquitin Western blots from tissue

In order to determine if any of the keratin species described in the previous section could be attributed to ubiquitination, extracts from normal and infected tissue were probed for ubiquitin. Ubiquitin blots were predicted to be easier to interpret than keratin blots due to the abundance of keratin and the relative scarcity of ubiquitinated proteins in epithelial tissue. However, ubiquitin blots proved to be problematic and were difficult to optimise, suggesting that very low levels of ubiquitin are present in samples. Free ubiquitin (8kDa) bands were observed in both samples, however due to the low levels of ubiquitin no other specifies could be detected before antibody background burnt out the blots (data not shown). On one occasion it was possible to identify a single band ~ 60 kDa in size in HPV2 extracts, (see next section). Although this may represent a mono-ubiquitinated keratin species, it was not possible to draw significant conclusions from

these experiments. Some of the problems encountered during theses experiments were subsequently resolved and are discussed in the next section.

5.5.4 Ubiquitin–keratin coimmunoprecipitation from lesions

In a final attempt to identify ubiquitinated keratin species *in vivo*, immunoprecipitations were attempted on protein extracts of slices taken from the mid layers of the tissue. Slices were boiled in 1 % (w/v) SDS/PBS and immunoprecipitations performed using the pan keratin antibody (C2562) and a keratin 14-specific antibody (C9097-14B). To reduce light chain antibody contamination samples were subsequently boiled in laemmli buffer without DTT. The keratin 14 antibody was shown to have pulled down keratin 14 (Fig 5.13 D), where as the C2562 antibody did not (data not shown). Lanes without antibody demonstrated that uncoupled beads bound protein, producing background. Interestingly earlier ubiquitin blots were restricted by the amount of protein that could be loaded into wells. Non-specific binding of protein to beads allowed the concentration of protein from samples, producing good ubiquitin blots. These control lanes lacking antibody, show low molecular weight ubiquitin species present in both normal and infected tissue (more low molecular weight ubiquitin was observed in the verruca sample Fig 13 A). In addition to this a possible ubiquitin smear starting at ~60 kDa (which is consistent with a ubiquitinated keratin 14 ladder) was observed in verruca but not in normal skin. Ubiquitin reactive bands were not observed in the pan specific keratin IP lanes indicating that the coupling of antibodies to beads inhibits non specific binding (Fig 5.13 A). Keratin 14 blots performed on samples, suggested that more protein had been loaded into the normal skin lane (see Fig 5.13 B) indicating that the verruca sample may contain elevated levels of free and conjugated ubiquitin (or reduced keratin levels). In addition to this, lanes containing sample blotted for keratin revealed that the low molecular weight keratin species described in section 5.5.3 were not present

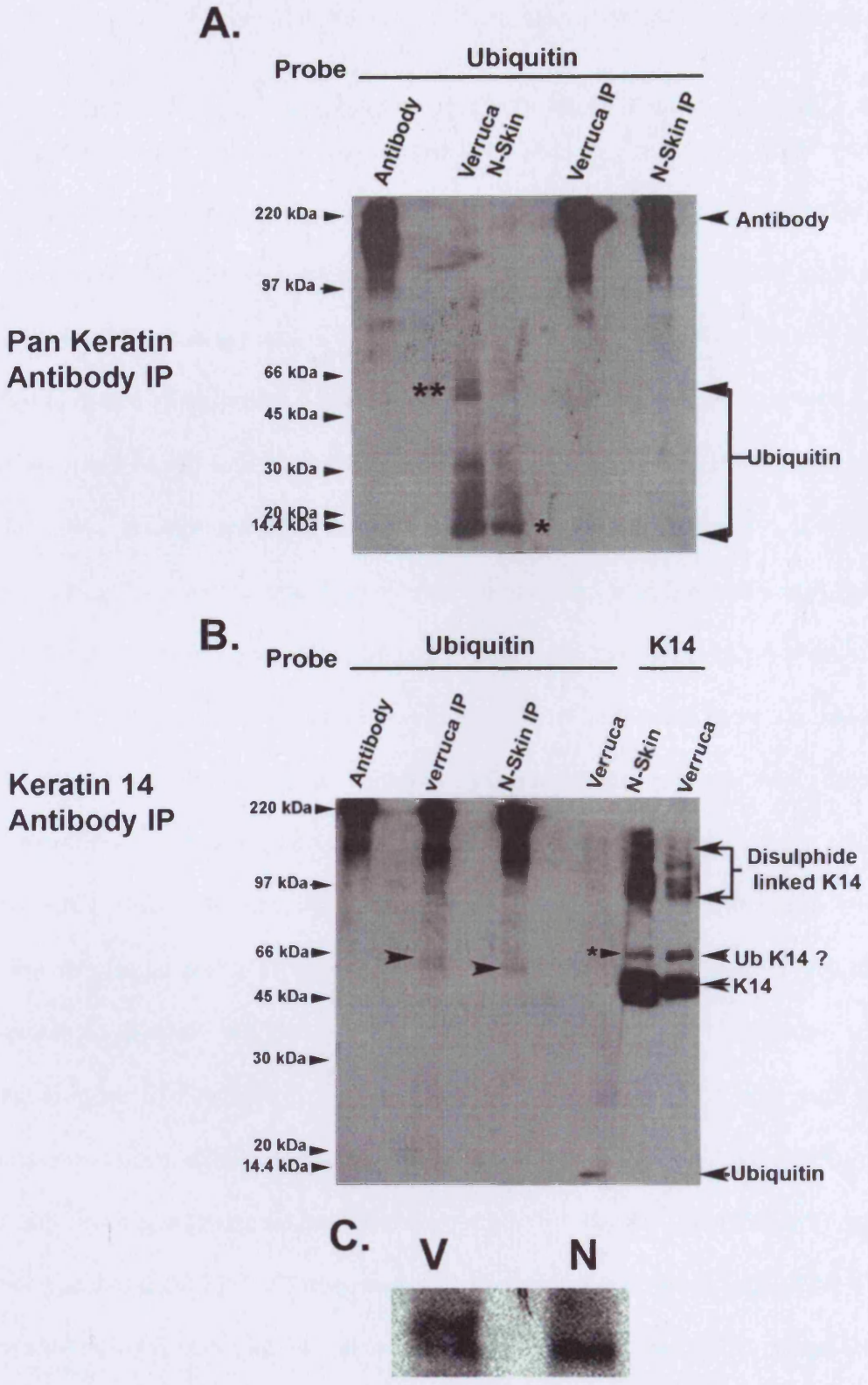
A.
Probe
Ubiquitin
Antibody
Verruca N-Skin
Verruca IP
N-Skin IP
220 kDa
97 kDa
66 kDa
45 kDa
30 kDa
20 kDa
14.4 kDa
**
*
Antibody
Ubiquitin
Pan Keratin Antibody IP
B.
Probe
Ubiquitin
K14
Antibody
verruca IP
N-Skin IP
Verruca
N-Skin
Verruca
220 kDa
97 kDa
66 kDa
45 kDa
30 kDa
20 kDa
14.4 kDa
Disulphide linked K14
Ub K14 ?
K14
Ubiquitin
Keratin 14 Antibody IP
C.
V
N

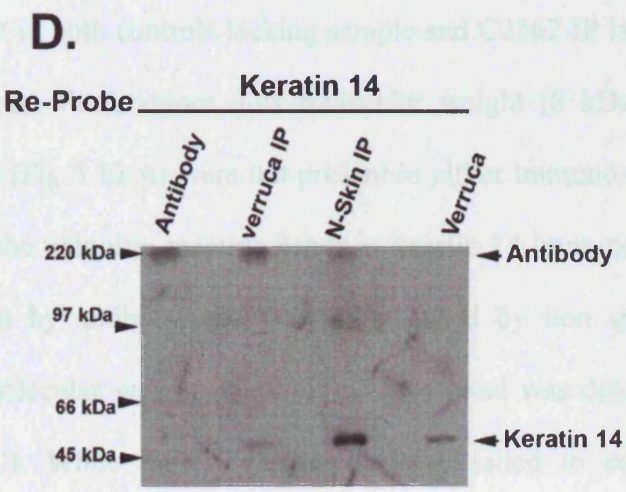

Figure 5.13 *In vivo* keratin-ubiquitin co-immunoprecipitation
Keratin was immunoprecipitated from a protein solution produced by boiling microtome sections from the mid layers of normal and infected skin in 1% (w/v) SDS/PBS. IPs were performed using a pan specific keratin antibody (C2562) (A) or a keratin 14-specific antibody (K0199-12) (B) and probed for ubiquitin (Sc-8017). Lanes containing antibody only reveal that the high molecular weight bands observed in IP lanes are caused by antibody contamination (A and B). Un-conjugated beads incubated with sample produced low molecular weight ubiquitin bands that were not observed on antibody-conjugated beads (A*). Verruca samples also contained a second ubiquitin reactive species ~60 kDa (A**). The pan-keratin antibody did not IP any detectable ubiquitin reactive species from either sample (A). The keratin 14 antibody may have pulled-down species from both samples (arrows B). Verruca sample probed for ubiquitin shows low levels of ubiquitin present in the sample (verruca lane, blot B). After image enhancement (C) the verruca sample could be seen to contain an additional band (B). Extracts probed for keratin 14 reveal multiple high molecular weight species. Although normal skin extracts contained more keratin 14, a ~60 kDa band (same as IPed ubiquitin-reactive species) is stronger in the verruca sample (B*). Blot B was re-probed for keratin 14; verruca and normal IP lanes both contained keratin 14, although significantly more protein had been pulled down from the normal sample (D).

in the absence of DTT indicating them to be disulphide linked species (see Fig 5.11 B). Weak ubiquitin reactive bands may have been pulled down by the keratin 14 antibody. Bands were absent in both controls lacking sample and C2562 IP lanes which, failed to pulled down keratin. Furthermore, low molecular weight (8 kDa) ubiquitin-reactive background bands (Fig 5.13 A) were not present in either immuno-precipitation, which may suggest that the ubiquitin reactive bands in keratin 14 immuno-precipitation lanes were pulled down by antibody and were not caused by non specific binding. An additional high molecular weight ubiquitin reactive band was detected in the verruca lane (Fig 5.13 C). While these experiments have failed to conclusively identify ubiquitinated keratins *in vivo,* initial data suggest further investigations may be worth while. Optimisation of immunoprecipitations or more sensitive techniques such as mass spectroscopy may be required to provide a definitive answer.

5.6 Discussion

The data generated in this study suggest that E1^E4 maintains its capacity to associate with and disrupt keratins *in vivo.* Despite this finding, several differences were observed between E1^E4-positive cells *in vivo* and *in vitro.* Firstly E1^E4-expression *in vivo* rarely leads to perinuclear collapse of keratin networks or the formation of E1^E4 aggregates as seen *in vitro,* suggesting that this is not its primary mode of action. However, E1^E4 association to keratins *in vivo* does appear to result in the disruption/reorganisation of networks, possibly leading to the loss or degradation of affected networks. Although epitope masking cannot be ruled out, it is thought to play a minor role for a number of reasons as discussed earlier in this chapter (see section 5.3.2).

In addition to causing the loss of keratin staining, a subset of HPV 16 E1^E4 positive cells near the surface of lesions cross-reacted with the phospho-specific keratin antibodies, 8250 and 2D6. These data must be viewed with some caution as keratins 4/13 and 5/14 do not contain identical epitopes to those to which the antibodies were raised, although this does not rule out the possibility of E1^E4-induced keratin phosphorylation occurring *in vivo*. Interestingly both of the sites on keratins that are observed to become phosphorylated in the presence of E1^E4 are linked to cell cycle arrest (Ku *et al.*, 1997b; Ku *et al.*, 1998), suggesting that E1^E4's role in G2 arrest by cytoplasmic sequestration of the cyclin B1/CDK1 complex (Davy *et al.*, 2005) may promote keratin reorganisation.

Furthermore, cells expressing high-levels of HPV 16 E1^E4 were found to contain altered ubiquitin profiles, with ubiquitin staining appearing in the cytoplasm of E1^E4 positive cells at the surface of tissue, whereas normal tissue only contained low level nuclear staining in the upper epithelial layers. HPV 2 lesions also contain altered ubiquitin profiles, with cells close to the basal layer containing cytoplasmic ubiquitin as has been previously reported (Sahin., 2001; Sato *et al.*, 1997). Levels of ubiquitin appeared to be especially high in E1^E4 positive cells. In addition to this in some lesions, E1^E4 positive cells continued to stain for ubiquitin into the cornified layer where no ubiquitin staining is detected in normal skin (Sahin. 2001). Although it is tempting to speculate that this is due to E1^E4-induced ubiquitination of keratins, there are also a number of other possible explanations for these observations including the activity of other viral proteins, cell stress and infiltration of immune cells (Kondo *et al.*, 2002; Sahin., 2001; Shackelford *et al.*, 2005).

Data generated in this study also pointed to multiple levels of HPV 16 E1^E4 being present in tissue, which may correspond to different events in the virus lifecycle. Work on mRNA transcripts suggests that HPV 16 E1^E4 may be expressed in the basal layer of cells (Baker *et al.*, 1996; Sherman *et al.*, 1992b; Wilson *et al.*, 2005). If this is the case, then initial levels are too low to be detected by immuno-fluorescence. The onset of detectable levels of E1^E4 occurs shortly before MCM expression is lost, allowing viral genome amplification to occur in a sub-population of cells (reviewed in (Doorbar, 2005)). Loss of MCM expression is followed by an elevation in E1^E4 levels, which in turn was shown to coincide with L1 expression, this may signify the onset of genome packaging. Only after this has occurred does E1^E4 expression move into the final stage, with protein levels building up further. In this population of cells E1^E4 can be seen to induce keratin loss and to colocalize with ubiquitin. In addition L1 relocates from the nucleus to the cytoplasm (possibly following nuclear envelope breakdown), suggesting that matured virions may be ready for release. This indicates that keratin disruption only occurs at the final stage of the virus lifecycle perhaps in order to facilitate egress of newly assembled virions. Keratin disruption must be carefully timed, as premature initiation could result in an EBS-like condition (Ishida-Yamamoto *et al.*, 1991; Lane *et al.*, 2004; Werner *et al.*, 2004), with infected epidermis being shed prior to the completion of the virus lifecycle. The hypothesis of multiple functions of 16 E1^E4 is supported by parallel observations made in HPV2 lesions.

HPV2 E1^E4 is differentially processed in different regions of the tissue, although the identity of each band was not confirmed, if processing is similar to 16 E1^E4 it is possible to speculate as to the identity of each band. These data would indicate that HPV2 E1^E4 may initially be expressed as a doublet containing a phosphorylated form.

In higher layers of the epithelium, multimerisation occurs possibly instigating keratin disruption as previously suggested (Wang *et al.*, 2004). An N-terminally cleaved form may also exist. Although its locations is uncertain, it may appear towards the surface of the tissue as previously seen with HPV 1E1^E4 (Breitburd *et al.*, 1987).

Western blot analysis of keratins from normal and HPV 2-infected tissue proved to be challenging. Because of the great abundance keratin in terminally differentiated epithelia tissue, the heterogeneous nature of HPV2 infections and the diffuse nature of E1^E4 expression in lesions, western bots are not a suitable method for confirming E1^E4-induced drop in keratin levels. Both keratin 10 and 14 appeared to contain high molecular weight species (possibly a dimer) that may have been enhanced by the presence of E1^E4. This observation is interesting when compared with data generated in chapter 6 which suggests that E1^E4 may stabilise keratin filaments. Despite the use of several different approaches no conclusive evidence of ubiquitination of keratin species was found. Although this does not rule out this as a possible mechanism of action of E1^E4 *in vivo,* more sensitive approaches such as mass spectroscopy may be required to resolve this issue.

5.6.1 Future experiments

In order to identify keratin and ubiquitin reactive species of interest, bands from a silver-stained gel could be sent of for analysis by N-terminal sequencing or mass spectroscopy analysis. It is hoped that the results would show whether E1^E4 induces biochemical modifications to keratins *in vivo.* It is also hoped to be able to acquire frozen HPV 16 sections expressing sufficient E1^E4 to perform top-to-bottom sectioning so as to look for modified keratin species. In addition to this it is hoped that

use of a laser dissection microscope may also be used to conclusively determine whether E1^E4 induces keratin loss.

Finally, in order to establish the true effect of E1^E4 on epidermal integrity, it is hoped to use HPV raft cultures and E1^E4 knockout viruses currently under development in the lab. If raft cultures can be produced expressing high levels of E1^E4 it may be possible to stress the surface of the tissue and quantify tissue fragility.

6 The effect of E1^E4 on cytokeratin network dynamics

6.1 Introduction

Having established that E1^E4 is able to disrupt keratins and induce biochemical modifications *in vitro* and potentially *in vivo* (see chapters 4 and 5), time lapse experiments were conducted to better understand the mechanism by which this process occurs. The association of E1^E4 to keratin networks *in vitro* results in their collapse to the perinuclear region, a phenomenon that is rarely observed *in vivo*. This study aimed to analyse the effect of E1^E4 on individual processes involved in the formation and turnover of the keratin network.

6.2 Keratin dynamics

Keratins provide mechanical strength to the cell whilst remaining highly dynamic in order to avoid interference with cellular processes such as mitosis, migration and wound healing. Cytokeratins were initially believed to form relatively stable cytoplasmic filament networks, but the possibility of a dynamic cytokeratin network was suggested when it was noticed that filaments disassemble during cell division (Aubin *et al.*, 1980; Lane *et al.*, 1982). The dynamic nature of keratin filament networks was first shown in the early nineties in a study that monitored the incorporation of biotin-labelled keratins microinjected into living cells. Incorporation of biotinilated keratins was observed within 15 min of injection. By 1.5-2 hours post infection extensive network labelling was observed suggesting that complete network turnover had occurred (Miller *et al.*, 1991; Miller *et al.*, 1993).

6.2.1 Time-lapse studies of keratin dynamics

Keratin network dynamics have been extensively studied by time-lapse microscopy, which has been able to identify individual processes involved in the turnover of keratin

networks. Keratin movement is an ATP-dependent process that can be inhibited by the addition of sodium azide and 2-deoxy-D-glucose (Windoffer *et al.*, 1999). Work investigating the recovery of dismantled filament networks after mitosis showed that network formation is energy dependent, occurs at the cell cortex (Fig 6.1B), and requires both the actin and microtubule filament networks (Windoffer *et al.*, 2001). The phosphorylation state of keratins plays an important role in regulating network stability. Keratin network disintegration, which mimics mitotic disruption can be induced by treating cells with phosphatase inhibitors. This network disintegration is rapid and reversible, and recovers after the removal of inhibitors (Strnad *et al.*, 2002).

6.2.2 Keratin network formation and turnover is dependent on both microtubules and actin networks

Recent studies have demonstrated that keratin filament assembly occurs almost exclusively at the cell cortex and that from here, the assembled filaments migrate towards the centre of the cell (Fig 6.1 A). The inward directed movement of newly formed keratin filaments and their precursors occurs at a rate of ~0.05-0.3 μm/min depending on the cell line being studied (Windoffer *et al.*, 1999; Yoon *et al.*, 2001). This movement is dependent on the actin cytoskeleton and can be inhibited by treating cells with cytochalasin (Werner *et al.*, 2004; Woll *et al.*, 2005). It has also been demonstrated that very few subunit exchanges occur along filaments as they migrate inwards (see Fig 6.1B). Once filaments migrate into the central region of the cell, they fuse with keratin bundles, where they are dismantled, the subunits are then transported back to the edge of the cells (Windoffer *et al.*, 2004). This movement is rapid (~18μm/min) and involves the transport of keratin particles to the edge of cell, which is facilitated by microtubules (Woll *et al.*, 2005). This outward-directed movement of keratin particles can be inhibited by microtubule depolymerising agents such as nocodazole. Analyses of multiple keratin subtypes (K5, 8, 13, 14 and 18) has

A.

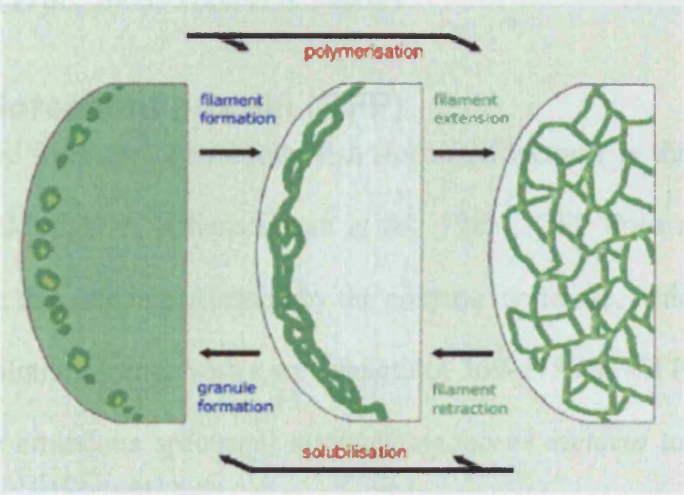

B.

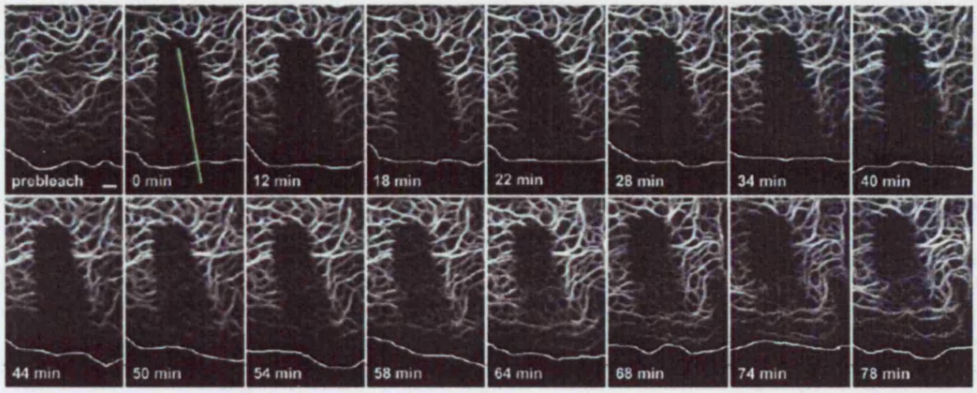

Figure 6.1 Mechanisms behind keratin filament formation and dynamics.
Diagram A shows the simplified two step model which highlights the major aspects of cytokeratin filament network assembly (from left to right), and disassembly (right to left) during mitosis. Granules at the centre of the cell are not depicted they do not directly contribute to network formation. Granule extension and ligation occurs during assembly vs. filament fragmentation and aggregate formation which occurs during disassembly. Radial filament extension and filament thinning occurs during network formation conversely filament retraction and thickening occurs during disassembly, (image taken from (Windoffer and Leube, 2001)). FRAP analysis on keratin filaments of PK18-5 cell demonstrates the differential recovery of central and peripheral cytokeratin filaments (white line indicates cell edge) (B). The first image shows the region prior to bleaching (green line indicates path of laser). Note the recurrence of fluorescence predominantly at the peripheral region where inward moving filaments can be distinguished. Image taken from (Windoffer et al., 2004).

revealed that basic keratin dynamics appear to be neither subtype-specific or cell type dependent (Woll *et al.*, 2005; Yoon *et al.*, 2001).

6.3 Green florescent protein (GFP)

GFP was isolated from the crystal jelly fish *Aequorea victoria* in the 1960's and first cloned in the mid eighties (Charbonneau *et al.*, 1985). GFP does not itself produce fluorescent light; this role is performed by the enzyme luciferase, which produces ATP-dependent chemiluminescence with a wavelength of 369-475 nm. GFP functions to alter the fluorescence emissions spectrum, allowing *Aequorea victoria* to emit green light with a wavelength of 508nm (reviewed in (Shimomura, 2005). In the laboratory GFP functions as a biological fluorophore and can be observed by excitation with an artificial light source such as a UV lamp or laser. The GFP protein contains a chromophore at its centre (Fig 6.2B) that has the ability to absorb light energy of specific wavelengths, this energy is then re-emitted by the molecule at a longer wavelength (fluorescence). The GFP protein catalyzes the formation of its own chromophore, which is contained within the centre of a beta–barrel structure formed by 11 beta strands (Fig 6.2A) (Phillips, 1997; Yang *et al.*, 1996). Since its discovery, GFP has been an invaluable tool in biological research, allowing the labelling and real-time monitoring of biological molecules in their natural environments. Many different GFP mutants have since been produced conferring various properties on the protein e.g. enhanced GFP (EGFP) fluoresces at a higher intensity and resists photobleaching when compared with wild type GFP. Monomeric and pH sensitive variants have also been produced. In addition, single amino acid mutations resulting in shifts in the absorbance and emission spectra have been generated resulting in yellow florescent protein (YFP) and cyan florescent protein (CFP) (reviewed by(Chudakov *et al.*, 2005).

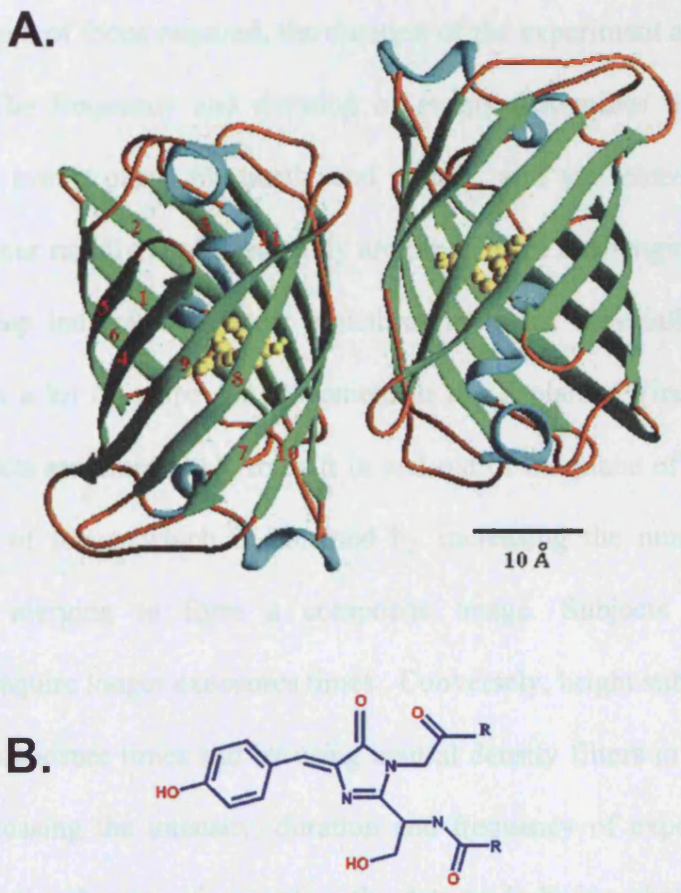

Figure 6.2 The structure of the Green florescent protein (GFP)
GFP exists as a dimer in solution at low ionic strengths. The protein is formed from eleven strands of β-sheet (green) which form the walls of a cylinder (A). Short segments of helices (blue) cap the top and bottom of the 'β-can' and provide a scaffold for the fluorophore (B) held near geometric centre of the can. Images taken from (Yang, Moss, and Phillips, 1996)

6.4 Basis of time-lapse imaging

To collect valid time-lapse data several factors must be taken into consideration. These include the depth of focus required, the duration of the experiment and the brightness of the subject. The frequency and duration of events determines the interval between frames. Some events occur frequently and rapidly, and are relatively easy to image. Events that occur rapidly but infrequently are much more challenging to film. It can be difficult to keep individual filament structures in focus, especially in rounded cells, where there is a lot of scope for movement in the Z-plane (Windoffer *et al.*, 1999). Dynamic objects are more likely to drift in and out of the plane of focus and require a greater depth of focus, which is obtained by increasing the number of Z sections, followed by merging to form a composite image. Subjects with low-intensity fluorescence require longer exposures times. Conversely, bright subjects can be imaged using shorter exposure times and by using neutral density filters to further reduce light intensity. Increasing the intensity, duration and frequency of exposure of samples to light increases the chances of corrupting the data by inducing phototoxic cell damage. The selection of fluorophore can also influence the phototoxicity incurred during imaging. For example, blue fluorophores such as CFP require shorter wavelength (higher energy) excitation sources resulting in more rapid accumulation of photo damage. Time-lapse imaging using multiple fluorophores requires a greater number of exposures and hence will increase phototoxic cell stress. All these factors must be taken into account when designing time-lapse experiments in order to generate valid data. As many of these factors are initially unknown and time-lapse experiments require a considerable amount of optimisation in order to establish a practical system.

6.4.1 Phototoxicity

Phototoxicity is a problem that is commonly encountered during time-lapse experiments. Phototoxicity and photobleaching are two distinct phenomena.

Phototoxicity results from the generation of free radicals by the exposure of cells to high energy light sources. Free radicals are chemically reactive species with lone pair electrons that are produced by the breaking of chemical bonds by high energy ultraviolet light. As free radicals accumulate in cells they react with bio-molecules and disrupt biological processes and this in turn can alter cellular dynamics leading to apoptosis, and distorts experimental data (Juven *et al.*, 1985). Phototoxicity can be minimised by reducing the duration and intensity of the light pulses used to excite fluorophores (Black, 2004; Juven *et al.*, 1985; Neumann *et al.*, 1999; Satoh *et al.*, 1996). Addition of antioxidants such as ascorbic acid, which mop up free radicals can also be used to reduce phototoxicity (Neumann *et al.*, 1999).

6.5 Results

6.5.1 Production and characterisation of a 16^E1^E4 YFP fusion protein

The YFP-E1^E4 fusion protein was produced by cloning E1^E4 from the existing MV11 vector, and ligating it into the pEYFP-C1 vector (Clonetec, see appendix IIII for vector map). This resulted in a YFP protein with E1^E4 attached to its C-terminus. The PCR reaction produced a 300 bp E1^E4 fragment (Fig 6.3 A), which was ligated into the vector and transformed into bacteria. Clones were screened by both endonuclease restriction digestion and PCR (Fig 6.3B). To ensure that the pYFP-E1^E4 construct expressed a functional protein, SiHa cells were transfected with the construct. Cells lysates were analysed by western blots, which were probed with an E1^E4-specific antibody (TVG 402). Extracts were shown to contain an E1^E4 reactive band of approximately 40 kDa which is consistent with a fusion between E1^E4 (12 kDa) and YFP (27kDa) (Fig 6.3 C). Separation on a 10 % gel showed that the band was composed of a doublet, suggesting that phosphorylation may occur as with wild type protein.

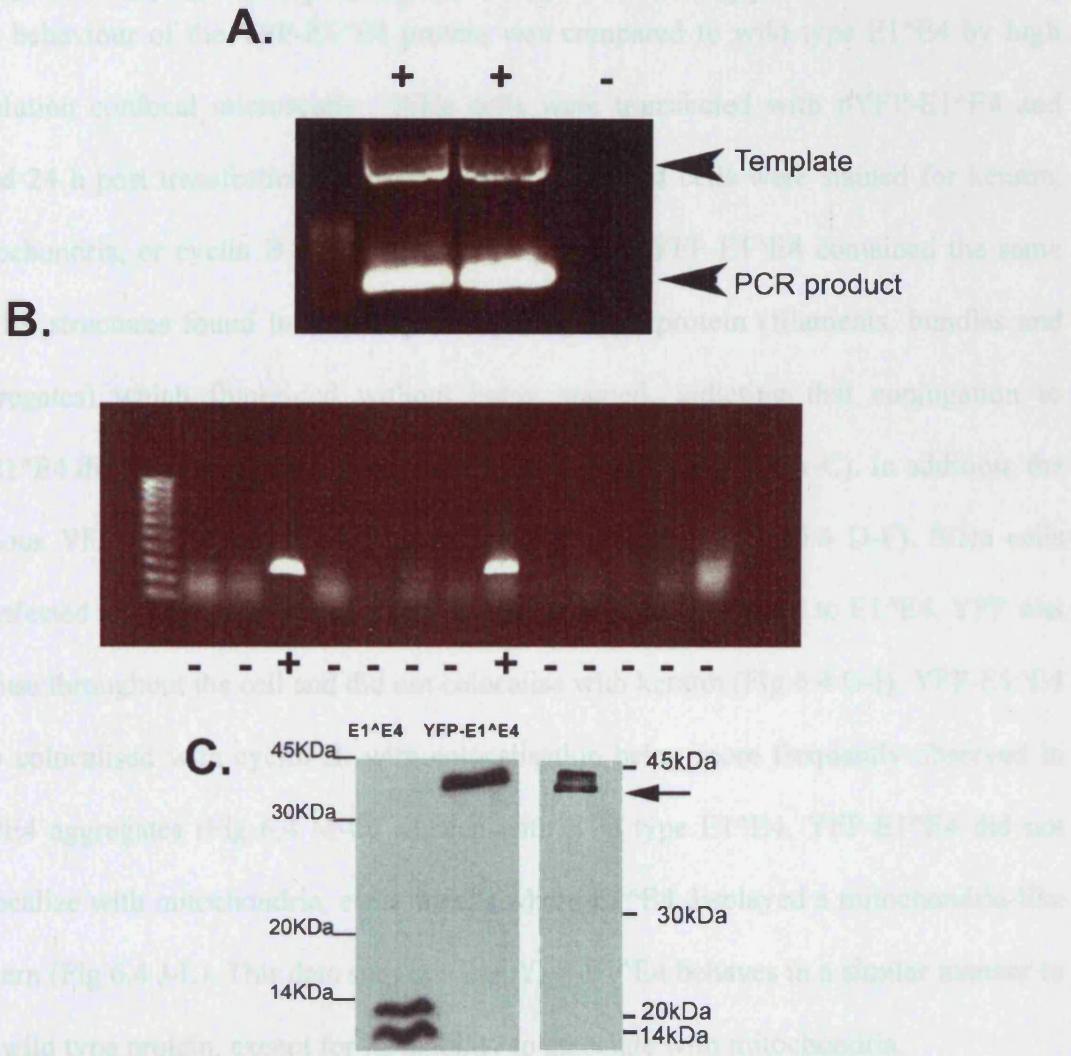

Figure 6.3 Cloning and identification of the YFP-E1^E4 fusion protein
The YFP-E1^E4 fusion protein was produced by cloning E1^E4 from pMV11 HPV 16 E1^E4 vector (Raj, 2004). PCR products were ~300 bp in size and only present in lanes containing template (A.). PCR products were ligated into the pEYFP-C1 vector (Clonetech) and electroporated into DH5α cells. Positive colonies were identified by PCR screening (B). Wild type and YFP-E1^E4 clones were transfected into SiHa cells and lysates analyzed by western blotting. Blots were probed with the E1^E4 specific antibody (TVG402). Wild type E1^E4 produced 2 bands ~12 kDa in size as previously reported. The YFP-fusion protein was ~40 kDa in size (C) and found to contain 2 bands when separated on a 10 % gel (arrow).

6.5.2 YFP-E1^E4 analysis by confocal microscopy

The behaviour of the YFP-E1^E4 protein was compared to wild type E1^E4 by high resolution confocal microscopy. SiHa cells were transfected with pYFP-E1^E4 and fixed 24 h post transfection with methanol. Transfected cells were stained for keratin, mitochondria, or cyclin B (Fig 6.4). Cells expressing YFP-E1^E4 contained the same E1^E4 structures found in cells expressing wild type protein (filaments, bundles and aggregates) which fluoresced without being stained, indicting that conjugation to 16E1^E4 did not disrupt the function of the YFP protein (Fig 6.4 A-C). In addition, the various YFP-E1^E4 structures all colocalised with keratin (Fig 6.4 D-F). SiHa cells transfected with the empty YFP vector showed that when not bound to E1^E4, YFP was diffuse throughout the cell and did not colocalise with keratin (Fig 6.4 G-I). YFP-E1^E4 also colocalised with cyclin B, with colocalisation being more frequently observed in E1^E4 aggregates (Fig 6.4 M-O) as seen with wild type E1^E4. YFP-E1^E4 did not colocalize with mitochondria, even in cells where E1^E4 displayed a mitochondria-like pattern (Fig 6.4 J-L). This data suggests that YFP-E1^E4 behaves in a similar manner to the wild type protein, except for its inability to associate with mitochondria.

6.5.3 Expression of YFP-E1^E4 in SW13 cells

To confirm that YFP-E1^E4 was incapable of associating with mitochondria; the construct was expressed in cells lacking cytokeratin networks. YFP-E1^E4 was transfected into SW13 T7K and SW13 C2 cell lines (C2 lack keratin networks, T7K cells express a K8/18 network). In SW13 T7K cells YFP-E1^E4 expression produced results similar to those in SiHa cells, producing filaments, bundles and aggregates that co-stained with keratin (see Fig 6.5 G-L). Expression of YFP-E1^E4 in SW13 C2 cells resulted in a diffuse pattern that did not appear to colocalize with mitochondria (see Fig 6.5 A-F).

Figure 6.4 Functionality of YFP-E1^E4 as determined by immunofluorescence in SiHa cells

SiHa cells were transfected with pYFP^E1^E4 and fixed with methanol 24 h post-transfection before being stained for DNA (DAPI, blue) and either keratin (C2562), cyclin B (GNS 11) or mitochondria (mitotracker, used prior to fixation) (red). YFP-16E1^E4 produced a variety of structures including filaments bundles and aggregates (A-C). YFP-E1^E4 associated to and disrupted keratin filaments (D-F). SiHa cells transfected with empty YFP vector, demonstrated that YFP was diffuse and did not associate to keratin (G-I). YFP-16E1^E4 could not be observed to associate with mitochondria (J-L). YFP-16E1^E4 maintained the ability to associate with cyclin B (M-O). Scale bars denote 5 μm.

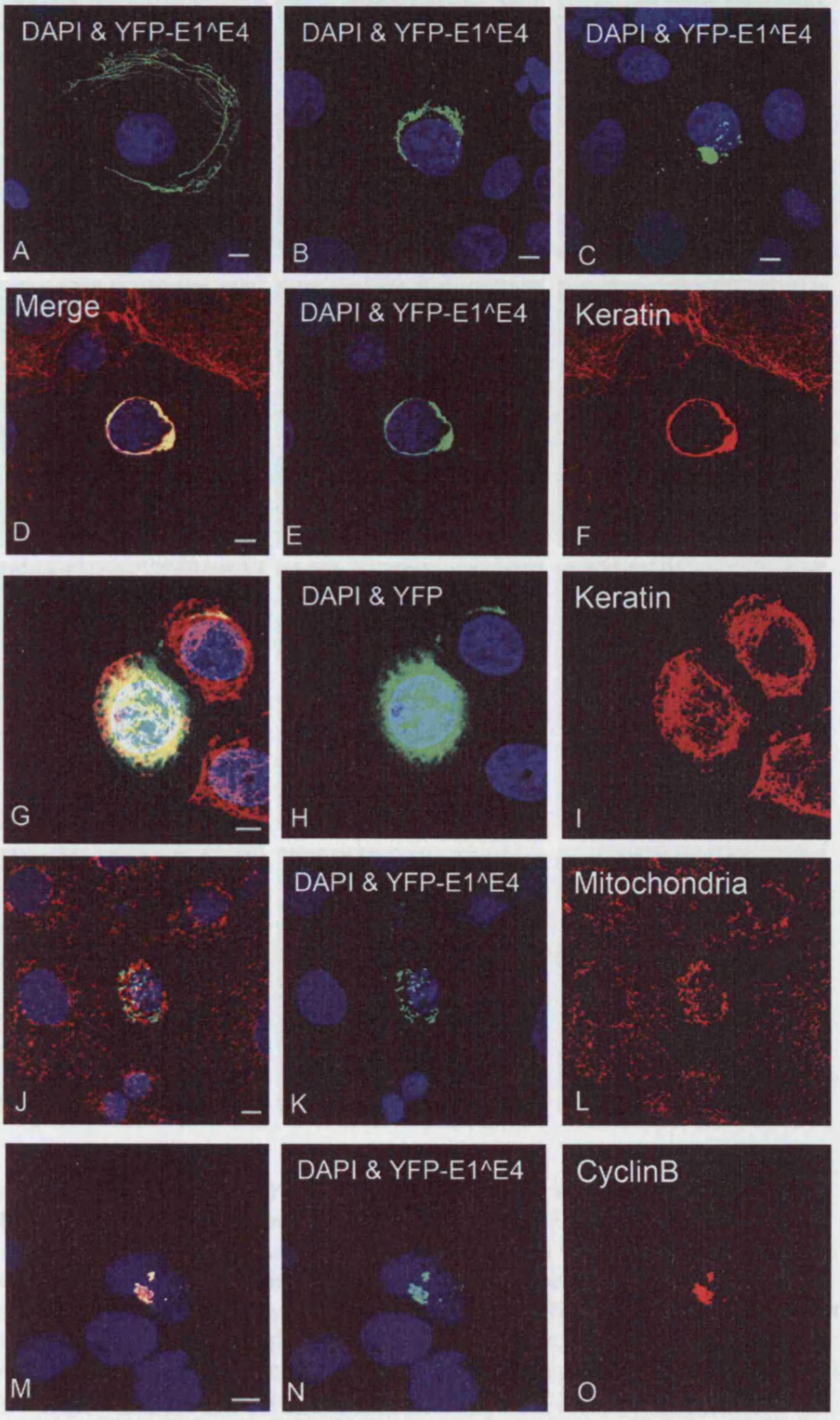
DAPI & YFP-E1^E4
A
DAPI & YFP-E1^E4
B
DAPI & YFP-E1^E4
C
Merge
D
DAPI & YFP-E1^E4
E
Keratin
F
G
DAPI & YFP
H
Keratin
I
J
DAPI & YFP-E1^E4
K
Mitochondria
L
M
DAPI & YFP-E1^E4
N
CyclinB
O

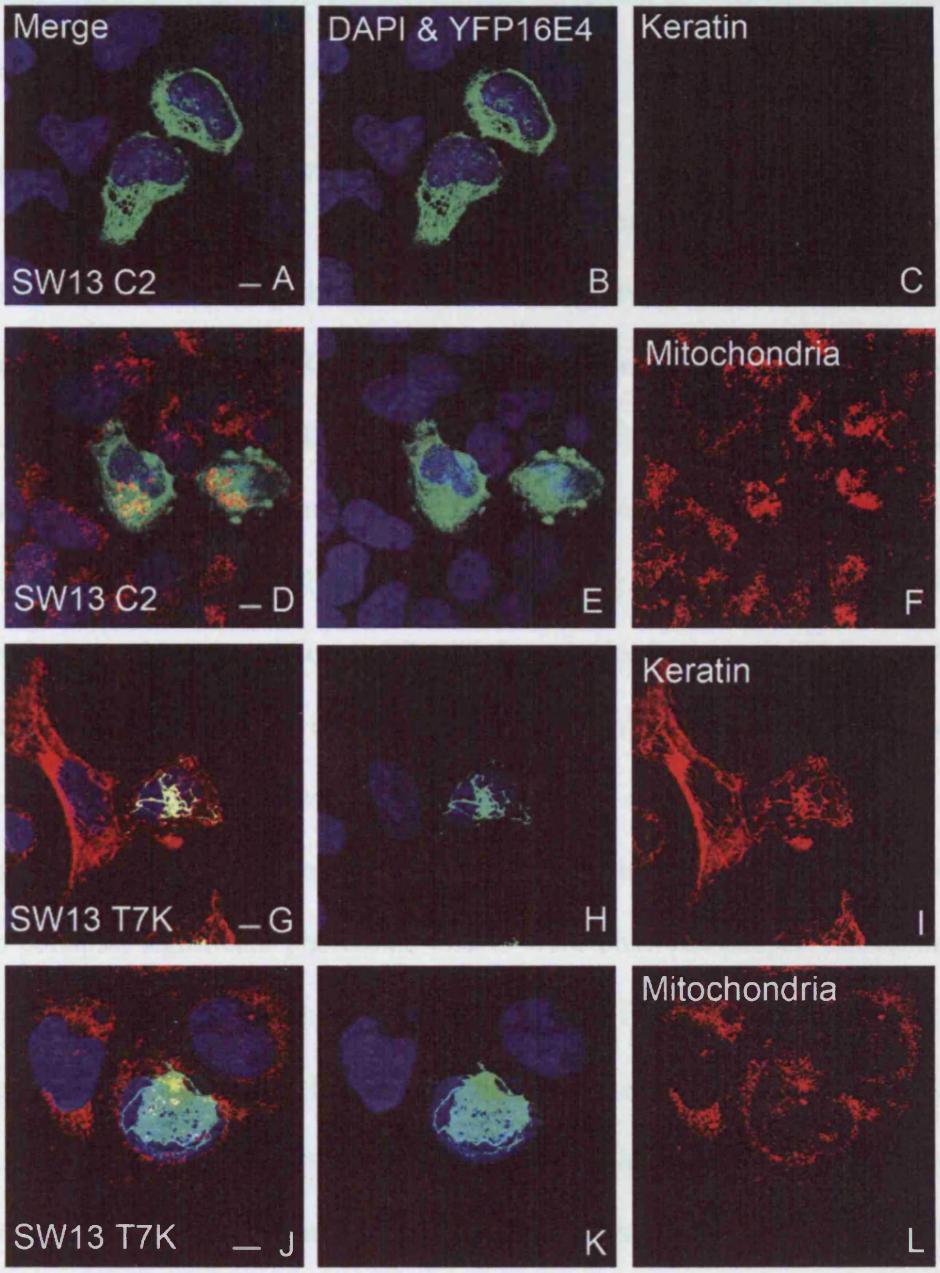

Figure 6.5 Expression of YFP-16E1^E4 in SW13 cells demonstrates that it is unable to associate with mitochondria

The ability of YFP E1^E4 to associate with mitochondria was established by transfecting pYFP-16^E1^E4 into C2 (K-ve) and T7K (keratin 8 & 18) SW13 cells. Cells were fixed 24 h post-transfection and stained for DNA (DAPI, Blue) and either keratin (C2562) or mitochondria (mitotracker added prior to fixation) (red). In the absence of keratin (SW13 C2 cell line) YFP^ E1^E4 was unable to bind mitochondria or form solid structures resulting in a diffuse cytoplasmic pattern (A-F). When expressed in SW13 T7K cells YFP E1^E4 was exclusively located to keratin (G-L). Scale bars denote 5 μm.

This data suggested that the fusion protein was incapable of forming solid structures in the absence of keratin.

6.6 Initial time-lapse strategies

Initial time-lapse experiments were carried out to observe both YFP-E1^E4 and CFP-keratin simultaneously using the AK-8 cell line expressing a CFP-tagged keratin 8/18 network (kindly provided by Rudolph Leube). The aims were to determine how robust the cells were, to observe E1^E4 behaviour in cells, and to determine the rate at which E1^E4 accumulates on keratin networks. Initial experiments showed that cells frequently drifted out of the plane of focus, suggesting that long duration movies may not produce usable data. Although YFP-E1^E4 was exclusively localised to the CFP keratin filaments, the network in the AK-8 cell line could not be clearly visualised, and only poor resolution images were obtained (this was also noted by Rudolph Leube, personal communication). Over the time frame required to observe E1^E4-induced keratin collapse, significant phototoxic effects were observed despite increasing time-lapse intervals. Cells were observed to ball up and fluorescent keratin formed into aggregates in the absence of E1^E4, indicating the initiation of apoptosis (Caulin *et al.*, 1997). The narrow margin between YFP-E1^E4 and phototoxicity-induced cytokeratin network collapse, meant that it was not possible to distinguish between the effects of E1^E4 and phototoxicity using this approach. Two colour imaging required double the number of exposures which contributed further to phototoxic damage. This problem was compounded by the use of CFP which requires short wave (high energy) excitation wavelengths. From these initial experiments it was concluded that long duration two colour imaging experiments were not possible to carry out due to high levels of phototoxic damage. In addition to this, the CFP cell line produced poor quality images.

Having been unable to produce usable data using the initial approach, it was decided to transfect YFP-E1^E4 into SiHa cells and to focus on the effect of YFP-E1^E4 on keratin network dynamics over a 1-2 hour frame using the AK 13 cell line as a control (Windoffer *et al.*, 1999). The GFP labelled keratin 13 networks expressed in this cell line were significantly sharper to visualise than the K8/K18 networks expressed in AK-8 cells. Both the process of keratin filament formation and the migration of individual filaments towards the centre of the cell could be captured using the available imaging systems. After generating data in this cell line it was discovered that although dynamics occurred at the same rate as previously reported for AK13 cells (Windoffer *et al.*, 1999) the rates of movement varied between different cell lines (Yoon *et al.*, 2001). As a result of this discovery a third strategy was investigated.

6.7 GFP keratin 13 transfected into SiHa cells

At the time of acquiring the AK8 and AK-13 cell lines, a GFP labelled keratin 13 plasmid (pHK13ΔP.EGFP) was also provided by Rudolph Leube. This plasmid was transfected into SiHa cells to investigate keratin filament formation and to allow the monitoring of keratin network dynamics in the same cellular background. SiHa cells express a keratin 8 and 18 network and so a GFP labelled keratin 8 or 18 would have been preferable. In addition to keratin 8/18, around 10 % of SiHa cells also express keratin 13 (see chapter 4), and so it was uncertain whether expressed GFP-K13 protein would be able to incorporate into keratin filaments in SiHa cells. To examine this, SiHa cells were transfected with the plasmid and stained for keratin (C2562). Transfected cells expressed high levels of the protein, and displayed various phenotypes. Fluorescent keratin aggregates (Fig 6.6 D-F) and filamentous structures were observed in cells (Fig 6.6 A-C), GFP-K13 filaments were indistinguishable from endogenous filament network (Fig 6.6 A-C). Cells were observed at 12 and 24 h post transfection; a

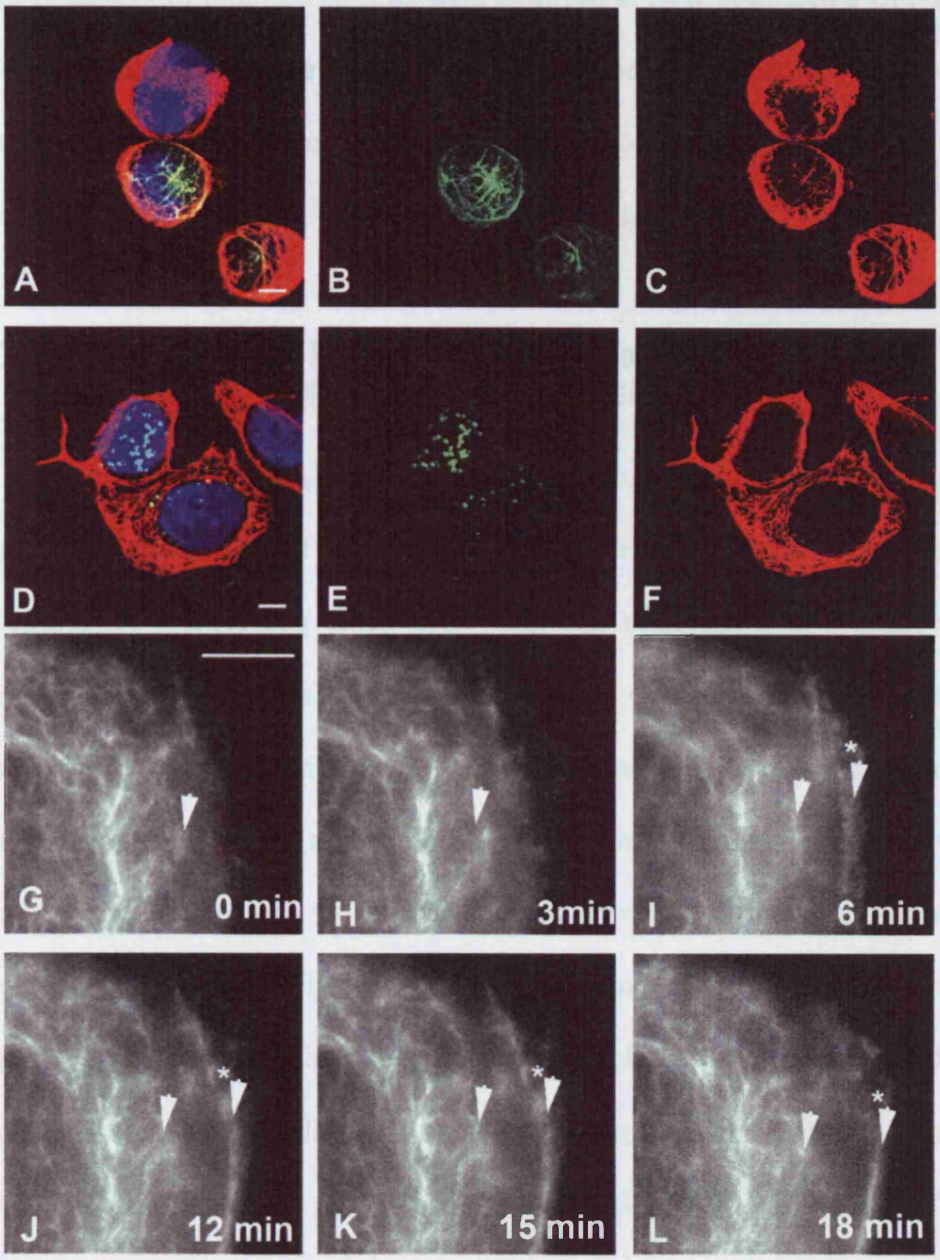

Figure 6.6 Formation of keratin filaments can be observed in GFP keratin 13 transfected SiHa cells

SiHa cells transfected with GFP-Keratin 13 plasmid (Windoffer and Leube, 1999) fixed with methanol and stained for keratin (C2562 red) and DNA (DAPI blue).GFP keratin 13 could be seen to incorporate into keratin networks in a sub population of cells (A-C), whereas it formed aggregate structures in others (D-F). (G-L) When GFP-keratin 13 is transfected into live cells, filaments could be seen to form from diffuse fluorescent material at the edge of the cell (*). Scale bars denote 5 μm.

greater number of filamentous cells were observed at 24 h. Although a GFP keratin 8 or 18 label would have been a more logical choice, from these observations it was decided that this system could be used as a control model to determine the affects of E1^E4 on keratin filament formation, migration and turnover in SiHa cells.

6.7.1 Formation of keratin filaments at the cell cortex can be observed in GFP K13 transfected SiHa cells

It was decided to investigate whether E1^E4 caused keratin collapse by disrupting keratin polymerisation and filament formation at the cell cortex. The process was first visualised by transfecting SiHa cells with the pHK13ΔP.EGFP plasmid. Diffuse fluorescent material at the edge of the cell edge was shown to condense and form filaments (Fig 6.6 G-L) with newly formed filaments migrating towards the centre of the cell (see Fig 6.8 A-C) (see movie GFP-K13) where they begin to fuse with centrally located keratin bundles. As filaments move inwards, diffuse fluorescent material condense behind the old filament, with new filaments gradually forming (small arrows Fig 6.8). These observations suggest that the pHK13ΔP.EGFP plasmid could be transfected into SiHa cells and used to observe keratin filament formation and migration, which occurs by a mechanism similar to that previously described (Windoffer *et al.*, 1999; Windoffer *et al.*, 2001).

6.7.2 E1^E4 does not initially disrupt filament formation

A reduction in soluble keratin in E1^E4-positive SiHa cells has previously been demonstrated using fractionation experiments (see Fig 4.16) (Wang *et al.*, 2004). This data would seem to suggest that the keratin "escalator" system may be inhibited. It was previously suggested that this was a result of E1^E4 associating with the soluble pool of

keratin and linking it to the insoluble filaments by a process of cross-linking and/or multimerisation (Wang *et al.*, 2004). During initial time-lapse analysis of cells, performed 24 h after transfection, no filament formation could be observed suggesting that the process of keratin polymerisation and filament formation was inhibited by E1^E4. However, analysis of SiHa cells 12 h after transfection with pYFP-E1^E4 shows that the build up of E1^E4 does not initially disrupt cytokeratin filament formation and subsequent inward translocation (Fig 6.7) (see movieYFP-E1^E4.1). In cells containing fine filamentous YFP-E1^E4 the process of filament formation could be observed. The formation of filaments from diffuse fluorescent E1^E4 occurred at the periphery of the cell, as observed in cells expressing fluorescently tagged keratin. Filaments joined with the existing filament network migrating towards the centre of the cell. The data was colleted using 5 z sections giving a focal depth of 2 μm confirming that filament formation was indeed being observed and that the data could not be explained simply by filaments drifting into the plane of focus. This data demonstrates that E1^E4 can associate with the soluble pool of keratin without initially disrupting keratin polymerisation and filament formation.

6.8 Tracking of the inward directed migration of GFP keratin 13 and YFP-E1^E4 filaments in SiHa cells

To determine whether E1^E4 was able to affect keratin network dynamics by disrupting their association with other cytoskeletal components or otherwise, SiHa cells were transfected with pYFP-E1^E4 or pHK13ΔP.EGFP. 2-hour time-lapse movies were produced and the rate of inwards directed migration of filaments from the edge of the cell was determined. Data sets were analysed to quantify variation between YFP-E1^E4 and GFP-K13 network dynamics using the in-house tracking software GM view, developed by Gregory Mashanov (Mashanov *et al.*, 2003; Mashanov *et al.*, 2004). Ten

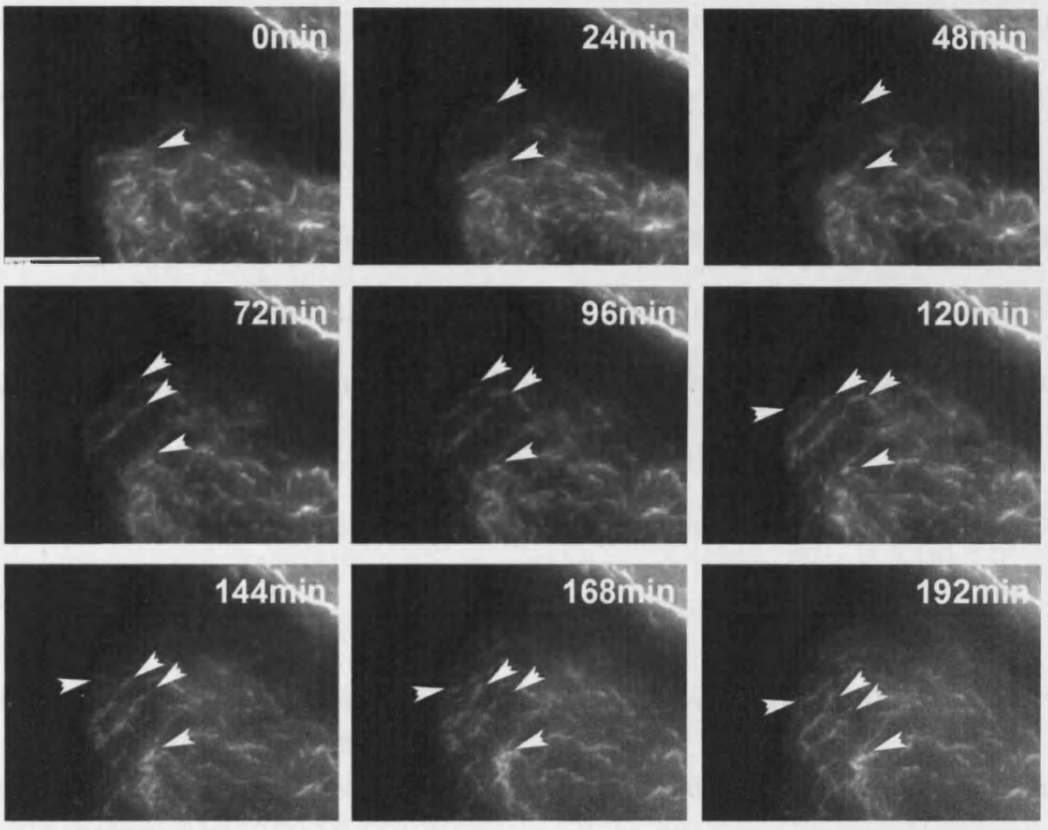

Figure 6.7 YFP-E1^E4 can be observed to assemble into filaments at the edge of the cell.
SiHa cells were transfected with pYFP-E1^E4 12 h prior to imaging on a Deltavision epifluorescence microscope. Diffuse YFP-E1^E4 at the edge of the cell was observed to assemble into filaments (marked by arrows). Filaments migrated towards the cell centre in a similar manner to that previously described for GFP labelled keratin filaments (Windoffer and Leube, 1999). Scale bar denotes 5 μm.

different identifiable objects at the edge of the cell were selected and tracked for each time point making a total of approximately 600 measurements /cell. Velocity values generated in GM view were double checked by frame to frame analysis of data sets in Softworks software (Applied Precision). To determine the effects of phototoxicity on data sets, 2-hour movies were split into three 40 min components and analysed separately in order to determine the cumulative effects of phototoxicity on dynamics. Average velocities were found to be stable over the 2 hour period (data not shown). Furthermore, cells appeared stable and did not show obvious signs of apoptosis, as observed in earlier recordings, suggesting that data was not being corrupted by phototoxicity.

6.8.1 Rates of filaments migration observed in GFP keratin 13 labelled SiHa cells.

The rate of inward movement of keratin filaments was determined by analysing time-lapse recordings of SiHa cells transfected with either GFP-K13 or YFP-E1^E4. The rate and uniformity of the movement was determined by analysing the average velocity and standard deviation values. Keratin filament migration was generally unidirectional (see Fig 6.8 A-C) (outward "pulses" of movements were occasionally observed see large arrow Fig 6.8 A-B) (see movie GFP-K13), the rate of which varied slightly from cell to cell and had an average velocity of 0.056 μm/min (with range of 0.03-0.084 μm/min) and an average standard deviation of 0.036 μm/ min (Fig 6.9A). New filament could be observed to form from diffuse material at the cell edge as the observed filament tracked inwards; demonstrating that filament turnover was ongoing (Fig 6.8 B small arrows) and indicating that phototoxicity was not affecting cells. Filament morphology appeared to be in a continuous state of flux with filaments stretching, condensing and fusing with one another. Filament mergers occurred in the perinuclear region of the cell sometimes forming large bundles, the morphology of which was also in a continual state of flux

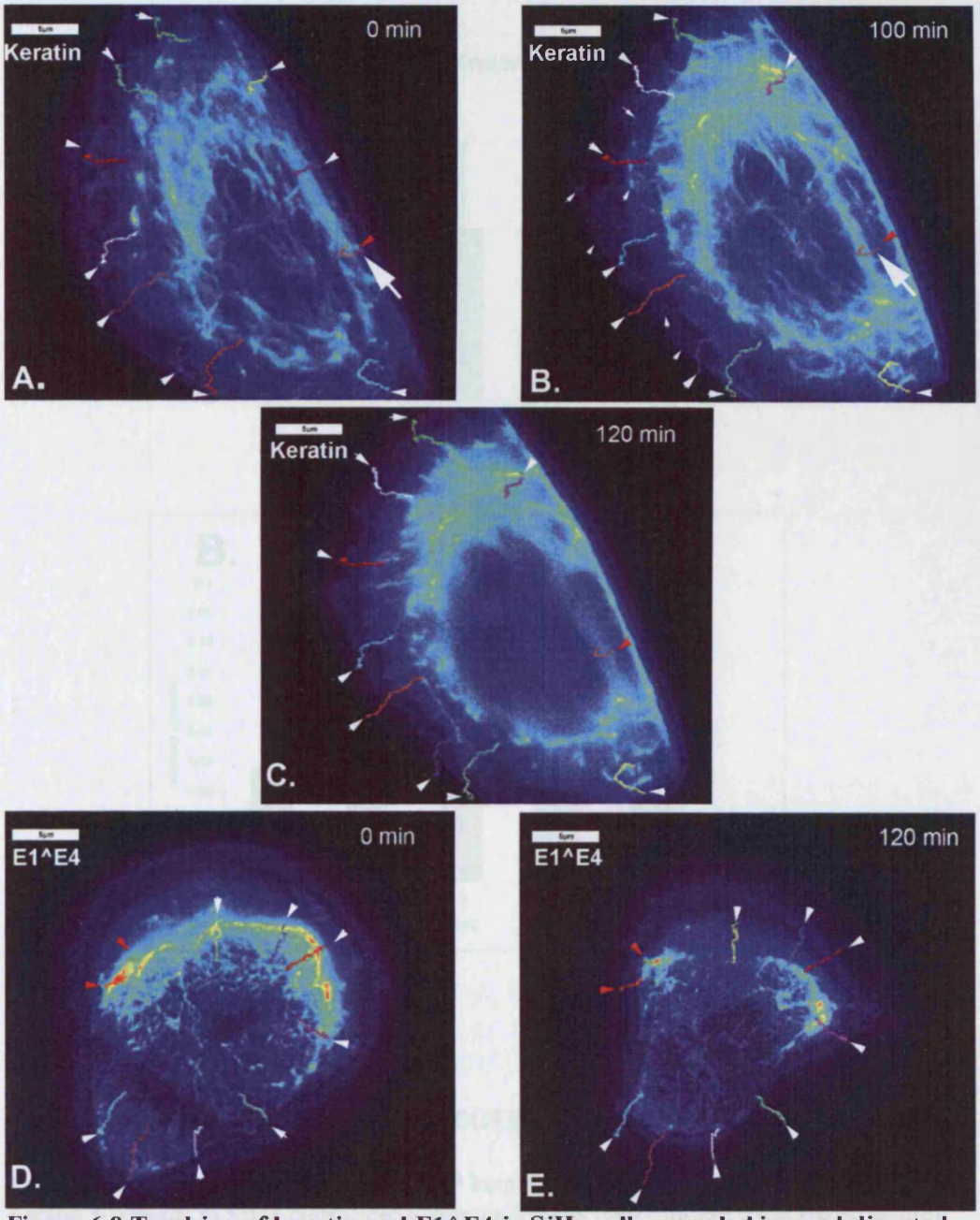

Figure 6.8 Tracking of keratin and E1^E4 in SiHa cells revealed inward directed movement of both YFP-E1^E4 and GFP keratin.

GFP-keratin 13 (A-C) or YFP-E1^E4 (D-E) was transfected in to SiHa cells and time lapse movies were produced. Data was analysed with GM view, paths (track initiation points denoted by arrows) of ten objects per cell were recorded. Images (A & D) show cells at T0. GFP keratin was observed to track into the centre of the cell continuously with an average rate of ~0.06μm/min (A-C). New filaments were observed to form behind old filaments as they tracked inwards (small arrows B). An outward spread of new filaments was also observed (large arrow A-B). Inward movement of YFP-E1^E4 fillaments was observed in cells as network collapse occurred, no new fluorescent material is observed at the edge of the cell (E). Maximum velocities did not exceed and were comparable to those of keratin movement (compare track lengths). YFP-E1^E4 and GFP keratin networks both contained relatively static points moved that little in 2 h (red arrows). Scale bar denotes 5 μm.

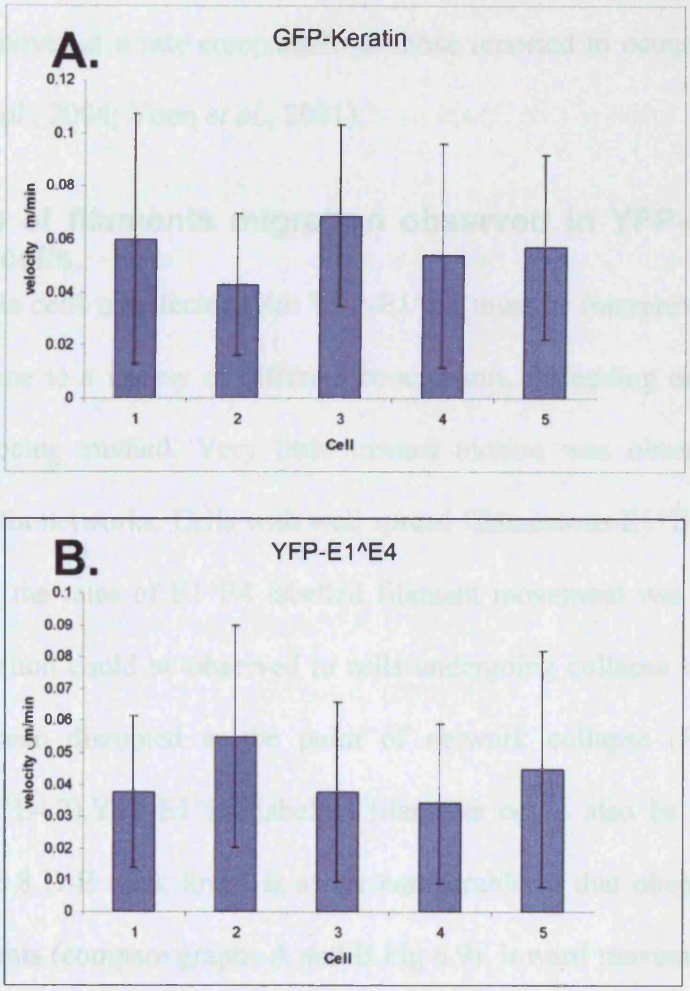

Figure 6.9 Average inward velocities of GFP keratin 13 and YFP-E1^E4 labelled keratin networks in SiHa cells

Graphs show the average velocity of GFP keratin 13 (A) or YFP-E1^E4 (B) labelled keratin filaments in SiHa cells (5cells /population) as they migrate from the edge into the centre of the cell (see Fig 6.8). Rates represent the average velocity of 10 objects per cell initiating at the cell edge and migrating inwards (see Fig 6.8), over the course of 2 hr using GM view tracking software, error bars represent the standard deviation. Average velocities of GFP keratin 13 and YFP-E1^E4 labelled keratin networks in SiHa cells were 0.059 and 0.043 μm/ min respectively.

(see movie GFP-K13). These data indicated that GFP-K13 labelled filament networks in SiHa cells turnover at a rate comparable to those reported to occur in other cell lines (Windoffer *et al.*, 2004; Yoon *et al.*, 2001).

6.8.2 Rates of filaments migration observed in YFP-E1^E4 labelled SiHa cells.

Data from SiHa cells transfected with YFP-E1^E4 must be interpreted carefully as it is possible to come to a variety of different conclusions, depending on the population of E1^E4 cells being studied. Very little inward motion was observed in cells with collapsed keratin networks. Cells with well spread filamentous E1^E4 were selected for this study and the rates of E1^E4 labelled filament movement was recorded. No new filament formation could be observed in cells undergoing collapse suggesting that this process has been disrupted at the point of network collapse (Fig 6.8 D-E) (see movieYFP-E1^E4.2).YFP-E1^E4 labelled filaments could also be observed to move inwards (Fig 6.8 D-E track lines) at a rate comparable to that observed for GFP-K13 labelled filaments (compare graphs A and B Fig 6.9). Inward movement had an average velocity of 0.043 μm/min (with a range of 0.019-0.072 μm/min) and a standard deviation of 0.029 μm/min. Although GFP-K13 labelled networks contained some relatively static regions (red arrow Fig 6.8 A-C), these were generally more abundant in YFP-E1^E4 networks, depending on the extent of network collapse (red arrows Fig 6.8 D-E), resulting in the reduced average velocities recorded. Points containing identifiable material 360° around the cells were selected. Data could have been skewed by selectively analysing highly dynamic regions and is therefore open to interpretation. Dynamic regions (non-collapsed) moved at comparable velocities in both YFP-E1^E4 and GFP–K13 transfected SiHa cells (YFP-E1^E4 max 0.072 μm/min, GFP K13 max 0.084 μm/min also, compare track lengths Fig 6.8 C and E).

Furthermore the usual complex shifting dynamics observed within normal keratin networks were not observed in E1^E4 associated networks. Filament stretching and mergers were not observed and filaments appeared to be of a uniform thickness. Individual filament junctions were stable over the 2 hour recordings (see Fig 6.10B and 6.11B). Dynamic regions of E1^E4 associated keratin filament moved inwards at a rate comparable to those observed in GFP-K13-labelled networks, suggesting that the association of E1^E4 to filaments appears not to disrupt the association to other components of the cell cytoskeleton responsible for keratin filaments dynamics. However, the association of E1^E4 appears to freeze dynamic alterations to the keratin network architecture that are apparent in normal keratin networks, possibly indicating the stabilisation of E1^E4 associated keratin filaments.

6.9 Fluorescence recovery after photobleaching (FRAP)

FRAP is a useful analytical technique that allows the study of protein diffusion and can provide data on protein-protein interactions in living cells. FRAP relies on the basic principal of photobleaching, which is where over stimulated fluorophores sustain photon-induced chemical damage and undergo covalent modification, destroying their fluorescent properties. Fluorophores can be photobleached with a brief pulse of bright light without damaging other cellular proteins (Prendergast, 1999). As lasers can be used to ablate fluorescence in localized regions within cells, fluorescence recovery can be monitored by time-lapse imaging to gain information on the kinetics and turnover of proteins within cells. It was hoped that such experiments would determine if keratin bound E1^E4 is in equilibrium with a diffuse population or whether keratin binding is a stable/irreversible event. In addition to this, by determining the E1^E4 recovery mechanism, it will be possible to determine if E1^E4 can bind polymerised keratin

filaments or whether it binds soluble keratin and is subsequently incorporated into networks during filament formation.

6.9.1 FRAP analysis of GFP labelled keratin filaments

Keratin FRAP has previously been performed by several researchers on cells expressing fluorescent tagged keratin chimeras in order to better understand keratin network turn-over. Experiments involving the bleaching of bars perpendicular to keratin filaments estimated a recovery half life of approximately 100 ±30 min. Recovery was not uniform across the length of the bleached region with fluorescence extending out from fluorescent ends of the filament. These experiments also demonstrated that parallel filaments less than 1μm apart moved at different rates and in different directions demonstrating the complex nature of keratin filament dynamics (Yoon *et al.*, 2001). A second study looked at the recovery of keratin filaments by bleaching wedge shaped regions at the periphery of cells. These experiments revealed very limited recovery in the central regions suggesting that limited subunit exchange occurs within polymerised filaments. Fluorescent recovery took place in a sub-membranous compartment, with diffuse fluorescent material forming new filaments which then migrated into the bleached region (see Fig 6.10 B). This observation was further supported by the bleaching of an entire cell and subsequent monitoring of a single unbleached peripheral filament. Little fluorescence reduction was detected over a 70 min period suggesting very limited release of fluorescent material into the soluble pool (Windoffer *et al.*, 2004). Over a 200 min period, the filament migrated towards the centre of the cell where fluorescent levels began to decrease, suggesting a recycling of fluorescent material into the soluble fraction. A corresponding increase in the fluorescence of nearby centrally located filaments was not observed indicating that shed fluorescent subunits were not being incorporated into adjacent filaments. These observations

demonstrated that the turnover of a keratin filament does not occur by exchange of subunits along its entire length and throughout the cytoplasm but is confined to the cell cortex (Windoffer *et al.*, 2004).

6.10 FRAP analysis of GFP keratin 13 labelled filaments in SiHa cells

Analysis of keratin FRAP was complicated by several factors including the duration and mechanism of recovery, and the highly dynamic nature of networks. Recovery of fluorescently tagged keratin in SiHa cells after the bleaching of perpendicular bars in cells occurs over more than 2 hours (Fig 6.10) (see movie GFP-K13). Fluorescence recovery occurred by a number of different processes. These include the migration of diffuse non-filamentous material into the bleached region. Unbleached filaments also migrated into the bleached regions as a result of normal network dynamics. Recovery was not uniform along the length of the filaments with limited recovery appearing to occur by bleached ends growing together to reform a fluorescent filament as previously reported (Yoon *et al.*, 2001). Due to the complex mechanism of recovery, data was not analysed using the imageJ software patch software used to analyse YFP-E1^E4 recovery, as it was only able to measure the uniform recovery of a single point and would not provide useful data on complex keratin recovery. Recovery of GFP-K13 labelled keratin networks in SiHa cells occurred at a similar rate and by comparable mechanisms as has been previously described in other cell lines (Windoffer *et al.*, 2004; Yoon *et al.*, 2001). Internal keratin network architecture is also in a continual state of flux, filament connection are not stable over the 2 h period of the recoding (Fig 6.10B) (see movie GFP-K13).

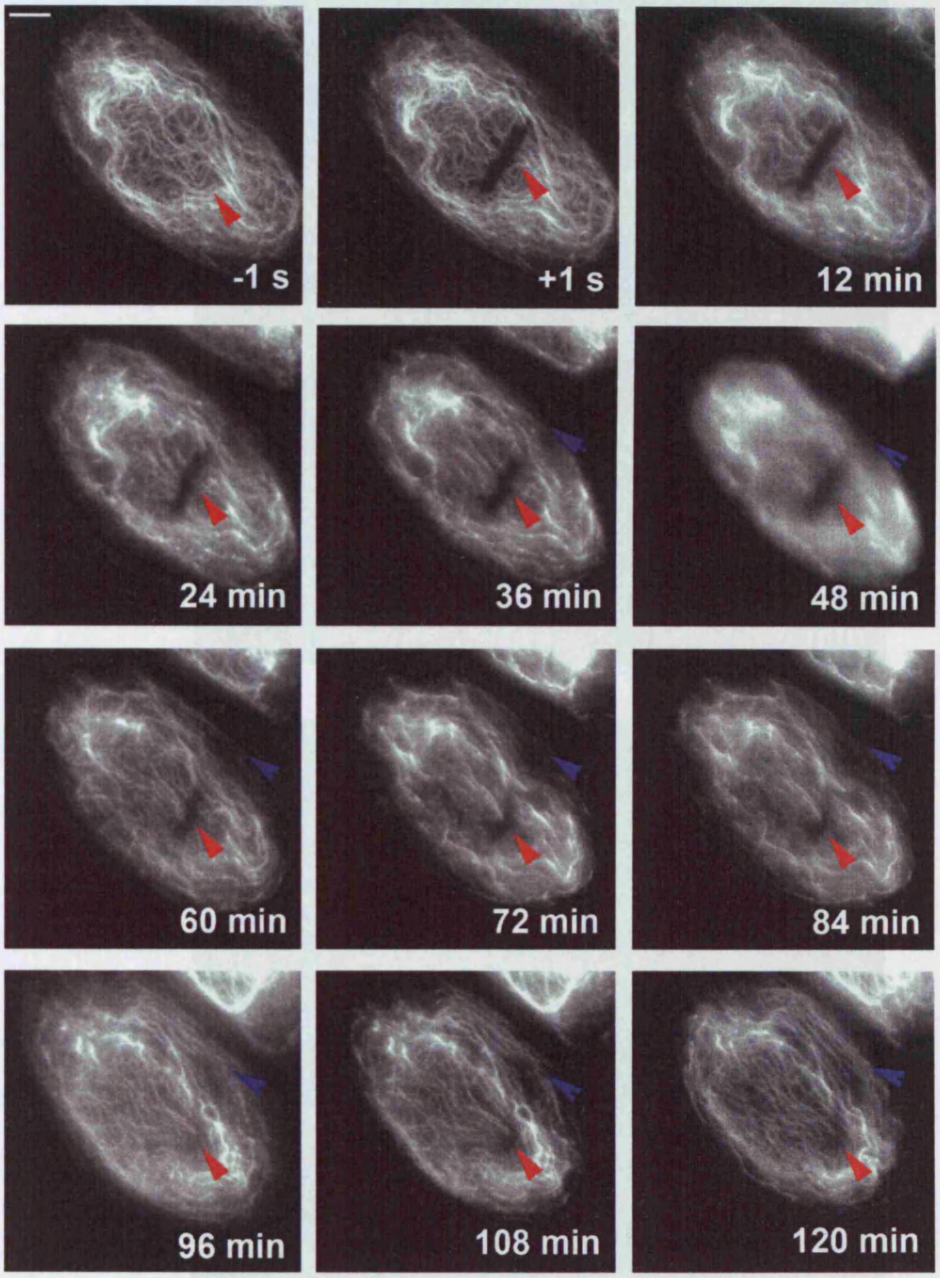

Figure 6.10A FRAP analysis of Keratin in SiHa cells
SiHa cells transfected with GFP Keratin 13 were subjected to FRAP analysis 24 h post transfection. Images were acquired (-1 s) before bars were bleached in cells (+1 s post bleach) (red arrow) using a 488 nm QLM module equipped deltavision microscope. Fluorescence recovery was recorded for two hours after bleaching. Recovery was almost completed within two hours, but was not uniform over the bleached region. Recovery primarily occurred by the migration of new fluorescent filaments into bleached regions. The ongoing processes of filament synthesis at the periphery of cells was clearly visible (blue arrow) Scale bar denotes 5 μm.

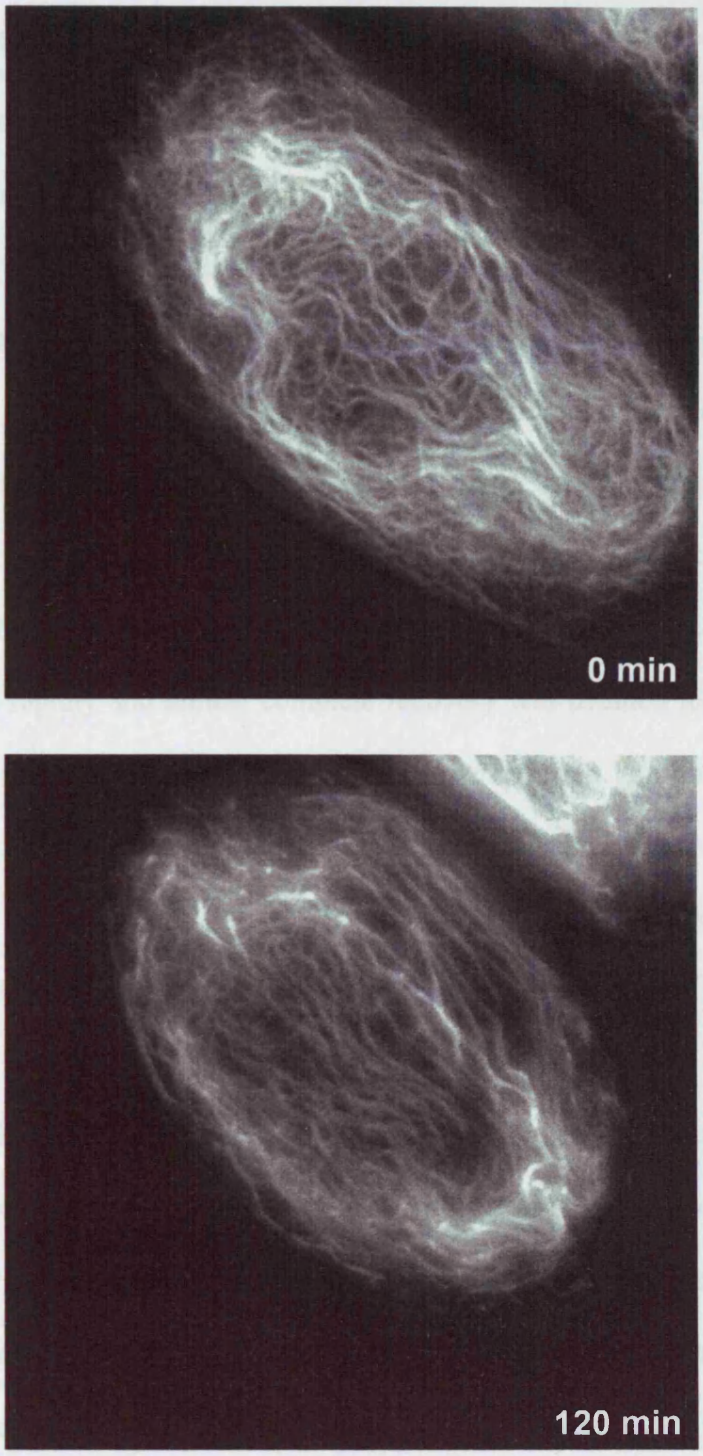

Figure 6.10B keratin filament networks are highly dynamic and in a continual state of flux

Figure shows enlarged images from figure 6.10, keratin network architecture is in a continual state of flux and no points or filament junctions are stable over a 2 h time frame.

6.10.1 FRAP analysis of YFP-E1^E4 in SiHa cells reveals rates of recovery varies in different structures

It was hoped that understanding the binding of E1^E4 to keratins would give insights into how keratin network disruption occurs. FRAP experiments were performed on cells containing both E1^E4 filaments and aggregates. Recovery of E1^E4 was not comparable to keratin in either time or mechanism. Furthermore, two separate rates of E1^E4 recovery were observed, depending on the structures studied. SiHa cells transfected with YFP-E1^E4 12 hrs prior to imaging which expressed E1^E4 with a fine filamentous pattern were selected for the first set of experiments. Bars were bleached through cells and images taken every 2 min subsequently. Fluorescence returned to the bleached regions rapidly and almost complete recovery was deemed to have occurred within approximately 30 min (N = 16) (Fig 6.11 and Fig 6.13) (see movie YFP-E1^E4.3). By monitoring fluorescence levels in unbleached regions it was possible to demonstrate that recovery was not due to new protein synthesis, as a comparable increase in fluorescence was not observed in control regions (Fig 6.13 C-D). Furthermore, unlike keratin, E1^E4 recovery appeared to be relatively uniform across the bleached region suggesting a dynamic equilibrium between the bound and soluble populations of protein (Fig 6.11 A-B). The rapid uniform recovery of fluorescence suggests that E1^E4 is able to bind, the polymerised filaments and the association is not dependent on keratin incorporation during filament formation at the cortex of the cell. Although the rates of recovery were consistent, there was a significant variation in the extent of recovery to pre-bleach levels, which ranged between 69% and 94% (Fig 6.13C and D). Fluorescence recovery occasionally involved an increase in protein synthesis during 2 experiments; a representative graph is also shown (Fig 6.13 E). This finding suggested that although a significant percentage of E1^E4 binding to keratin is transient; a second populations may be irreversibly bound, or have a significantly

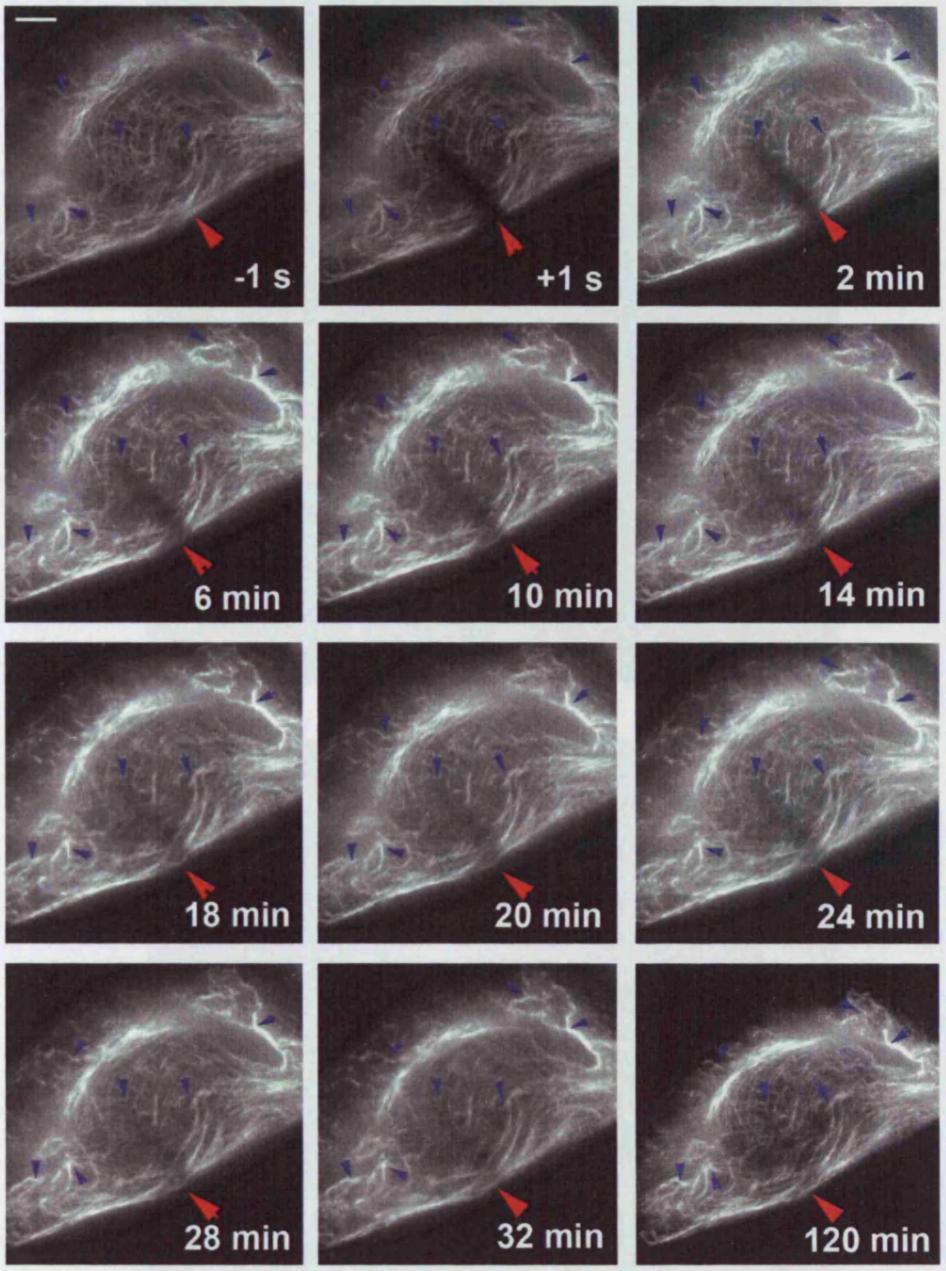

Figure 6.11A FRAP analysis of filamentous E1^E4 in SiHa cells
SiHa cells transfected with YFP-E1^E4 cell expressing filamentous E1^E4 were subjected to FRAP analysis 12 h post transfection. Images were acquired (-1 s) before bars were bleached (red arrow) in cells (+1 s post bleach) using a 488 nm QLM module equipped deltavision microscope. Fluorescence recovery occurred in 30 min with recovery occurring uniformly over the bleached region (red arrow). Filament network architecture was not observed to alter significantly over two hours and multiple individual filaments were still detectable (Blue arrows) showing increased stability of E1^E4 associated filaments. Scale bar denotes 5μm.

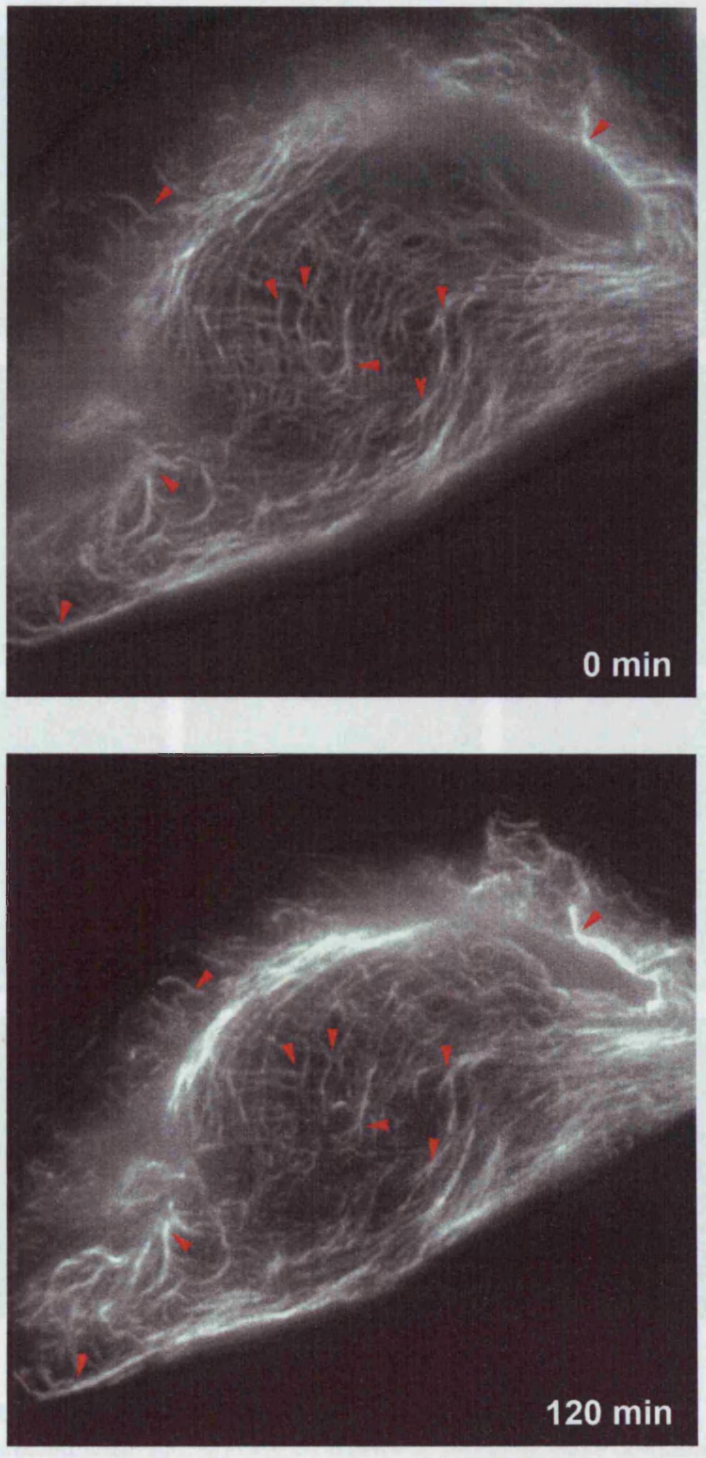

Figure 6.11B E1^E4 association to keratin stabilises keratin filament networks. Figure shows enlarged images from figure 6.11, the association of E1^E4 to the keratin network freezes network architecture over 2 h. Individual filament junctions are stable over 2 h (see arrows).

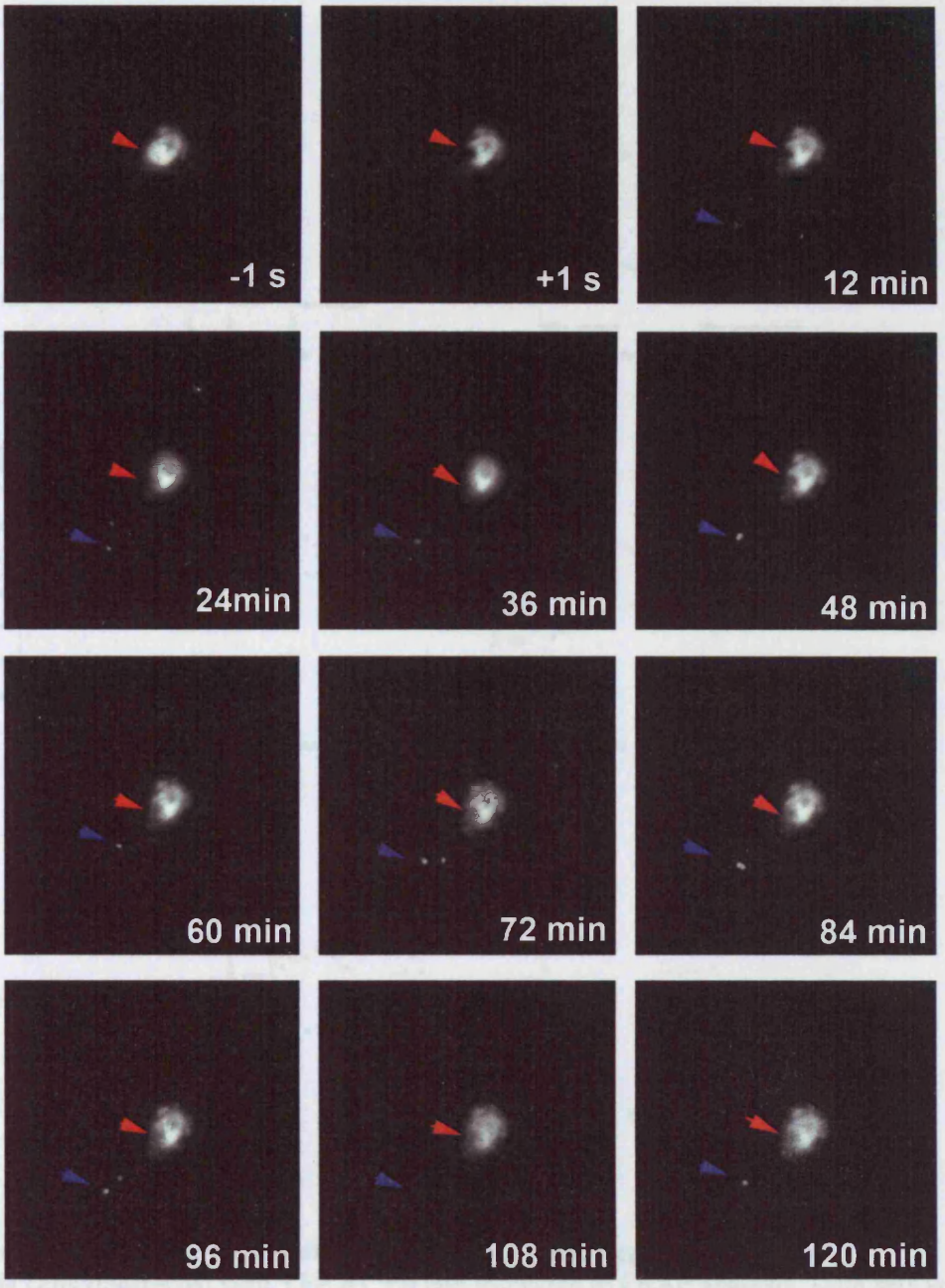

Figure 6.12 FRAP analysis of E1^E4 aggregates in SiHa cells
SiHa cells transfected with YFP-E1^E4 24 h prior to imaging, cells containing aggregates were subjected to FRAP analysis. Images were acquired (-1 s) before spots were bleached with a single laser pulse (+1 s post bleach) (red arrow) using a 488 nm QLM module equipped deltavision microscope. Only limited fluorescence recovery was observed over a 2 h period. Small E1^E4 aggregate structures were highly dynamic and were observed to under go rapid bidirectional translocation (blue arrow) scale bar denote 5 μm.

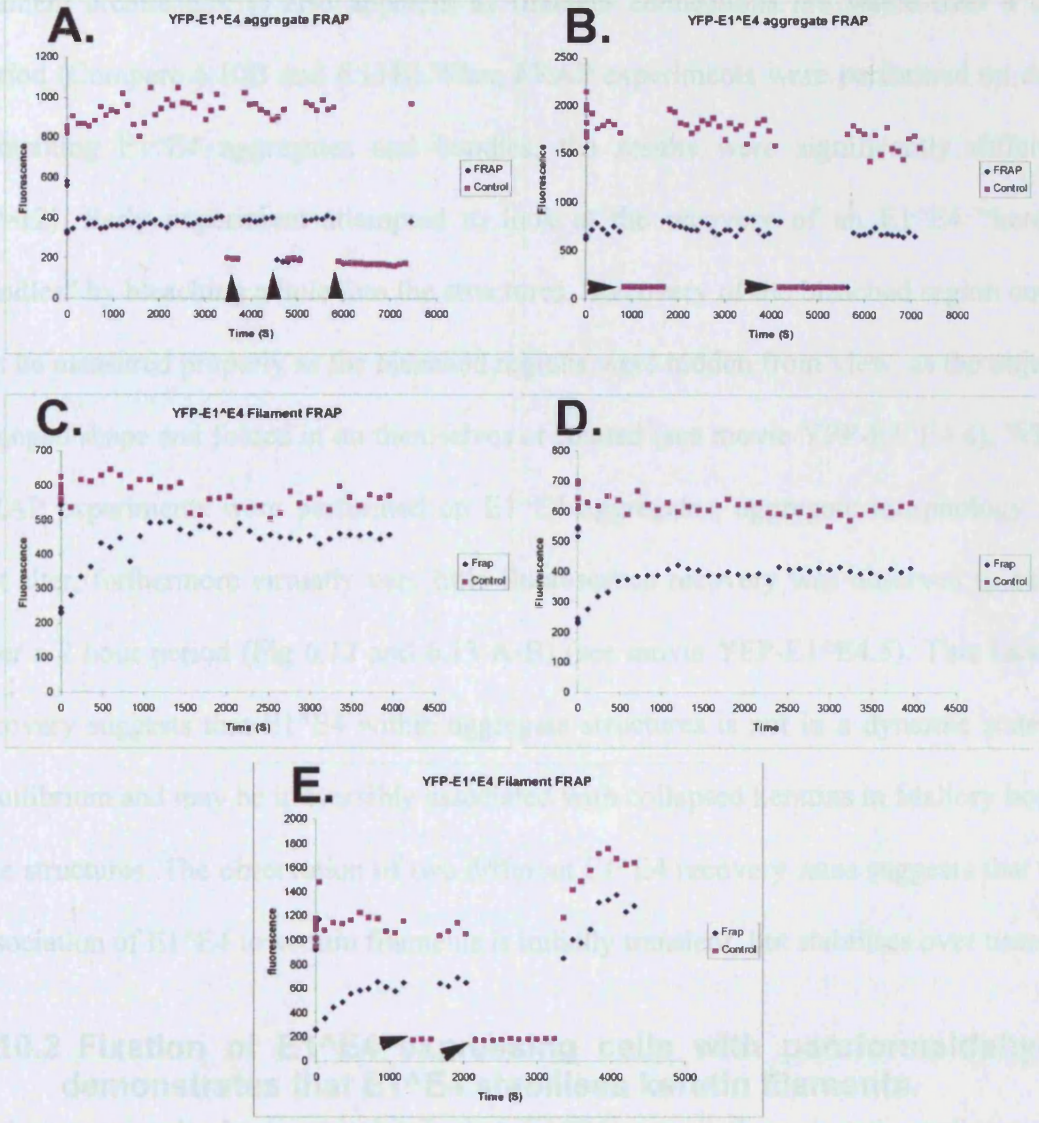

Figure 6.13 Recovery rates of E1^E4 filaments and aggregates
SiHa cells transfected with YFP E1^E4 and subjected to FRAP analysis. Data sets were analyzed in image J and revealed several different mechanisms of recovery (values denote grey scale ranging from 0-2500). E1^E4 aggregates (A-B) showed very little recovery over 2 h. Control unbleached regions (Pink) were stable over 2 h indicating that protein synthesis and photobleaching were not significantly affecting data sets. When disruption of data sets by focal drift occurred data was discarded (black arrows). Recovery analysis of filamentous E1^E4 produced smooth recovery curves that flatten out between 1500-2000 s. Unbleached control regions did not reflect recovery curves, suggesting that recovery was not due to additional protein synthesis (C-D). Significant increases in control regions (which mimicked recovery curves) were observed in some recordings suggesting protein synthesis may be involved in the fluorescence recovery during some experiments (E).

slower dissociation rate.The inhibition of internal dynamics of E1^E4 associated filament architecture is also apparent as filament connections are stable over a 2 h period (Compare 6.10B and 6.11B).When FRAP experiments were performed on cells containing E1^E4 aggregates and bundles, the results were significantly different (N=12). Early experiment attempted to look at the recovery of an E1^E4 "keratin bundles" by bleaching a hole into the structures. Recovery of the bleached region could not be measured properly as the bleached regions were hidden from view, as the objects changed shape and folded in on themselves or rotated (see movie YFP-E1^E4.4). When FRAP experiments were performed on E1^E4 aggregates, aggregate morphology did not alter, furthermore virtually very little fluorescence recovery was observed to occur over a 2 hour period (Fig 6.12 and 6.13 A-B) (see movie YFP-E1^E4.5). This lack of recovery suggests that E1^E4 within aggregate structures is not in a dynamic state of equilibrium and may be irreversibly associated with collapsed keratins in Mallory body-like structures. The observation of two different E1^E4 recovery rates suggests that the association of E1^E4 to keratin filaments is initially transient, but stabilises over time.

6.10.2 Fixation of E1^E4 expressing cells with paraformaldehyde demonstrates that E1^E4 stabilises keratin filaments.

It has previously been speculated that E1^E4 may induce keratin collapse by multimerisation or cross-linking (Wang *et al.*, 2004). Data generated in this study has shown that E1^E4 depletes the soluble pool of keratins over time (see Fig 4.16) and that keratin filament formation (but not subunit polymerisation) is inhibited, by E1^E4 (see section 6.7.2). Furthermore, FRAP analysis has demonstrated that, although E1^E4's association to keratin is initially transient, E1^E4 association appears to stabilise over time, possibly via a process of multimerisation as previously suggested (Wang *et al.*, 2004). This process may result in the stabilisation of keratin filaments. To examine this hypothesis, SiHa cells were transfected with HPV 16 E1^E4 and fixed with

paraformaldehyde, which disrupts keratin filaments (See Fig 3.3). E1^E4-associated keratin structures were found to be resistant to paraformaldehyde induced disruption, whereas no filamentous keratin could be observed in E1^E4 negative neighbouring cells (Fig 6.14). This observation supports the hypothesis that E1^E4 association stabilises keratin filaments and may lead to the contrasting methods of keratin disruption observed *in vitro* and *in vivo.*

6.11 Discussion

The YFP-E1^E4 fusion protein generated for this study was shown to behave in an identical fashion to the wild type E1^E4 protein in all respects except that it lacked the ability to associate with mitochondria. For the purpose of this study this loss of function was beneficial as it was discovered that the protein was unable to form solid structures in the absence of keratin. This finding is significant as the LLXLL motif required for keratin binding is also required for the association with mitochondria (Raj *et al.*, 2004), demonstrating that separate domains are required for mitochondrial and keratin association, or that binding occurs by a different mechanism and that the YFP-protein causes steric hindrance. Therefore, YFP-E1^E4 may be used to investigate the apoptotic properties of E1^E4 in the absence of mitochondrial association.

Initial experiments expressing YFP-E1^E4 in AK 8 cells expressing CFP keratin were abandoned due to the poor resolution of keratin filament in the cells and the high levels of phototoxicity produced by multiple exposures of high energy excitation wavelengths required to visualise CFP.

The transfection of GFP keratin 13 into SiHa cells allowed the visualisation of the keratin network, which were found to behave as previously described (Windoffer *et al.*,

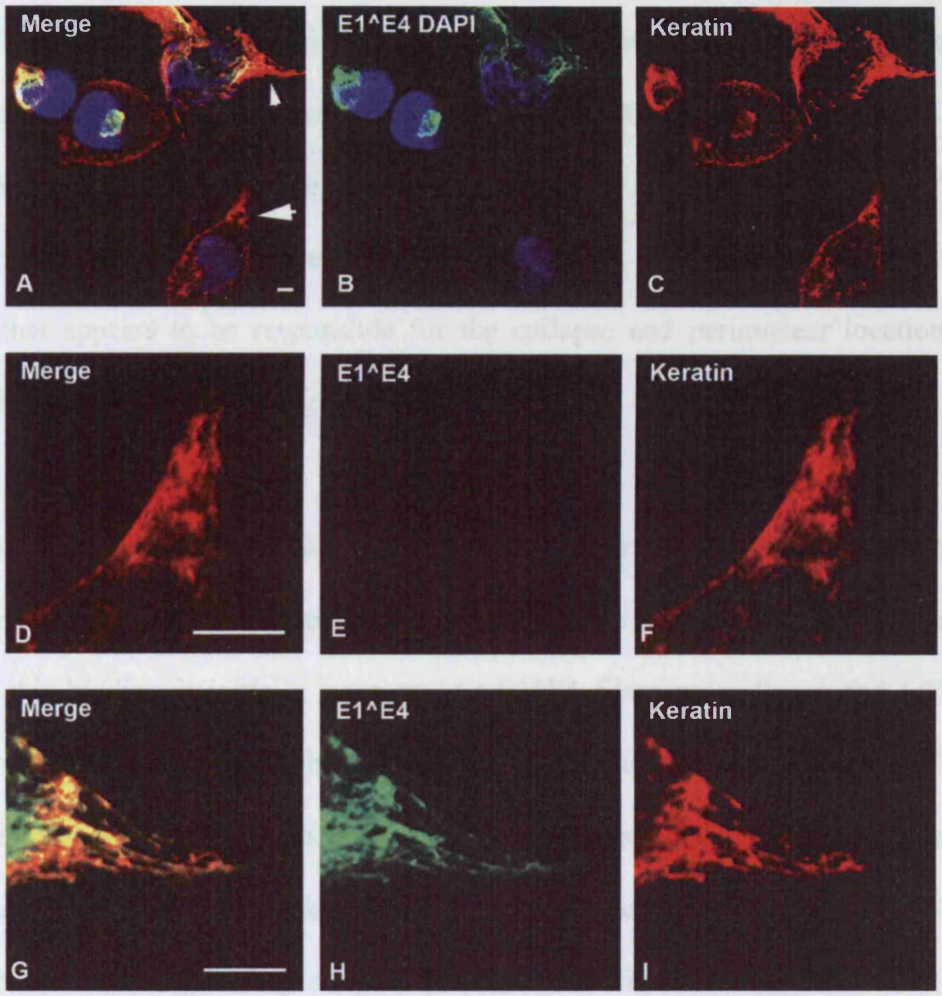

Figure 6.14 E1^E4 protects keratin filaments from paraformaldehyde mediated disruption.
SiHa cells were transfected with wild type E1^E4 and fixed with 5 % paraformaldehyde (5 min) 24 h post transfection. Paraformaldehyde fixation does not disrupt the interaction between E1^E4 and keratin in either filamentous or condensed E1^E4 structures (A-C). Higher magnifications of these cells (regions indicated by arrows A) show that no intact keratin filaments can be observed in E1^E4 negative cells (D-F, region indicated by large arrow A), conversely E1^E4 associated keratin filaments (regions indicated by small arrow A) are intact and not disrupted by paraformaldehyde (G-I). Scale bars denote 5 μm.

1999). Expression of YFP-E1^E4 in SiHa cells demonstrated that E1^E4 appears not to initially inhibit keratin polymerisation and filament formation. Despite this observation, at early time points, it would appear that keratin filament formation is disrupted at the point of keratin network collapse, for reasons that will be discussed later. E1^E4 association did not appear to directly inhibit the inward directed motion of keratin filaments that appears to be responsible for the collapse and perinuclear location of collapsed keratin filaments (see Fig 6.8 and 6.9).

FRAP experiments demonstrated that E1^E4 recovery occurs at a different rate and by a different mechanism than keratin recovery. E1^E4 is able to bind to polymerised keratin filaments; this binding is initially transient. As E1^E4 filaments collapse and E1^E4 aggregate structures form, E1^E4 binding appears to stabilise the keratin network. The percentage recovery of E1^E4 fluorescence varies, suggesting that the percentage of stably bound E1^E4 may increase at latter time points as filaments collapse. It is thought that the stable binding of E1^E4 to keratins filaments may stabilise the filaments. This hypothesis is supported by the finding that E1^E4 association is able to protect filaments against paraformaldehyde mediated disruption and by the observation that keratin filament architecture cannot be altered when it is E1^E4 bound (see Fig 6.10B and 6.11B).

From observations made in this chapter it is possible to speculate about how E1^E4 association with keratin can result in the two contrasting events seen *in vivo* and *in vitro.* Although initially transient, as E1^E4 levels build up on keratin filaments and binding stabilises (possibly by multimerisation, as previously suggested) (Wang *et al.*, 2004), it is possible that the concentration of E1^E4 on keratin filaments may nucleate

multimerisation reactions. The binding of E1^E4 stabilises the keratin filaments; which would prevent the disassembly of filaments as they migrate to the centre of the cell. Inhibition of filament disassembly would result in a depletion of the soluble keratin pool as observed in figure 4.16. As the pool is depleted no new materials are available for incorporation into new filaments (approximately 2 % of total keratin is synthesised per h (Windoffer *et al.*, 2004)), which are continually moved inwards by actin (Woll *et al.*, 2005). This inward movement causes networks to pull away from the edge of the cell and collapse. It is likely that this process puts mechanical stress on filaments, which results in their becoming phosphorylated and ubiquitinated, as observed *in vitro* (see chapter 4). The finding that keratin collapse occurs at the same rate as inward directed keratin migration, suggests that it is dependent on network dynamics, which explains why keratin filament collapse is rarely observed *in vivo*. Differentiation-dependent cross-linking and modifications that keratins undergo within tissue probably inhibits inward keratin dynamics *in vivo*. The build up of E1^E4 *in vivo* may also put stress on networks resulting in their disruption, whether this process results in keratin ubiquitination and subsequent degradation remains unclear.

7 Final Discussion

7.1 Specific functions are conserved to different degrees between divergent E1^E4 proteins

E1^E4 proteins from different HPV types are very divergent at the amino acid level, raising the question as to whether they perform a similar role in the virus life cycle and if so whether this achieved by similar modes of action. Preliminary analysis of E1^E4 proteins from several α-group HPV types (including HPV types 2, 16, 18, 31, 35 and 45), and two γ-group viruses (HPV 4 and 65), has shown that the E1^E4 proteins of all possess an ability to associate with the cell cytoskeleton. Several reports suggested that this function also extends to the E1^E4 proteins of the μ-group HPV viruses (Doorbar *et al.*, 1996; Roberts *et al.*, 1993; Rogel-Gaillard *et al.*, 1992b). Despite this conserved ability, significant differences still exist between different groups. The α-group E1^E4 proteins are able to bind and disrupt the keratin networks of cells in culture, with the HPV 16 E1^E4 protein having the ability to bind and disrupt the keratin network expressed in HaCat cells in a keratin subtype independent manner. HPV 1 E1^E4, which is a μ-group HPV type, has been reported to bind keratins transiently, without inducing collapse, before forming aggregates (Doorbar *et al.*, 1996; Roberts *et al.*, 1993). The γ-group viruses, HPV 4 and 65 were shown here to bind to microtubules when expressed in SiHa cells but have since been shown to have the capacity to associate with the differentiation-dependent keratin 4/13 networks when expressed in NIKS cells, although no network collapse was observed (personal communication, Woei Peh).

The expression profile of E1^E4 proteins in lesions may explain the differences in keratin binding observed *in vitro*. The expression of HPV 16 E1^E4 *in vivo* varies in its

timing, and can occur before or after the first appearance of the differentiation-dependent keratin 4/13 network in lesions (personal communication, John Doorbar), with reorganisation of the assembled network occurring in the E1^E4-expressing cells. It appears that the α-group E1^E4 proteins may have evolved the ability to target and disrupt the terminally differentiated keratin network after formation (which may be reinforced by covalent cross linking), which is likely to be necessary considering the late onset of E1^E4 expression in the α virus lifecycle (Middleton *et al.*, 2003; Peh *et al.*, 2002). HPV 1 E1^E4 also has the ability to bind keratin but lacks the ability to collapse or reorganise pre-existing intact networks *in vitro* (Roberts *et al.*, 1993). Interestingly HPV1 E1^E4 expression occurs much lower down in the epithelium, and the differentiation-dependent keratin 1/10 network does not establish itselves in HPV 1 E1^E4-positive cells (Breitburd *et al.*, 1987; Doorbar *et al.*, 1997). This observation may indicate that HPV1 E1^E4 expression is able to disrupt the keratin 1/10 network as it is formed (and thus inhibits network assembly), possibly by preventing the polymerisation of K1/10 subunits.

The absence of differentiation-dependent keratins has also been observed in HPV 65 lesions (personal communication, John Doorbar), in which E1^E4 expression occurs close to the basal layer. Selective targeting of differentiation-dependent keratins by HPV 65 may allow early E1^E4 expression without compromising the mechanical integrity of the cells in these layers, which are expressing K5/14 networks, that are lost anyway during differentiation. If this hypothesis is correct, it may be that E1^E4 proteins maintain the ability to disrupt keratin networks by subtly different mechanisms, depending on the region of epithelium where late events are triggered.

Although the reasons for the cytokeratin interactions have not yet been conclusively demonstrated, it is reasonable to speculate that keratin disruption may facilitate virion release, and that the protein has a role that has been conserved during evolution. Although less well understood, the association with mitochondria was observed in all α-group viruses examined, but not observed amongst the E1^E4 proteins of the γ-group viruses, suggesting that this may be a more recently evolved function. By contrast Cyclin B association (as visualised by immunofluorescence) was not even conserved across all members of the α-group viruses. In addition to this, the γ-group E1^E4 proteins were shown to associate with microtubules in the absence of differentiation-dependent keratins. Amongst the viruses examined here, this function was unique to γ-group proteins. Although its purpose is unknown, it may facilitate cell cycle arrest in the absence of a cyclin-binding domain, in order to facilitate viral genome amplification. The fact that most functions are not conserved between E1^E4 proteins from different phylogenetic groups suggests that the highly conserved ability of the E1^E4 proteins to interact with keratins may be essential for the successful completion of the papillomavirus lifecycle.

7.2 The disruption of keratins *in vivo* and *in vitro*

The ability of the HPV 16 E1^E4 proteins to disrupt keratins *in vitro* was further investigated in order to better understand the processes involved. The analysis of cells expressing keratin 4/13 networks would have been ideal for this work, but due to the limited amount of molecular information available on these networks SiHa cells expressing the better studied keratin 8/18 network were used instead.

E1^E4 has previously been reported to induce the collapse of the keratin network in SiHa cells (Wang *et al.*, 2004). This ability has also been demonstrated in HaCat cells,

which express more robust, differentiation-dependent keratins. Although the network present in HaCat cells was more resistant to network reorganisation, collapse was in fact generally observed, suggesting that 16 E1^E4 has the ability to associate with and induce collapse of, multiple types of intact keratin network. This finding suggests that the lack of apparent network collapse *in vivo* cannot simply be attributed to the presence of certain types of keratin network and indicates that other factors may be responsible for the observed differences.

Western blotting and immunofluorescence studies were able to demonstrate the presence of highly phosphorylated keratins *in vitro* following E1^E4 expression. Some evidence that phosphorylated keratins accumulate in cells expressing 16 E1^E4 was also obtained from *in vivo* studies. However, the antibodies used in the study were specific for keratins 8 and 18, and it was uncertain whether the phosphorylation of differentiation-dependent keratins also took place. 2D gel electrophoresis of HaCat cell lysates and/or tissue extracts may be able to answer these questions. Western blotting analysis of cell extracts revealed that HPV 16 E1^E4 expression induced the formation of high molecular weight keratin ladders. The use of proteasome inhibitors, IP assays and isopeptidase demonstrated that the keratin ladders were caused by the ubiquitination of keratin species. The molecular mass of the ladders (which indicated conjugation of more than 4 ubiquitin molecules), coupled with the results from experiments using proteasome inhibitors, suggested that keratins were being targeted for proteasome-mediated degradation by E1^E4. Interestingly, the accumulation of ubiquitinated keratins, also appeared to induce proteasome inhibition, which has also been reported for other protein aggresomes (Bence *et al.*, 2001; Bennett *et al.*, 2005). Although it has been speculated that proteasome inhibition may occur in the presence of keratin

aggresomes (Janig *et al.*, 2005), this has not previously been experimentally demonstrated. The effect on proteasome activity was not investigated *in vivo,* but such a function may allow the build up of viral proteins in the upper epithelial layers, and could play a role in the completion of virus life cycle. The immunofluorescence studies have also demonstrated that E1^E4 staining coincides with ectopic ubiquitin expression in HPV 2 and 16 lesions, but it was not possible to show conclusive evidence for keratin ubiquitination *in vivo*. Even so, initial experiments were able to identify the presence of a high molecular weigh ubiquitin species in extracts from lesions, and this now warrants further investigation.

7.3 The involvement of the conserved LLXLL motif in keratin disruption

Experiments using the mutant M2 16 E1^E4 protein, which lacks the highly conserved LLXLL keratin binding motif, demonstrated that although keratin binding was initially greatly reduced, the protein still maintained the ability to bind and disrupt the keratin network at later time points. Despite this ability to disrupt keratin networks, no elevation in keratin biochemical modifications was observed when compared to β-Gal control cells, even at late time points. Keratins undergo biochemical modifications during cell cycle progression (specifically increased phosphorylation (Liao *et al.*, 1995)). Therefore, it is important to distinguish keratin modifications that may occur as a result of E1^E4-induced cell cycle arrest (Davy *et al.*, 2002), from those induced by E1^E4's interaction with keratins. The work presented here suggests that keratin ubiquitination and phosphorylation are not a down-stream consequence of E1^E4-induced cell cycle arrest, but that it occurs as a result of the direct interaction between E1^E4 and keratins. Furthermore, it was noticed that the disruption of keratins by M2 E1^E4 occurred by a slightly different mechanism than was seen with the wild type protein. The percentage of M2 E1^E4 protein colocalising with keratin gradually

increased over time, and gradually damaged the networks. In contrast, wild type E1^E4 appears to associate directly with keratin networks, saturating them and inducing network collapse. These observations may suggest that the mechanism of wild type E1^E4 induced keratin disruption, which involves the highly conserved LLXLL motif, promotes the phosphorylation and ubiquitination of affected keratin. This observation may suggest that the LLXLL domain conserved though out the α-group E1^E4 proteins, may specifically disrupt keratins in a manner that promotes the proteolytic degradation of affected networks.

7.4 The timing of keratin disruption may be important for completion of the virus lifecycle.

Quantitative imaging of HPV 16 lesions showed that E1^E4 levels rise towards the surface of the tissue and that they correlate with specific events in the virus lifecycle. Relatively low levels of E1^E4 were found in MCM-positive cells, where viral genome amplification has been reported to occur (Doorbar *et al.*, 1997; Middleton *et al.*, 2003). Significantly higher E1^E4 levels were found to coincide with cells expressing the L1 capsid protein, where viral packaging is believed to occur. E1^E4 levels appeared to rise still further after the onset of L1 expression, indicating the possible activation of additional protein functions. Cells expressing very high levels of E1^E4 displayed low-level or disrupted keratin staining, and in some cases ectopic ubiquitin staining. This finding suggests that the keratin-disrupting function of E1^E4 is carefully controlled by the virus, and is only activated after viral genome amplification and packaging has occurred. This timing may be important for the successful completion of the virus lifecycle, as keratin disruption could otherwise cause the untimely shedding of affected tissue as seen in the skin blistering disease EBS (Coulombe *et al.*, 1991). The deregulation of E1^E4 induced keratin damage could lead to blistering and skin damage, and may prevent successful completion of the virus lifecycle. Interestingly

HPV 2 lesions, which express E1^E4 and L1 much lower in the tissue than is seen in HPV 16 lesions, show a slightly different pattern of E1^E4 expression. HPV 16 lesions show relativity solid regions of E1^E4 expression but only at the surface of lesions, and it may be that its role is to damage the top few cell layers in order to allow the release of mature virions. HPV2 lesions show a much more sporadic presence of E1^E4-positive cells throughout the lesion. This may weaken individual cells in order to facilitate virion release, without significantly compromising the mechanical strength of the tissue. This may be particularly important, as the damaging of tissue normally subject to mechanical stress may cause infected sites to be shed away (i.e. blisters or ulcers may form exposing the dermis which cannot harbour the virus) before the virus has completed its lifecycle.

7.5 The hypothesis of E1^E4-induced keratin filament stabilisation can help to explain the differences observed *in vivo* and *in vitro*

Data generated by time lapse analysis of YFP-labelled E1^E4 was able to provide some insight as to the mechanism of E1^E4-induced keratin disruption, and may provide a partial explanation for the different patterns of keratin disruption that are seen *in vivo* and *in vitro*. The experiments showed that E1^E4 expression did not initially inhibit the formation of keratin filaments at the cell edge, suggesting that 16 E1^E4 does not necessarily directly inhibit keratin polymerisation. Following continued E1^E4 expression, filament formation eventually ceases at the point of keratin network collapse. E1^E4-associated keratin networks collapse inwards at a rate comparable to that observed for the inward movement of GFP-labelled keratin filaments. This indicates that E1^E4 association may not necessarily disrupt the inward movement of keratin filaments, which occurs through contacts with other components of the cytoskeleton (microtubules and actin) (Woll *et al.*, 2005). FRAP experiments showed

that in cells containing GFP-keratin 13 labelled networks, fluorescence recovery of bleached regions took place over ~ 2h. The process involved new fluorescent filaments migrating into the bleached region, demonstrating that keratin subunits can only incorporate into filaments at the cell edge as previously reported (Windoffer *et al.*, 2004). E1^E4 fluorescence recovery occurred by a different mechanism showing that E1^E4 can associate with polymerised keratin filaments and is not just incorporated during filament formation. Fluorescence recovery was uniform over the bleached region, suggesting that E1^E4 association to keratin is initially transient, with complete turn over occurring in approximately 30 min. By contrast, very little recovery was observed in E1^E4 aggregates over 2 h. Although the rate of recovery of filamentous E1^E4 was very consistent, the extent to which recovery restored to pre-bleach levels varied. These observations may suggest that E1^E4 is associated with keratin in two different states. E1^E4 is predominantly bound irreversibly (or with higher binding affinity) in keratin aggregates, whereas >50% of E1^E4 appeared to be transiently bound to filamentous structures. This finding is compatible with the hypothesis that 16 E1^E4 may multimerise or polymerise on keratin filaments (Wang *et al.*, 2004) in order to cause keratin disruption towards the surface of the lesion. In undifferentiated cells, keratin networks are highly dynamic (Windoffer *et al.*, 1999), and E1^E4 associates with and stabilises keratin filaments that migrate to the centre of the cell. High affinity / multimeric E1^E4 binding may prevent keratin filaments from disassembling and returning to the soluble factions (Fig 7.1). This would result in depletion of the soluble keratin pool as was observed in keratin fractionation experiments (seen in section 4.10.5 and (Wang *et al.*, 2004)). Depletion of the soluble keratin fraction would eventually prevent the formation of new keratin filaments, causing networks to rip away from the

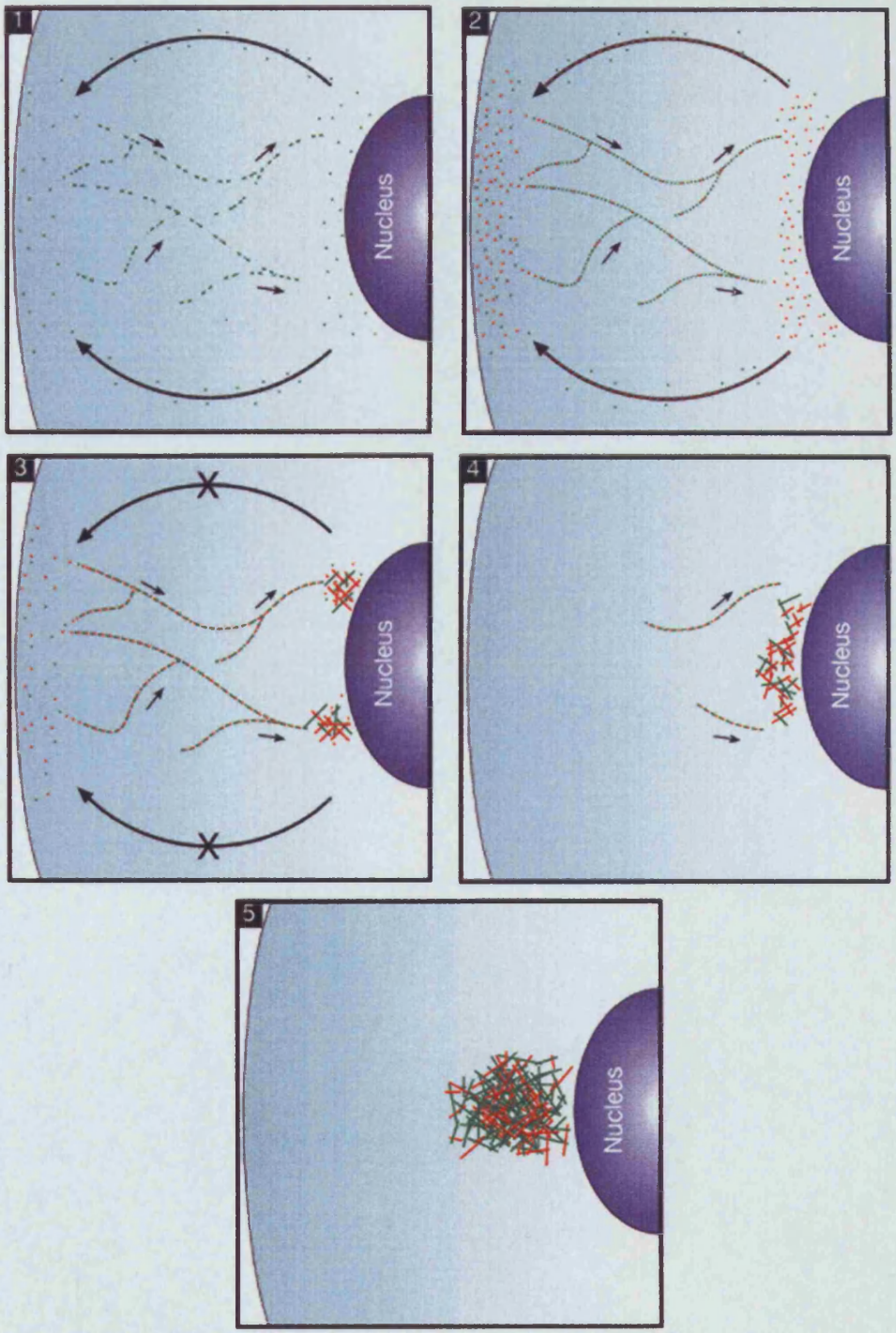

Figure 7.1 The mechanism of 16 E1^E4 induced keratin networks disruption
In a normal cell keratin tetramers (green) assemble into filaments at the cell edge, and gradually migrate towards the centre of the cells where they disassemble and are subsequently transported along microtubules back to the cell edge, where they are reincorporated into new filaments. As E1^E4 (red) levels begin to elevate, keratin binding is transient and the cycle of keratin filaments formation is not initially disrupted. As E1^E4 levels build up, binding begins to stabilise. This in turn stabilises keratin filaments which continue to migrate inwards. Stable E1^E4 binding prevents keratin filaments from disassembling at the centre of the cell depleting the soluble pool of keratin that is required for new filament formation. When the soluble pool of keratin drops below a certain threshold, new filaments cannot form. Peripheral filaments continue to migrate inwards causing them to rip away from the cell edge. Keratins end up in peri-nuclear aggregates containing E1^E4 and highly phosphorylated and ubiquitinated keratins.

edge of the cell as peripheral filaments continue to migrate inwards, leading ultimately to network collapse, as seen *in vitro* (Fig 7.1).

This hypothesis is supported by the finding that 16 E1^E4-binding protected the keratin network from paraformaldehyde-mediated disruption, which normally destroys the filamentous appearance of keratins as visualised by immunofluorescence staining. The ability of the 4 and 65 E1^E4 proteins to protect microtubules from paraformaldehyde-mediated disruption (see Fig 3.3 and 3.5) may indicate that cytoskeletal filament stabilisation is a conserved mechanism that is employed by E1^E4 proteins from evolutionary divergent viruses.

The same mechanism that is seen *in vitro* is also likely to be employed by E1^E4 *in vivo,* but due to the differentiation-dependant cross-linking modifications that reinforce keratin networks *in vivo* (e.g. filaggrin binding, disulphide bonding and transglutaminase linkage), it is likely that the networks are much less dynamic. This would explain why perinuclear keratin collapse is rarely observed *in vivo.* The observation that E1^E4 can occasionally cause perinuclear keratin reorganisation *in vivo* (Doorbar *et al.*, 1997; Wang *et al.*, 2004) may reflect the presence of poorly differentiated cells containing dynamic keratin networks. By contrast when keratin disruption observed in the upper layers of the epithelium, keratins are either undetectable suggesting that they may have been degraded, or are seen to reorganise to the cell periphery. The high affinity binding or multimerisation of E1^E4 on keratin filaments *in vivo* may put networks under mechanical stress which may damage networks and lead to their reorganisation. Reorganisation of filaments to the cell edge, as opposed to the perinuclear region, may also reflect the differentiation-dependent up-

regulation of desmosomes, which tightly anchor keratin networks to the epidermal junctions between cells (Arnemann *et al., 1993;* Presland *et al., 2002).* Expression of E1^E4 in a keratinocyte cell line such as NIKS, followed by differentiated in semi-solid methyl cellulose media, could be used to test this hypothesis.

7.6 In summary

This study has been able to demonstrate the ability of multiple E1^E4 proteins to interact with the cell cytoskeleton, and more specifically, the keratin network. This suggests a general need amongst papillomaviruses to disrupt keratin networks, which would otherwise present a barrier that hinders virion release (Dohner *et al.*, 2005; Seksek *et al.*, 1997). Keratin disruption has been observed to occur by different mechanisms (e.g. enzymatic cleavage (Chen *et al.*, 1993) and phosphorylation followed by subsequent ubiquitination (Murata *et al.*, 2002)), by other viruses infecting epithelial tissue. It is believed that the association of E1^E4 to keratin filaments may stabilise the affected filaments, possibly by E1^E4 multimerisation. *In vitro,* this results in the perinuclear collapse of the affected networks, and leads to the phosphorylation and ubiquitination of keratins. *In vivo* networks appear to reorganise to the edge of the cell and may be subsequently degraded, allowing progeny virions to be released into the environment.

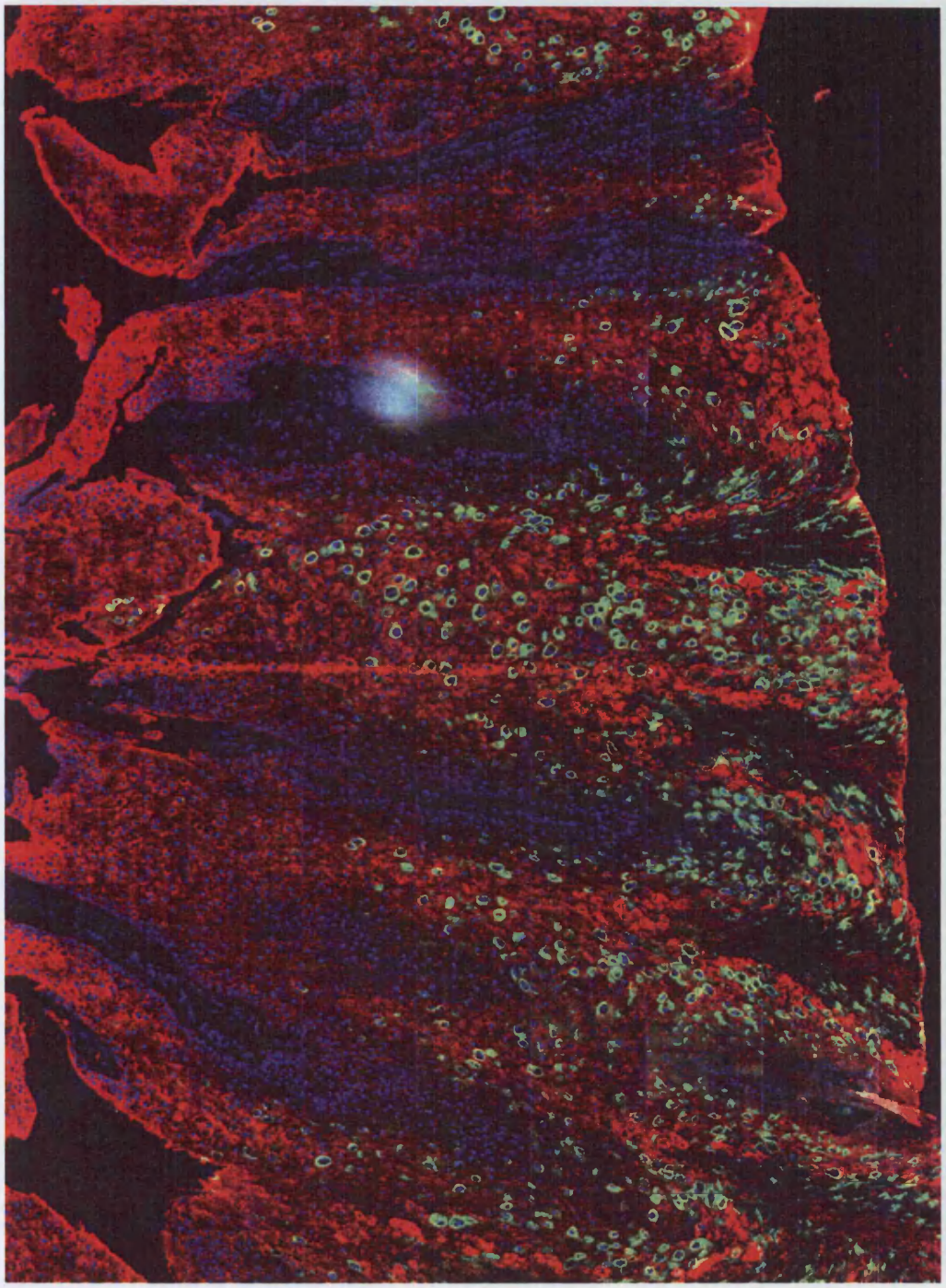

Appendix I
Image shows the HPV 2 lesion used in section 5.5, that was cut in half, half was used for biochemical analysis and the other half was section and stained. Image shows lesion stained for keratin (red), E1^E4 (green) and DNA (DAPI, Blue). The image was created by taking multiple images on a deltavision microscope using a 20 X objective lens and stitching them together to produce a composite image of the lesion.

Appendix II
Image shows the HPV 2 lesion used in section 5.5, that was cut in half, half was used for biochemical analysis and the other half was section and stained. Image shows lesion stained for Ubiquitin (red), E1^E4 (green) and DNA (Blue). The image was created by taking multiple images on a deltavision microscope using a 20 X objective lens and stitching them together to produce a composite image of the lesion.

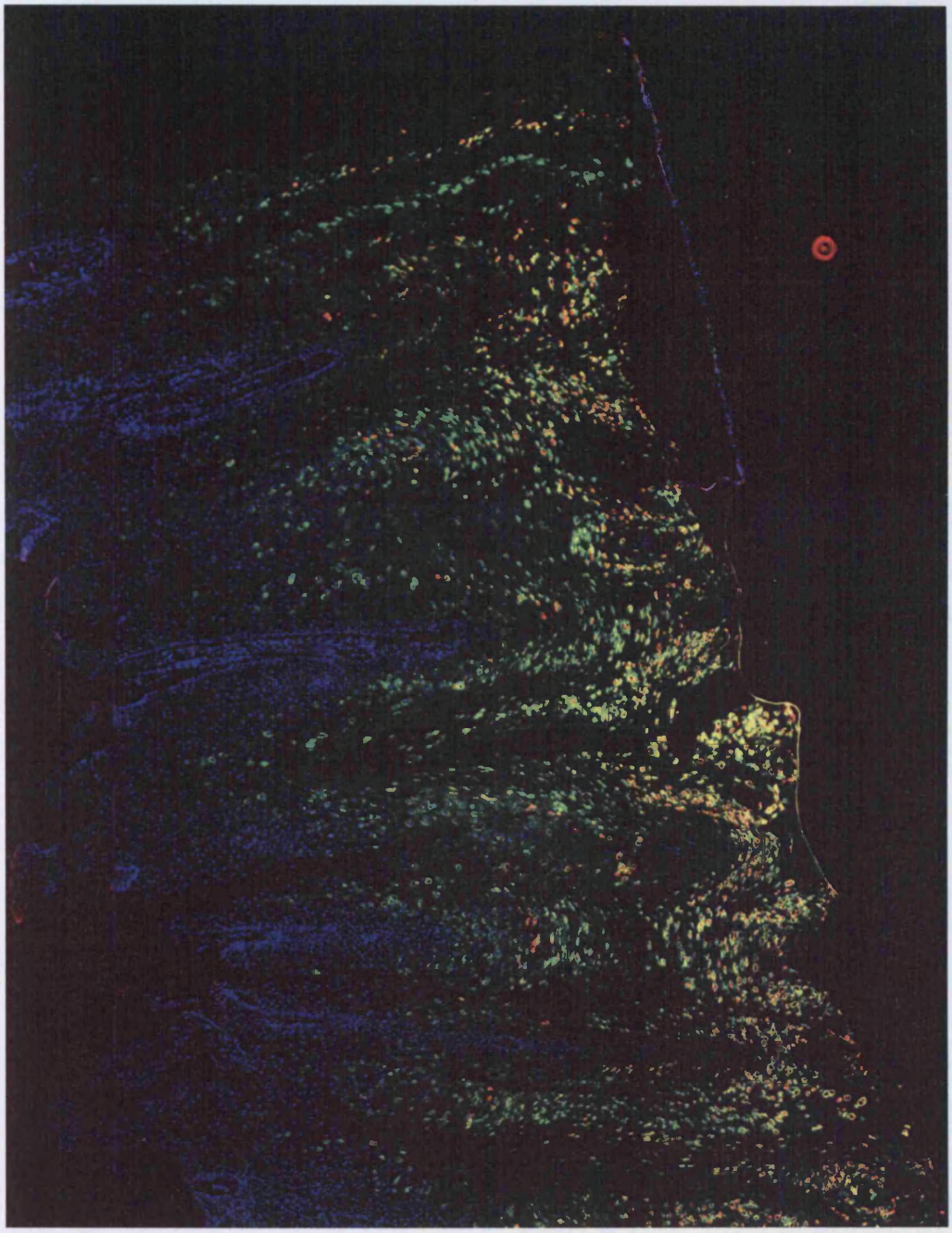

Appendix III
Image shows the HPV 2 lesion used in section 5.5, that was cut in half, half was used for biochemical analysis and the other half was section and stained. Image shows lesion stained L1 (red), E1^E4 (green) and DNA (Blue). The image was created by taking multiple images on a deltavision microscope using a 20 X objective lens and stitching them together to produce a composite image of the lesion.

pEYFP-C1 Vector Information PT3176-5

Catalog #6005-1

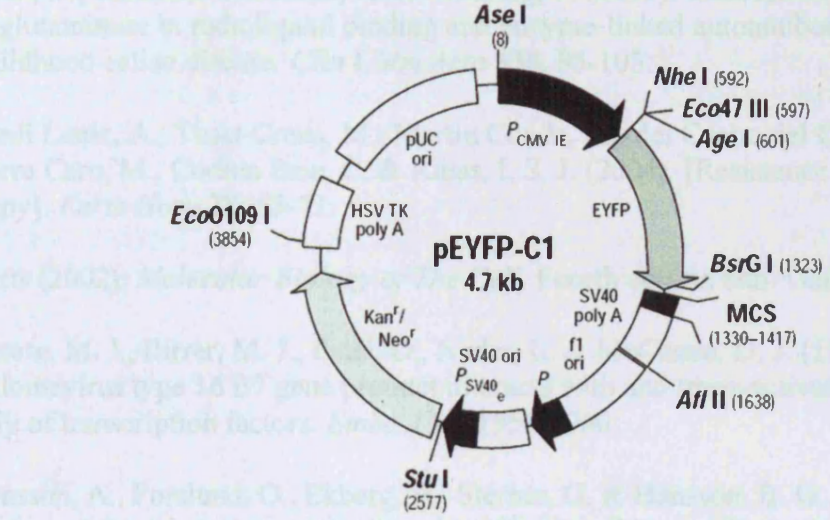

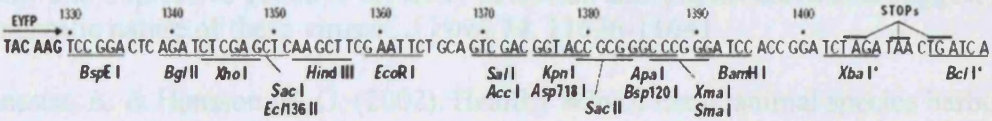

Restriction map and multiple cloning site (MCS) of pEYFP-C1. All restriction sites are shown are unique. The *Xba* I and *Bcl* I sites (*) are methylated in the DNA provided by BD Biosciences Clontech. If you wish to digest the vectors with these enzymes, you will need to transform the vector into a *dam*r host and make fresh DNA.

Appendix IIII

Plasmid map was obtained from

http://orders.clontech.com/clontech/techinfo/vectors_dis/pEYFP-C1.shtml

References

Agardh, D., Roth, B., Lernmark, A. & Stenberg, P. (2005). Calcium activation of tissue transglutaminase in radioligand binding and enzyme-linked autoantibody immunoassays in childhood celiac disease. *Clin Chim Acta* **358**, 95-103.

Alberdi Leniz, A., Tuset Creus, M., Martin Conde, M., del Cacho del Cacho, E., Nigorra Caro, M., Codina Jane, C. & Ribas, I. S. J. (2004). [Resistance to antiretroviral therapy]. *Farm Hosp* **28**, 55-71.

Alberts (2002). *Molecular Biology of The Cell*, Fourth edition edn: Garland Science.

Antinore, M. J., Birrer, M. J., Patel, D., Nader, L. & McCance, D. J. (1996). The human papillomavirus type 16 E7 gene product interacts with and trans-activates the AP1 family of transcription factors. *Embo J* **15**, 1950-1960.

Antonsson, A., Forslund, O., Ekberg, H., Sterner, G. & Hansson, B. G. (2000). The ubiquity and impressive genomic diversity of human skin papillomaviruses suggest a commensalic nature of these viruses. *J Virol* **74**, 11636-11641.

Antonsson, A. & Hansson, B. G. (2002). Healthy skin of many animal species harbors papillomaviruses which are closely related to their human counterparts. *J Virol* **76**, 12537-12542.

Arends, M. J., Buckley, C. H. & Wells, M. (1998). Aetiology, pathogenesis, and pathology of cervical neoplasia. *J Clin Pathol* **51**, 96-103.

Arnemann, J., Sullivan, K. H., Magee, A. I., King, I. A. & Buxton, R. S. (1993). Stratification-related expression of isoforms of the desmosomal cadherins in human epidermis. *J Cell Sci* **104 (Pt 3)**, 741-750.

Ashmole, I., Gallimore, P. H. & Roberts, S. (1998). Identification of conserved hydrophobic C-terminal residues of the human papillomavirus type 1 E1E4 protein necessary for E4 oligomerisation in vivo. *Virology* **240**, 221-231.

Ashrafi, G. H., Tsirimonaki, E., Marchetti, B., O'Brien, P. M., Sibbet, G. J., Andrew, L. & Campo, M. S. (2002). Down-regulation of MHC class I by bovine papillomavirus E5 oncoproteins. *Oncogene* **21**, 248-259.

Ashrafi, G. H., Haghshenas, M. R., Marchetti, B., O'Brien, P. M. & Campo, M. S. (2005). E5 protein of human papillomavirus type 16 selectively downregulates surface HLA class I. *Int J Cancer* **113**, 276-283.

Aubin, J. E., Osborn, M., Franke, W. W. & Weber, K. (1980). Intermediate filaments of the vimentin-type and the cytokeratin-type are distributed differently during mitosis. *Exp Cell Res* **129**, 149-165.

Baker, C. & Calef, C. (1996). Maps of Papillomavirus mRNA Transcripts. In *HPV website: wwwstdgenlanlgov/stdgen/virus/hpv/indexhtml*.

Baker, T. S., Newcomb, W. W., Olson, N. H., Cowsert, L. M., Olson, C. & Brown, J. C. (1991). Structures of bovine and human papillomaviruses. Analysis by cryoelectron microscopy and three-dimensional image reconstruction. *Biophys J* **60**, 1445-1456.

Band, V., Dalal, S., Delmolino, L. & Androphy, E. J. (1993). Enhanced degradation of p53 protein in HPV6 and BPV1 E6 immortalized human mammary epithelial cells. *EMBO J* **12**, 1847-1853.

Banks, L., Spence, P., Androphy, E., Hubbert, N., Matlashewski, G., Murray, A. & Crawford, L. (1987). Identification of human papillomavirus type 18 E6 polypeptide in cells derived from human cervical carcinomas. *J Gen Virol* **68**, 1351-1359.

Barboule, N., Chadebech, P., Baldin, V., Vidal, S. & Valette, A. (1997). Involvement of p21 in mitotic exit after paclitaxel treatment in MCF-7 breast adenocarcinoma cell line. *Oncogene* **15**, 2867-2875.

Bardag-Gorce, F., van Leeuwen, F. W., Nguyen, V., French, B. A., Li, J., Riley, N., McPhaul, L. W., Lue, Y. H. & French, S. W. (2002). The role of the ubiquitin-proteasome pathway in the formation of mallory bodies. *Exp Mol Pathol* **73**, 75-83.

Bardag-Gorce, F., Riley, N. E., Nan, L., Montgomery, R. O., Li, J., French, B. A., Lue, Y. H. & French, S. W. (2004). The proteasome inhibitor, PS-341, causes cytokeratin aggresome formation. *Exp Mol Pathol* **76**, 9-16.

Barksdale, S. K. & Baker, C. C. (1995). Differentiation specific alternative splicing of bovine papillomavirus late mRNAs. *JVirol* **69**, 6553-6556.

Bartolo, I., Epalanga, M., Bartolomeu, J., Fonseca, M., Mendes, A., Gama, A. & Taveira, N. (2005). High genetic diversity of human immunodeficiency virus type 1 in Angola. *AIDS Res Hum Retroviruses* **21**, 306-310.

Bastien, N. & McBride, A. A. (2000). Interaction of the papillomavirus E2 protein with mitotic chromosomes. *Virology* **270**, 124-134.

Bechtold, V., Beard, P. & Raj, K. (2003). Human papillomavirus type 16 E2 protein has no effect on transcription from episomal viral DNA. *J Virol* **77**, 2021-2028.

Bedell, M. A., Jones, K. H., Grossman, S. R. & Laimins, L. A. (1989). Identification of human papillomavirus type 18 transforming genes in immortalized and primary cells. *J Virol* **63**, 1247-1255.

Belin, M. T. & Boulanger, P. (1987). Processing of vimentin occurs during the early stages of adenovirus infection. *J Virol* **61**, 2559-2566.

Belnap, D. M., Olson, N. H., Cladel, N. M., Newcomb, W. W., Brown, J. C., Kreider, J. W., Christensen, N. D. & Baker, T. S. (1996). Conserved features in papillomavirus and polyomavirus capsids. *J Mol Biol* **259**, 249-263.

Bence, N. F., Sampat, R. M. & Kopito, R. R. (2001). Impairment of the ubiquitin-proteasome system by protein aggregation. *Science* **292**, 1552-1555.

Bennett, E. J., Bence, N. F., Jayakumar, R. & Kopito, R. R. (2005). Global impairment of the ubiquitin-proteasome system by nuclear or cytoplasmic protein aggregates precedes inclusion body formation. *Mol Cell* **17**, 351-365.

Bernard, H. U., Chan, S. Y. & Delius, H. (1994). Evolution of papillomaviruses. *Curr Top Microbiol Immunol* **186**, 33-54.

Beutner, K. R., Spruance, S. L., Hougham, A. J., Fox, T. L., Owens, M. L. & Douglas, J. M., Jr. (1998). Treatment of genital warts with an immune-response modifier (imiquimod). *J Am Acad Dermatol* **38**, 230-239.

Black, H. S. (2004). Mechanisms of pro- and antioxidation. *J Nutr* **134**, 3169S-3170S.

Bonnez, W., Rose, R. C., da Rin, C., Borkhuis, C., de Mesy Jensen, K. L. & Reichman, R. C. (1993). propogation of human papillomavirus type 11 in human xenografts using the severe combined immunodeficiency (SCID) mouse and comparison to the nude mouse model. *Virology* **197**, 455-458.

Bosma, G. C., Custer, R. P. & Bosma, M. J. (1983). A severe combined immunodeficiency mutation in the mouse. *Nature* **301**, 527-530.

Boukamp, P., Petrussevska, R. T., Breitkreutz, D., Hornung, J., Markham, A. & Fusenig, N. E. (1988). Normal keratinization in a spontaneously immortalized aneuploid human keratinocyte cell line. *J Cell Biol* **106**, 761-771.

Bousarghin, L., Hubert, P., Franzen, E., Jacobs, N., Boniver, J. & Delvenne, P. (2005). Human papillomavirus 16 virus-like particles use heparan sulfates to bind dendritic cells and colocalize with langerin in Langerhans cells. *J Gen Virol* **86**, 1297-1305.

Bouvard, V., Matlashewski, G., Gu, Z. M., Storey, A. & Banks, L. (1994). The human papillomavirus type 16 E5 gene cooperates with the E7 gene to stimulate proliferation of primary cells and increases viral gene expression. *Virology* **203**, 73-80.

Boyer, S. N., Wazer, D. E. & Band, V. (1996). E7 protein of human papilloma virus-16 induces degradation of retinoblastoma protein through the ubiquitin-proteasome pathway. *Cancer Res* **56**, 4620-4624.

Boyle, P. & Ferlay, J. (2005). Cancer incidence and mortality in Europe, 2004. *Ann Oncol* **16**, 481-488.

Brandsma, J. L., Yang, Z., Barthold, S. W. & Johnson, E. A. (1991). Use of a rapid, efficient inoculation method to induce papillomas by cottontail rabbit papillomavirus DNA shows that the E7 gene is required. *PNAS* **88**, 4816-4820.

Brandsma, J. L., Yang, Z. H., DiMaio, D., Barthold, S. W., Johnson, E. & Xiao, W. (1992). The putative E5 open reading frame of cottontail rabbit papillomavirus is dispensable for papilloma formation in domestic rabbits. *J Virol* **66**, 6204-6207.

Brandsma, J. L., Brownstein, D. G., Xiao, W. & Longley, B. J. (1995). Papilloma formation in human foreskin xenografts after inoculation of human papillomavirus type 16 DNA. *JVirol* **69**, 2716-2721.

Bravo, I. G. & Alonso, A. (2004). Mucosal hutumours invading encode four different E5 proteins whose chemistry and phylogeny correlate with malignant or benign growth. *J Virol* **78**, 13613-13626.

Breitburd, F., Croissant, O. & Orth, G. (1987). Expression of Human Papillomavirus type-1 E4 gene products in warts. In *Cancer Cells 5*, pp. 115-122. Cold Spring Harbor, New York: Cold Spring Harbor Laboratory press.

Breitburd, F., Kirnbauer, R., Hubbert, N. L., Nonnenmacher, B., Trin-Dinh-Desmarquet, C., Orth, G., Schiller, J. T. & Lowy, D. R. (1995). Immunization with viruslike particles from cottontail rabbit papillomavirus (CRPV) can protect against experimental CRPV infection. *J Virol* **69**, 3959-3963.

Breitkreutz, D., Boukamp, P., Ryle, C. M., Stark, H. J., Roop, D. R. & Fusenig, N. E. (1991). Epidermal morphogenesis and keratin expression in c-Ha-ras-transfected tumorigenic clones of the human HaCaT cell line. *Cancer Res* **51**, 4402-4409.

Breitkreutz, D., Stark, H. J., Plein, P., Baur, M. & Fusenig, N. E. (1993). Differential modulation of epidermal keratinization in immortalized (HaCaT) and tumorigenic human skin keratinocytes (HaCaT-ras) by retinoic acid and extracellular Ca2+. *Differentiation* **54**, 201-217.

Brisson, J., Morin, C., Fortier, M. & other authors (1994). Risk factors for cervical intraepithelial neoplasia: differences between low- and high-grade lesions. *Am J Epidemiol* **140**, 700-710.

Brown, D. R. & Bryan, J. T. (2000). Abnormalities of cornified cell envelopes isolated from human papillomavirus type 11-infected genital epithelium. *Virology* **271**, 65-70.

Brown, D. R., Brown, C. R. & Lehr, E. E. (2004). Intracellular expression patterns of the human papillomavirus type 59 E1/E4 protein in COS cells, keratinocytes, and genital epithelium. *Intervirology* **47**, 321-327.

Brown, M. T., McBride, K. M., Baniecki, M. L., Reich, N. C., Marriott, G. & Mangel, W. F. (2002). Actin can act as a cofactor for a viral proteinase in the cleavage of the cytoskeleton. *J Biol Chem* **277**, 46298-46303.

Brusa, G., Benvenuti, M., Mazzacurati, L. & other authors (2003). p53 loss of function enhances genomic instability and accelerates clonal evolution of murine myeloid progenitors expressing the p(210)BCR-ABL tyrosine kinase. *Haematologica* **88**, 622-630.

Bryan, J. T., Fife, K. H. & Brown, D. R. (1998). The intracellular expression pattern of the human papillomavirus type 11 E1--E4 protein correlates with its ability to self associate. *Virology* **241**, 49-60.

Bryan, J. T. & Brown, D. R. (2000a). Association of the human papillomavirus type 11 E1()E4 protein with cornified cell envelopes derived from infected genital epithelium. *Virology* **277**, 262-269.

Bryan, J. T., Han, A., Fife, K. H. & Brown, D. R. (2000b). The human papillomavirus type 11 E1E4 protein is phosphorylated in genital epithelium. *Virology* **268**, 430-439.

Bryan, J. T. & Brown, D. R. (2001). Transmission of human papillomavirus type 11 infection by desquamated cornified cells. *Virology* **281**, 35-42.

Butz, K., Ristriani, T., Hengstermann, A., Denk, C., Scheffner, M. & Hoppe-Seyler, F. (2003). siRNA targeting of the viral E6 oncogene efficiently kills human papillomavirus-positive cancer cells. *Oncogene* **22**, 5938-5945.

Cadrin, M., Anderson, N. M., Aasheim, L. H., Kawahara, H., Franks, D. J. & French, S. W. (1995). Modifications in cytokeratin and actin in cultured liver cells derived from griseofulvin-fed mice. *Lab Invest* **72**, 453-460.

Campo, M. S., Jarrett, W. F., Barron, R., O'Neil, B. W. & Smith, K. T. (1992). Association of bovine papillomavirus type 2 and bracken fern with bladder cancer in cattle. *Cancer Res* **52**, 6898-6904.

Campo, M. S., Grindlay, G. J., O'Neil, B. W., Chandrachud, L. M., McGarvie, G. M. & Jarrett, W. F. (1993). Prophylactic and therapeutic vaccination against a mucosal papillomavirus. *J Gen Virol* **74 (Pt 6)**, 945-953.

Campo, M. S. & Jarrett, W. F. (1994). Vaccination against cutaneous and mucosal papillomavirus in cattle. *Ciba Found Symp* **187**, 61-73; discussion 73-67.

Campo, M. S. (2002). Animal models of papillomavirus pathogenesis. *Virus Res* **89**, 249-261.

Caulin, C., Salvesen, G. S. & Oshima, R. G. (1997). Caspase cleavage of keratin 18 and reorganization of intermediate filaments during epithelial cell apoptosis. *J Cell Biol* **138**, 1379-1394.

Chambers, V. C. & Evans, C. A. (1959). Canine oral papillomatosis. I. Virus assay and observations on the various stages of the experimental infection. *Cancer Res* **19**, 1188-1195.

Chan, S. Y., Bernard, H. U., Ong, C. K., Chan, S. P., Hofmann, B. & Delius, H. (1992). Phylogenetic analysis of 48 papillomavirus types and 28 subtypes and variants: a showcase for the molecular evolution of DNA viruses. *J Virol* **66**, 5714-5725.

Chan, S. Y., Delius, H., Halpern, A. L. & Bernard, H. U. (1995a). Analysis of genomic sequences of 95 papillomavirus types: uniting typing, phylogeny, and taxonomy. *J Virol* **69**, 3074-3083.

Chan, S. Y., Bernard, H. U., Ratterree, M., Birkebak, T. A., Faras, A. J. & Ostrow, R. S. (1997). Genomic diversity and evolution of papillomaviruses in rhesus monkeys. *J Virol* **71**, 4938-4943.

Chan, S.-Y., Delius, H., Halpern, A. L. & Bernard, H.-U. (1995b). Analysis of genomic sequences of 95 papillomavirus types: Uniting typing, phylogeny and taxonomy. *J Virol* **69**, 3074-3083.

Charbonneau, H., Walsh, K. A., McCann, R. O., Prendergast, F. G., Cormier, M. J. & Vanaman, T. C. (1985). Amino acid sequence of the calcium-dependent photoprotein aequorin. *Biochemistry* **24**, 6762-6771.

Chellappan, S., Kraus, V. B., Kroger, B., Munger, K., Howley, P. M., Phelps, W. C. & Nevins, J. R. (1992). Adenovirus E1A, simian virus 40 tumour antigen, and human papillomavirus E7 protein share the capacity to disrupt the interaction between transcription factor E2F and the retinoblastoma gene product. *PNAS* **89**, 4549-4553.

Chen, P. H., Ornelles, D. A. & Shenk, T. (1993). The Adenovirus 13 23-kilodalton proteinase cleaves the amino-terminal head domain from cytokeratin 18 and disrupts the cytokeratin network of Hela cells. *J Virol* **67**, 3507-3514.

Cheng, S., Schmidt-Grimminger, D. C., Murant, T., Broker, T. R. & Chow, L. T. (1995). Differentiation-dependent up-regulation of the human papillomavirus E7 gene reactivates cellular DNA replication in suprabasal differentiated keratinocytes. *Genes Dev* **9**, 2335-2349.

Cho, C. W., Poo, H., Cho, Y. S. & other authors (2002). HPV E6 antisense induces apoptosis in CaSki cells via suppression of E6 splicing. *Exp Mol Med* **34**, 159-166.

Chong, J. P., Hayashi, M. K., Simon, M. N., Xu, R. M. & Stillman, B. (2000). A double-hexamer archaeal minichromosome maintenance protein is an ATP-dependent DNA helicase. *Proc Natl Acad Sci U S A* **97**, 1530-1535.

Chou, C. F. & Omary, M. B. (1993a). Mitotic arrest-associated enhancement of O-linked glycosylation and phosphorylation of human keratins 8 and 18. *J Biol Chem* **268**, 4465-4472.

Chou, C. F., Riopel, C. L., Rott, L. S. & Omary, M. B. (1993b). A significant soluble keratin fraction in 'simple' epithelial cells. Lack of an apparent phosphorylation and glycosylation role in keratin solubility. *J Cell Sci* **105 (Pt 2)**, 433-444.

Chow, L. T. & Broker, T. R. (1997). In vitro experimental systems for HPV: epithelial raft cultures for investigations of viral reproduction and pathogenesis and for genetic analyses of viral proteins and regulatory sequences. *Clin Dermatol* **15**, 217-227.

Christensen, N. D., Han, R. & Kreider, J. W. (2000). Cottontail rabbit papillomavirus (CRPV). In *Persistent viral infections*, pp. 485-502. Edited by R. Ahmed & I. Chen. Sussex, England: John Wiley & Sons Ltd.

Chudakov, D. M., Lukyanov, S. & Lukyanov, K. A. (2005). Fluorescent proteins as a toolkit for in vivo imaging. *Trends Biotechnol.*

Ciccozzi, M., Gori, C., Boros, S. & other authors (2005). Molecular diversity of HIV in Albania. *J Infect Dis* **192**, 475-479.

Ciuffo, G. (1907). Innesto positivo con filtrate di verruca vulgare. *Giornale Italiano delle malatte veneree* **42**, 12-17.

Clayson, E. T., Brando, L. V. & Compans, R. W. (1989). Release of simian virus 40 virions from epithelial cells is polarized and occurs without cell lysis. *J Virol* **63**, 2278-2288.

Cole, S. T. & Danos, O. (1987). Nucleotide sequence and comparative analysis of the human papillomavirus type 18 genome. Phylogeny of papillomaviruses and repeated structure of the E6 and E7 gene products. *J Mol Biol* **193**, 599-608.

Conrad, M., Bubb, V. J. & Schlegel, R. (1993). The human papillomavirus type 6 and 16 E5 proteins are membrane-associated proteins which associate with the 16kd pore forming protein. *JVirol* **67**, 6170-6178.

Coulombe, P. A., Kopan, R. & Fuchs, E. (1989). Expression of keratin K14 in the epidermis and hair follicle: insights into complex programs of differentiation. *J Cell Biol* **109**, 2295-2312.

Coulombe, P. A., Hutton, M. E., Letai, A., Hebert, A., Paller, A. S. & Fuchs, E. (1991). Point mutations in human keratin 14 genes of epidermolysis bullosa simplex patients: genetic and functional analyses. *Cell* **66**, 1301-1311.

Coulombe, P. A., Bousquet, O., Ma, L., Yamada, S. & Wirtz, D. (2000). The 'ins' and 'outs' of intermediate filament organization. *Trends Cell Biol* **10**, 420-428.

Coulombe, P. A. & Omary, M. B. (2002). 'Hard' and 'soft' principles defining the structure, function and regulation of keratin intermediate filaments. *Curr Opin Cell Biol* **14**, 110-122.

Cripe, T. P., Haugen, T. H., Turk, J. P., Tabatabai, F., Schmid, P., Durst, M., Gissman, L., Roman, A. & Turek, L. P. (1987). Transcriptional regulation of the human papillomavirus 16 E6-E7 promoter by a keratinocyte dependent enhancer, and by viral E2 trans-activator and repressor gene products; implications for cervical carcinogenesis. *EMBO J* **6**, 3745-3753.

Crook, T., Tidy, J. A. & Vousden, K. H. (1991). Degradation of p53 can be targeted by HPV E6 sequences distinct from those required for p53 binding and transactivation. *Cell* **67**, 547-556.

Culp, T. D. & Christensen, N. D. (2004). Kinetics of in vitro adsorption and entry of papillomavirus virions. *Virology* **319**, 152-161.

Culp, T. D., Budgeon, L. R. & Christensen, N. D. (2006). Human papillomaviruses bind a basal extracellular matrix component secreted by keratinocytes which is distinct from a membrane-associated receptor. *Virology* **347**, 147-159.

Dahlmann, B. (2005). Proteasomes. *Essays Biochem* **41**, 31-48.

Daling, J. R., Sherman, K. J., Hislop, T. G., Maden, C., Mandelson, M. T., Beckman, A. M. & Weiss, N. S. (1992). Cigarette-smoking and the risk of anogenital cancer. *Am J Epidemiol* **135**, 180-189.

Danos, O., Georges, E., Orth, G. & Yaniv, M. (1985). Fine structure of the cottontail rabbit papillomavirus mRNAs expressed in the transplantable VX2 carcinoma. *J Virol* **53**, 735-741.

Das, P. (2005).Pending thesis.

Davy, C., Raj, K., Masterson, P., Millar, J., Jackson, D., Zumbach, K., Cuthill, S. & Doorbar, J. (2000).The E1^E4 protein of HPV16 causes human keratinocytes and *S.pombe* to arrest at G2 with redistribution of cyclin B and p34cdc2 to the insoluble fraction. In *18th International Papillomavirus Conference*. Barcelona, Spain.

Davy, C. E., Jackson, D. J., Wang, Q. & other authors (2002). Identification of a G(2) arrest domain in the E1 wedge E4 protein of human papillomavirus type 16. *J Virol* **76**, 9806-9818.

Davy, C. E., Jackson, D. J., Raj, K. & other authors (2005). Human papillomavirus type 16 E1 E4-induced G2 arrest is associated with cytoplasmic retention of active Cdk1/cyclin B1 complexes. *J Virol* **79**, 3998-4011.

Day, P. M., Roden, R. B. S., Lowy, D. R. & Schiller, J. T. (1998). The papillomavirus minor capsid protein, L2, induces localization of the major capsid protein, L1, and the viral transcription/replication protein, E2, to PML oncogenic domains. *J Virol* **72**, 142-150.

Day, P. M., Lowy, D. R. & Schiller, J. T. (2003). Papillomaviruses infect cells via a clathrin-dependent pathway. *Virology* **307**, 1-11.

De Geest, K., Turyk, M. E., Hosken, M. I., Hudson, J. B., Laimins, L. A. & Wilbanks, G. D. (1993). Growth and differentiation of human papillomavirus type 31b positive human cervical cell lines. *Gynecol Oncol* **49**, 303-310.

de Villiers, E. M., Fauquet, C., Broker, T. R., Bernard, H. U. & zur Hausen, H. (2004). Classification of papillomaviruses. *Virology* **324**, 17-27.

DiMaio, D., Guralski, D. & Schiller, J. T. (1986). Translation of open reading frame E5 of bovine papillomavirus is required for its transforming activity. *Proc Natl Acad Sci U S A* **83**, 1797-1801.

DiMaio, D. & Mattoon, D. (2001). Mechanisms of cell transformation by papillomavirus E5 proteins. *Oncogene* **20**, 7866-7873.

Disbrow, G. L., Hanover, J. A. & Schlegel, R. (2005). Endoplasmic reticulum-localized human papillomavirus type 16 E5 protein alters endosomal pH but not trans-Golgi pH. *J Virol* **79**, 5839-5846.

Dohner, K. & Sodeik, B. (2005). The role of the cytoskeleton during viral infection. *Curr Top Microbiol Immunol* **285**, 67-108.

Dollard, S. C., Wilson, J. L., Demeter, L. M., Bonnez, W., Reichman, R. C., Broker, T. R. & Chow, L. T. (1992). Production of human papillomavirus and modulation of the infectious program in epithelial raft culture. *Genes and Development* **6**, 1131-1142.

Dong, X. P. & Pfister, H. (1999). Overlapping YY1- and aberrant SP1-binding sites proximal to the early promoter of human papillomavirus type 16. *J Gen Virol* **80 (Pt 8)**, 2097-2101.

Doorbar, J. & Gallimore, P. H. (1987). Identification of proteins encoded by the L1 and L2 open reading frames of human papillomavirus type 1a. *JVirol* **61**, 2793-2799.

Doorbar, J., Evans, H. S., Coneron, I., Crawford, L. V. & Gallimore, P. H. (1988a). Analysis of HPV1 E4 gene expression using epitope-defined antibodies. *EMBO J* 7, 825-833.

Doorbar, J., Evans, H. S., Coneron, I., Crawford, L. V. & Gallimore, P. H. (1988b). Analysis of HPV-1 E4 gene expression using epitope-defined antibodies. *Embo J* 7, 825-833.

Doorbar, J., Parton, A., Hartley, K., Banks, L., Crook, T., Stanley, M. & Crawford, L. (1990a). Detection of novel splicing patterns in a HPV 16-containing keratinocyte cell line. *Virology* **178**, 254-262.

Doorbar, J., Parton, A., Hartley, K., Banks, L., Crook, T., Stanley, M. & Crawford, L. (1990b). Detection of novel splicing patterns in a HPV16-containing keratinocyte cell line. *Virology* **178**, 254-262.

Doorbar, J. (1991). An emerging function for E4. *Papillomavirus Report* **2**, 145-148.

Doorbar, J., Ely, S., Sterling, J., McLean, C. & Crawford, L. (1991). Specific interaction between HPV-16 E1-E4 and cytokeratins results in collapse of the epithelial cell intermediate filament network. *Nature* **352**, 824-827.

Doorbar, J., Ely, S., Coleman, N., Hibma, M., Davies, D. H. & Crawford, L. (1992). Epitope-mapped monoclonal antibodies against the HPV16E1--E4 protein. *Virology* **187**, 353-359.

Doorbar, J. (1996). The E4 proteins and their role in the viral life cycle. In *Papillomavirus Reviews: Current Research on Papillomaviruses*, pp. 31-38. Edited by C. Lacey. Leeds: Leeds Medical Information, Leeds University Press.

Doorbar, J., Medcalf, E. & Napthine, S. (1996). Analysis of HPV1 E4 complexes and their association with keratins in vivo. *Virology* **218**, 114-126.

Doorbar, J., Foo, C., Coleman, N. & other authors (1997). Characterization of events during the late stages of HPV16 infection in vivo using high-affinity synthetic Fabs to E4. *Virology* **238**, 40-52.

Doorbar, J., Elston, R., Napthine, S. & other authors (2000). The E1^E4 protein of human papillomavirus type 16 associates with a putative RNA helicase through sequences in its C terminus. *J Virol* **74**, 10081-10095.

Doorbar, J. (2005). The papillomavirus life cycle. *J Clin Virol* **32 Suppl 1**, S7-15.

Doorbar, J. & Cubie, H. (2005). Molecular basis for advances in cervical screening. *Mol Diagn* **9**, 129-142.

Doorbar, J. (2006). Molecular biology of human papillomavirus infection and cervical cancer. *Clin Sci (Lond)* **110**, 525-541.

Dray, M., Russell, P., Dalrymple, C., Wallman, N., Angus, G., Leong, A., Carter, J. & Cheerala, B. (2005). p16(INK4a) as a complementary marker of high-grade intraepithelial lesions of the uterine cervix. I: Experience with squamous lesions in 189 consecutive cervical biopsies. *Pathology* **37**, 112-124.

Drobni, P., Naslund, J. & Evander, M. (2004). Lactoferrin inhibits human papillomavirus binding and uptake in vitro. *Antiviral Res* **64**, 63-68.

Dunne, E. F., Karem, K. L., Sternberg, M. R., Stone, K. M., Unger, E. R., Reeves, W. C. & Markowitz, L. E. (2005). Seroprevalence of human papillomavirus type 16 in children. *J Infect Dis* **191**, 1817-1819.

Dyson, N., Howley, P. M., Munger, K. & Harlow, E. (1989). The human papilloma virus-16 E7 oncoprotein is able to bind to the retinoblastoma gene product. *Science* **243**, 934-937.

Dyson, N. (1998). The regulation of E2F by pRB-family proteins. *Genes Dev* **12**, 2245-2262.

Eckert, B. S. & Yeagle, P. L. (1988). Acrylamide treatment of PtK1 cells causes dephosphorylation of keratin polypeptides. *Cell Motil Cytoskeleton* **11**, 24-30.

Egawa, K. (2003). Do human papillomaviruses target epidermal stem cells? *Dermatology* **207**, 251-254.

Enemark, E. J., Chen, G., Vaughn, D. E., Stenlund, A. & Joshua-Tor, L. (2000). Crystal structure of the DNA binding domain of the replication initiation protein E1 from papillomavirus. *Mol Cell* **6**, 149-158.

Evander, M., Frazer, I. H., Payne, E., Mei Qi, Y., Hengst, K. & McMillan, N. A. J. (1997). Identification of the alpha 6 integrin as a candidate receptor for papillomaviruses. *J Virol* **71**, 2449-2456.

Fausther, M., Villeneuve, L. & Cadrin, M. (2004). Heat shock protein 70 expression, keratin phosphorylation and Mallory body formation in hepatocytes from griseofulvin-intoxicated mice. *Comp Hepatol* **3**, 5.

Favre, M., Orth, G., Majewski, S., Baloul, S., Pura, A. & Jablonska, S. (1998). Psoriasis: A possible reservoir for human papillomavirus type 5, the virus associated with skin carcinomas of epidermodysplasia verruciformis. *J Invest Dermatol* **110**, 311-317.

Fay, A., Yutzy, W. H. t., Roden, R. B. & Moroianu, J. (2004). The positively charged termini of L2 minor capsid protein required for bovine papillomavirus infection function separately in nuclear import and DNA binding. *J Virol* **78**, 13447-13454.

Fehrmann, F., Klumpp, D. J. & Laimins, L. A. (2003). Human papillomavirus type 31 E5 protein supports cell cycle progression and activates late viral functions upon epithelial differentiation. *J Virol* **77**, 2819-2831.

Ferlay, J., Bray, F., Pisani, P. & Parkin, D. M. (2001). *GLOBOCAN 2000: Cancer Incidence, Mortality and Prevalence Worldwide, Version 1.0.* Lyon: IARC CancerBase, Lyon, IARCPress,.

Ferran, M. C. & McBride, A. A. (1998). Transient viral DNA replication and repression of viral transcription are supported by the C-terminal domain of the bovine papillomavirus type 1 E1 protein. *J Virol* **72**, 796-801.

Ferreira, P., Oliveira, M. J., Beraldi, E. & other authors (2005). Loss of functional E-cadherin renders cells more resistant to the apoptotic agent taxol in vitro. *Exp Cell Res* **310**, 99-104.

Fields (2001). *Virology.*

Fischetti, V. A. (2005). Bacteriophage lytic enzymes: novel anti-infectives. *Trends Microbiol* **13**, 491-496.

Flores, E. R., Allen-Hoffmann, B. L., Lee, D., Sattler, C. A. & Lambert, P. F. (1999). Establishment of the human papillomavirus type 16 (HPV-16) life cycle in an immortalized human foreskin keratinocyte cell line. *Virology* **262**, 344-354.

Flores, E. R., Allen-Hoffmann, B. L., Lee, D. & Lambert, P. F. (2000). The Human Papillomavirus Type 16 E7 Oncogene Is Required for the Productive Stage of the Viral Life Cycle. *J Virol* **15**, 6622-6631.

Florin, L., Sapp, C., Streeck, R. E. & Sapp, M. (2002). Assembly and Translocation of Papillomavirus Capsid Proteins. *Journal of Virology* **76**, 10009-10014.

Frattini, M. G. & Laimins, L. A. (1994). Binding of the human papillomavirus E1 origin recognition protein is regulated through complex formation with the E2 enhancer-binding protein. *PNAS* **91**, 12398-12402.

Freeman, A., Morris, L. S., Mills, A. D., Stoeber, K., Laskey, R. A., Williams, G. H. & Coleman, N. (1999). Minichromosome maintenance proteins as biological markers of dysplasia and malignancy. *Clin Cancer Res* **5**, 2121-2132.

Frega, A., Cenci, M., Stentella, P., Cipriano, L., De Ioris, A., Alderisio, M. & Vecchione, A. (2003). Human papillomavirus in virgins and behaviour at risk. *Cancer Lett* **194**, 21-24.

Fuche, E. & Byrne, C. (1994). The epidermis: rising to the surface. *Current Opinion in Genetics and Development* **4**, 725-736.

Fuchs, E. (1994). Intermediate filaments and disease: mutations that cripple cell strength. *J Cell Biol* **125**, 511-516.

Funk, J. O., Waga, S., Harry, J. B., Espling, E., Stillman, B. & Galloway, D. A. (1997). Inhibition of CDK activity and PCNA-dependent DNA replication by p21 is blocked by interaction with the HPV16 E7 oncoprotein. *Genes and Development* **11**, 2090-2100.

Gage, J. R., Meyers, C. & Wettstein, F. O. (1990). The E7 proteins of the nononcogenic human papillomavirus type 6b (HPV-6b) and of the oncogenic HPV-16 differ in retinoblastoma protein binding and other properties. *J Virol* **64**, 723-730.

Garcia-Vallve, S., Alonso, A. & Bravo, I. G. (2005). Papillomaviruses: different genes have different histories. *Trends Microbiol* **13**, 514-521.

Gardiol, D., Kuhne, C., Glaunsinger, B., Lee, S. S., Javier, R. & Banks, L. (1999). Oncogenic human papillomavirus E6 proteins target the discs large tumour suppressor for proteasome-mediated degradation. *Oncogene* **18**, 5487-5496.

Garnett, G. P. & Waddell, H. C. (2000). Public health paradoxes and the epidemiological impact of an HPV vaccine. *J Clin Virol* **19**, 101-111.

Garrod, D. R. (2004). Intercellular junctions in normal epidermis. *Exp Dermatol* **13**, 652-653.

Geisen, G. & Khan, T. (1996). Promoter activity of sequences located upstream of the human papillomavirus type 16 and type 18 late regions. *J Gen Virol* **77**, 2193-2200.

Genther, S. M., Sterling, S., Duensing, S., Munger, K., Sattler, C. & Lambert, P. F. (2003). Quantitative role of the human papillomavirus type 16 E5 gene during the productive stage of the viral life cycle. *Journal of Virology* **77**, 2832-2842.

Gilmartin, M. E., Culbertson, V. B. & Freedberg, I. M. (1980). Phosphorylation of epidermal keratins. *J Invest Dermatol* **75**, 211-216.

Giri, I. & Yaniv, M. (1988). Structural and mutational analysis of E2 trans-activating proteins of papillomaviruses reveals three distinct functional domains. *EMBO Journal* **7**, 2823-2829.

Giroglou, T., Florin, L., Schafer, F., Streeck, R. E. & Sapp, M. (2001a). Human papillomavirus infection requires cell surface heparan sulfate. *J Virol* **75**, 1565-1570.

Giroglou, T., Sapp, M., Lane, C., Fligge, C., Christensen, N. D., Streeck, R. E. & Rose, R. C. (2001b). Immunological analyses of human papillomavirus capsids. *Vaccine* **19**, 1783-1793.

Gomez-Lorenzo, M. G., Valle, M., Frank, J., Gruss, C., Sorzano, C. O., Chen, X. S., Donate, L. E. & Carazo, J. M. (2003). Large T antigen on the simian virus 40 origin of replication: a 3D snapshot prior to DNA replication. *Embo J* **22**, 6205-6213.

Goodwin, E. C. & DiMaio, D. (2000). Repression of human papillomavirus oncogenes in HeLa cervical carcinoma cells causes the orderly reactivation of dormant tumor suppressor pathways. *Proc Natl Acad Sci U S A* **97**, 12513-12518.

Grand, R. J. A., Doorbar, J., Smith, K. J., Coneron, I. & Gallimore, P. H. (1989). Phosphorylation of the human papillomavirus type 1 E4 proteins *in vivo* and *in vitro*. *Virology* **170**, 201-213.

Griffin, H., Elston, R., Jackson, D., Ansell, K., Coleman, M., Winter, G. & Doorbar, J. (2006). Inhibition of papillomavirus protein function in cervical cancer cells by intrabody targeting. *J Mol Biol* **355**, 360-378.

Gu, Z. & Matlashewski, G. (1995). Effect of human papillomavirus type 16 oncogenes on MAP kinase activity. *J Virol* **69**, 8051-8056.

Ham, J., Dostatni, N., Arnos, F. & Yaniv, M. (1991). Several different upstream promoter elements can potentiate transactivation by the BPV-1 E2 protein. *EMBO Journal* **10**, 2931-2940.

Hamilton, E. H., Payne, R. E., Jr. & O'Keefe, E. J. (1991). Trichohyalin: presence in the granular layer and stratum corneum of normal human epidermis. *J Invest Dermatol* **96**, 666-672.

Handley, J. M., Maw, R. D., Bingham, E. A., Horner, T., Bharucha, H., Swann, A., Lawther, H. & Dinsmore, W. W. (1993). Anogenital warts in children. *Clin Exp Dermatol* **18**, 241-247.

Harper, D. M., Franco, E. L., Wheeler, C. M. & other authors (2006). Sustained efficacy up to 4.5 years of a bivalent L1 virus-like particle vaccine against human papillomavirus types 16 and 18: follow-up from a randomised control trial. *Lancet* **367**, 1247-1255.

Harwood, C. A., Perrett, C. M., Brown, V. L., Leigh, I. M., McGregor, J. M. & Proby, C. M. (2005). Imiquimod cream 5% for recalcitrant cutaneous warts in immunosuppressed individuals. *Br J Dermatol* **152**, 122-129.

Hawley-Nelson, P., Vousden, K. H., Hubbert, N. L., Lowy, D. R. & Schiller, J. T. (1989). HPV16 E6 and E7 proteins cooperate to immortalize human foreskin keratinocytes. *Embo J* **8**, 3905-3910.

Heck, D. V., Yee, C. L., Howley, P. M. & Munger, K. (1992). Efficiency of binding the retinoblastoma protein correlates with the transforming capacity of the E7 oncoproteins of the human papillomaviruses. *Proc Natl Acad Sci U S A* **89**, 4442-4446.

Hedberg, K. K. & Chen, L. B. (1986). Absence of intermediate filaments in a human adrenal cortex carcinoma-derived cell line. *Exp Cell Res* **163**, 509-517.

Herwig, S. & Strauss, M. (1997). The retinoblastoma protein: a master regulator of cell cycle, differentiation and apoptosis. *Eur J Biochem* **246**, 581-601.

Hicke, L. (2001). Protein regulation by monoubiquitin. *Nat Rev Mol Cell Biol* **2**, 195-201.

Higgins, G. D., Uzelin, D. M., Phillips, G. E., McEvoy, P., Marin, R. & Burrell, C. J. (1992). Transcription patterns of human papillomavirus type 16 in genital intraepithelial neoplasia: evidence for promoter usage within the E7 open reading frame during epithelial differentiation. *J Gen Virol* **73 (Pt 8)**, 2047-2057.

Hirohashi, S. (1998). Inactivation of the E-cadherin-mediated cell adhesion system in human cancers. *Am J Pathol* **153**, 333-339.

Ho, L., Chan, S. Y., Burk, R. D. & other authors (1993). The genetic drift of human papillomavirus type 16 is a means of reconstructing prehistoric viral spread and the movement of ancient human populations. *J Virol* **67**, 6413-6423.

Hofseth, L. J., Hussain, S. P. & Harris, C. C. (2004). p53: 25 years after its discovery. *Trends Pharmacol Sci* **25**, 177-181.

Holmgren, S. C., Patterson, N. A., Ozbun, M. A. & Lambert, P. F. (2005). The minor capsid protein L2 contributes to two steps in the human papillomavirus type 31 life cycle. *J Virol* **79**, 3938-3948.

Hopfl, R., hristensen, N. D., Angell, M. G. & Kreider, J. W. (1995). Leukocyte proliferation in vitro against cottontail rabbit papillomavirus in rabbits with persisting papillomas/cancer or after regression. *Arch Dermatol Res* **287**, 652-658.

Horner, S. M., DeFilippis, R. A., Manuelidis, L. & DiMaio, D. (2004). Repression of the human papillomavirus E6 gene initiates p53-dependent, telomerase-independent senescence and apoptosis in HeLa cervical carcinoma cells. *J Virol* **78**, 4063-4073.

Horwitz, B. H., Burkhardt, A. L., Schlegel, R. & DiMaio, D. (1988). 44-amino acid E5 transforming protein of Bovine papillomavirus requires a hydrophobic core and specific carboxyl terminal amino acids. *Mol Cell Biol* **8**, 4071-4078.

Howley, P. M. (1996). Papillomaviriae: The viruses and their replication. In *Virology*, pp. 2077-2109. Edited by Fields N.B, Knipe D.M, Howley M.P, Chanock M.R, Melnick J.L, Monath T.P, Roizman B & Straus S.E: Lippincott-Raven.

Howley, P. M. & Lowy, D. R. (2001). Papillomaviruses and their replication. In *Virology*, pp. 2197-2229. Edited by B. N. Fields, D. N. Knipe & P. M. Howley: Lippincott Williams and Wilkins.

Hsu, K. F., Huang, S. C., Hsiao, J. R., Cheng, Y. M., Wang, S. P. & Chou, C. Y. (2003). Clinical significance of serum human papillomavirus DNA in cervical carcinoma. *Obstet Gynecol* **102**, 1344-1351.

Hubbert, N. L., Schiller, J. T., Lowy, D. R. & Androphy, E. J. (1988). Bovine papilloma virus-transformed cells contain multiple E2 proteins. *Proc Natl Acad Sci U S A* **85**, 5864-5868.

Huibregtse, J. M., Scheffner, M., Beaudenon, S. & Howley, P. M. (1995). A family of proteins structurally and functionally related to the E6-AP ubiquitin-protein ligase. *Proc Natl Acad Sci U S A* **92**, 2563-2567.

Hummel, M., Hudson, J. B. & Laimins, L. A. (1992). Differentiation-induced and constitutive transcriptionof human papillomavirus type 31b in cell lines containing viral episomes. *JVirol* **66**, 6070-6080.

Hummel, M., Lim, H. B. & Laimins, L. A. (1995). Human papillomavirus type 31b late gene expression is regulated through protein kinase C-mediated changes in RNA processing. *J Virol* **69**, 3381-3388.

Ilves, I., Kivi, S. & Ustav, M. (1999). Long-term episomal maintenance of bovine papillomavirus type 1 plasmids is determined by attachment to host chromosomes, which Is mediated by the viral E2 protein and its binding sites. *J Virol* **73**, 4404-4412.

Ilves, I., Kadaja, M. & Ustav, M. (2003). Two separate replication modes of the bovine papillomavirus BPV1 origin of replication that have different sensitivity to p53. *Virus Res* **96**, 75-84.

Inada, H., Izawa, I., Nishizawa, M., Fujita, E., Kiyono, T., Takahashi, T., Momoi, T. & Inagaki, M. (2001). Keratin attenuates tumor necrosis factor-induced cytotoxicity through association with TRADD. *J Cell Biol* **155**, 415-426.

Ishida-Yamamoto, A., McGrath, J. A., Chapman, S. J., Leigh, I. M., Lane, E. B. & Eady, R. A. (1991). Epidermolysis bullosa simplex (Dowling-Meara type) is a genetic disease characterized by an abnormal keratin-filament network involving keratins K5 and K14. *J Invest Dermatol* **97**, 959-968.

Jablonska, S., Orth, G., Jarzabek-Chorzelska, M., Rzesa, G., Obalek, S., Glinski, W., Favre, M. & Croissant, O. (1978). [Malignancies induced by human papilloma virus]. *Przegl Dermatol* **65**, 497-450.

Jablonska, S. & Majewski, S. (1994). Epidermodysplasia Verruciformis: immunological and clinical aspects. In *Human Pathogenic Papillomaviruses*. Edited by H. zur Hausen. Heidelberg: Springer Verlag.

Janig, E., Stumptner, C., Fuchsbichler, A., Denk, H. & Zatloukal, K. (2005). Interaction of stress proteins with misfolded keratins. *Eur J Cell Biol* **84**, 329-339.

Janoff, E. N., Orenstein, J. M., Manischewitz, J. F. & Smith, P. D. (1991). Adenovirus colitis in the acquired immunodeficiency syndrome. *Gastroenterology* **100**, 976-979.

Jarrett, W. F. (1980). Bracken fern and papilloma virus in bovine alimentary cancer. *Br Med Bull* **36**, 79-81.

Jeon, S., Allen-Hoffmann, B. L. & Lambert, P. F. (1995a). Integration of human papillomavirus type 16 into the human genome correlates with a selective growth advantage of cells. *J Virol* **69**, 2989-2997.

Jeon, S. & Lambert, P. F. (1995b). Integration of human papillomavirus type 16 DNA into the human genome leads to increased stability of E6 and E7 mRNAs: implications for cervical carcinogenesis. *Proc Natl Acad Sci U S A* **92**, 1654-1658.

Jermy, T. (1984). Evolution of insect/host relationships. *Am Nat* **124**, 609-630.

Jones, D. L., Alani, R. M. & Munger, K. (1997). The human papillomavirus E7 oncoprotein can uncouple cellular differentiation and proliferation in human keratinocytes by abrogating p21CIP1 mediated inhibition of cdk2. *Genes and Development* **11**, 2101-2111.

Jordan, M. A., Wendell, K., Gardiner, S., Derry, W. B., Copp, H. & Wilson, L. (1996). Mitotic block induced in HeLa cells by low concentrations of paclitaxel (Taxol) results in abnormal mitotic exit and apoptotic cell death. *Cancer Res* **56**, 816-825.

Joyce, J. G., Tung, J. S., Przysiecki, C. T., Cook, J. C., Lehman, E. D., Sands, J. A., Jansen, K. U. & Keller, P. M. (1999). The L1 major capsid protein of human papillomavirus type 11 recombinant virus-like particles interacts with heparin and cell-surface glycosaminoglycans on human keratinocytes. *J Biol Chem* **274**, 5810-5822.

Juven, B. J. & Rosenthal, I. (1985). Effect of free-radical and oxygen scavengers on photochemically generated oxygen toxicity and on the aerotolerance of Campylobacter jejuni. *J Appl Bacteriol* **59**, 413-419.

Kabsch, K. & Alonso, A. (2002a). The human papillomavirus type 16 (HPV-16) E5 protein sensitizes human keratinocytes to apoptosis induced by osmotic stress. *Oncogene* **21**, 947-953.

Kabsch, K. & Alonso, A. (2002b). The human papillomavirus type 16 E5 protein impairs TRAIL- and FasL-mediated apoptosis in HaCaT cells by different mechanisms. *J Virol* **76**, 12162-12172.

Kabsch, K., Mossadegh, N., Kohl, A., Komposch, G., Schenkel, J., Alonso, A. & Tomakidi, P. (2004). The HPV-16 E5 protein inhibits TRAIL- and FasL-mediated apoptosis in human keratinocyte raft cultures. *Intervirology* **47**, 48-56.

Kalinin, A., Marekov, L. N. & Steinert, P. M. (2001). Assembly of the epidermal cornified cell envelope. *J Cell Sci* **114**, 3069-3070.

Kamper, N., Day, P. M., Nowak, T., Selinka, H. C., Florin, L., Bolscher, J., Hilbig, L., Schiller, J. T. & Sapp, M. (2006). A membrane-destabilizing peptide in capsid protein L2 is required for egress of papillomavirus genomes from endosomes. *J Virol* **80**, 759-768.

Keating, J. T., Ince, T. & Crum, C. P. (2001). Surrogate biomarkers of HPV infection in cervical neoplasia screening and diagnosis. *Adv Anat Pathol* **8**, 83-92.

Kee, S. H. & Steinert, P. M. (2001). Microtubule disruption in keratinocytes induces cell-cell adhesion through activation of endogenous E-cadherin. *Mol Biol Cell* **12**, 1983-1993.

Kessis, T. D., Slebos, R. J. & Nelson, W. G. (1993). Human papillomavirus 16 E6 expression disrupts the p53-mediated cellular response to DNA damage. *PNAS* **90**, 3988-3992.

Kessis, T. D., Connolly, D. C., Hedrick, L. & Cho, K. R. (1996). Expression of HPV16 E6 or E7 increases integration of foreign DNA. *Oncogene* **13**, 427-431.

Kirnbauer, R., Booy, F., Cheng, N., Lowy, D. R. & Schiller, J. T. (1992). Papillomavirus L1 major capsid protein self-assembles into virus-like particles that are highly immunogenic. *Proc Natl Acad Sci U S A* **89**, 12180-12184.

Kiyono, T., Hiraiwa, A., Fujita, M., Hayashi, Y., Akiyama, T. & Ishibashi, M. (1997). Binding of high-risk human papillomavirus E6 oncoproteins to the human homologue of the Drosophila discs large tumor suppressor protein. *Proc Natl Acad Sci U S A* **94**, 11612-11616.

Kjellberg, L., Hallmans, G., Ahren, A. M., Johansson, R., Bergman, F., Wadell, G., Angstrom, T. & Dillner, J. (2000). Smoking, diet, pregnancy and oral contraceptive use as risk factors for cervical intra-epithelial neoplasia in relation to human papillomavirus infection. *Br J Cancer* **82**, 1332-1338.

Knight, G. L., Grainger, J. R., Gallimore, P. H. & Roberts, S. (2004). Cooperation between different forms of the human papillomavirus type 1 E4 protein to block cell cycle progression and cellular DNA synthesis. *J Virol* **78**, 13920-13933.

Koller, L. D. & Olson, C. (1971). Subcutaneous papillomatous cysts produced by bovine papilloma virus. *J Natl Cancer Inst* **47**, 891-898.

Koller, L. D. & Olson, C. (1972). Attempted transmission of warts from man, cattle, and horses and of deer fibroma, to selected hosts. *J Invest Dermatol* **58**, 366-368.

Kondo, T., Tanaka, J., Ishida, Y., Mori, R., Takayasu, T. & Ohshima, T. (2002). Ubiquitin expression in skin wounds and its application to forensic wound age determination. *Int J Legal Med* **116**, 267-272.

Koutsky, L. A., Ault, K. A., Wheeler, C. M., Brown, D. R., Barr, E., Alvarez, F. B., Chiacchierini, L. M. & Jansen, K. U. (2002). A controlled trial of a human papillomavirus type 16 vaccine. *N Engl J Med* **347**, 1645-1651.

Kreider, J. W., Howett, M. K., Lill, N. L., Bartlett, G. L., Zaino, R. J., Sedlacek, T. V. & Mortel, R. (1986). In vivo transformation of human skin with human papillomavirus type 11 from condylomata acuminata. *J Virol* **59**, 369-376.

Kreider, J. W., Howett, M. K., Stoler, M. H., Zaino, R. J. & Welsh, P. (1987). Susceptibility of various human tissues to transformation in vivo with human papillomavirus type 11. *Int J Cancer* **39**, 459-465.

Kreider, J. W., Patrick, S. D., Cladel, N. M. & Welsh, P. A. (1990). Experimental infection with human papillomavirus type 1 of human hand and foot skin. *Virology* **177**, 415-417.

Kreimer, A. R., Alberg, A. J., Viscidi, R. & Gillison, M. L. (2004). Gender differences in sexual biomarkers and behaviors associated with human papillomavirus-16, -18, and -33 seroprevalence. *Sex Transm Dis* **31**, 247-256.

Ku, N. O. & Omary, M. B. (1994). Identification of the major physiologic phosphorylation site of human keratin 18: potential kinases and a role in filament reorganization. *J Cell Biol* **127**, 161-171.

Ku, N. O., Michie, S., Oshima, R. G. & Omary, M. B. (1995). Chronic hepatitis, hepatocyte fragility, and increased soluble phosphoglycokeratins in transgenic mice expressing a keratin 18 conserved arginine mutant. *J Cell Biol* **131**, 1303-1314.

Ku, N. O., Michie, S. A., Soetikno, R. M., Resurreccion, E. Z., Broome, R. L., Oshima, R. G. & Omary, M. B. (1996). Susceptibility to hepatotoxicity in transgenic mice that express a dominant-negative human keratin 18 mutant. *J Clin Invest* **98**, 1034-1046.

Ku, N. O., Liao, J. & Omary, M. B. (1997a). Apoptosis generates stable fragments of human type I keratins. *J Biol Chem* **272**, 33197-33203.

Ku, N. O. & Omary, M. B. (1997b). Phosphorylation of human keratin 8 in vivo at conserved head domain serine 23 and at epidermal growth factor-stimulated tail domain serine 431. *J Biol Chem* **272**, 7556-7564.

Ku, N. O., Liao, J. & Omary, M. B. (1998). Phosphorylation of human keratin 18 serine 33 regulates binding to 14-3-3 proteins. *Embo J* **17**, 1892-1906.

Ku, N. O. & Omary, M. B. (2000). Keratins turn over by ubiquitination in a phosphorylation-modulated fashion. *J Cell Biol* **149**, 547-552.

Ku, N. O. & Omary, M. B. (2001). Effect of mutation and phosphorylation of type I keratins on their caspase-mediated degradation. *J Biol Chem* **276**, 26792-26798.

Ku, N. O., Azhar, S. & Omary, M. B. (2002a). Keratin 8 phosphorylation by p38 kinase regulates cellular keratin filament reorganization: modulation by a keratin 1-like disease causing mutation. *J Biol Chem* **277**, 10775-10782 Epub 12002 Jan 10711.

Ku, N. O., Michie, S., Resurreccion, E. Z., Broome, R. L. & Omary, M. B. (2002b). Keratin binding to 14-3-3 proteins modulates keratin filaments and hepatocyte mitotic progression. *Proc Natl Acad Sci U S A* **99**, 4373-4378.

Ku, N. O., Fu, H. & Omary, M. B. (2004). Raf-1 activation disrupts its binding to keratins during cell stress. *J Cell Biol* **166**, 479-485.

Ku, N. O., Lim, J. K., Krams, S. M., Esquivel, C. O., Keeffe, E. B., Wright, T. L., Parry, D. A. & Omary, M. B. (2005). Keratins as susceptibility genes for end-stage liver disease. *Gastroenterology* **129**, 885-893.

Kundu, A. & Wade, A. A. H. (1995). Warts in the oral cavity. *Genitourin Med* **71**, 195.

Kuo, S.-R., Liu, J.-S., Broker, T. R. & Chow, L. T. (1994). Cell-free replication of the human papillomavirus DNA with homologous viral E1 and E2 proteins and human cell extracts. *Journal of Biological Chemistry* **269**, 24058-24065.

Lacey, J. V., Jr., Swanson, C. A., Brinton, L. A. & other authors (2003). Obesity as a potential risk factor for adenocarcinomas and squamous cell carcinomas of the uterine cervix. *Cancer* **98**, 814-821.

Laimins, L. A. (1996). Human Papillomaviruses target differentiating epithelia for virion production and malignant conversion. *Seminars in Virology* **7**, 305-313.

Lambert, P. F., Spalholz, B. A. & Howley, P. M. (1987). A transcriptional repressor encoded by BPV-1 shares a common carboxy-terminal domain with the E2 transactivator. *Cell* **50**, 69-78.

Lambertsen, R. H., Kohn, B. A., Sundberg, J. P. & Buergelt, C. D. (1987). Genital papillomatosis in sperm whale bulls. *J Wildl Dis* **23**, 361-367.

Lancaster, W. D., Olson, C. & Meinke, W. (1977). Bovine papilloma virus: presence of virus-specific DNA sequences in naturally occurring equine tumors. *Proc Natl Acad Sci U S A* **74**, 524-528.

Lane, D. P. (1992). Cancer. p53, guardian of the genome. *Nature* **358**, 15-16.

Lane, E. B., Goodman, S. L. & Trejdosiewicz, L. K. (1982). Disruption of the keratin filament network during epithelial cell division. *Embo J* **1**, 1365-1372.

Lane, E. B., Rugg, E. L., Navsaria, H., Leigh, I. M., Heagerty, A. H., Ishida-Yamamoto, A. & Eady, R. A. (1992). A mutation in the conserved helix termination peptide of keratin 5 in hereditary skin blistering. *Nature* **356**, 244-246.

Lane, E. B. & McLean, W. H. (2004). Keratins and skin disorders. *J Pathol* **204**, 355-366.

Leachman, S. A., Tigelaar, R. E., Shlyankevich, M. & other authors (2000). GM-CSF Priming Plus Papillomavirus E6 DNA Vaccination: Effects on Papilloma Formation and Regression in the CRPV-Rabbit Model. *J Virol* **74**, 8700-8708.

Lee, C. & Laimins, L. A. (2004). Role of the PDZ domain-binding motif of the oncoprotein E6 in the pathogenesis of human papillomavirus type 31. *J Virol* **78**, 12366-12377.

Lee, S. S., Glaunsinger, B., Mantovani, F., Banks, L. & Javier, R. T. (2000). Multi-PDZ domain protein MUPP1 is a cellular target for both adenovirus E4-ORF1 and high-risk papillomavirus type 18 E6 oncoproteins. *J Virol* **74**, 9680-9693.

Leechanachai, P., Banks, L., Moreau, F. & Matlashewski, G. (1992). The E5 gene from human papillomavirus type 16 is an oncogene which enhances growth factor-mediated signal transduction to the nucleus. *Oncogene* **7**, 19-25.

Leers, M. P., Kolgen, W., Bjorklund, V. & other authors (1999). Immunocytochemical detection and mapping of a cytokeratin 18 neo-epitope exposed during early apoptosis. *J Pathol* **187**, 567-572.

Lehr, E., Jarnik, M. & Brown, D. R. (2002). Human papillomavirus type 11 alters the transcription and expression of loricrin, the major cell envelope protein. *Virology* **298**, 240-247.

Lehr, E. & Brown, D. R. (2003). Infection with the oncogenic human papillomavirus type 59 alters protein components of the cornified cell envelope. *Virology* **309**, 53-60.

Li, R., Knight, J. D., Jackson, S. P., Tjian, R. & Botchan, M. R. (1991). Direct interaction between Sp1 and the BPV enhancer E2 protein mediates synergistic activation of transcription. *Cell* **65**, 493-505.

Li, X. & Coffino, P. (1996). High-risk human papillomavirus E6 protein has two distinct binding sites within p53, of which only one determines degradation. *J Virol* **70**, 4509-4516.

Liao, J., Lowthert, L. A., Ku, N. O., Fernandez, R. & Omary, M. B. (1995). Dynamics of human keratin 18 phosphorylation: polarized distribution of phosphorylated keratins in simple epithelial tissues. *J Cell Biol* **131**, 1291-1301.

Liao, J. & Omary, M. B. (1996). 14-3-3 proteins associate with phosphorylated simple epithelial keratins during cell cycle progression and act as a solubility cofactor. *J Cell Biol* **133**, 345-357.

Liao, J., Ku, N. O. & Omary, M. B. (1997). Stress, apoptosis, and mitosis induce phosphorylation of human keratin 8 at Ser-73 in tissues and cultured cells. *J Biol Chem* **272**, 17565-17573.

Lilley, B. N. & Ploegh, H. L. (2005). Viral modulation of antigen presentation: manipulation of cellular targets in the ER and beyond. *Immunol Rev* **207**, 126-144.

Luby-Phelps, K. (1994). Physical properties of cytoplasm. *Curr Opin Cell Biol* **6**, 3-9.

Luesley, D., Blomfield, P., Dunn, J., Shafi, M., Chenoy, R. & Buxton, J. (1994). Cigarette smoking and histological outcome in women with mildly dyskaryotic cervical smears. *Br J Obstet Gynaecol* **101**, 49-52.

Lutzner, M., Croissant, O., Ducasse, M. F., Kreis, H., Crosnier, J. & Orth, G. (1980). A potentially oncogenic human papillomavirus (HPV-5) found in two renal allograft recipients. *J Invest Dermatol* **75**, 353-356.

Lynley, A. M. & Dale, B. A. (1983). The characterization of human epidermal filaggrin. A histidine-rich, keratin filament-aggregating protein. *Biochim Biophys Acta* **744**, 28-35.

Ma, L., Xu, J., Coulombe, P. A. & Wirtz, D. (1999). Keratin filament suspensions show unique micromechanical properties. *J Biol Chem* **274**, 19145-19151.

Madine, M. A., Khoo, C. Y., Mills, A. D., Musahl, C. & Laskey, R. A. (1995). The nuclear envelope prevents reinitiation of replication by regulating the binding of MCM3 to chromatin in Xenopus egg extracts. *Curr Biol* **5**, 1270-1279.

Magal, S. S., Jackman, A., Ish-Shalom, S., Botzer, L. E., Gonen, P., Schlegel, R. & Sherman, L. (2005). Downregulation of Bax mRNA expression and protein stability by the E6 protein of human papillomavirus 16. *J Gen Virol* **86**, 611-621.

Mao, C., Koutsky, L. A., Ault, K. A. & other authors (2006). Efficacy of human papillomavirus-16 vaccine to prevent cervical intraepithelial neoplasia: a randomized controlled trial. *Obstet Gynecol* **107**, 18-27.

Marchetti, B., Ashrafi, G. H., Tsirimonaki, E., O'Brien, P. M. & Campo, M. S. (2002). The bovine papillomavirus oncoprotein E5 retains MHC class I molecules in the Golgi apparatus and prevents their transport to the cell surface. *Oncogene* **21**, 7808-7816.

Margottin, F., Bour, S. P., Durand, H., Selig, L., Benichou, S., Richard, V., Thomas, D., Strebel, K. & Benarous, R. (1998). A novel human WD protein, h-beta TrCp, that interacts with HIV-1 Vpu connects CD4 to the ER degradation pathway through an F-box motif. *Mol Cell* **1**, 565-574.

Markl, J. & Schechter, N. (1998a). Fish intermediate filament proteins in structure, evolution, and function. *Subcell Biochem* **31**, 1-33.

Markl, J. & Schechter, N. (1998b). intermediate filaments. In *subcellular biochemistry*, pp. 1-34: Plenum Publishing.

Martens, J., Baars, J., Smedts, F., Holterheus, M., Kok, M. J., Vooijs, P. & Ramaekers, F. (1999). Can keratin 8 and 17 immunohistochemistry be of diagnostic value in cervical cytology? A feasibility study. *Cancer* **87**, 87-92.

Mashanov, G. I., Tacon, D., Knight, A. E., Peckham, M. & Molloy, J. E. (2003). Visualizing single molecules inside living cells using total internal reflection fluorescence microscopy. *Methods* **29**, 142-152.

Mashanov, G. I., Tacon, D., Peckham, M. & Molloy, J. E. (2004). The spatial and temporal dynamics of pleckstrin homology domain binding at the plasma membrane measured by imaging single molecules in live mouse myoblasts. *J Biol Chem* **279**, 15274-15280.

Matsukura, T., Koi, S. & Sugase, M. (1989). Both episomal and integrated forms of human papillomavirus type 16 are involved in invasive cervical cancers. *Virology* **172**, 63-72.

Matthews, K., Leong, C. M., Baxter, L., Inglis, E., Yun, K., Backstrom, B. T., Doorbar, J. & Hibma, M. (2003). Depletion of Langerhans cells in human papillomavirus type 16-infected skin is associated with E6-mediated down regulation of E-cadherin. *J Virol* **77**, 8378-8385.

McBride, A. A., Schlegel, R. & Howley, P. M. (1988). The carboxy-terminal domain shared by the bovine papillomavirus E2 transactivator and repressor proteins contains a specific DNA binding activity. *Embo J* **7**, 533-539.

McBride, A. A., Bolen, J. B. & Howley, P. M. (1989). Phosphorylation sites of the E2 transcriptional regulatory protein of bovine papillomavirus type 1. *J Virol* **63**, 5076-5085.

Melendy, T., Sedman, J. & Stenlund, A. (1995). Cellular factors required for papillomavirus DNA replication. *J Virol* **69**, 7857-7867.

Mendelsohn, J. A. (2002). 'Like all that lives': biology, medicine and bacteria in the age of Pasteur and Koch. *Hist Philos Life Sci* **24**, 3-36.

Meneguzzi, G., Cerni, C., Kieny, M. P. & Lathe, R. (1991). Immunization against human papillomavirus type 16 tumor cells with recombinant vaccinia viruses expressing E6 and E7. *Virology* **181**, 62-69.

Merle, E., Rose, R. C., LeRoux, L. & Moroianu, J. (1999). Nuclear import of HPV11 L1 capsid protein is mediated by karyopherin alpha2beta1 heterodimers. *J Cell Biochem* **74**, 628-637.

Micali, G., Dall'Oglio, F., Nasca, M. R. & Tedeschi, A. (2004). Management of cutaneous warts: an evidence-based approach. *Am J Clin Dermatol* **5**, 311-317.

Middleton, K., Peh, W., Southern, S. & other authors (2003). Organization of human papillomavirus productive cycle during neoplastic progression provides a basis for selection of diagnostic markers. *J Virol* **77**, 10186-10201.

Middleton, K., Peh, W., Southern, S.A., Griffin, H.M., Sotlar, K., Nakahara, T., El-Sherif, A., Morris, L., Seth, R., Hibma, M., Jenkins, D., Lambert, P.F., Coleman, N. and Doorbar, J. (2003). Organisation of the human papillomavirus productive cycle during neoplastic progression provides a basis for the selection of diagnostic markers. *JVirol* **77**, 10186-10201.

Miller, R. K., Vikstrom, K. & Goldman, R. D. (1991). Keratin incorporation into intermediate filament networks is a rapid process. *J Cell Biol* **113**, 843-855.

Miller, R. K., Khuon, S. & Goldman, R. D. (1993). Dynamics of keratin assembly: exogenous type I keratin rapidly associates with type II keratin in vivo. *J Cell Biol* **122**, 123-135.

Mohr, I. J., Clark, R., Sun, S., Androphy, E. J., MacPherson, P. & Botchan, M. R. (1990). Targeting the E1 replication protein to the papillomavirus origin of replication by complex formation with the E2 transactivator. *Science* **250**, 1694-1699.

Moreno, V., Bosch, F. X., Munoz, N., Meijer, C. J., Shah, K. V., Walboomers, J. M., Herrero, R. & Franceschi, S. (2002). Effect of oral contraceptives on risk of cervical cancer in women with human papillomavirus infection: the IARC multicentric case-control study. *Lancet* **359**, 1085-1092.

Munoz, N., Bosch, F. X., deSanjose, S. & Shah, K. V. (1994). The role of HPV in the etiology of cervical cancer. *Mutation Res* **305**, 293-301.

Munoz, N. & Bosch, F. X. (1997). Cervical cancer and human papillomavirus: epidemiological evidence and perspectives for prevention. *Salud Publica Mex* **39**, 274-282.

Munoz, N., Bosch, F. X., de Sanjose, S., Herrero, R., Castellsague, X., Shah, K. V., Snijders, P. J. & Meijer, C. J. (2003). Epidemiologic classification of human papillomavirus types associated with cervical cancer. *N Engl J Med* **348**, 518-527.

Murata, T., Goshima, F., Nishizawa, Y., Daikoku, T., Takakuwa, H., Ohtsuka, K., Yoshikawa, T. & Nishiyama, Y. (2002). Phosphorylation of cytokeratin 17 by herpes simplex virus type 2 US3 protein kinase. *Microbiol Immunol* **46**, 707-719.

Murthy, N. S. & Mathew, A. (2000). Risk factors for pre-cancerous lesions of the cervix. *Eur J Cancer Prev* **9**, 5-14.

Myers, G., Androphy, E.J. (1995). The E6 protein in human papillomaviruses. 47-57.

Nagao, T., Saito, K., Hirayama, E., Uchikoshi, K., Koyama, K., Natori, S., Morisaki, N., Iwasaki, S. & Matsushima, T. (1989). Mutagenicity of ptaquiloside, the carcinogen in bracken, and its related illudane-type sesquiterpenes. I. Mutagenicity in Salmonella typhimurium. *Mutat Res* **215**, 173-178.

Nakahara, T., Nishimura, A., Tanaka, M., Ueno, T., Ishimoto, A. & Sakai, H. (2002). Modulation of the cell division cycle by human papillomavirus type 18 E4. *J Virol* **76**, 10914-10920.

Nakahara, T., Peh, W. L., Doorbar, J., Lee, D. & Lambert, P. F. (2005). Human papillomavirus type 16 E1circumflexE4 contributes to multiple facets of the papillomavirus life cycle. *J Virol* **79**, 13150-13165.

Nakamichi, I., Hatakeyama, S. & Nakayama, K. I. (2002). Formation of Mallory body-like inclusions and cell death induced by deregulated expression of keratin 18. *Mol Biol Cell* **13**, 3441-3451.

Nakamichi, I., Toivola, D. M., Strnad, P., Michie, S. A., Oshima, R. G., Baribault, H. & Omary, M. B. (2005). Keratin 8 overexpression promotes mouse Mallory body formation. *J Cell Biol* **171**, 931-937.

Nakano, N., Nakao, A., Ishidoh, K., Tsuboi, R., Kominami, E., Okumura, K. & Ogawa, H. (2005). CDK5 regulates cell-cell and cell-matrix adhesion in human keratinocytes. *Br J Dermatol* **153**, 37-45.

Narechania, A., Terai, M. & Burk, R. D. (2005). Overlapping reading frames in closely related human papillomaviruses result in modular rates of selection within E2. *J Gen Virol* **86**, 1307-1313.

Nasseri, M., Hirochika, R., Broker, T. R. & Chow, L. (1987). A human papillomavirus type 11 transcript encoding an E1^E4 protein. *Virology* **159**, 433-439.

Neumann, N. J., Holzle, E., Wallerand, M., Vierbaum, S., Ruzicka, T. & Lehmann, P. (1999). The photoprotective effect of ascorbic acid, acetylsalicylic acid, and indomethacin evaluated by the photo hen's egg test. *Photodermatol Photoimmunol Photomed* **15**, 166-170.

Nieh, S., Chen, S. F., Chu, T. Y., Lai, H. C., Lin, Y. S., Fu, E. & Gau, C. H. (2005). Is p16(INK4A) expression more useful than human papillomavirus test to determine the outcome of atypical squamous cells of undetermined significance-categorized Pap smear? A comparative analysis using abnormal cervical smears with follow-up biopsies. *Gynecol Oncol* **97**, 35-40.

Nishimura, A., Ono, T., Ishimoto, A., Dowhanick, J. J., Frizzell, M. A., Howley, P. M. & Sakai, H. (2000). Mechanisms of human papillomavirus E2-mediated repression of viral oncogene expression and cervical cancer cell growth inhibition. *J Virol* **74**, 3752-3760.

O'Banion, M. K., Sundberg, J. P., Reszka, A. A. & Reichmann, M. E. (1987). Cross-hybridization and relationships of various papillomavirus DNAs at different degrees of stringency. *Intervirology* **28**, 114-121.

O'Banion, M. K., Jacobson, E. R. & Sundberg, J. P. (1992). Molecular cloning and partial characterization of a parrot papillomavirus. *Intervirology* **33**, 91-96.

O'Brien, P. M. & Saveria Campo, M. (2002). Evasion of host immunity directed by papillomavirus-encoded proteins. *Virus Res* **88**, 103-117.

Offord, E. A. & Beard, P. (1990). A member of the activator protein 1 family found in keratinocytes but not in fibroblasts required for transcription from a human papillomavirus type 18 promoter. *J Virol* **64**, 4792-4798.

Ohta, M., Marceau, N., Perry, G. & other authors (1988). Ubiquitin is present on the cytokeratin intermediate filaments and Mallory bodies of hepatocytes. *Lab Invest* **59**, 848-856.

Oka, H., Shiozaki, H., Kobayashi, K. & other authors (1992). Immunohistochemical evaluation of E-cadherin adhesion molecule expression in human gastric cancer. *Virchows Arch A Pathol Anat Histopathol* **421**, 149-156.

Oksala, O., Salo, T., Tammi, R., Hakkinen, L., Jalkanen, M., Inki, P. & Larjava, H. (1995). Expression of proteoglycans and hyaluronan during wound healing. *J Histochem Cytochem* **43**, 125-135.

Okun, M. M., Day, P. M., Greenstone, H. L., Booy, F. P., Lowy, D. R., Schiller, J. T. & Roden, R. B. (2001). L1 interaction domains of papillomavirus l2 necessary for viral genome encapsidation. *J Virol* **75**, 4332-4342.

Omary, M. B., Ku, N. O., Liao, J. & Price, D. (1998). Keratin modifications and solubility properties in epithelial cells and in vitro. *Subcell Biochem* **31**, 105-140.

Ong, C. K., Chan, S. Y., Campo, M. S. & other authors (1993). Evolution of human papillomavirus type 18: an ancient phylogenetic root in Africa and intratype diversity reflect coevolution with human ethnic groups. *J Virol* **67**, 6424-6431.

Orth, G., Breitburd, F., Favre, M. & Croissant, O. (1977). Papillomaviruses:possible role in human cancer. *Cold Spring Harbor Cell Prolif* **4**, 1043-1068.

Oshima, R. G. (2002). Apoptosis and keratin intermediate filaments. *Cell Death Differ* **9**, 486-492.

Otsuga, D., Keegan, B. R., Brisch, E., Thatcher, J. W., Hermann, G. J., Bleazard, W. & Shaw, J. M. (1998). The dynamin-related GTPase, Dnm1p, controls mitochondrial morphology in yeast. *J Cell Biol* **143**, 333-349.

Ozbun, M. A. & Meyers, C. (1997). Characterisation of late gene transcripts expressed during vegetative replication of human papillomavirus type 31b. *JVirol* **71**, 5161-5172.

Ozbun, M. A. & Meyers, C. (1998a). Temporal Usage of Multiple Promoters during the life cycle of Human Papillomavirus type 31b. *J Virol* **72**, 2715-2722.

Ozbun, M. A. & Meyers, C. (1998b). Human papillomavirus type 31b E1 and E2 transcript expression correlates with vegetative viral genome amplification. *Virology* **248**, 218-230.

Ozbun, M. A. & Meyers, C. (1999). Two novel promoters in the upstream regulatory region of human papillomavirus type 31b are negatively regulated by epithelial differentiation. *J Virol* **73**, 3505-3510.

Paladini, R. D., Takahashi, K., Bravo, N. S. & Coulombe, P. A. (1996). Onset of re-epithelialization after skin injury correlates with a reorganization of keratin filaments in wound edge keratinocytes: defining a potential role for keratin 16. *J Cell Biol* **132**, 381-397.

Panici, P. B., Scambia, G., Perrone, L. & other authors (1992). Oral condyloma lesions in patients with extensive genital human papillomavirus infection. *Am J Obstet Gynecol* **167**, 451-458.

Paramio, J. M., Casanova, M. L., Segrelles, C., Mittnacht, S., Lane, E. B. & Jorcano, J. L. (1999). Modulation of cell proliferation by cytokeratins K10 and K16. *Mol Cell Biol* **19**, 3086-3094.

Paramio, J. M. & Jorcano, J. L. (2002). Beyond structure: do intermediate filaments modulate cell signalling? *Bioessays* **24**, 836-844.

Parkin, D. M., Bray, F., Ferlay, J. & Pisani, P. (2005). Global cancer statistics, 2002. *CA Cancer J Clin* **55**, 74-108.

Patel, S. S. & Picha, K. M. (2000). Structure and function of hexameric helicases. *Annu Rev Biochem* **69**, 651-697.

Patterson, N. A., Smith, J. L. & Ozbun, M. A. (2005). Human papillomavirus type 31b infection of human keratinocytes does not require heparan sulfate. *J Virol* **79**, 6838-6847.

Peh, W. L. (2002).The Role of the Papillomavirus E4 Protein During the Late Stage of the Virus Life Cycle using in vivo Model Systems. In *Virology*, pp. 297. London: University of London.

Peh, W. L., Middleton, K., Christensen, N. & other authors (2002). Life cycle heterogeneity in animal models of human papillomavirus-associated disease. *J Virol* **76**, 10401-10416.

Peh, W. L., Brandsma, J. L., Christensen, N. D., Cladel, N. M., Wu, X. & Doorbar, J. (2004). The viral E4 protein is required for the completion of the cottontail rabbit papillomavirus productive cycle in vivo. *J Virol* **78**, 2142-2151.

Peng, H., Liu, S., Mann, V., Rohan, T. & Rawls, W. (1991). Human papillomavirus types 16 and 33, herpes simplex virus type and other risk factors for cervical cancer in Sichuan Province, China. *Int J Cancer* **47**, 711-716.

Pettersson, U. & Hoglund, S. (1969). Sructural proteins of adenoviruses. 3. Purification and characterization of the adenovirus type 2 penton antigen. *Virology* **39**, 90-106.

Phillips, G. N., Jr. (1997). Structure and dynamics of green fluorescent protein. *Curr Opin Struct Biol* 7, 821-827.

Pickart, C. M. (2001). Mechanisms underlying ubiquitination. *Annu Rev Biochem* **70**, 503-533.

Pim, D., Storey, A., Thomas, M., Massimi, P. & Banks, L. (1994). Mutational analysis of HPV-18 E6 identifies domains required for p53 degradation in vitro, abolition of p53 transactivation in vivo and immortalisation of primary BMK cells. *Oncogene* **9**, 1869-1876.

Pim, D. & Banks, L. (1999). HPV-18 E6*I protein modulates the E6-directed degradation of p53 by binding to full-length HPV-18 E6. *Oncogene* **18**, 7403-7408.

Pray, T. R. & Laimins, L. A. (1995a). Differentiation-dependent expression of E1^E4 proteins in cell lines maintaining episomes of human papillomavirus type 31b. *Virology* **206**, 679-685.

Pray, T. R. & Laimins, L. A. (1995b). Differentiation-dependent expression of E1--E4 proteins in cell lines maintaining episomes of human papillomavirus type 31b. *Virology* **206**, 679-685.

Prendergast, F. G. (1999). Biophysics of the green fluorescent protein. *Methods Cell Biol* **58**, 1-18.

Presland, R. B. & Dale, B. A. (2000). Epithelial structural proteins of the skin and oral cavity: function in health and disease. *Crit Rev Oral Biol Med* **11**, 383-408.

Presland, R. B. & Jurevic, R. J. (2002). Making sense of the epithelial barrier: what molecular biology and genetics tell us about the functions of oral mucosal and epidermal tissues. *J Dent Educ* **66**, 564-574.

Putral, L. N., Bywater, M. J., Gu, W., Saunders, N. A., Gabrielli, B. G., Leggatt, G. R. & McMillan, N. A. (2005). RNA interference against human papillomavirus oncogenes in cervical cancer cells results in increased sensitivity to cisplatin. *Mol Pharmacol* **68**, 1311-1319.

Querido, E., Blanchette, P., Yan, Q. & other authors (2001). Degradation of p53 by adenovirus E4orf6 and E1B55K proteins occurs via a novel mechanism involving a Cullin-containing complex. *Genes Dev* **15**, 3104-3117.

Raj, K., Berguerand, S., Southern, S., Doorbar, J. & Beard, P. (2004). E1 empty set E4 protein of human papillomavirus type 16 associates with mitochondria. *J Virol* **78**, 7199-7207.

Reid, R., Stanhope, C. R., Herschman, B. R., Booth, E., Phibbs, G. D. & Smith, J. P. (1982). Genital warts and cervical cancer. I. Evidence of an association between subclinical papillomavirus infection and cervical malignancy. *Cancer* **50**, 377-387.

Renz, J. F., Lin, Z., de Roos, M., Dalal, A. A. & Ascher, N. L. (1996). SCID mouse as a model for transplantation studies. *J Surg Res* **65**, 34-41.

Ridge, K. M. (2004).Mitochondrial-generated ROS promote the disassembly of keratin intermediate filaments. In *GCR on Intermediate Filaments*. Queens college, Oxford, UK.

Ridge, K. M., Linz, L., Flitney, F. W., Kuczmarski, E. R., Chou, Y. H., Omary, M. B., Sznajder, J. I. & Goldman, R. D. (2005). Keratin 8 phosphorylation by protein kinase C delta regulates shear stress-mediated disassembly of keratin intermediate filaments in alveolar epithelial cells. *J Biol Chem* **280**, 30400-30405.

Riley, N. E., Bardag-Gorce, F., Montgomery, R. O., Li, J., Lungo, W., Lue, Y. H. & French, S. W. (2003). Microtubules are required for cytokeratin aggresome (Mallory body) formation in hepatocytes: an in vitro study. *Exp Mol Pathol* **74**, 173-179.

Roberts, S., Ashmole, I., Johnson, G. D., Kreider, J. W. & Gallimore, P. H. (1993). Cutaneous and mucosal human papillomavirus E4 proteins form intermediate filament-like structures in epithelial cells. *Virology* **197**, 176-187.

Roberts, S., Ashmole, I., Gibson, L. J., Rookes, S. M., Barton, G. J. & Gallimore, P. H. (1994). Mutational analysis of human papillomavirus E4 proteins: identification of structural features important in the formation of cytoplasmic E4/cytokeratin networks in epithelial cells. *J Virol* **68**, 6432-6445.

Roberts, S., Ashmole, I., Rookes, S. M. & Gallimore, P. H. (1997). Mutational analysis of the human papillomavirus type 16 E1--E4 protein shows that the C terminus is dispensable for keratin cytoskeleton association but is involved in inducing disruption of the keratin filaments. *J Virol* **71**, 3554-3562.

Roberts, S., Hillman, M. L., Knight, G. L. & Gallimore, P. H. (2003). The ND10 component promyelocytic leukemia protein relocates to human papillomavirus type 1 E4 intranuclear inclusion bodies in cultured keratinocytes and in warts. *J Virol* **77**, 673-684.

Roden, R. B., Lowy, D. R. & Schiller, J. T. (1997). Papillomavirus is resistant to desiccation. *J Infect Dis* **176**, 1076-1079.

Rogel-Gaillard, C., Breitburd, F. & Orth, G. (1992a). Human papillomavirus type 1 E4 proteins differing by their N-terminal ends have distinct cellular locations when transiently expressed in vitri. *JVirol* **66**, 816-823.

Rogel-Gaillard, C., Breitburd, F. & Orth, G. (1992b). Human papillomavirus type 1 E4 proteins differing by their N-terminal ends have distinct cellular localizations when transiently expressed in vitro. *J Virol* **66**, 816-823.

Rogel-Gaillard, C., Pehau-Arnaudet, G., Breitburd, F. & Orth, G. (1993). Cytopathic effect in human papillomavirus type 1-induced inclusion warts: *In vitro* analysis of the contribution of two forms of the viral E4 protein. *JInvestDermatol* **101**, 843-851.

Sahin., I. P. T. E. N. A. Y. (2001). Expression of 8 kDa Heat Shock protein (Ubiquitin) in Psoriasis. *Turksh Journal of medical science* **31**, 69-72.

Sailaja, G., Watts, R. M. & Bernard, H. U. (1999). Many different papillomaviruses have low transcriptional activity in spite of strong epithelial specific enhancers. *J Gen Virol* **80 (Pt 7)**, 1715-1724.

Sanders, C. M. & Maitland, N. J. (1994). Kinetic and equilibrium binding studies of the human papillomavirus type-16 transcription regulatory protein E2 interacting with core enhancer elements. *Nucleic Acids Res* **22**, 4890-4897.

Sanders, C. M. & Stenlund, A. (1998). Recruitment and loading of the E1 initiator protein: an ATP-dependent process catalysed by a transcription factor. *Embo J* **17**, 7044-7055.

Sanders, C. M. & Stenlund, A. (2000). Transcription factor-dependent loading of the E1 initiator reveals modular assembly of the papillomavirus origin melting complex. *J Biol Chem* **275**, 3522-3534.

Sandler, A. B., Vande Pol, S. B. & Spalholz, B. A. (1993). Repression of bovine papillomavirus type 1 transcription by the E1 replication protein. *J Virol* **67**, 5079-5087.

Santucci, S., Bonne-Andrea, C. & Clertant, P. (1995). Bovine papillomavirus type 1 E1 ATPase activity does not depend on binding to DNA nor to viral E2 protein. *J Gen Virol* **76 (Pt 5)**, 1129-1140.

Sargent, S. J. (1992). The 'other' sexually transmitted diseases. Chlamydial, herpes simplex virus, and human papillomavirus infections. *Postgrad Med* **91**, 359-362, 371-354, 377.

Sarian, L. O., Derchain, S. F., Pittal Dda, R., Andrade, L. A., Morais, S. S. & Figueiredo, P. G. (2005). Human papillomavirus detection by hybrid capture II and residual or recurrent high-grade squamous cervical intraepithelial neoplasia after large loop excision of the transformation zone (LLETZ). *Tumori* **91**, 188-192.

Sato, K., Waguri, S., Ohsawa, Y., Nitatori, T., Kon, S., Kominami, E., Watanabe, T., Gotow, T. & Uchiyama, Y. (1997). Immunocytochemical localization of lysosomal cysteine and aspartic proteinases, and ubiquitin in rat epidermis. *Arch Histol Cytol* **60**, 275-287.

Satoh, K. & Sakagami, H. (1996). Ascorbyl radical scavenging activity of polyphenols. *Anticancer Res* **16**, 2885-2890.

Scheffner, M., Werness, B. A., Huibregtse, J. M., Levine, A. J. & Howley, P. M. (1990). The E6 oncoprotein encoded by human papillomavirus types 16 and 18 promotes the degradation of p53. *Cell* **63**, 1129-1136.

Scheffner, M., Huibregtse, J. M. & Howley, P. M. (1994). Identification of a human ubiquitin conjugating enzyme that mediates the E6AP-dependent ubiquitination of p53. *PNAS* **91**, 8797-8801.

Scheffner, M., Nuber, U. & Huibregtse, J. M. (1995). Protein ubiquitination involving an E1-E2-E3 enzyme ubiquitin thioester cascade. *Nature* **373**, 81-83.

Scherneck, S., Feunteun, J., Vogel, F., Boettger, M., Krause, H., Prokoph, H., Zimmermann, W. & Geissler, E. (1983). Evolutionary relationships between papovaviruses and their hosts. *Arch Geschwulstforsch* **53**, 197-206.

Schiffman, M., Bauer, H., Hoover, R. & other authors (1993). Epidemiologic Evidence Showing That Human Papillomavirus Infection Causes Most Cervical Intraepithelial Neoplasia. *J Natl Cancer Inst* **85**, 958-964.

Schiffman, M., Wheeler, C. M. & Castle, P. E. (2002). Human papillomavirus DNA remains detectable longer than related cervical cytologic abnormalities. *J Infect Dis* **186**, 1169-1172.

Schutte, B., Henfling, M., Kolgen, W. & other authors (2004). Keratin 8/18 breakdown and reorganization during apoptosis. *Exp Cell Res* **297**, 11-26.

Seifert, G. J., Lawson, D. & Wiche, G. (1992). Immunolocalization of the intermediate filament-associated protein plectin at focal contacts and actin stress fibres. *Eur J Cell Biol* **59**, 138-147.

Seksek, O., Biwersi, J. & Verkman, A. S. (1997). Translational diffusion of macromolecule-sized solutes in cytoplasm and nucleus. *J Cell Biol* **138**, 131-142.

Seo, Y. S., Muller, F., Lusky, M., Gibbs, E., Kim, H. Y., Phillips, B. & Hurwitz, J. (1993a). Bovine papilloma virus (BPV)-encoded E2 protein enhances binding of E1 protein to the BPV replication origin. *Proc Natl Acad Sci U S A* **90**, 2865-2869.

Seo, Y. S., Muller, F., Lusky, M. & Hurwitz, J. (1993b). Bovine papilloma virus (BPV)-encoded E1 protein contains multiple activities required for BPV DNA replication. *Proc Natl Acad Sci U S A* **90**, 702-706.

Shackelford, J. & Pagano, J. S. (2005). Targeting of host-cell ubiquitin pathways by viruses. *Essays Biochem* **41**, 139-156.

Shafti-Keramat, S., Handisurya, A., Kriehuber, E., Meneguzzi, G., Slupetzky, K. & Kirnbauer, R. (2003). Different heparan sulfate proteoglycans serve as cellular receptors for human papillomaviruses. *J Virol* **77**, 13125-13135.

Sherman, L., Alloul, N., Golan, I., Durst, M. & Baram, A. (1992a). Expression and splicing patterns of human papillomavirus type 16 mRNAs in precancerous lesions and carcinoma of the cervix, in human keratinocytes immortalized by HPV16, and in cell lines established from cervical cancers. *Int J Cancer* **50**, 356-364.

Sherman, L., Alloul, N., Golan, I., Durst, M. & Baram, A. (1992b). Expression and splicing patterns of human papillomavirus type-16 mRNAs in pre-cancerous lesions and carcinomas of the cervix, in human keratinocytes immortalized by HPV 16, and in cell lines established from cervical cancers. *Int J Cancer* **50**, 356-364.

Sherman, L. & Schlegel, R. (1996). Serum-induced and calcium-induced differentiation of human keratinocytes is inhibited by the E6 protein of human papillomaviruses. *J Virol* **70**, 3269-3279.

Shimomura, O. (2005). The discovery of aequorin and green fluorescent protein. *J Microsc* **217**, 1-15.

Shope (1933). Infectous papillomatosis of rabbits. *Journal of Experimental Medicine* **58**, 607-604.

Short, M. B. & Rosenthal, S. L. (2006). Fostering acceptance of human papillomavirus and herpes simplex virus vaccines among adolescents and parents. *Curr Opin Pediatr* **18**, 53-57.

Sibbet, G., Romero-Graillet, C., Meneguzzi, G. & Campo, M. S. (2000). alpha6 integrin is not the obligatory cell receptor for bovine papillomavirus type 4. *J Gen Virol* **81**, 327-334.

Smedts, F., Ramaekers, F., Robben, H., Pruszczynski, M., van Muijen, G., Lane, B., Leigh, I. & Vooijs, P. (1990). Changing patterns of keratin expression during progression of cervical intraepithelial neoplasia. *Am J Pathol* **136**, 657-668.

Smith, G. A. & Enquist, L. W. (2002). Break ins and break outs: viral interactions with the cytoskeleton of Mammalian cells. *Annu Rev Cell Dev Biol* **18**, 135-161.

Smotkin, D. & Wettstein, F. O. (1986). Transcription of human papillomavirus type 16 early genes in a cervical cancer and a cancer-derived cell line and identification of the E7 protein. *Proc Natl Acad Sci U S A* **83**, 4680-4684.

Smotkin, D., Prokoph, H. & Wettstein, F. O. (1989). Oncogenic and nononcogenic human genital papillomaviruses generate the E7 mRNA by different mechanisms. *J Virol* **63**, 1441-1447.

Soubeyrand, B. & Leparc, J. (2005). [Vaccination against human papillomavirus: a new vaccination for the female adolescent?]. *Med Mal Infect.*

Spalholz, B. A., Yang, Y. C. & Howley, P. M. (1985). Transactivation of a bovine papilloma virus transcriptional regulatory element by the E2 gene product. *Cell* **42**, 183-191.

Spalholz, B. A., Byrne, J. C. & Howley, P. M. (1988). Evidence for cooperativity between E2 binding sites in E2 trans-regulation of bovine papillomavirus type 1. *J Virol* **62**, 3143-3150.

Spink, K. M. & Laimins, L. A. (2005). Induction of the human papillomavirus type 31 late promoter requires differentiation but not DNA amplification. *J Virol* **79**, 4918-4926.

Stacey, S. N., Jordan, D., Snijders, P. J., Mackett, M., Walboomers, J. M. & Arrand, J. R. (1995). Translation of the human papillomavirus type 16 E7 oncoprotein from bicistronic mRNA is independent of splicing events within the E6 open reading frame. *J Virol* **69**, 7023-7031.

Stanley, M. (2005). Immune responses to human papillomavirus. *Vaccine*.

Stark, G. R. & Taylor, W. R. (2004). Analyzing the G2/M checkpoint. *Methods Mol Biol* **280**, 51-82.

Steenbergen, R. D., Parker, J. N., Isern, S., Snijders, P. J., Walboomers, J. M., Meijer, C. J., Broker, T. R. & Chow, L. T. (1998). Viral E6-E7 transcription in the basal layer of organotypic cultures without apparent p21cip1 protein precedes immortalization of human papillomavirus type 16- and 18-transfected human keratinocytes. *J Virol* **72**, 749-757.

Sterling, J. C., Skepper, J. N. & Stanley, M. A. (1993a). Immunoelectron Microscopical localization of the human papillomavirus type 16 L1 and E4 proteins in cervical keratinocytes cultured in vitro. *JInvestDermatol* **100**, 154-158.

Sterling, J. C., Skepper, J. N. & Stanley, M. A. (1993b). Immunoelectron microscopical localization of human papillomavirus type 16 L1 and E4 proteins in cervical keratinocytes cultured in vivo. *J Invest Dermatol* **100**, 154-158.

Sterlinko Grm, H., Weber, M., Elston, R., McIntosh, P., Griffin, H., Banks, L. & Doorbar, J. (2004). Inhibition of E6-induced degradation of its cellular substrates by novel blocking peptides. *J Mol Biol* **335**, 971-985.

Stoler, M. H., Whitbeck, S. M., Wolinsky, S. M., Broker, T. R., Chow, L. T., Howett, M. K. & Kreider, J. W. (1990). Infectious cycle of human papillomavirus type 11 in human foreskin xenografts in nude mice. *JVirol* **64**, 3310-3318.

Stoler, M. H., Rhodes, C. R., Whitbeck, A., Wolinsky, S. M., Chow, L. T. & Broker, T. R. (1992). Human papillomavirus type 16 and 18 gene expression in cervical neoplasias. *Hum Pathol* **23**, 117-128.

Storey, A. (2002). Papillomaviruses: death-defying acts in skin cancer. *Trends Mol Med* **8**, 417-421.

Straight, S. W., Hinkle, P. M., Jewers, R. J. & McCance, D. J. (1993). The E5 oncoprotein of human papillomavirus type 16 transforms fibroblasts and effects the downregulation of the epidermal growth factor receptor in keratinocytes. *J Virol* **67**, 4521-4532.

Strnad, P., Windoffer, R. & Leube, R. E. (2001). In vivo detection of cytokeratin filament network breakdown in cells treated with the phosphatase inhibitor okadaic acid. *Cell Tissue Res* **306**, 277-293.

Strnad, P., Windoffer, R. & Leube, R. E. (2002). Induction of rapid and reversible cytokeratin filament network remodeling by inhibition of tyrosine phosphatases. *J Cell Sci* **115**, 4133-4148.

Stubenrauch, F. & Pfister, H. (1994). Low-affinity E2-binding site mediates downmodulation of E2 transactivation of the human papillomavirus type 8 late promoter. *J Virol* **68**, 6959-6966.

Stubenrauch, F., Colbert, A. M. & Laimins, L. A. (1998). Transactivation by the E2 protein of oncogenic human papillomavirus type 31 is not essential for early and late viral functions. *J Virol* **72**, 8115-8123.

Stubenrauch, F., Hummel, M., Iftner, T. & Laimins, L. A. (2000). The E8E2C protein, a negative regulator of viral transcription and replication, is required for extrachromosomal maintenance of human papillomavirus type 31 in keratinocytes. *J Virol* **74**, 1178-1186.

Stumptner, C., Omary, M. B., Fickert, P., Denk, H. & Zatloukal, K. (2000). Hepatocyte cytokeratins are hyperphosphorylated at multiple sites in human alcoholic hepatitis and in a mallory body mouse model. *Am J Pathol* **156**, 77-90.

Stuurman, N., Heins, S. & Aebi, U. (1998). Nuclear lamins: their structure, assembly, and interactions. *J Struct Biol* **122**, 42-66.

Sun, T. T. & Green, H. (1978). Keratin filaments of cultured human epidermal cells. Formation of intermolecular disulfide bonds during terminal differentiation. *J Biol Chem* **253**, 2053-2060.

Sverdrup, F. & Khan, S. A. (1994). Replication of human papillomavirus (HPV) DNAs supported by the HPV type 18 E1 and E2 proteins. *J Virol* **68**, 505-509.

Sverdrup, F. & Khan, S. A. (1995). Two E2 binding sites alone are sufficient to function as the minimal origin of replication of human papillomavirus type 18 DNA. *J Virol* **69**, 1319-1323.

Swanbeck, G. & Thyresson, N. (1965). The role of keratohyalin material in the keratinization process and its importance for the barrier function. *Acta Derm Venereol* **45**, 21-25.

Swindle, C. S., Zou, N., Van Tine, B. A., Shaw, G. M., Engler, J. A. & Chow, L. T. (1999). Human papillomavirus DNA replication compartments in a transient DNA replication system. *Journal of Virology* **73**, 1001-1009.

Tachezy, R., Rector, A., Havelkova, M., Wollants, E., Fiten, P., Opdenakker, G., Jenson, B., Sundberg, J. & Van Ranst, M. (2002). Avian papillomaviruses: the parrot Psittacus erithacus papillomavirus (PePV) genome has a unique organization of the early protein region and is phylogenetically related to the chaffinch papillomavirus. *BMC Microbiol* **2**, 19 Epub 2002 Jul 2010.

Takahashi, K., Coulombe, P. A. & Miyachi, Y. (1999). Using transgenic models to study the pathogenesis of keratin-based inherited skin diseases. *J Dermatol Sci* **21**, 73-95.

Tang, A., Amagai, M., Granger, L. G., Stanley, J. R. & Udey, M. C. (1993). Adhesion of epidermal Langerhans cells to keratinocytes mediated by E-cadherin. *Nature* **361**, 82-85.

Taniguchi, A., Kikuchi, K., Nagata, K. & Yasumoto, S. (1993). A cell-type-specific transcription enhancer of type 16 human papillomavirus (HPV 16)-P97 promoter is defined with HPV-associated cellular events in human epithelial cell lines. *Virology* **195**, 500-510.

Tanner, N. K. & Linder, P. (2001). DExD/H box RNA helicases: from generic motors to specific dissociation functions. *Mol Cell* **8**, 251-262.

Thomas, M. & Banks, L. (1999). Human papillomavirus (HPV) E6 interactions with Bak are conserved amongst E6 proteins from high and low risk HPV types. *J Gen Virol* **80 (Pt 6)**, 1513-1517.

Thomas, M., Glaunsinger, B., Pim, D., Javier, R. & Banks, L. (2001). HPV E6 and MAGUK protein interactions: determination of the molecular basis for specific protein recognition and degradation. *Oncogene* **20**, 5431-5439.

Toivola, D. M., Zhou, Q., English, L. S. & Omary, M. B. (2002). Type II keratins are phosphorylated on a unique motif during stress and mitosis in tissues and cultured cells. *Mol Biol Cell* **13**, 1857-1870.

Ustav, M. & Stenlund, A. (1991). Transient replication of BPV1 requires two viral polypeptides encoded by the E1 and E2 open reading frames. *EMBO J* **10**, 449-457.

Vaeteewoottacharn, K., Chamutpong, S., Ponglikitmongkol, M. & Angeletti, P. C. (2005). Differential localization of HPV16 E6 splice products with E6-associated protein. *Virol J* **2**, 50.

Van Bressem, M. F., Kastelein, R. A., Flamant, P. & Orth, G. (1999a). Cutaneous papillomavirus infection in a harbour porpoise (Phocoena phocoena) from the North Sea. *Vet Rec* **144**, 592-593.

Van Bressem, M. F., Van Waerebeek, K. & Raga, J. A. (1999b). A review of virus infections of cataceans and the potential impact of morbilliviruses, poxviruses and papillomaviruses on host population dynamics. *Dis Aquat Organ* **38**, 53-65.

Van Ranst, M., Fuse, A., Fiten, P., Beuken, E., Pfister, H., Burk, R. D. & Opdenakker, G. (1992). Human papillomavirus type 13 and pygmy chimpanzee papillomavirus type 1: comparison of the genome organizations. *Virology* **190**, 587-596.

Vernon, S. D., Unger, E. R., Miller, D. L., Lee, D. R. & Reeves, W. C. (1997). Association of human papillomavirus type 16 integration in the E2 gene with poor survival from cervical cancer. *Int J Cancer* **74**, 50-56.

Villa, L. L., Costa, R. L., Petta, C. A. & other authors (2005). Prophylactic quadrivalent human papillomavirus (types 6, 11, 16, and 18) L1 virus-like particle vaccine in young women: a randomised double-blind placebo-controlled multicentre phase II efficacy trial. *Lancet Oncol* **6**, 271-278.

Villiers de, E. M. (2001). Taxonomic Classification of Papillomaviruses. *Papillomavirus Reports* **12**, 57-63.

Walboomers, J., Jacobs, M., Manos MM & other authors (1999). Human papillomavirus is a necessary cause of invasive cervical cancer worldwide. *J Pathol* **189**, 12-19.

Waldeck, W., Rosl, F. & Zentgraf, H. (1984). Origin of replication in episomal bovine papilloma virus type 1 DNA isolated from transformed cells. *Embo J* **3**, 2173-2178.

Walker, D. C., Brown, B. H., Blackett, A. D., Tidy, J. & Smallwood, R. H. (2003). A study of the morphological parameters of cervical squamous epithelium. *Physiol Meas* **24**, 121-135.

Wang, Q., Griffin, H., Southern, S. & other authors (2004). Functional analysis of the human papillomavirus type 16 E1=E4 protein provides a mechanism for in vivo and in vitro keratin filament reorganization. *J Virol* **78**, 821-833.

Warner, C. A. & McCance, D. J. (1989). Screening for cervical carcinoma. *Med Lab Sci* **46**, 215-222.

Waseem, A., Karsten, U., Leigh, I. M., Purkis, P., Waseem, N. H. & Lane, E. B. (2004). Conformational changes in the rod domain of human keratin 8 following heterotypic association with keratin 18 and its implication for filament stability. *Biochemistry* **43**, 1283-1295.

Werner, N. S., Windoffer, R., Strnad, P., Grund, C., Leube, R. E. & Magin, T. M. (2004). Epidermolysis bullosa simplex-type mutations alter the dynamics of the keratin cytoskeleton and reveal a contribution of actin to the transport of keratin subunits. *Mol Biol Cell* **15**, 990-1002 Epub 2003 Dec 1010.

Werness, B. A., Levine, A. J. & Howley, P. M. (1990). Association of human papillomavirus types 16 and 18 E6 proteins with p53. *Science* **248**, 76-79.

Wettstein, F. O., Barbosa, M. S. & Nasseri, M. (1987). Identification of the major cottontail rabbit papillomavirus late RNA cap site and mapping and quantitation of an E2 and minor E6 coding mRNA in papillomas and carcinomas. *Virology* **159**, 321-328.

Williams, G. H., Romanowski, P., Morris, L., Madine, M., Mills, A. D., Stoeber, K., Marr, J., Laskey, R. A. & Coleman, N. (1998). Improved cervical smear assessment using antibodies against proteins that regulate DNA replication. *Proc Natl Acad Sci U S A* **95**, 14932-14937.

Wilson, R., Fehrmann, F. & Laimins, L. A. (2005). Role of the E1--E4 protein in the differentiation-dependent life cycle of human papillomavirus type 31. *J Virol* **79**, 6732-6740.

Wilson, V. G., West, M., Woytek, K. & Rangasamy, D. (2002). Papillomavirus E1 proteins: form, function, and features. *Virus Genes* **24**, 275-290.

Windoffer, R. & Leube, R. E. (1999). Detection of cytokeratin dynamics by time-lapse fluorescence microscopy in living cells. *J Cell Sci* **112**, 4521-4534.

Windoffer, R. & Leube, R. E. (2001). De novo formation of cytokeratin filament networks originates from the cell cortex in A-431 cells. *Cell Motil Cytoskeleton* **50**, 33-44.

Windoffer, R., Woll, S., Strnad, P. & Leube, R. E. (2004). Identification of novel principles of keratin filament network turnover in living cells. *Mol Biol Cell* **15**, 2436-2448.

Wolf, P., Seidl, H., Back, B. & other authors (2004). Increased prevalence of human papillomavirus in hairs plucked from patients with psoriasis treated with psoralen-UV-A. *Arch Dermatol* **140**, 317-324.

Woll, S., Windoffer, R. & Leube, R. E. (2005). Dissection of keratin dynamics: different contributions of the actin and microtubule systems. *Eur J Cell Biol* **84**, 311-328.

Xiao, W. & Brandsma, J. L. (1996). High efficiency, long-term clinical expression of cottontail rabbit papillomavirus (CRPV) DNA in rabbit skin following particle-mediated DNA transfer. *NAR* **24**, 2620-2622.

Yaffe, M. P. (1999). Dynamic mitochondria. *Nat Cell Biol* **1**, E149-150.

Yang, F., Moss, L. G. & Phillips, G. N., Jr. (1996). The molecular structure of green fluorescent protein. *Nat Biotechnol* **14**, 1246-1251.

Yang, L., Mohr, I., Fouts, E., Lim, D. A., Nohaile, M. & Botchan, M. (1993). The E1 protein of bovine papillomavirus 1 is an ATP-dependent DNA helicase. *PNAS* **90**, 5086-5090.

Yang, R., Yutzy, W. H. t., Viscidi, R. P. & Roden, R. B. (2003a). Interaction of L2 with beta-actin directs intracellular transport of papillomavirus and infection. *J Biol Chem* **278**, 12546-12553 Epub 12003 Jan 12530.

Yang, R., Yutzy, W. H. t., Viscidi, R. P. & Roden, R. B. (2003b). Interaction of L2 with beta-actin directs intracellular transport of papillomavirus and infection. *J Biol Chem* **278**, 12546-12553.

Yang, X. F., Qu, X. Z., Wang, K., Zheng, J., Si, L. S., Dong, X. P. & Wang, Y. L. (2005). Construction of Prophylactic Human Papillomavirus Type 16 L1 Capsid Protein

Vaccine Delivered by Live Attenuated Shigella flexneri Strain sh42. *Acta Biochim Biophys Sin (Shanghai)* **37**, 743-750.

Yoon, K. H., Yoon, M., Moir, R. D., Khuon, S., Flitney, F. W. & Goldman, R. D. (2001). Insights into the dynamic properties of keratin intermediate filaments in living epithelial cells. *J Cell Biol* **153**, 503-516.

Yuan, Q. X., Nagao, Y., Gaal, K., Hu, B. & French, S. W. (1998). Mechanisms of mallory body formation induced by okadaic acid in drug-primed mice. *Exp Mol Pathol* **65**, 87-103.

Zatloukal, K., Stumptner, C., Fuchsbichler, A. & other authors (2002). p62 Is a common component of cytoplasmic inclusions in protein aggregation diseases. *Am J Pathol* **160**, 255-263.

Zhang, B., Li, P., Wang, E., Brahmi, Z., Dunn, K. W., Blum, J. S. & Roman, A. (2003). The E5 protein of human papillomavirus type 16 perturbs MHC class II antigen maturation in human foreskin keratinocytes treated with interferon-gamma. *Virology* **310**, 100-108.

Zhang, Y. & Schneider, R. J. (1994). Adenovirus inhibition of cell translation facilitates release of virus particles and enhances degradation of the cytokeratin network. *J Virol* **68**, 2544-2555.

Zhou, J., Doorbar, J., Sun, X. Y., Crawford, L. V., McLean, C. S. & Frazer, I. H. (1991a). Identification of the nuclear localization signal of human papillomavirus type 16 L1 protein. *Virology* **185**, 625-632.

Zhou, J., Sun, X. Y., Stenzel, D. J. & Frazer, I. H. (1991b). Expression of vaccinia recombinant HPV 16 L1 and L2 ORF proteins in epithelial cells is sufficient for assembly of HPV virion-like particles. *Virology* **185**, 251-257.

Zhou, X., Liao, J., Hu, L., Feng, L. & Omary, M. B. (1999). Characterization of the major physiologic phosphorylation site of human keratin 19 and its role in filament organization. *J Biol Chem* **274**, 12861-12866.

Ziegert, C., Wentzensen, N., Vinokurova, S., Kisseljov, F., Einenkel, J., Hoeckel, M. & von Knebel Doeberitz, M. (2003). A comprehensive analysis of HPV integration loci in anogenital lesions combining transcript and genome-based amplification techniques. *Oncogene* **22**, 3977-3984.

Zur Hausen, H. (1996). Papillomavirus infections-a major cause of human cancers. *Biochimica et Biophysica Acta* **1288**, F55-F78.